Development and Performance Analysis of Self-Aspirated Porous Radiant Burners for Kerosene Pressure Stove

A thesis submitted in partial fulfillment of the requirements for the degree of

Doctor of Philosophy

by

Gyan Sagar Sinha

(Roll No: 126103012)

Department of Mechanical Engineering

Indian Institute of Technology Guwahati

Guwahati – 781039, India

November 2017

भारतीय प्रौद्योगिकी संस्थान गुवाहाटी
Indian Institute of Technology Guwahati

Department of Mechanical Engineering
Indian Institute of Technology Guwahati
Guwahati – 781039, India

THESIS CERTIFICATE

It is certified that the work contained in the thesis entitled **Development and Performance Analysis of Self-Aspirated Porous Radiant Burners for Kerosene Pressure Stove** by **Gyan Sagar Sinha,** a student in the Department of Mechanical Engineering, Indian Institute of Technology Guwahati, India, for the award of the degree of the **Doctor of Philosophy** has been carried out under our supervision and that this work has not been submitted elsewhere for the degree.

Dr. P. Muthukumar
Professor
Department of Mechanical Engineering
Indian Institute of Technology Guwahati
Guwahati – 781039, Assam, India.

(Late) Dr. Subhash C. Mishra
Professor
Department of Mechanical Engineering
Indian Institute of Technology Guwahati
Guwahati – 781039, Assam, India.

भारतीय प्रौद्योगिकी संस्थान गुवाहाटी
Indian Institute of Technology Guwahati

Dedicated to

My Mother

भारतीय प्रौद्योगिकी संस्थान गुवाहाटी
Indian Institute of Technology Guwahati

Acknowledgement

I am heartily thankful to my thesis supervisors, **Prof. Subhash C. Mishra** and **Prof. P. Muthukumar**, whose guidance and support from the initial level to final level have enabled me to develop an understanding of the subject. The constant encouragements, strength and attention given by them to me have been a great motivation to take up the work as challenge and complete the same with great enthusiasm. Begining from framing the problems to the final experimental results and their physical interpretations, they remained deeply involved in my thesis work. Their wide knowledge and their logical way of thinking have been of great value for me. Their understanding, encouraging and personal guidance have provided a good basis for the present thesis. I have immensely benefited from each and every moment of my association with them. I am highly inspired by their intellectual prowess and exemplary professionalism. I enjoyed each and every moment working with their supervision and learnt a lot of things from them, which will be an asset for my future research.

I wish to express my deep gratitude to all those who have helped me in various ways during the tenure of my PhD work at IIT Guwahati. I have been supported and accompanied by many people and each one has played an indispensable role during my work. I am grateful to all of them.

I am thankful to my Doctoral Committee members, Prof. P. Mahanta, Prof. U. K. Saha and Dr. Chandan Das for their valuable suggestions and encouragement during the period of my research work.

I heart fully thank to Prof. S. Kanagaraj and Prof. V. S. Mohalkar to allowed me to their lab to perform important experiment.

I specially thank to Dr. Niraj Kumar Mishra for their help during the course of fabrication of the setup and also their assistance when needed during my experimental studies.

I personally thank to my close colleague and lab mate Mr. Hakeem Niyas for their proper support during my thesis correction.

I am thankful to Dr. S. Anbarasu, Dr. Rupesh Singh, Dr. Koushik Das, Mr. Luv Kumar Koushik, Miss. Sanjukta Devi, Mr. Snehasish Panigrahy, Mr. Chilaka Ravi Chandra Rao, Mr. B. Kiran, Mr. Vivek Selvan, Dr. Vijay Mishra and Miss. Sunita Deb with whom I had healthy discussions and they made my stay a pleasant one at IIT Guwahati. I may have missed out a few names in the following list; my sincere apologies are due for any such inadvertent oversight.

I would like to express my sincere gratitude to my parents Sri Madhukar Prasad Singh and Late Mrs. Rekha Sinha, my brothers Mr. Gopi Krishna sinha, Mr. Sruti Sharwan Sinha, Mr. Priyavart Sinha and My younger sister Miss. Priyanka Bharti Sinha whose blessings, prayers and never ending support is the real impetus that continuously motivates me to produce my best. Last but not the least, my deepest gratitude goes to my friend Miss. Sweta Kumari for her constant encouragement, patience and motivation for the completion of this thesis work.

I bow my head and record my sincere gratitude to the God Almighty for giving me the strength, health and the spirit to complete my research work.

Gyan Sagar Sinha

Abstract

In the rural part of India or any other developing and under developed nation, people use biomass and kerosene for cooking application because of the low cost as compared to LPG. The thermal efficiency of biomass is about 5 – 10 %. Severe usage of biomass not only lead to deforestation, but also create an imbalance of natural resources in the ecological system. Though, LPG is a clean fuel when compared to other fuels for cooking purpose, due to its high cost and less accessibility in remote areas, people in the rural areas cannot afford LPG. Hence, due to the low cost and easy availability of kerosene, low-income group people in rural, suburban and urban areas can certainly utilize kerosene for the cooking applications. Average thermal efficiency of pressure kerosene stove is 45 %. Kerosene stoves release huge amount of CO and NO_x emissions in the form of exhaust because of its incomplete combustion. Therefore, it is of vital importance to incorporate modifications in the design of kerosene pressure stove. The main purpose of the design modifications is to utilise the input energy to the maximum possible extent and to minimize the pollutant emissions. A conventional combustion device is associated with free-flame wherein the combustion takes place in the open-air environment, in which convection heat transfer is dominant. Free flame combustion comes with very low thermal conductivities and emissivities, so in conventional combustion devices, contributions of conduction and radiation is insignificant. Thus, due to poor heat transport, these devices are less efficient, and they have undesirable features such as low power density, high level of pollutant emissions, etc. Conventional kerosene pressure stoves fall under this category. Performance of biomass stove when compared to LPG and kerosene stove is very low. Since the last decade, depending upon the economic conditions of the people, there has been a gradual shift from the usage of biomass to kerosene or LPG fuels. In kerosene stove, a premixed air-fuel

mixture combust in the gaseous (air) environment and the flame stabilizes over the metallic burner head. The measured thermal efficiencies (laboratory conditions) of the conventional domestic kerosene pressure cooking stoves (1.5 – 3 kW) available in the Indian market are in the range of 48.5 – 58 %. CO and NO_x emissions from conventional domestic kerosene pressure stoves (1.5 – 3 kW) are in the range of 610 ppm to 915 ppm and 19 ppm to 35 ppm, respectively. These emissions levels are above the current standards of World Health Organization. Thus, curtailment of CO and NO_x emissions further necessitates development of efficient burners for cooking applications. PMC has emerged as an important technology for reduction of emissions of CO and NO_x. In PMC, the combustion takes place within a highly conductive and radiative solid porous medium (matrix) having very large surface area. Apart from preheating of the incoming premixed fuel-air mixture, several factors such as volumetric radiation, increased conduction and convection owing to higher surface area per unit volume of the porous matrix and homogenization of temperature lead to the elongation in the volume of the reaction zone. These aspects result in a higher thermal efficiency and reduced emissions. Some researchers have extended usage of porous matrix to kerosene pressure stoves. They have reported enhanced thermal efficiency and reduced emissions. A critical review of previous studies reveals that their developments were mainly focused on the development of burners based PMC technology with the supply of compressed air and hence they could not be used for domestic cooking. The supply of compressed air is not feasible, and it is also unnecessary for the cooking applications. The present work, addresses this issue through the development of self-aspirated porous radiant burners (PRB) for kerosene pressure domestic stoves. The present work utilizes the principles of PMC for the development of kerosene pressure cooking stoves. For domestic cooking, burner power in the range of 1.5 – 3 kW is developed. The developed cooking stoves with PRB are stand-alone systems. These burners does not

require any supply of external air for their operation. Design of the cooking stoves has been substantially changed to work without the supply of external air. The changes are discussed in detail in the thesis. The work contained in the thesis has been carried out in two parts. The first part of the study is dedicated to the development of self-aspirated domestic kerosene pressure cooking stove with a PRB. The development of self-aspirated PRB for kerosene pressure cooking stoves with nanoparticle-blended kerosene is the second study. To compare the improvements in terms of thermal efficiency and emissions in the developed kerosene pressure stoves, experiments were performed with both the newly developed self-aspirated (with PRB) and conventional (same power input) kerosene pressure stoves. In the first part of the study, the burner input power range considered was 1.5 – 3 kW. The combustion behaviour within the burner has been also studied with the temperature details, measured at certain radial and axial locations. Use of compressed air has been one of the major limitations in using the kerosene pressure stoves with PRB for cooking applications. To eradicate this limitation, the design modifications in terms of kerosene supply pressure, orifice, burner port, and burner casing were done. With the improved design of the burner assembly, thermal efficiency, emission characteristics and temperature distribution were studied. A significant improvement in thermal efficiency (55.5 – 64.3 %), and large reduction in emissions (CO: 180 – 290 ppm and NO_x: 1.5 – 4.1 ppm) were observed. For different power inputs, the thermal efficiency of the conventional burners was found in the range 48.5 – 58 %. This increase in thermal efficiency is attributed to the improved combustion in the PRB. Nanoparticle blended kerosene was also tested in the kerosene pressure stoves of the same power range (1.5 – 3 kW) with self-aspirated PRB and conventional burners. The thermal efficiency was found to improve significantly (58.5 – 67.1 %), and the emissions (CO: 120 – 220 ppm and NO_x: 1.2 – 3.5 ppm) also reduced considerably in the kerosene pressure stove with the self-aspirated PRB.

भारतीय प्रौद्योगिकी संस्थान गुवाहाटी
Indian Institute of Technology Guwahati

Nomenclature

S_L	Laminar flame speed (mm/s)
d_m	Equivalent pore diameter (mm)
L	Heat of vaporization of water at 373 K, (kJ/kg)
ρ	Density (kg/m^3)
k	Thermal conductivity of the fuel-air mixture (W/m-K)
Q_{rad}	Total radiative power emitted by the burner, (MJ)
Q_{chem}	Energy release rate for ideal combustion at standard state (MJ)
m_w	Mass of water (kg)
C_w	Specific heat of water (kJ/kg-K)
T_2	Final temperature of water ($^\circ$C)
T_1	Initial temperature of water ($^\circ$C)
$T_{w,0}$	Water temperature at the outlet (K)
$T_{w,i}$	Water temperature at the inlet (K)
m_f	Mass of fuel consumed (kg)
LCV	Lower calorific value (kJ/kg)
m_p	Mass of vessel, kg
C_p	Specific heat of vessel (kJ/kg-K)
m_{ev}	Mass of water evaporated (kg)
η_{th}	Thermal efficiency
η_R	Radiation efficiency
ϕ	Equivalence ratio

φ	Upstream porosity
φ_2	Downstream porosity
wt. %	Weight by percentage
Wn	Weight of nanoparticle (gm)
WF	Weight fraction
Ws	Weight of kerosene (gm)
Wt	Weight of nanofuel (gm)

Abbreviations

PMC	Porous Medium Combustion
PM	Porous media
PB	Porous Burner
PRB	Porous Radiant Burner
PSZ	Partially Stabilized Zirconia
CB	Conventional Burner
ppm	Parts per million
ppi	Pores per inch
ppc	Pores per centimeter
cpsi	Cell per square inch
LPG	Liquefied petroleum gas
SiC	Silicon carbide
Al_2O_3	Alumina
ZrO_2	Zirconia
TMT	Thousand Metric Tonnes
OSC	Oxygen Storage capacity
TWC	Three Ways Catalyst
CTAB	Cetyl Trimethyl Ammonium Bromide
SDS	Sodium Dodecyl Sulfate
CeO_2	Cerium oxide or Ceria
WBT	Water boiling Test
BIS	Bureau of Indian Standards

CV	Calorific Value
WHO	World Health Organization
CO	Carbon Mono-oxide
NO_x	Nitrogen Oxide
SOL	Sol-gel
COP	Co–precipitation
TPR	Temperature Reduction Program
TGA	Thermogravimetric Analyzer
XRD	X-rays Diffractometric Technique
UHC	Unburnt Hydrocarbon
YSZ	Yttria Stabilized Zirconia
YZA	Zirconia/Alumina composite
ZTM	zirconia-toughened Mullite

Contents

List of Figures

भारतीय प्रौद्योगिकी संस्थान गुवाहाटी
Indian Institute of Technology Guwahati

List of Tables

Chapter 1

Introduction

1.1 Motivation

In the developing nation like India, the major part of the energy requirements in cooking applications is fulfilled via traditional combustion devices working on fossil fuels. The concern on increase in environmental pollution originating from combustion processes and decrease in fossil fuel sources have imposed the need to look for an alternative source of energy. Concurrently, it is also required to make necessary modifications in the existing combustion systems for achieving better combustion efficiency. The main objective of these design modifications is to utilise the energy to the maximum possible extent and to minimize the pollutant emissions.

Generally, the free flame combustion exists in conventional combustion device. Free flame combustion takes place in the open air environment in which the convection is the predominant mode of heat transfer. In conventional combustion device, the contributions of conduction and radiation modes of heat transfer from the post flame to pre flame zone is insignificant, because gases have a very low thermal conductivity and low emissivity. Due to insignificant contributions from conduction and radiation modes of heat transfer, the performance of conventional combustion devices is poor, and they have undesirable features such as low flammability limits, low power density, high level of pollutant emissions, etc.

Conventional pressure kerosene cooking stove is one of such devices that falls under the category of free flame combustion. In developing countries like India especially in rural

areas, for cooking purpose, kerosene is the most commonly used fuel. Kerosene is synthesized by refining petroleum, and is usually derived from fossil fuel sources. Kerosene has a high calorific value than biomass (firewood and chips, dungcake and gobar gas). It is also a clean fuel and its usage is much easier. The properties of kerosene are presented in Appendix – I.

In India, large share of energy requirement for cooking applications mainly comes from three different fuels, viz., biomass, kerosene and liquefied petroleum gas (LPG). Table 1.1 indicates the share of different cooking fuels used in rural and urban Indian households. In urban areas, LPG is extensively used as a fuel for cooking and in rural, kerosene and biomass are used. Due to the presence of high-income people and easy availability, LPG is consumed more in urban areas while in rural areas, people could not access LPG due to higher cost and poor distribution network (Dixit *et al.*, 2006). However, in urban areas also, low-income people could not use LPG. So low-income people still use kerosene and biomass. Kerosene is preferred more as compared to biomass because of its clean combustion. Indian government is also providing subsidy on kerosene mainly for the poor class people.

Table 1.1: Cooking Fuel Usage, percentage of households (NSSR, 2010)

S. No.	**Primary cooking fuel**	**Year: 2009-2010**	
		Rural	Urban
1	Firewood, chips	76.3	17.5
2	Dung cake	6.3	1.3
3	LPG	11.5	64.5
4	Kerosene	0.8	6.5
5	Others	0.8	2.3

1.1.1 Conventional Pressure Kerosene Cooking Stove

Two types of kerosene stoves viz., wick type and pressure type are generally used in cooking applications. Due to high thermal efficiencies, pressure type stove is mostly preferred (Natarajan *et al.,* 2008). Pressure kerosene stove has an average thermal efficiency of about 45 % (Thukral and Bhandari, 1994; Smith *et al.*, 2000). Thermal efficiency also depends on power input and operating condition. In case of traditional biomass stove, thermal efficiency varies only 5-10%, which is lower than that of pressure kerosene stove (Dendukuri and Mittal, 1993). In the context of emissions, pressure kerosene stoves have lower emissions as compared to wick type and biomass stove. Reason behind this is higher thermal and combustion efficiencies of kerosene pressure stove, which emits low amount of carbon dioxide (CO_2) and carbon monoxide (CO). Kerosene stoves as an individual have high carbon monoxide (CO) emissions, which is higher than the prescribed limit of the World health organization (WHO) for indoor air pollution (Kandpal *et al.*, 1995; Zhang *et al.,* 1999). Fuel combustion with deficiency of oxygen (O_2) produces CO. Prolonged exposure of CO can cause severe health problems. CO react with hemoglobin form carboxy-hemoglobin, which decreases the overall capacity of the blood to carry O_2 to the cells. Besides, it is believed that CO is an indirect greenhouse gas, which is solely responsible for global warming. Thus, control of CO emissions from the cooking stove is necessary and this further adds to the motivation to improve the design of the combustion devices. Pressure kerosene cooking stove burner has two ascending and two descending tubes with a flat circular chamber at the top called burner head. Lower portions of the ascending tube is connected to the top of the fuel passage tube, which is called rising tube. The bottom end of the rising tube is connected to the pressure tank. A spray nozzle is attached in between the two descending tubes. Figure 1.1 shows the schematic of the burner assembly. In the pressure kerosene cooking stove, combustion takes place on the top of the

burner head and the combustion that happens in the conventional burner (CB) is always fuel rich. Generally, combustion in the pressure kerosene cooking stove takes place in a gaseous environment and the flame becomes stable over the metallic surface (flame ring) of the burner as shown in Figure 1.2. This type of combustion is called as free flame combustion. In free flame combustion, the reaction zone is very thin and because of which the temperature gradient across the flame is very high. Due to the above reasons, the free flame combustion is not desirable for cooking stoves.

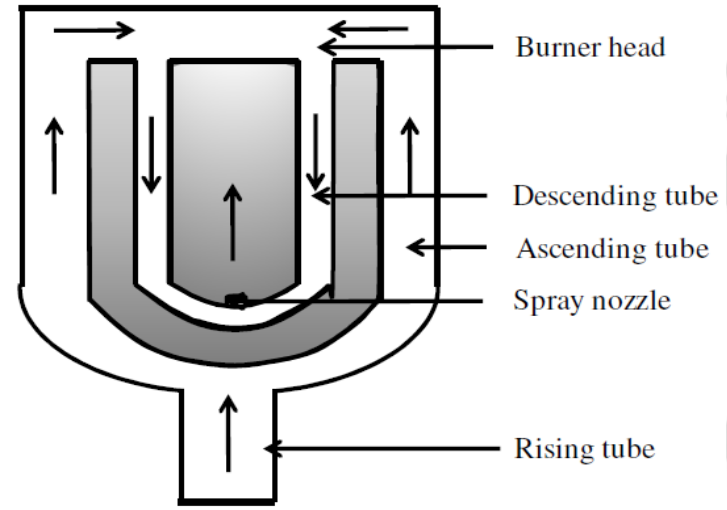

Fig. 1.1: Schematic of the primus stove burner (Primus stove, Wikipedia, 2010).

Fig. 1.2: Pictorial view of the free flame in conventional cooking kerosene stove.

1.1.2 Energy Analysis

Figure 1.3 shows the export and import of kerosene by the Govt of India during 2011-2016. Earlier, India has imported a huge amount of kerosene to meet the cooking demand. In 2011, the total import of kerosene was about 564 Thousand Metric Tonnes (TMT). However, after 2011, it was almost stopped. The kerosene import during the years, 2012, 2013, 2014, 2015 and 2016 are 0, 0, 30, 41 and 0 TMT, respectively. The reason behind this are the incorporation of new technology and the production of kerosene from various private and government organisations. Now, India is in a position to export kerosene due to the excess production of kerosene. Though, the kerosene production was accelerated during the period from 2012 to 2016, there was a decrease in kerosene export, which is due to the increase in local demand. Figure 1.4 shows the consumption and production of kerosene. It is observed from Figure 1.4 that the consumption rate of kerosene has been gradually decreased during the last five years. It is obviously due to the higher usage of LPG and electricity. In urban areas, two types of people live, low and high income people. High-income people can afford LPG and high cost electricity. However, the low-income people cannot afford LPG and electricity even after subsidies. Low-income people totally rely on either traditional biomass or kerosene stove. Traditional biomass stove has low thermal efficiency (5-10 %) and is highly smoky. In case of pressure kerosene stove, the efficiency is greater (average thermal efficiency is 45 %) than the traditional biomass stove and it is lower in particulate emissions. However, through the public distribution system, the quantity of kerosene is limited to few litres per household per month. So to meet the cooking requirements, the low-income people have to buy the kerosene from the commercial market, which costs Rs. 33-50 per litre (annual report of ministry of petroleum and natural gas, 2016-17). To avoid the highly priced kerosene, the low-income people tend to use either coal, wood, dung cake or wood chips.

This is the major reason for the low consumption of kerosene in the recent years.

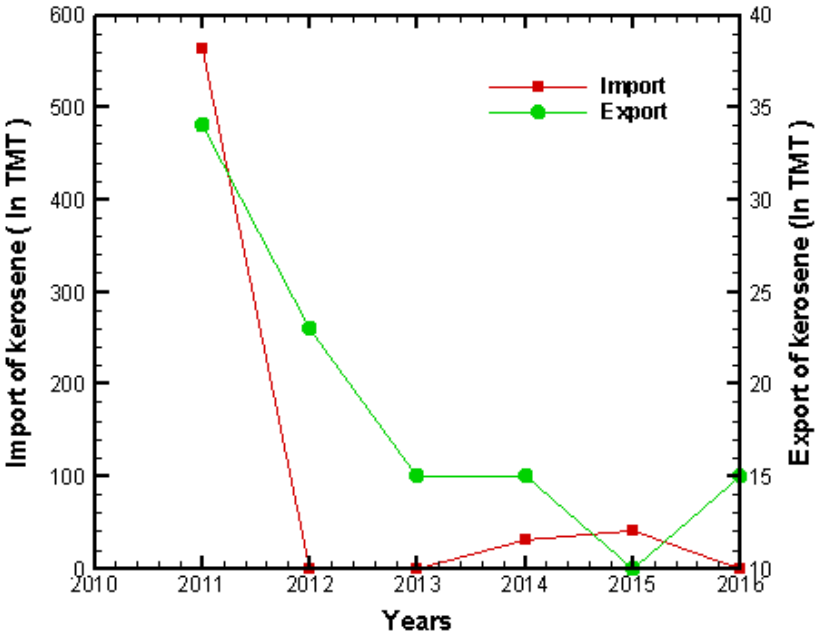

Fig. 1.3: Year wise import and export of kerosene (Annual Report, Ministry of Petroleum and Natural Gas, 2016-17).

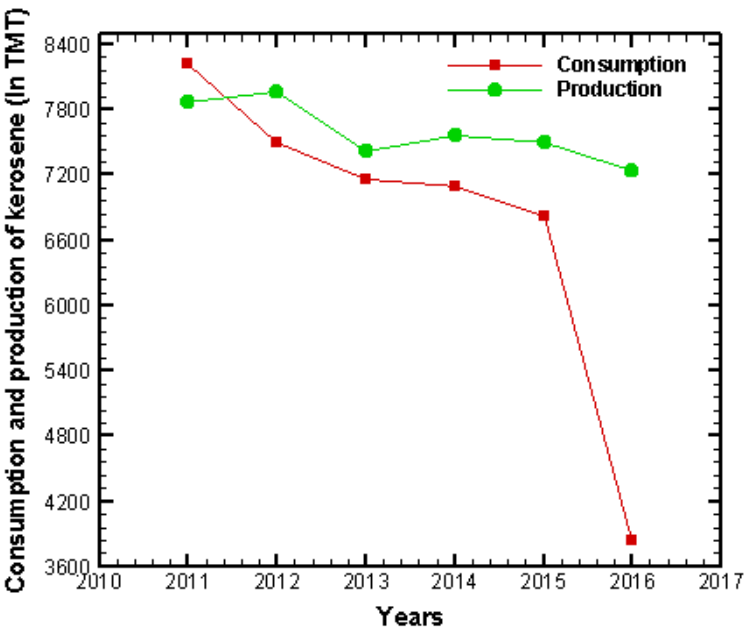

Fig. 1.4: Year wise production and consumption of kerosene (Annual Report, Ministry of Petroleum and Natural Gas, 2016-17).

In rural areas, due to poor network of LPG and electricity, people use wood for cooking, which not only produces smoke, but also leads to deforestation, resulting in ecological

imbalance. So people in rural areas have only option of using kerosene pressure stove. Porous burner (PRB) with pressure kerosene cooking stove has promising future for people surviving in either rural or urban areas. Because PRB with kerosene stove operates with high efficiency as well as low emissions. Government of India provides huge amount of subsidy for kerosene every year, which is shown in Figure 1.5. In order to cut down the increasing subsidies, the amount of kerosene consumed should be reduced by improving the combustion characteristics of the existing burners.

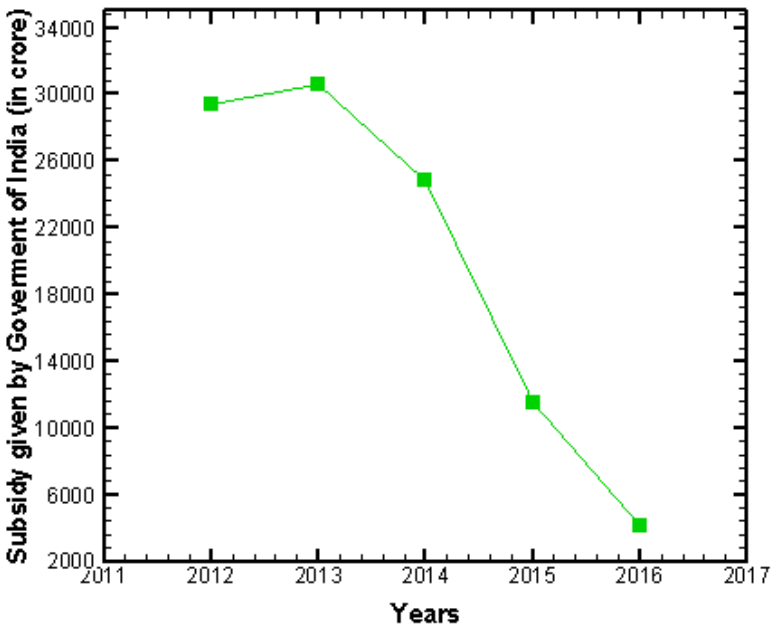

Fig. 1.5: Year wise subsidy by Government of India on kerosene (Annual Report, Ministry of Petroleum and Natural Gas, 2016-17).

1.1.3 Pollutant Formation and Their Effects

There are two major outcomes derived from the combustion process: the first one is heat and the second one is air pollution in terms of exhaust, which severely affects the environment and health in several ways. There are two type of air pollutants: primary and secondary. Primary air pollutants are the one, which are emitted directly from the source. Secondary air pollutants are generally formed through the reactions involving primary pollutants in the atmosphere. Carbon monoxide (CO), nitric oxide (NO) and nitrogen

dioxide (NO_2) are the primary pollutants that has been exhausted by any combustion device as they dominate during the combustion process. Physical properties, available sources and the general effects of primary air pollutants are presented in Table 1.2. Carbon monoxide is the most abundant pollutant in the lower atmosphere. The major ill effects include headache, vomiting and in large exposure, it can lead to coma or even death. Figure 1.6 illustrates the different effects of CO exposure levels. CO is the major species formed during the rich combustion. For stoichiometric and slightly lean mixtures, CO is found in substantial quantities at typical combustion temperatures because of the dissociation of CO_2. Carbon monoxide concentrations rapidly fall with temperature (Turns, 2000). According to Basu *et al.* (2012), 0.1 s of residence time is necessary for complete combustion. However, in IC engines, as the variation of temperature is high, the residence time is not sufficiently long enough for complete combustion. There are various requirements to be met for reducing the concentration of CO in flue gases: (i) the residence time must be as long as possible (ii) higher combustion temperatures and (iii) usage of lean mixture (excess air). For fuel rich mixture, the CO emission is higher and the CO equilibrium concentration is high. One should emphasize that the above considerations are valid only for pre-mixed combustion processes.

Oxides of nitrogen are also one of the important pollutants formed from the combustion of fossil fuels. The major sources are automobiles and power plants using coal, oil and gas. Nitric oxide (NO) and nitrogen dioxide ($NO_{2)}$ are part of the oxides of nitrogen and generally known as NO_x. NO is a precursor for the formation of NO_2 and other oxides of nitrogen. Nitric oxide is generally formed from atmospheric nitrogen (N_2 present in air) and nitrogen contained in some fuels by breaking the triple bond between the nitrogen atom. The major source of NO_x among the above two is atmospheric nitrogen. Nitric oxide is generally formed, because of the high-temperature oxidation of N_2. Low amount of nitrogen

oxides, which is present in ambient air, would not affect the human beings. Higher exposure of nitrogen oxides may occur by burning kerosene, wood or if one smokes, which could lead to unhealthy environment.

Table 1.2: Some important physical properties and effects of the primary pollutants (Avdic, 2004)

Pollutant	Physical properties	Source		Effects on humans
		Humans	Natural	
CO	Colourless, odourless, flammable, toxic gas, slightly soluble in water	Combustion of fossil fuels	Atmospheric oxidation of methane and other biogenic hydrocarbons	Decreases the oxygen carrying capacity of blood. The other effects vary from headache, vomit, collapse and death depends on the levels of exposure.
NO	Colourless, Odourless gas, non-flammable, slightly soluble in water, toxic	Combustion of fossil fuels	Bacterial action, Natural combustion processes.	Damage respiratory air ways, can cause burns on the skin/eyes.
NO_2	Reddish-orange brown gas with sharp pungent odour, toxic and highly corrosive.	Combustion of fossil fuels	---	Risk of respiratory symptoms such as acute bronchitis, cough and phlegm, particularly in children.

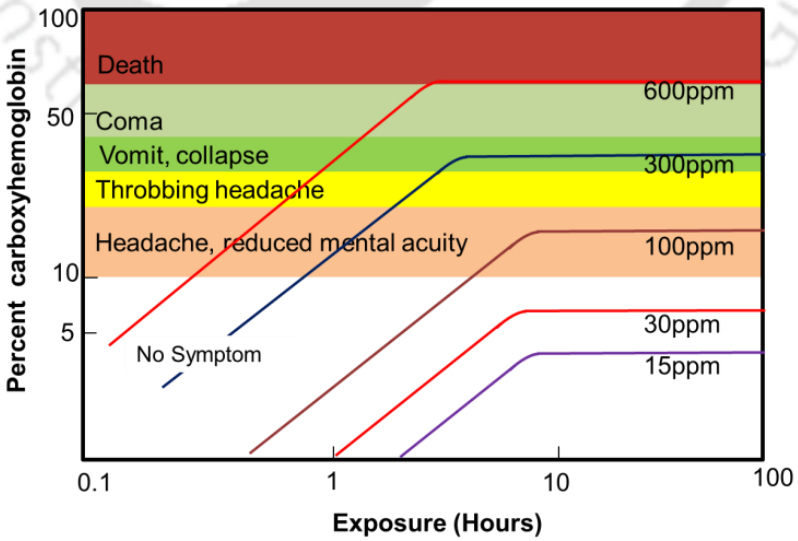

Fig. 1.6: Effects of different levels of CO exposure on humans (Turn, 2000).

1.2 Porous Medium Combustion

Porous media combustion (PMC) is totally a different type of combustion, which makes use of a novel concept of combusting in a highly conductive and radiative porous solid medium for better heat transport. This is a flameless combustion, which is significantly different from the conventional combustion. The conventional combustion is characterized by a free-flame where the combustion takes place in a gaseous environment.

In conventional combustion, convection mode of heat transfer remains dominant. In the PMC, unlike the conventional combustion, the reaction zone remains fully submerged in the inert porous matrix with almost no visible flame at the exit of the burner (Mital *et al.*, 1997). Due to the higher conductivity and emissivity of the solid matrix material, the effect of conduction and radiation heat transfers are significant. The convective heat transfer is also improved because of the large internal surface area of the porous media. In the PMC, temperature of combustion zone is much lower than the conventional combustion due to an internally self-organized process of heat recuperation (Weinberg, 1971). Figure 1.7 shows the photographic view of the porous radiant burner (PRB) taken at Thermal Science Lab, IIT Guwahati. The better heat transport (through the combined modes of conduction, convection and radiation) leads to a homogeneous temperature distribution in the combustion zone. Due to better conductive, radiative and convective heat transfers, the porous radiant burner has several advantages, such as higher thermal efficiency, higher power density, higher power modulation, lower NOx emission, etc. (Howell *et al.*, 1996). Stabilization of the flame may occurs either inside or on the surface of the porous matrix, which depend on the flow velocity and thermo-physical properties of the porous material. Besides that, due to the higher effective diffusion and heat transfer between the phases in porous burner, the combustible mixture stabilizes over a wide range of reactant velocities, air-fuel ratios and heat input (Mujeebu *et al.*, 2009a).

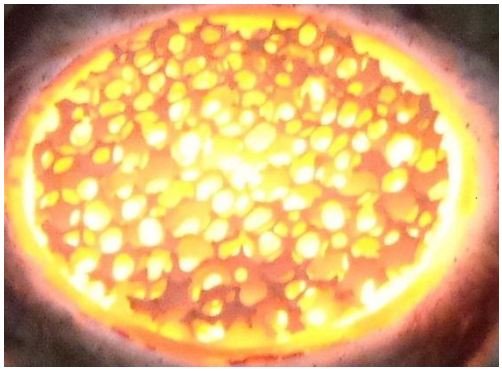

Fig. 1.7: The photographic views of PRB taken at IIT Guwahati.

Unlike the conventional burners, a low calorific fuel can also be combusted in the porous radiant burners. Figure 1.8 shows the schematic of heat transfer mechanism in porous media constructed with four spherical solids where combustion takes places within the pores of the solids. The air-fuel mixture flows in the porous media through its convoluted path when it is passed from the bottom of solid media. The exhaust gases are expelled from the top of the porous burner. Stabilization of reaction zone occurs within the porous bed and there is a transfer of heat occurs from the reaction zone to the incoming mixture, which involves all the three modes, viz., conduction, convection and radiation. Conduction takes place inside the porous radiant burner, as the solids are interconnected. Convection remains present when there is a transfer of heat from the hot combustion products to the porous solids. Radiation remains active when the solid media takes the sensible heat from the hot gases and becomes incandescent. Owing to the self-organized internal heat recirculation, PMC has a unique characteristic. It facilitates preheating of reactants, which thereby allows the combustion to start at a relatively low temperature. There are several advantage of preheating such as increase in flammability limit, reduction of CO, increase in burn rate, increase in flame speed, etc. In case of conventional burner (CB), due to poor heat conductivity of gases, chemical reaction takes place in a smaller circular region of combustion zone.

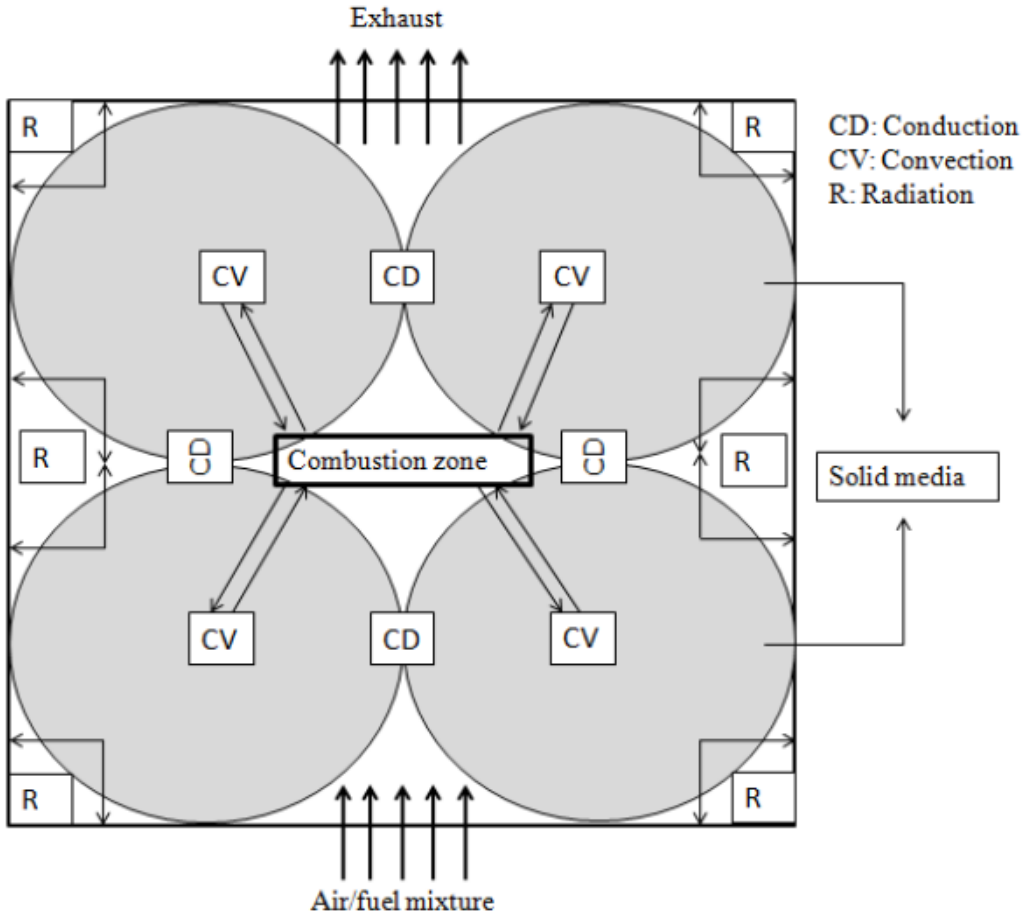

Fig.1.8: Heat recirculation in a porous radiant burner.

Due to the small region of combustion zone, maximum energy is released in that region itself, while the rest of the combustion chamber remains unused. This leads to the increased formation of NO_x as the temperature gradient across the combustion zone of the CB is very steep.

Nowadays, PRB gains popularity as it offers the benefits of infrared heating, due to which it provides much faster heating as compared to the CB, which has only convective heat transfer. Temperature of the source and the absorption characteristics of the product being heated determine the rate of heat transfer in an infrared heater. Since the radiation output is proportional to the fourth power of the temperature, source temperature dominates the performance.

1.2.1 Advantages of Porous Medium Combustion

The major advantages of PMC are as follows;

- PMC has better heat transfer properties and it keeps the burner's surface temperature low, which in turn reduces NO_x emissions.
- Due to the increase in residence time, the formation of CO emission is low.
- A portion of heat released is transported in the upstream direction, which preheats the fresh mixture causing the greater flame speeds as compared to free flame combustion.
- Operates at lower equivalence ratios.
- The burner can be operated on wide range of power modulation.
- Various complex combustion chamber geometries are possible in case of a porous burner.
- This method improves the heat transfer process due to good radiation and conduction properties of porous medium (Mujeebu *et al.*, 2009a).

1.2.2 Applications of Porous Medium Combustion

Nowadays, the applications of porous media combustion are widespread. Wood and Harris (2008) reported a detailed review of the various commercially available porous burners that are based on gas fired combustion, which are used in manufacturing processes such as paper drying, paper finishing, powder and paint curing, baking, textile drying, glass and chemical processing, polymer processing, metal heat treating, etc. Porous burners are also used in IC engines, gas turbine combustion chamber, steam generator etc. Use of porous burner in domestic cooking applications are limited and not much literature is available on this. Till date, Pantangi *et al.* (2010) and Mishra *et al.* (2015) analyzed the combustion behaviour of LPG stoves using a porous radiant burner. Patangi *et al.* (2010) used the complete concept

of porous media combustion in which they combusted the LPG within the porous radiant burner with an external air supply, while Mishra *et al.* (2015) used two layer of porous radiant burner in which they combusted the LPG between the two layers. Kakati *et al.* (2007) and Sharma *et al.* (2009) studied the performance of conventional kerosene stoves. Kakati *et al.* (2007) used the porous media as radiant inserts only, while Sharma *et al.* (2009) used two layers of porous media with different porosities for combusting the kerosene in between the two layers. The bottom layer is used to preheat the incoming air and the upper layer is used to increase the heat transfer. They found that significant improvement in efficiency were found in the porous radiant burners over the conventional burners.

1.3 Introduction of Nanofuel

Now a days, emphasis has been focussed on the research area of nanofuel for enhancing performance of kerosene and diesel engine over conventional hydrocarbon. Nanoparticle in nanofluid exhibit increase in surface area, improvement in thermal conductivity etc. In current years, a special attention has been given to synthesize and characterize the solid solutions based on cerium oxide (CeO_2) for cleaning the combustion emission, because the redox properties of the catalysts can contribute to lower the emission (Masui *et al.*, 2006). CeO_2 is found to be widely used a three way catalyst (TWC) for exhaust gas treatment device because of its attractive characteristics such as low temperature reduction, large specific surface area and cubic structure. It enables to operate the after-combustion-device more efficiently irrespective of the fuel mixture in an IC engine (Kaspar *et al.*, 2003). Due to wide range of applications of rare-earth metal oxides like ceria, more emphasis is being given by many research scientist in the related area of research. The inherent attractive characteristics such as elevated oxygen transport capacity, which is also called oxygen storage capacity (OSC), associated with the ability of changing the valency state from Ce^{3+}

to Ce^{4+} or vice versa made ceria for the many different application. The redox characteristics of ceria were more effective when the particles were in the range of nanosize (Yetter *et al.,* 2009). The main role of ceria in catalytic applications is to provide oxygen buffering capacity during the rich/lean oscillation of exhaust gases. Ceria has the ability to donate its oxygen for the oxidation of CO and hydrocarbon during the oxygen deficient portion and absorbs excess oxygen for the reduction of NO_x. The required oxygen for complete combustion of the fuel can be supplied by the ceria when it was used during the combustion stage.

Ceria nanoparticles dispersed in biodiesel increased the total combustion of heat, while the concentration of smoke and NO_x was decreased in the exhaust of a diesel engine (Sajith *et al.,* 2010). Another important advantage of nanoparticles in liquid is their size, because there is no chance for fuel injector and filter clogging as in the case of micron size of nanoparticles (Ganesh *et al.,* 2011). Addition of low boiling point component in diesel also promoted the spray evaporation and mixture formation processes (Li *et al.,* 2009a). In order to ensure the same characteristics of ceria dispersed diesel and pure diesel, the nanoparticles are always dispersed in tiny amounts at ppm level in diesel. It was found that the use of ceria as a TWC was explored in automobile applications. But it was not used in PRB with pressure kerosene stove. In order to reduce exhaust emission of PRB with pressure kerosene stove and improve its performance, an attempt is being made to enhance the oxygen storage capacity of ceria and its application in kerosene pressure stove with PRB performance as a nanofuel, nanoparticles dispersed kerosene.

1.4 Research Gap

Necessity of the development of a low emission and high efficient cooking stove is strongly felt to curtail energy crisis and to reduce the formation of pollutants especially from fossil

fuel fired devices. In this context, commonly in other applications (Delalic *et al.*, 2004; Avdic *et al*., 2010) and some studies made with cooking stoves (Kakati *et al.*, 2007; Sharma *et al.*, 2009; Pantangi *et al.*, 2010; Mishra *et al.*, 2015), the use of PMC is beneficial. In the last ten years, several applications of this technology have been explored. It was observed that most of the researchers explored the use of porous medium combustion in cooking applications with the help of an external air supply. It was seen that no works have been reported on the use of self-aspirated PRB in domestic pressure kerosene cooking stove. It was also found that no researcher tested the PRB with ceria-based nano fuel in pressure kerosene cooking stove. Hence, this thesis is dedicated to investigate the applications of the PRB particularly concentrating on the self-aspirated domestic pressure kerosene cooking stove with simple kerosene fuel and ceria-based nano fuel.

1.5 Objectives of the Present Study

The overall objective of this study is to investigate the application of PRB in the conventional pressure kerosene stoves. In a broad sense, considering the scope of the present study, the following objectives have been set.

1. Development of a self-aspirated PRB incorporated pressure kerosene stove.
2. Synthesis and combustion performance assessment of a ceria-based nano fuel.
3. Performance evaluation of the developed pressure kerosene stove with PRB in terms of temperature profile, thermal efficiency and emissions.
4. Comparison of the performance of the self – aspirated pressure kerosene stove PRB and conventional stove using simple kerosene and nano fuel.

1.6 Organization of Thesis

This thesis consists of eight chapters and the contents presented in each chapter are discussed in the following sections. The first chapter gives a brief introduction about the concepts and applications of porous media combustion devices. Chapter 1 also discuss about cerium based nanofuel.

In the second chapter, history and the various stages of development of pressure kerosene cooking stoves are discussed. A complete review of PMC, which include different significant developments till date and important aspects of PMC such as flame stabilization, heat recirculation etc. are presented. Chapter 2 also discuss about the different potential materials chosen for PRB. Performance evaluation of cerium based nanofuel has been discussed in this chapter. A brief review covering various applications of PRBs, ranging from industry to domestic sectors and patents associates with PRB have been also provided. The chapter ends with the concluding remarks of the literature review and present the aims of the PhD thesis.

Chapter 3 encompasses the detailed descriptions of the various experimental tools and measurement techniques that are relevant for the present work. The formulations used for the calculations of different parameters are also discussed.

Chapter 4 presents the different configurations of self-aspirated domestic pressure kerosene cooking stove with PRB and the arrangement of air entertainment in PRB.

Chapter 5 presents the development of ceria-based nano fuel, which is tested in the developed self-aspirated pressurised kerosene cooking stove with PRB for domestic cooking applications for the input power of 1.5 kW. This chapter also discusses the different methods of preparation of nanoparticle and nano fuel.

Chapter 6 discuss about the thermal performance of self-aspirated PRB in terms of thermal efficiency, emissions and temperature profile for the input power range of 1.5 – 3 kW. Comparative analysis of thermal performance have been also done between the PRB and conventional kerosene stove. Chapter 6 also presents the effect of environmental temperature on the thermal efficiency of PRB and conventional stoves.

Chapter 7 presents comparative analysis of thermal performance between the pressure kerosene stove with PRB and conventional pressure kerosene stove with and without nanofuel. The effect of the environmental temperature on thermal efficiency of kerosene stove with PRB and conventional kerosene stove with nano fuel is also presented. Conclusions and scope of future work are presented in Chapter 8.

Chapter 2

State-of-the-Art

In this chapter, an extensive literature survey on the initial developments of porous medium combustion that lead to the establishment of the technology for different applications have been presented. The experimental and numerical investigations on flame stability, emission characteristics, and radiation output of porous medium combustion carried out by different researchers are discussed. Research works done on porous surface burners are also discussed. The various applications of Porous Radiant Burner (PRB) are discussed in detail. The objectives of the thesis are presented at the end of this chapter followed by the closure of the literature survey.

2.1 Introduction

Combustion is an ancient technology of humankind and it has wide range of applications such as cooking, heating and cooling, generation of mechanical power, production of electrical energy, etc. Fossil fuel provides majority of energy requirements, nevertheless, the frequent application of fossil fuels creates a crucial menace to the civilisation due to the increased emissions of CO, NO_x, unburned hydrocarbon and other harmful gases. Prodigious use of fossil fuel poses fast depletion in fossil fuel resources. Due to the emissions of harmful gases from the combustion creates a situation of Global warming and climate change, which has become a serious issue (Hansen *et al*., 2016). Over a decade, policy makers and researchers have been working on the development energy efficient combustion device, which are not only produces low emissions but also provide high conversion efficiency. Nowadays the substitute technology has gained more importance

and reducing the harmful gases emissions like green house by means of improved combustion device has been a high priority research topic.

Porous media combustion (PMC) is a novel concept that gained substantial attention because it deals with multifaceted benefits as compared to traditional combustion technology functioning on free-flame method. Two types of combustion may take place in PMC, matrix stabilized combustion (flame trapped in porous matrix) or surface stabilized combustion (flame appears on surface of porous media) that depends upon the working conditions which has been shown in Figure 2.1(a) and 2.1(b) (Marbach *et al.*, 2003).

For understanding the behaviour of flame during combustion a comprehensive literature review have been done. Deportment of the flame in either type, and the matrix stabilized combustion have gained great attention due to their extended flammability limit, higher firing rate operation, silent operation etc. (Mital *et al.*, 1997). The fundamental studies on matrix stabilized combustion reported during 1985- 1999 (Mital *et al.*, 1997; Takeno *et al.*, 1986; Echigo *et al.*, 1991; Chen *et al.*, 1987; Viskanta, 1995; Yoshio *et al.*, 1988; Sathe *et al.*, 1991; Hsu *et al.*, 1993; Min *et al.*, 1991; Echigo, 1982; Echigo *et al.*, 1986) and the concept of matrix stabilized combustion are now more understood.

In the late eighties and early nineties, scientists and experts were more concentrated about the heat transfer and combustion behaviour within the PM. It has been observed that at the starting of the 21st century, the attention was shifted towards the understanding of stabilization mechanism and burner development for practical applications (Leonardi *et al.*, 2002; Avdic, 2004; Echigo, 1984; Fleming, 1987; Barra *et al.*, 2004; Mishra *et al.*, 2006; Mathis *et al.*, 2003; Leonardi *et al.*, 2003; Talukdar *et al.*, 2004). Major developments occurred during last five years because there have been lot of studies reported on porous burner in context of practical aspect with gaseous and liquid fuels. The recent focus is

shifted towards the development of porous radiant burners for domestic cooking applications (Mujeebu *et al.*, 2011; Mujeebu *et al.*, 2013; Pantangi *et al.*, 2007; Pantangi *et al.*, 2011; Muthukumar *et al.*, 2011; Muthukumar and Shyamkumar, 2013; Kakati *et al.*, 2007; Sharma *et al.*, 2009; Sharma *et al.*, 2011; Mishra *et al.*, 2015).

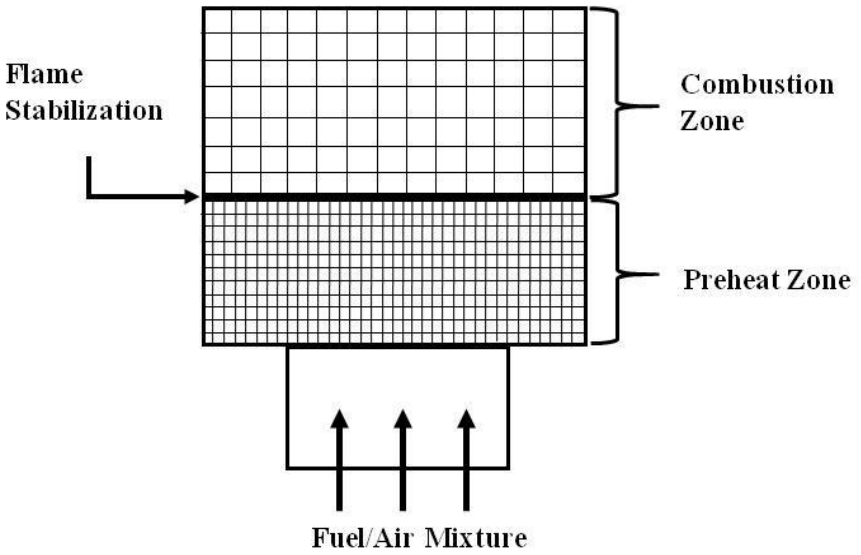

(a)

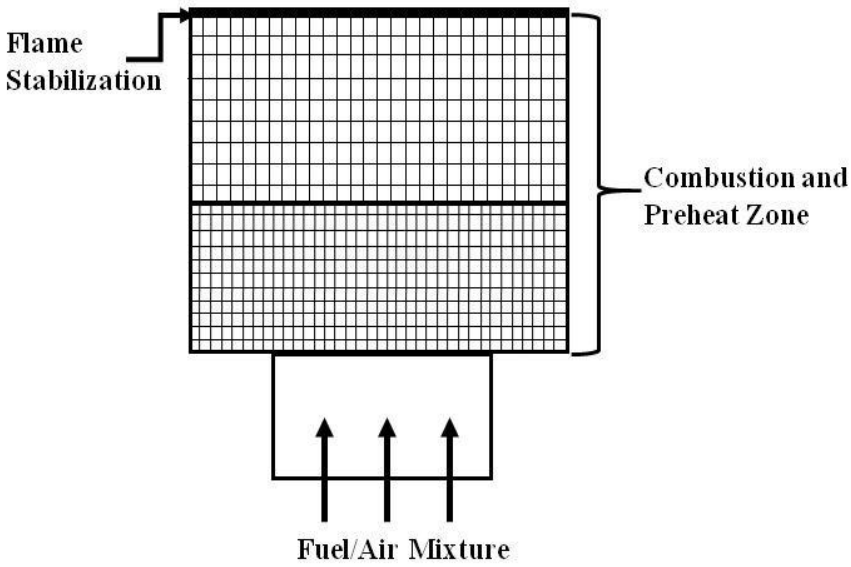

(b)

Fig. 2.1: Porous burner (a) matrix stabilized (b) surface stabilized (Marbach and Agrawal, 2005).

In early 2000, commercial or high wattage scale burners developed and the centre of attention also given to application of liquid fuels (Durst *et al.,* 1997; Vijayakant and Agrawal, 2006; Takami *et al.,* 1998; Jugjai *et al.,* 2002; Jugjai and Polmart, 2003; Trimis *et al.,* 2001; Fuse *et al.,* 2003; Fuse *et al.,* 2005; Jugjai and Phothiya, 2007; Wei *et al.,* 2002; Vijayakant and Agrawal, 2007).

A number of researchers have also reviewed the progress of PMC technology over the different point of stage (Howell *et al.,* 1996; Mujeebu *et al.,* 2009a; Mujeebu *et al.,* 2010; Malico and Mujeebu, 2015; Surange *et al.,* 2014). Howell *et al.* (1996) first studied experimentally, the combustion behaviour of gaseous and liquid fuels in different porous media. Wood and Harris (2008) sketch out the investigation on lean methane combustion in PRB. Not long ago, Malico and Mujeebu (2015) have drafted the possible application of PMC for domestic burners. Various developments in PMC have been recorded till 2010, but after this period no report excluding Surange *et al.*(2014) who discussed the performance evaluation of few domestic burner. The performances of the newly developed burners were assessed in terms of efficiency and emissions.

The literature review has been arranged in following manner. First, introduction and development of various stoves have been discussed then principle of PMC has been discussed, followed by a brief introduction to the material and its latest development. Next, the flame stabilization techniques in line to the fundamental studies on radiation performance of the burners are highlighted. Following this, various burners and their performances in terms of efficiency and pollutant emission are discussed. After this, some recent patents in the area of PMC are presented and in the last, study on nanofuel has been reviewed. Summary of the literature survey is provided at the end.

2.2 History of Kerosene Pressure Stove

The first kerosene pressure stove was developed in 1892 by a Swedish researchers named Frans Wilhelm Lidqvist (Primus stove, Wikipedia, 2010). The stove was known as the primus stove. This stove has gained popularity since its early days, as it was found reliable and durable in everyday use and also under adverse conditions. In yesteryears, a number of similarly-designed stoves of different models and sizes were built and commercialized. The modern kerosene pressure stoves are basically the modified version of the primus stove.

The first model of the primus stove (Figure 2.2) consisted of a fuel tank with a hand operated plunger, a spirit cup and a burner. A steel ring was provided on the top of the burner for supporting cooking vessel.

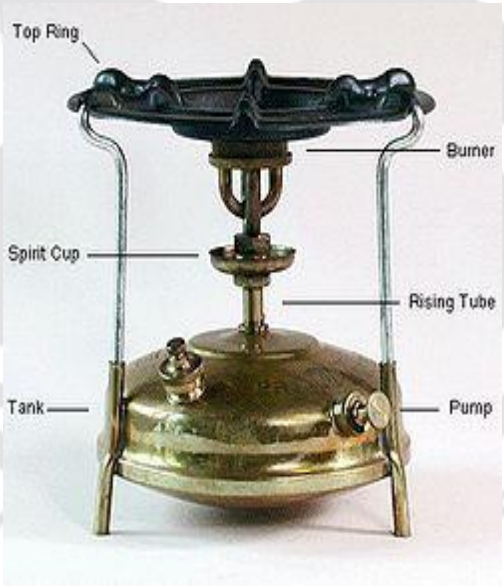

Fig. 2.2: Picture of a primus stove and its various components (Primus stove, Wikipedia, 2010).

In primus stove, the burner is an assembly of two ascending and two descending tubes with a flat circular chamber at the top called burner head. The lower portions of the ascending tubes are connected to another tube called rising tube which on the other end is connected to the pressure tank as discussed in Figure 1.1. A spray nozzle is provided in between the

two descending tubes. The operation of the stove is as follows. Initially, a small amount of alcohol poured in the spirit cup, provided in between the rising tube and the ascending and descending tubes, is ignited with the help of a burning wick. Once heated, the fuel tank is pressurized by means of the hand operated plunger and the pressure forces kerosene from the tank up through the rising tube and the ascending tubes to the pre-heated burner head. The burner head receives the heat from the spirit cup through convection and the kerosene receives heat from it on its way through the ascending tubes and gets converted to vapour. The kerosene vapour is then forced under pressure through the descending tubes and is sprayed through the nozzle, where it mixes with air and burns. The burner head then receives heat from the kerosene/air flame and the alcohol flame at the spirit cup is put off. Thus, the vaporization and combustion cycle continues during the cooking process.

The basic designs of the modern primus-style stoves are same as the older version. They are operated in a similar way. However, there are constructional differences between the earlier and the latter versions. Figure 2.3 shows the schematic of a kerosene pressure stove available in the market. In this, the fuel tank is not just below the burner but little away. For easy cleaning, the tank is made detachable. The dimensions of the burners are also different; the new burner is well optimized for higher thermal efficiency. Prior to the invention of the primus stove, the kerosene stoves were constructed in the same manner as the oil lamps, which use a wick to draw fuel from the tank to the burner. These stoves are known as wick stoves and are still very popular due to its easy construction and low initial cost. But these stoves produce soot due to incomplete combustion. The primus stove's design, which uses pressure and heat to vaporize kerosene before ignition, results in efficient combustion, leading to relatively lower emissions of CO. The reports on emission measurement of the primus stove are, however, limited, although there have been ample reports on efficiency measurements (Thukral and Bhandari, 1994; Jungbluth *et al.*, 1997; Pohekar *et al.*, 2005).

In the Indian context, emission characteristics of the primus stove have been reported by Zhang *et al.*, 1999; Smith *et al.*, 2000; and Kakati *et al.*, 2007.

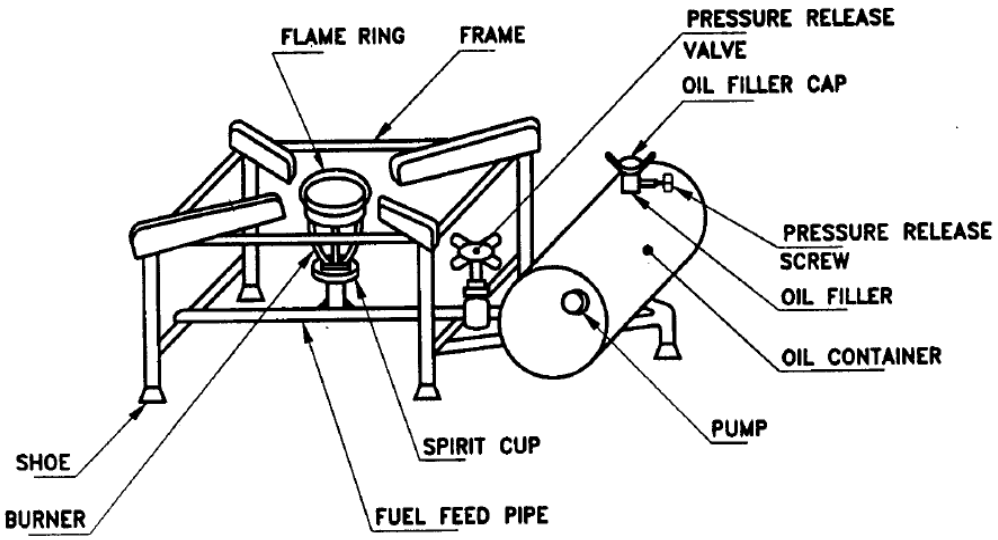

Fig. 2.3: Schematic of a BIS specified kerosene pressure stove (IS: 10109, 2002).

Zhang *et al.* (1999) measured the CO emission from different kinds of stoves available in the Indian market, and they found that the CO emissions from the kerosene stoves were higher than the LPG stoves. Kakati *et al.* (2007) examined the CO emission characteristics of a conventional BIS pressure stove and also of a stove incorporated with a PM. They found that the PM incorporated stove exhibited better thermal performance over the conventional counterpart due to improved heat transfer. In recent times, the use of PM has been prevalent in many other thermal systems as outlined in Chapter 1.

2.3 Principle of PMC

The combustion in PM makes use of a porous solid matrix wherein fuel and air are entered and they are ignited using a pilot flame. Once the heat of combustion is released, a premixed or diffusion (non-premixed) flame is enveloped within the matrix and it got stabilized at a particular location depending on the operating conditions (Marbach and Agrawal, 2003;

Marbach *et al.*, 2007; Nakamura *et al.*, 1993). The chemical enthalpy of gas is then absorbed by the solid and the media becomes radiatively participating. The PM being highly conductive starts transferring heat through conduction too to the upstream and the large surface area of it makes convective heat transfer sufficiently large. The incoming air fuel mixture is thus preheated with the recirculated heat coming though the combined modes of radiation, conduction and convection. Figure 2.4(a)-(b) shows the heat transfer mechanisms of CB and PRB respectively.

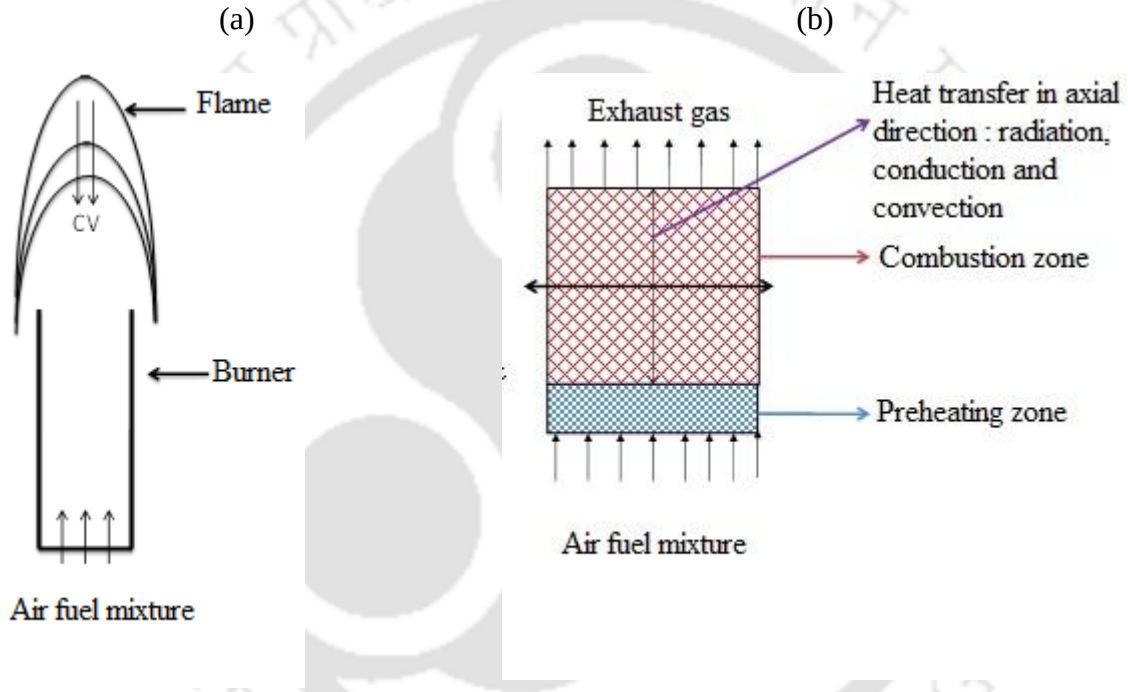

Fig.2.4: (a) Convection dominated free-flame in CB (b) radiation dominated PRB (Sharma *et al.*, 2016).

As illustrated in Figure 2.4, PRB involves better heat recirculation mechanism than CB due to the contribution of three heat transfer mechanisms making the reaction zone widen and the temperature gradient lesser. The excess enthalpy flame defined as the flame whose temperature higher than the adiabatic temperature and it happens due the effect of recuperation (absorption of net energy from burned gases to the unburnt mixture) (Weinberg, 1971). There have been numerous records where the characteristic of the excess

enthalpy flame is described in detail (Nakamura *et al.*, 1993; Sharma *et al.*, 2016; Weinberg, 1971). Hardesty and Weinberg (1973) exposed theoretically that the flammability limits get extended more than those for a conventional flame and this happens due to excess enthalpy combustion and this allows leaner mixture to be burnt suitably with reduced CO emissions. Flame situations and the flammability limit also depends on Burner types and operating conditions.

2.4 Porous Radiant Burner Type: Single-layered, Double-layered

A PRB can be made of a single material having high porosity (void fraction), or it can be made of two different materials having different porosities and thermo-physical, radiative properties. The former is known as single-layered and the latter as double-layered burner. A double-layered burner consists of two distinct zones: preheating zone and combustion zone, and the interface of the two zones serves as a flame holder (Viskanta, 1995; Barra and Ellzey, 2004; Trimis and Durst, 1996). Figure 2.5 (a) and 2.5 (b) shows the schematic of a single and a double layered burner. In the recent times, applications of double-layered burner have received more fame due to its better flame stability compared to single-layered burner (Hsu *et al.*, 1993). Nevertheless, flame position remarkably depends on material characteristic and porosity (Trimis and Durst, 1996; Malico and Pereira, 2001; Kulkarni and Peck, 1996). Malico and Pereira (2001) through their numerical studies showed the importance of thermal radiation and radiative properties such as extinction coefficient, scattering albedo, optical thickness etc. on the flame stabilization.

Research have revealed that the preheating zone of the burner should be thinner and have low porosity, low thermal conductivity, low volumetric heat transfer coefficient, large albedo, short optical path length, high optical thickness and high radiative extinction coefficient so as to prevent possibility of ignition and flame propagation thereby occurrence

of flashback (Barra and Ellzey, 2004; Kulkarni and Peck, 1996; Barra *et al.*, 2003). While combustion zone supporting flame propagation and heat recirculation to the preheating zone should have high conductivity, high volumetric heat transfer coefficient, intermediate extinction coefficient and non-scattering. Porosity decides the optical and thermal properties such as optical thickness, extinction coefficient, heat transfer coefficient, thermal conductivity etc. The porous bed can be of same material with different pore sizes (Bubnovich *et al.*, 2006) or can be of two different materials (Mital., 1997; Pantangi *et al.*, 2007; Mishra *et al.*, 2015).

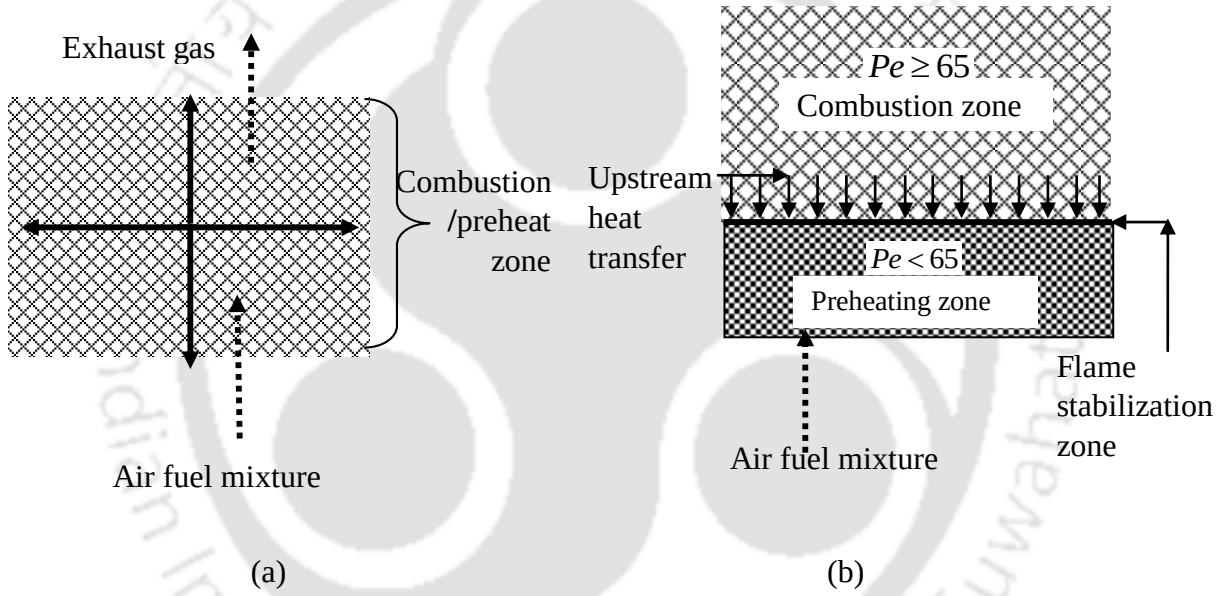

Fig. 2.5: Schematic of (a) single layered (b) double layered PRB.

Babkin *et al.* (1991) gave the stabilization criteria through Peclet number. They showed that the stability of the hydrocarbon flame in a double-layered burner as a function of Peclet number (*Pe*: ratio of heat flow by convection transport to heat flow by conduction), based on the mean pore diameter. They proposed the following limiting condition for the flame to propagate.

$$Pe \geq 65$$

$$\text{where,} \quad Pe = \frac{S_L d_m c_p \rho}{k}$$

Any burner possesses *Pe* greater than 65 or equal would allow flame to propagate and thus the combustion zone of the burner should be constructed in such a way that the *Pe* in this region should be greater than 65 and the preheating zone should be below 65 (Babkin *et al.*, 1991). For Hydrogen flame (H_2), however the limit was found to be 37 by Dillon (1999). A careful selection of the pore diameter and thermal conductivities of the two zones allows the flame to stabilize at the interface of the two zones and upstream zone (preheat zone) to receive the heat. The size of the pores in this region should be small to enough to quench the flame and eliminate flashback while the pores in the downstream section should be large enough to allow significant thermal feedback to the reactants.

2.5 Materials and Properties of Porous Media

Porous media with certain specific characteristics such as high thermal and chemical stress resistance, large inner surface area, good heat transport properties, high heat capacity etc. are found suitable for combustion applications, and Aluminium oxide (Al_2O_3), Silicon carbide (SiC), Zirconium dioxide/Zirconia (ZrO_2), Mullite, Cordierite, metal etc. are the collection of ceramics which meet the requirements(Weclas, 2005; Mößbauer *et al.*, 2002; Pickenäcker *et al.*, 1999; Cookson *et al.*, 2007; Tong and Li, 1995). Metallic materials such as stainless steel, Fe-Cr alloy (nickel-iron chromium) etc. are also found suitable (Dhamrat and Ellzey, 2006; Bakry, 2008; Krittacom and Kamiuto, 2009; Yu *et al.*, 2013; Gao *et al.*, 2014). However, due to their inadequate thermal stability at high temperature, and high thermal inertia, ceramics are largely preferred (Gao *et al.*, 2014). The notable benefits of ceramics are high melting temperature, high oxidation resistance, high permeability and superior creep resistance (Tiwari *et al.*, 2016). Table 2.1 enlists a few important thermal and radiative properties of the commonly used ceramics. Ceramics are available in different forms: reticulated foams, honeycomb, lamellae, pebbles, balls etc. (as shown in Figure 2.6), and due to certain advantages, such as better gas mixing, higher porosity, lesser pressure

Table 2.1: Ceramic material properties (Hsu *et al.*, 1993; Pickenäcker *et al.*, 1999; Gao *et al.*, 2014; Hale and Bohn, 1993; Orenstein and Green, 1992; Delalic *et al.*, 2004; Younis and Viskanta, 1993; Hendricks and Howell, 1996; Djordjevic et al., 2012).

Material		A	B	C	D	E	F	G	H	I
Maximum allowable temperature in air (^oC)		1600	1900	1800	1400-1750	1380	1700			
Thermal conductivity (W/mK)		20-50	5-6	2-4	40-120	110-160	80-145	2.6	0.37	
		at (1000 ^oC)			at (20-100 ^oC)					
Total emissivity at 2000K		0.9	0.28	0.31	-	-	-			
Thermal expansion coefficient from 20-1000 ^oC (10^{-6} K^{-1})		4-5	8	10-13	-		-			
Heat capacity (25-800 ^oC) (kJ/kgK)		-	1.05	0.59	0.84	0.84	0.84	0.80		
Optical thickness	10 ppi 65 ppi			28.2 300						
Scattering albedo	10 ppi	0.55-0.88		0.87-0.99		0.7		0.76	0.84	
Extinction coefficient (m^{-1})	10 ppi 20 ppi 25 ppi 30 ppi	234.1 468.1 585.2 702.2	210 300	234.1	100	178 244		270	202	23 4.1

* SSiC: sintered silicon carbide; * SiSiC: silicon infiltrated silicon carbide; * HPSiC: hot pressed infiltrated silicon carbide

(A). SiC: Silicon carbide; (B). Al_2O_3: Aluminium oxide; (C). ZrO_2: Zirconium dioxide/Zirconia; (D). SSiC: sintered silicon carbide; (E). SiSiC: silicon infiltrated silicon carbide; (F). HPSiC: hot pressed infiltrated silicon carbide; (G). Cordierite; (H). Mullite; (I). FeCrAl: Fecralloy (nickel-iron chromium)

drop etc., foams are found to be largely employed (Gao *et al.*, 2012). However, they are prone to have larger damage on exposure to high temperature environment due to their rigid structures. On the other hand, the durability and heat capacities of discrete particles are better than the foams due to their small, robust shape (Gao *et al.*, 2012). Al_2O_3 is generally available in discrete shapes; balls, flakes, lamellae etc., while SiC, ZrO_2, Cordierite etc. comes in the form of foam. Honeycomb slabs and foam form of Al_2O_3 are not very common though they were used in a few studies, while balls (diameters ranging from 3-20 mm) have found wide usages (Gao *et al.*, 2014; Gao *et al*., 2012; Gao *et al.*, 2011; Gao *et al.*, 2013; Gao *et al.*, 2014; Yoksenakul and Jugjai, 2011; Arrieta and Amell, 2014). The most attractive features of Al_2O_3 are higher durability, larger allowable temperature rating, and higher chemically stability. While SiC and ZrO_2 have higher thermal conductivity, and this provides a good basis for them to be used in a double-layered burner with Al_2O_3 as one layer. Recently, a number of successful demonstrations have been reported where Al_2O_3 was used in upstream and SiC in the downstream to have a better flame stability due to the differences in conductivity values (Mujeebu *et al.*, 2011; Mishra *et al.*, 2015; Wongwatcharaphon *et al.*, 2013). However, porosity has larger impact on the effective thermal conductivity (accounting the combined effect of conduction and radiation) (Hsu and Howell, 1992; Fu *et al.*, 1998) and heat transfer coefficient (Younis and Viskanta., 1993; Fu *et al.*, 1998).

At a temperature of about 1000^{o}C, Hsu *et al.* (1992) reported the thermal conductivity of a 65 ppi PSZ to be 1.6 W/m-K, against 0.5 W/m-K for a 10 ppi PSZ (partially stabilized zirconia). A few researchers have predicted the effective thermal conductivities of other materials like Al_2O_3 and reticulated vitreous carbon etc. by developing conduction models and however the findings are still scarce considering different material having wide range of porosities (Zumbrunnen *et al.*, 1986; Singh and Kasana, 2004). Further, forms of material

also affect the conductivity and thereby affecting heat transfer and stability.

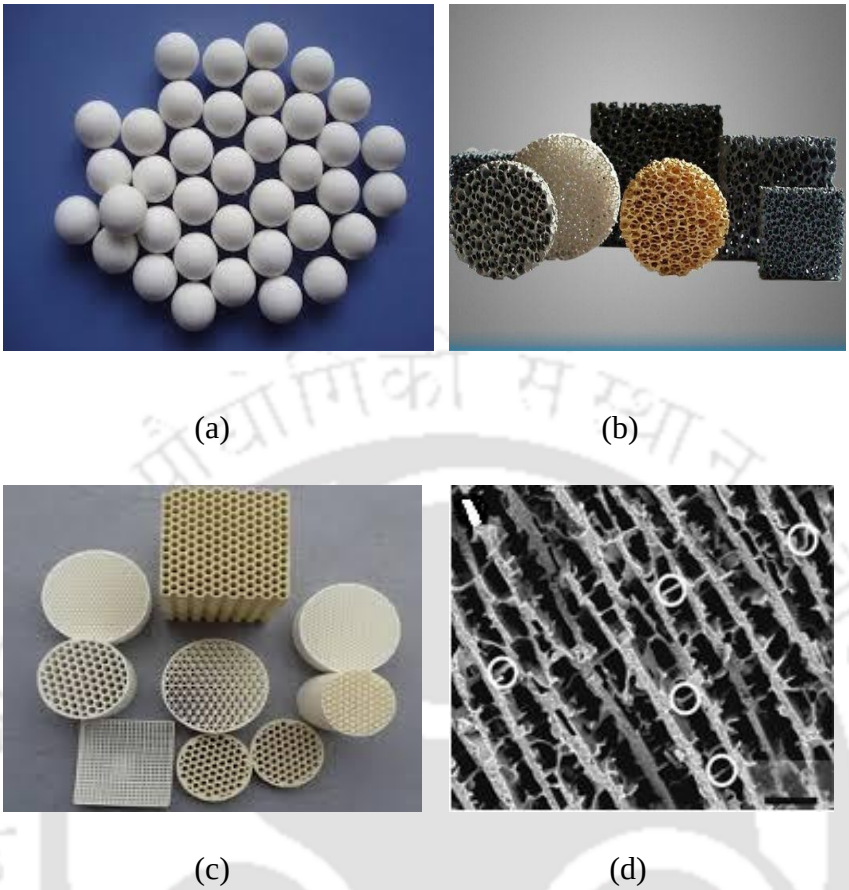

(a) (b)

(c) (d)

Fig. 2.6: Forms of porous structure (a) balls (b) foam (c) honeycomb (d) lamellae.

SiC has been found to have wide usage in the double-layered burner (Pantangi *et al.*, 2011; Muthukumar *et al.*, 2011; Mishra *et al.*, 2015; Gao *et al.*, 2014; Keramiotis *et al.*, 2012; Herrera *et al.*, 2015) followed by ZrO_2 either in pure or stabilized by other material such as magnesia or yttria (Mathis and Ellzey, 2003; Dhamrat and Ellzey, 2006; Gao *et al.*, 2014; Djordjevic *et al.*, 2012; Smucker and Ellzey, 2004; Ellzey and Goel, 1995). Avdic *et al.* (2010) used ZrO_2 foam in the preheating zone and Al_2O_3 lamellae in the combustion zone while in some studies ZrO_2 or SiC were used alone (Kaplan and Hall, 1995). The use of mullite and cordierite were limited (Mital *et al.*, 1997; Takami *et al.*, 1998; Yu *et al.*, 2013; Mital *et al.*, 1998; Abdelaal *et al.*, 2013). Cordierite exhibits higher extinction coefficient (Table 2.1) than SiC or Al_2O_3 having same pore density (expressed in terms of ppi: pores

per inch). Hendricks and Howell (1996) measured the transmittance and reflectance of PSZ and SiC having pore sizes of 10,20 ,66 ppi and found that SiC retained its properties at all wavelength; while PSZ showed a significant change, in the wavelength range 2500-3000 nm.

Summarizing the development of materials for PMC, it can be said that a variety of materials ranging from metal to ceramic are uncovered. Metal has lower temperature resistance while ceramics have received more attention due to its higher resistance to thermal and chemical shock. SiC and Al_2O_3 are observed to be used in large scale due to their easy availability better heat thermal and radiative properties and low cost (Pantangi *et al.*, 2011; Muthukumar *et al.*, 2011; Muthukumar and Shyamkumar, 2013). Double-layered burners are found to be constructed with Al_2O_3 – SiC or Al_2O_3 - ZrO_2 as a combination. Al_2O_3 is reported to be used mostly in the form of balls while other ceramics such as SiC, ZrO_2 as reticulated structure. Discrete particles (like balls, wires) are found to provide better stability at high temperature while reticulated ceramics provide good mixing of fuel and air.

2.6 Studies on Combustion Stability

2.6.1 Flame Speed Characterization and Flame Stabilization-Gaseous Fuel

Flame stabilization in a PRB is an important phenomenon and flame speed is found to be the key deciding factor affecting stability. In the recent years, many experimental and numerical studies were conducted towards its measurement and computing in different PM with different fuels (Yoshio *et al.*, 1988; Sathe *et al.*, 1991; Hsu *et al.*, 1993). The flame speed in a PM is much higher than the laminar flame speed of the same air-fuel mixture in a free space and it happens due to internal heat recirculation mechanism. This mechanism supports the stable combustion for a wide range of equivalence ratios (ratio of

stoichiometric air fuel ratio to actual air fuel ratio) and firing rates (Barra and Ellzey, 2004; Kotani *et al.,* 1985; Khanna *et al.,* 1994). Increase in air fuel ratio from leaner condition (equivalence ratio less than 1) results in higher flame speed; the peak occurs near stoichiometry and then it starts decreasing due to the higher radial heat loss through radiation. Flame can stabilize in two different sections of the PRB: adjacent to exit edge of the PM and in the interior upstream half of the medium. For a particular equivalence ratio and a range of firing rates, (Sathe *et al.,* 1991; Hsu *et al.,* 1993).

Barra and Ellzey (2004) examined the effective flame speed of a methane-air mixture for different equivalence ratios and reported that for the flame located within the upstream half of the porous solid (i.e. the interface of two different solids in a double-layered PRB), the effective flame speed was controlled by solid conduction as well as radiation. Further, at low equivalence ratio, conduction was found more important than radiation and the characteristics of the flame at low equivalence ratios were stated to be primarily determined by the properties of the upstream material. Figure. 2.7 shows the variations of flame speed ratio with equivalence ratio, and Figure. 2.8 compares the heat recirculation efficiency, conduction efficiency and radiation efficiency of a methane-air mixture at three different equivalence ratios (0.55, 0.65, and 0.90).

It is observed from Figure 2.7 that the change in equivalence ratio was found to affect the critical flame speeds. The lower limit of the flame speed ratio (ratio of effective flame speed to the laminar flame speed) was found to decrease with increase in equivalence ratio due to the lower heat recirculation (~16-26% at an equivalence ratio of 0.55, unlike 5-13% at equivalence ratio 0.90) while the upper limit was found to decrease slightly and then rise.

Liu and Hsieh (2004) however ruled out the existence of two critical flame speeds against a particular equivalence ratio.

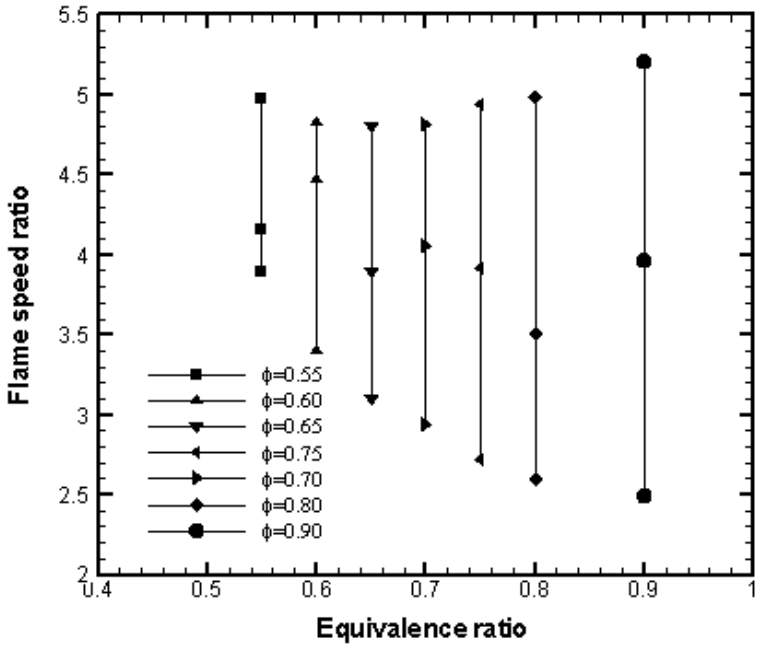

Fig. 2.7: Variation of flame speed ratio as a function of equivalence ratio (Barra and Ellzey, 2004).

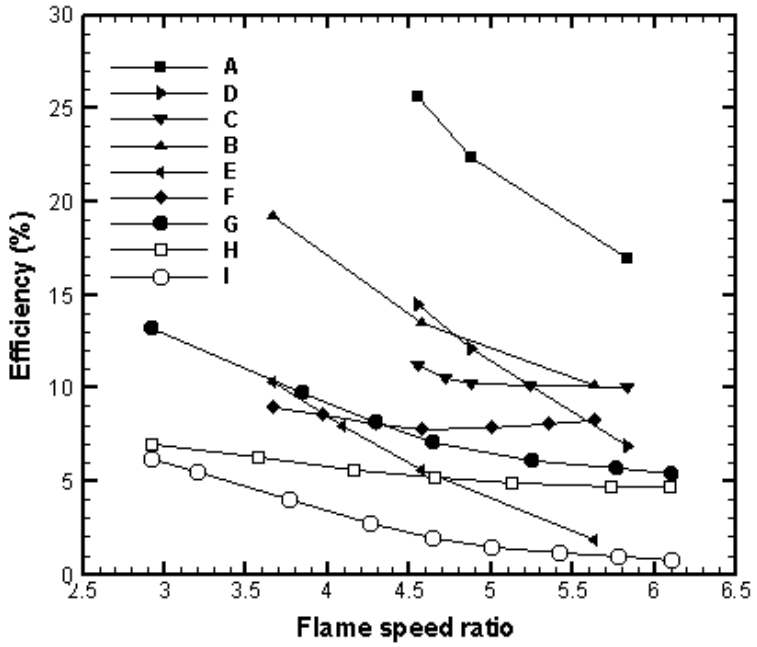

Fig. 2.8: Variations of heat recirculation, preheat conduction and preheat radiant efficiencies with flame speed ratio (Barra and Ellzey, 2004).

A: Heat Recirculation Efficiency, ϕ= 0.55; B: Preheat Conduction Efficiency, ϕ =0.55; C: Preheat Radiant Efficiency, ϕ =0.55; D: Heat Recirculation Efficiency, ϕ= 0.65; E: Preheat

Conduction Efficiency, ϕ =0.65; F: Preheat Radiant Efficiency, ϕ =0.65; G: Heat Recirculation Efficiency, ϕ= 0.90; H: Preheat Conduction Efficiency, ϕ =0.90; I: Preheat Radiant Efficiency, ϕ =0.90

In their study with PRB fired with LPG and embedded cooling tubes, and stated that the combustion with cooling tube was significantly different from the combustion without cooling tube. It is because in the system with cooling tube due to the intense heat removal process, a unique phenomenon metastable combustion occurs and it drives to maintain stable combustion against a single flame speed (higher than the laminar flame speed) at a particular equivalence ratio.

Higher flame speed in the PRB is found beneficial to support stable combustion for an increased range of firing rates (Mathis and Ellzey, 2003). However, the increasing firing rate results in a condition that the rate at which the unburnt mixture is supplied to the combustion zones exceeds the rate at which the mixture can be consumed and that causes reaction zone to move downstream until a match between the two rates is re-established.

After a critical limit, the flame speed experience a nonlinear enhancement due to the increase in radiative and conductive heat feedback rate, and a particular equivalence ratio, the flame comes back to the upstream until a balance between the two rates is established again. Thus, the excessive increase in heat feedback results in flashback, a condition where flame travels to the farthest upstream of the PM affecting stabilization. The stable operating range i.e., without flash back or blow off (a condition where flame travels to the downstream) is different for different fuels and burner materials.

A balance among the heat release, heat recirculation and heat losses results in stabilization at a particular location, and it is guided by different factors viz., thermo-physical properties of the solid, fluids, porosity, convective heat transfer coefficient between the solid and

fluid, geometry of PM etc. (Mital *et al.*, 1997; Du and Xie, 2006; Di Mare *et al.*, 2000). Any changes in operating conditions or material type make the flame to propagate either upstream or downstream. Adjustment of porosity brings stabilization of the flame within the media through a balance between the chemical reaction rate and two phase energy transfer rate. Pore size has large influence; effective flame speed is lower for small pore materials than the larger pore, and highest flame speed is recorded for the flame located at the centre of the burner (Tseng and Howell, 1996). Qiu *et al.* (2006) reported that the gas velocity increases by a factor of 1/porosity of the solid matrix. Yoshio *et al.* (1988) demonstrated the importance of radiative properties in determining temperature profile and flame speed.

The radiative properties of the media are largely affected by the materials' porosity and so the amount of heat recirculation and radiative preheating (Yoshio *et al.*, 1988). Hsu *et al.* (1993) experimentally demonstrated that the variation of flame speeds in double-layered PRB by varying pore sizes is an effective means of stabilizing the flame at the interface of the two layers. Kaplan and Hall (1995) described two possible means for better stability offered by two different pore sized materials (i) change in optical path lengths (upstream: 0.8 versus downstream: 1.5 μm) causing reduction of flame speed and (ii) low turbulence intensity at in small pore material and hence lower flame speed attributing stabilization.

Hsu *et al.* (1993) studied the influence of pore size on the stability of methane-air combustion in a PSZ burner comprised of 65 ppi preheat zone and 10, 30 and 45 ppi combustion zone. It was revealed that the smaller combustion zone pore size allows flashback to occur at higher burning rates that with a burner with larger pore size. Higher back scattering to the preheat region with smaller pore material resulted in higher flame temperature or higher burning rate in the preheat zone. The lean limit (complete extinguishment of the flame) for the 10, 30 and 45 ppi were found at the equivalence ratio

of 0.41, 0.44, and 0.51 respectively, and they are lower than the lean limit for the free flame that occurs at the equivalence ratio of ~0.52.

Djordevic *et al.* (2012) studied the combustion of natural gas-air mixture in burners made of Al_2O_3 and SiSiC with pore densities 10 and 20 ppi in the combustion zone 45 ppi PSZ in the preheat zone and reported similar observation as that of (Hsu *et al.*, 1993) that flame stability decreases with increase in pore size. Further, they observed that SiSiC burner exhibited more effective flame stabilization than the Al_2O_3 burner and it was reported to be attributed to better heat transport properties of SiSiC. Similar finding was reported by Xiong *et al.* (1995) who studied the combustion of natural gas-air mixture in PRB made of SiC and Al_2O_3 and found SiC as a more promising candidate as the flame in the SiC bed was stabilized over a wide range of excess air than the Al_2O_3 bed. Gao *et al.* (2012) later reported that the stable operating region enlarges with increase in Al_2O_3 diameter due to a better control on flame speed.

Mital *et al.* (1997) studied the stability range of methane-air combustion inside a double-layered burner consists of 66 ppi cordierite in the preheat zone and 20 ppi cordierite in the combustion zone at a thermal load of 150-475 kW/m^2 and equivalence ratio 0.70-0.95. They found the lift off phenomena occurred at an equivalence ratio range of 0.6-0.7 and lean limit at an equivalence ratio of 0.5-0.6. Flash back was observed near stoichiometry but at the higher thermal load (higher than 300 kW/m^2) attributing to higher heat recirculation resulting in higher preheating of the incoming air-fuel mixture. However, they had not quantified the amount of recirculated heat and its role with respect to pore density.

Smucker and Ellzey (2004) investigated a double layered PRB made of yttria stabilized zirconia (YSZ) with propane-air and methane-air mixtures and observed that the stable operating limits in terms of firing rate followed similar patterns for both propane and

methane. In each case, both the upper and lower stability limits were increased with the increasing equivalence ratio and the increase of upper limit was sharper than the lower limit. Min and Shin (1991) investigated the stability characteristics of propane-air flame in cordierite and reported the equivalence ratios corresponding to lean limit and flashback to be 0.49 and 0.66 respectively.

Mathis and Ellzey (2003) studied flame stabilization phenomena of methane-air combustion in two separate but identical burners (60 ppi preheat zone, 10 ppi combustion zone) made up of zirconia/alumina composite (YZA) and zirconia-toughened mullite (ZTM) and reported that material of the solid matrix has strong influence on flame stability. They found YSZ a better candidate to offer higher stability than ZTM (for the same equivalence ratio: 0.65 flash back was observed in ZTM with higher upstream temperature). However, the reason behind the better stabilization in YSZ was stated to be not explained due to the lack of knowledge on property of the media. Further, there was no report of ZTM stability at a lower thermal load (~313 kW/m^2) like YSZ though flash back was likely to be occurred only beyond a critical firing rate.

For the PRB, the accountability of equivalence ratio and firing rates are so high that any change in either of the two results in changes in combustion mode (Cho *et al.,* 2001; Colorado *et al.,* 2015). Qiu and Hayden (2006) who studied the combustion characteristics of natural gas-air mixture in a micro-porous (10 μm) ceramic fibre felt (Yb_2O_3:93.5 wt. % and CeO_2:3.0 wt. % with minor additives as hardening agents) burner reported that when the firing rate exceeded a particular range, the combustion had shifted from the radiant to the convective mode and there was a substantial decrease in the downstream surface temperature. The upper limit of the radiant mode of operation of the PRB was reported to be controlled by the balance between flame speed and the gas mixture velocity. Stability

was found to be increased with air preheating (preheating temperature: 550°C) and stable flame was observed over a wide range of firing rates at a low level of excess air.

Gao *et al.* (2011) studied biogas (composed of CH_4 and CO_2) air combustion in an Al_2O_3 PRB with varying CO_2 compositions and reported that in comparison to methane, the range biogas equivalence ratios for stable flame moved to a higher level, and the biogas stable flame speed was lower. The upper and lower limits of the biogas were found to be in the equivalence ratio range of 0.75-0.95 and 0.8-0.95, against CO_2 concentrations of 25-35 and 40%, respectively. While for methane, the same limit is between 0.55-0.70. The upper stability limits and the stable flame region was found to be decreased with increasing CO_2 concentrations. For about 15% increase in CO_2 concentrations in the biogas was observed to lead to ~60% decrease in flame speed. Later they (Gao *et al.*, 2013) examined the effects of three different diluents (CO_2, N_2, and Ar) on combination with pure CH_4 on flame stability and reported that the CO_2 dilution induced lower flame stability limits than the N_2 and Ar dilutions because of the larger heat capacity of CO_2 dilution and its dissociation. Francisco *et al.* (2009) studied the combustion of H_2 gaseous fuels and reported that the laminar flame speed increases with increase in H_2 content.

In an another study, Gao *et al.* (2014) examined the stability limits of methane-air combustion in four different burners made of Al_2O_3, ZrO_2, SiC, and FeCrAl and reported that the flame stability limits expanded with increased foam conductivity or decreased pore density. The maximum stable velocity was found to be increased in the order of Al_2O_3, ZrO_2, SiC, and FeCrAl, and the minimum stable velocity was almost unchanged. The pore densities of SiC were however different (20, 25, and 30 ppi) than the other materials (10 ppi) and that might alter the conclusion. The same group of authors (Gao *et al.*, 2014) investigated the effect of foams of PM on stability and reported that the flame stability limits decreased in the order of foams (10 ppi), balls (13 mm bead), and honeycombs (200

cpsi; cell per square inch). It is however felt that the comparison does not hold well as the flow field created with 13 mm diameter ball and 10 ppi foams or 200 cspi honeycomb structure might not be similar.

Keramiotis *et al.* (2012) studied the combustion phenomena of CH_4-air and LPG-air in a PRB made of 10 ppi SiSiC foam in the downstream and Al_2O_3 in the upstream section. They varied the thermal load from 200 to 1000 kW/m^2 and excess air ratios (inverse of equivalence ratio) from 1.2-1.8, and reported that the stability was more affected by thermal load variation than the equivalence ratio. Further, they observed slightly higher temperature in LPG-air mixture than CH_4-air at all excess air ratio. The burner was found to provide a wide flexibility when operated at lean combustion regimes with excess air ratio higher than 1.2. Lammers and Goey (2003) identified equivalence ratio corresponding to flash back of CH_4-air mixture to be 0.8-1.0.

Krittacom and Kamiuto (2009) studied the stability limit of CH_4-air combustion in three types of Ni-Cr PRB having different pore densities (8.5, 21.5 and 39.5 ppi) and optical thicknesses (1.213, 2.828 and 6.523) and reported that the flash back limit of 8.5 ppi burner was ~0.54 and for the 21.5 and 39.5 ppi, the same were higher than 0.80. The observation is similar to the findings of Hsu *et al.* (1993) who concluded that the upstream porosity plays a significant role in flame stabilization. Bakry (2008) demonstrated that the flame stabilization technique in double-layered PRB (95% porosity) can be further improved by replacing the less porous material in the preheating by non-porous quenching parallel slots. In an another study, Bakry *et al.* (2011) studied the dependence of stable flame condition at higher temperature and pressure. They found that the lean blow-out limit was strongly affected by the preheating temperature of the mixture but nearly independent on pressure. Qui and Hayden (2009) reported another way of improving stability is through oxygen enrichment that eventually results in higher radiation output and efficiency.

2.6.2 Flame Stabilization Studies of Liquid Fuels

Flame stabilization of liquid fuels inside the PRB is more challenging than that of gases as it involves two important steps: vaporization and combustion, and each step has unique requirement of heat energy to proceed further. Inadequate vaporization gives rise to large droplet burning and higher emission of pollutants while combustion needs sufficient energy to be self-sustained and transfer heat for vaporization (Kayal and Chakravarty, 2006). Drop in temperature would promote condensation and coking of oil vapour (Trimis *et al.*, 2001). Vaporization mechanism has thus been an interesting area of research and ample emphasis has been given for the appropriate vaporizer design. In the early days of research however vaporization concepts were little complicated like the use of separate fuel flash vaporizer or the use of atomizer (Wei *et al.*, 2002; Kaplan and Hall, 1995) while the recent trend demonstrates the use of PM itself as a vaporizer (Takami *et al.*, 1998; Jugjai *et al.*, 2002; Jugjai and Polmart, 2003; Jugjai and Pongsai, 2007) besides supporting combustion. For practical application however the use of injector is still thought to be a better choice while literature reveals both the uses, and different fuels like heptane, kerosene, etc., are found to be explored.

To begin, Tseng and Howell (1996) studied the combustion of liquid heptane in a PRB made of PSZ (both preheat and the combustion zones) with pore densities 30 and 20 ppi respectively. Flash back and blow off limits were determined and flame speeds were estimated for a range of equivalence ratios (0.3-0.8). Flammability limit was found to be widened at the low flame speed, and flame was seen to be sustained at a very low equivalence ratio 0.3 with an average droplet diameter of about 10 μm. The stability was reported to be significantly influenced by the aerodynamic behaviour of air and fuel droplets. Takami *et al*. (1998) studied kerosene-air mixture in mullite PRB with porosity 36% and pore size is 180 μm. They reported that the mixture was flammable even at very

low flow rate of kerosene and low equivalence ratio 0.1. The concept of using PM as vaporizer was first demonstrated by them, and later Jugjai *et al.* (2002, 2003, 2007) have adopted and improvised the technique through a series of studies. The fundamental concept of PM as vaporizer is as follows. The fuel was supplied drop wise to the top surface the PRB instead of fine droplets and the PM was made sufficiently hot by an external source. While passing through the pores to the other side of the PM, the combustible mixture gets heated and vaporized. On mixing with air supplied from the wall of the combustion chambers, vapour gets burnt and after some time the process becomes self-sustained. The burning becomes then similar to gaseous combustion. Jugjai *et al.* (2002) examined the vaporizing behaviour of PM with the concept provided by Takami *et al.* (1998) and however they added a new component in their experimental setup i.e. a porous emitter, installed at the exit of the combustion chamber comprising steel wire mesh as PRB and swirl air supply ducts. They studied the evaporation mechanism and combustion characteristics of kerosene and reported that stable combustion was observed at a thermal load of 2.62-3.49 kW/m^2 and equivalence ratio of 0.37-0.55. Porous emitter was found to improve the downstream temperature and an optical thickness of 2.54 of the porous emitter was found optimal.

In an another study Jugjai and Polmart (2003) reported the use of Al_2O_3 balls as a porous emitter and probably (not mentioned) the same material as PRB, and studied the effect of air supply (three-way supply unlike single way in the previous study (Jugjai *et al.*, 2002), the bed height of the emitter and its installation distance on evaporation and combustion of kerosene. They observed more intense combustion at higher input throughout the cross section of the burner and attributed it to be the use of three-way air supply. The flammability regions were mapped for a wide range of equivalence ratios (0.2-0.6) and stability was found in effective. With the introduction of water coils and water jackets for extracting heat

from the porous emitter and however Jugjai and Phothiya (2007) found that range of equivalence ratio supporting stable combustion was narrower (0.4-0.60) while the lean limit was 0.50 against 0.60 (equivalence ratio) in the CB of similar wattage.

Fuse *et al.* (2003) studied kerosene in two different PRBs (Al_2O_3: 85 porosity with 6 cells per inch and 36% porosity with 20 cell/inch) with optical thickness (2.4 and 0.54) and kerosene was supplied from four corners and centre of the bottom of the fuel evaporating. The stable combustion range of 20 cells/inch plate was found to increase up to 1 kW to the lower load compared with 6 cells/inch ceramic plate at the same equivalence ratio. While the stable combustion region increased to 10 kW in 0.4-0.8 of equivalence ratio when 6 cells/inch ceramic was used. For high burning load operation therefore higher porosity ceramic is appropriate. Low porosity material functions as a radiative shield between the combustion and vaporization side. In another study, Fuse *et al.* (2005) investigated the combustion characteristics of ethanol in a PRB made of Al_2O_3 (75% porosity) and observed complete combustion in the equivalence ratio range of 0.63-0.80. Vaporization was initially carried out by ultrasonic irradiation, and later by backward radiation promoted by PM.

Periasamy *et al.* (2007) investigated the combustion characteristics of kerosene-air mixture and confirmed the fact that the use of PM is beneficial in distributing the fuel vapour-air mixture uniformly. They used SiC-coated carbon-carbon foam as the PM and the aviation-type kerosene as the fuel. Atomizer was used for spraying kerosene and it was first sprayed into a co-flowing, preheated air environment and the mixture then subsequently entered the PM. The minimum combustion heat feedback rate required for complete vaporization was measured and it was found to increase when the distance between the PM and the injector was decreased. Complete vaporization was achieved at a co-flow air temperature of 400 K. Further, they found that at an equivalence ratio of 0.3 and the combustion heat feedback rate of 1%, the average vapour concentrations was 63% (equivalence ratio 0.6) while the

same was 43% when there was no heat feedback. This finding is very important and a numerical study compliments the facts (Periasamy and Gollahalli, 2010). Later, the same authors (Periasamy and Gollahalli, 2011) studied the flame stability characteristics at the near lean extinction limit and reported that the PM was able to withstand the combustion continuously for 2 hours and the structural stability was maintained for ~100 hours.

2.7 Radiation Output/Efficiency

Radiation output of a PRB is the function of several parameters such as porosity, flame position, flame speed, equivalence ratio, firing rate etc. Sathe *et al.* (1991, 1989a, 1989b) computed flame speed and radiation output for the flame stabilized at different locations and suggested that maximum output can be obtained by stabilizing the flame at centre of the burner. Following this, Kulkarni and Peck (1996) through their theoretical study on a double-layered burner concluded that the radiative output of the burner can be improved by optimizing the burner properties, upstream and downstream of the flame. They examined the radiation output variations with upstream porosities (φ) and downstream porosities (φ_2) (as shown in Fig.2.9) and observed that the radiation output, efficiency, and flame speed peaked at a porosity level of the downstream section of 95-97% for all the values of upstream section porosities. Reduction of radiation output and efficiency at a very high value of downstream porosities was linked to lesser availability of solid to participate in radiative heat transfer while lower porosity material was described to act as a heat sink. Further, upstream porosity was found to have larger effect on radiation output and flame speed. Both radiant output and flame speed were found to rise with the reduction of upstream porosity due to higher conductive heat transfer.

Khanna *et al.* (1994; 1992) examined the radiation output of a PSZ burner with methane-air combustion at different equivalence ratios (0.6, 0.65, 0.70. 0.75, 0.8.0, 0.87) and

reported that radiation output increases with increase in flame speed or with firing rate and equivalence ratio. However, the increase of radiant emission was not as significant as that of the heat input and this result in lower radiation efficiency.

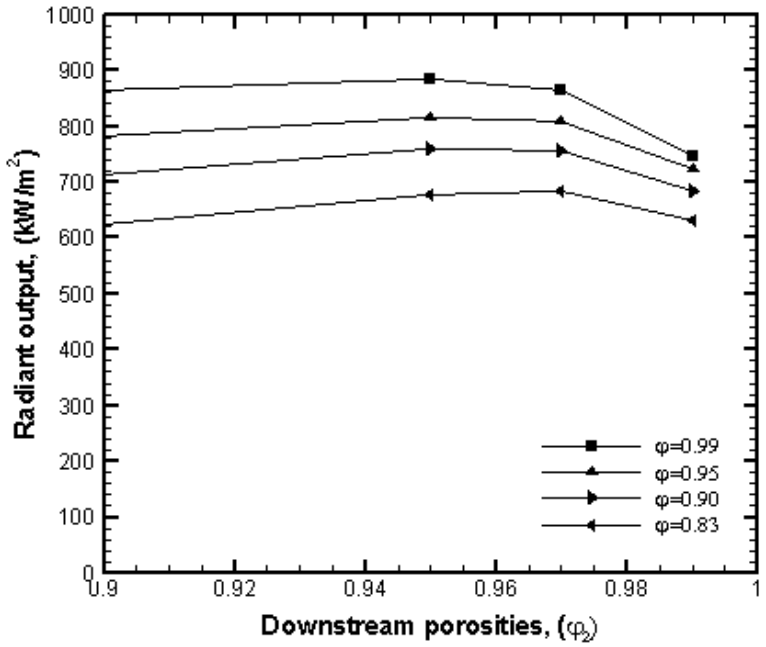

Fig. 2.9: Variations of radiation output with upstream and downstream porosities of PM (Kulkarni and Peck, 1996).

Similar observations that the efficiency decreases with increase in firing rat were reported by various other researchers such as Yoksenakul and Jugjai (2011), Bouma and Goey (1999) and Leonardi *et al.* (2003) etc. Williams *et al.* (1992) reported that the radiation efficiency increases with increase in equivalence ratios and then peaks somewhere near stoichiometry and then decreases (as shown in Fig. 2.10). Mital *et al.* (1998) observed similar trend with respect to firing rate, and Barra and Ellzey (2004) observed decreasing efficiencies with increase in equivalence ratio for a fixed flame speed ratio.

Measurements or computations of radiation efficiencies were also reported by a number of researchers for different burners. For instance, Yoksenakul and Jugjai (2011) conducted a theoretical study and reported the radiation efficiency of an Al_2O_3 PRB (ball diameter: 15

mm) at a firing rate range of 23-61 kW. They found at 23 kW, the efficiency was ~23% while the same was ~ 15% at 61 kW. Bouma and Goey (1999) observed ~33% efficiency at a thermal load of ~100 kW/m^2 against ~8% against the thermal load of ~600 kW/m^2.

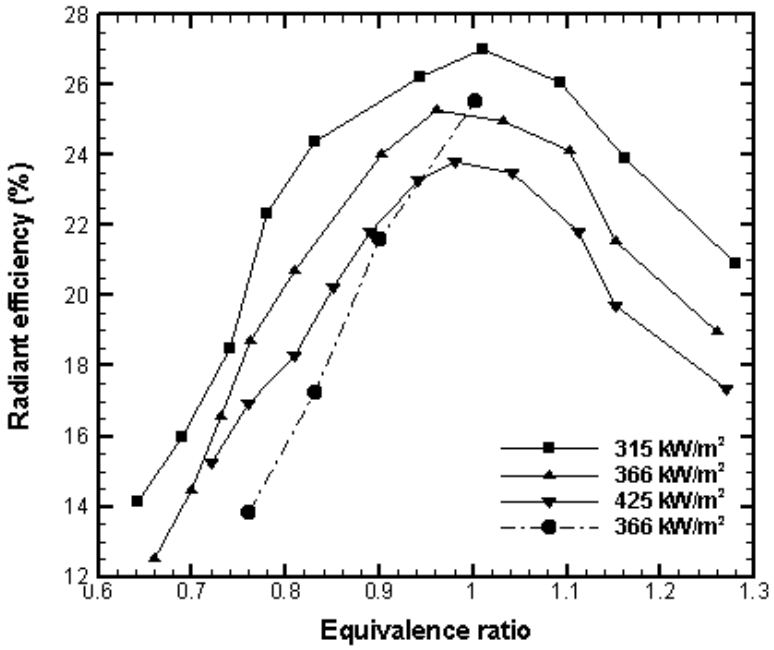

Fig. 2.10: Variations of radiant efficiency with equivalence ratio and thermal load (Williams *et al.*, 1992).

Qiu and Hayden (2006) measured the radiation efficiency as a function of firing rate for various combustion air temperatures (25 ^{o}C, 300 ^{o}C, and 550 ^{o}C) and reported that the radiation efficiency improves with air pre-heating. At a thermal load of ~ 190 kW/m^2, the radiation efficiency of the no-preheat case was found to be ~ 14 % and the same for the preheated temperature of 300 ^{o}C, 550 ^{o}C were 17 % and 19 % respectively. Further, they reported that the effect of firing rate was more prominent in the case of no-preheating case.

Wongwatcharaphon and Theinnoi (2013) predicted about ~10 % decrease in efficiency when the porosity of the combustor was increased from 40 % to 90%. Williams *et al.* (1992) on the other hand observed about 26 % efficiency at the same porosity level (~90%) in a surface burner operating at a thermal load of 315 kW/m^2 and equivalence ratio 1.0. Further,

they stated that operating the burner at an equivalence ratio higher than stoichiometric limit results in decrease in efficiency (as shown in Figure 2.10) and this could be the reason for obtaining low level of efficiencies in the study conducted by Yoksenakul and Jugjai (2011) as they operated the burner at an extremely high equivalence ratio (2.08). Further, they also studied the method vaporization kerosene.

Kulkarni and Peck (1996) reported that the radiant efficiency of the double-layered burner has not much influenced by upstream section's porosity, while for the single-layer burner efficiency dropped significantly with the reduction of porosity or increase of thermal conductivity (Sathe *et al.*, 1990). Mital *et al.* (1997) observed ~5% decrease in efficiency when pore density of the downstream section was varied from 10 to 20 ppi. Further, they observed that the length of the porous bed in the downstream section affects radiation efficiency to a large extend.

It is evident from Figure 2.11 that at lower thermal load (< 300 kW/m^2), the burner with a thicker (6.5 mm) downstream section has lower radiation efficiency than that of a thinner (3.2 mm) layer, while at higher firing rates, the trend reverses. Leonardi *et al.* (2002, 2003) has however observed higher efficiency in the case of 4 mm (double layer) thick downstream section compared with 2 mm (single layer). Mital *et al.* (1998) reported that the average radiative efficiencies of the cellular ceramic burner varied between 20-35 %. Table 2.2 compiles some efficiency data presented by various researchers for various firing rates and equivalence ratios.

It is evident from Table 2.2 that radiation efficiency was predicted out mostly for CH_4-air combustion and they were in the range of 20-25 %. With other fuels such as natural gas or LPG, the radiation efficiency values are on the lower side and difference might be attributed to differences in material, porosity, operating conditions or due to difference in fuel types.

Effect of combustion zone thickness on radiation efficiency (as shown in Fig. 2.11)			
Φ = 0.9	Combustion zone		Symbol
	Thickness, mm	ppc	
Preheat zone 26 ppc Thickness 19 mm	3.2	4	○
	6.5	4	◇
	3.2	8	△

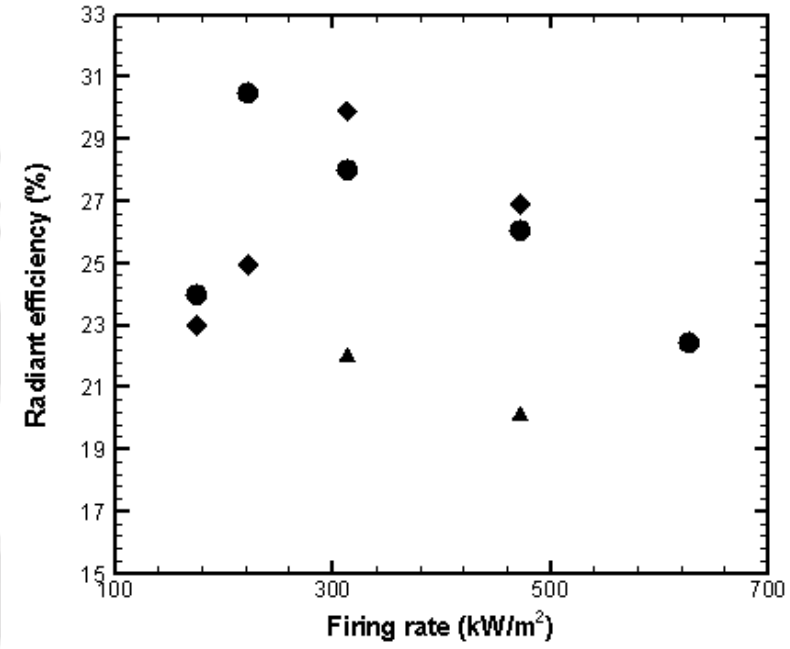

Fig. 2.11: Radiation efficiency as a function of firing rate and pore densities of combustion zone (Mital *et al.*, 1997).

Keramiotis *et al.* (2015) reported due to lower CO_2 concentration, biogas/syngas mixture demonstrated higher radiation efficiency than biogas alone. Due to the nonappearance of CO_2 unlike biogas Natural gas/syngas mixture 'showed the highest efficiency. CH_4-air mixture was little bit lower efficiency than the natural gas/syngas mixture. The maximum reported efficiency was ~65% and it was found for a thermal load of 200 kW/m^2. Gao *et al.* (2011) reported that radiation efficiency depends upon the CO_2 concentrations. For biogas-air combustion the radiation efficiency were in the range of 14-28%.

Table 2.2: Radiation efficiencies of different burners as a function of firing rate, equivalence ratios (Mital *et al.*, 1997; Bouma and De Goey, 1999; Leonardi *et al.*, 2002; Williams *et al.*, 1992; Qiu and Hayden, 2006; Yoksenakul and Jugjai, 2011; Wongwatcharaphon and Theinnoi, 2013; Keramiotis *et al.*, 2015).

Description of porous media and fuel	Firing rate (kW)	Thermal load (kW/m^2)	Equivalence ratio	Radiation Efficiency (%)
Cordierite upstream pore density: 65 ppi downstream pore density: 10, 20 ppi Fuel: CH_4-air (premixed)		200-600	0.90	20-30
Ceramic foam burner, pore size: 0.4 mm, porosity:90% Fuel: CH_4-air(premixed)		100-600	0.90	33-9
Fibrous metal Fuel: CH_4-air (premixed)		170-340	0.90-1.1	19-27
Ceramic fiber Porosity: 90 % Fuel: CH_4 -air (premixed)		300-450	0.75-0.95	14-25
Ceramic fiber felt, fiber diameter: 10 μm Fuel: natural gas-air (premixed)		200-500	0.60-0.90	14-12
Al_2O_3 balls; ball diameter: 15 mm Fuel: LPG-air (partially premixed)	23-61		2.08-2.5	23-15
Stainless steel and Al_2O_3 combo porosity:40-90% Fuel: LPG and kerosene (partially premixed)	5.74		0.4	19(40% porosity) 9(90% porosity)
SiSiC Pore density: 10 ppi Fuel: CH_4 , biogas and mixture Case A: CH_4:47.3%, H_2: 19.8%, CO:32.9%, Case B: CH_4:38%, H_2: 16%, CO:26%, CO_2: 20 % (biogas syngas mixture) Case C: CH_4:28%, H_2: 12%, CO:20%, CO_2: 40 % Biogas (40% CO_2+60 % CH_4) CH_4		200-800	0.83	 30-65 30-55 45-25 28-25 52-25

Gao *et al.* 2012 studied the alteration of efficiencies of CH_4 -air mixture with different types of diluents: Ar, N_2, and CO_2. They reported that the efficiency reduces in the order of CO_2, N_2 and Ar for the same dilution and equivalence ratio.

Arrieta and Amell (2014) stated that the radiation efficiency rises with the adding of syngas to the methane related to the methane only. The statement was come when they examined the combustion of methane-syngas occurrence in a surface-stabilized Al_2O_3 burner (cell density: 400 square cells per square inch). It was happened because of the elevated surface temperature achievement. The reason behind this was reduction in the ratio of unburnt gas velocity to the adiabatic laminar burning velocity. Table 2.3 compiles the efficiency value provided for different firing rates and excess air ratios.

It is evident from Table 2.3 that the radiation efficiency decreases ~66 % when the air fuel ratio was increased from 1.1 to 1.4. Same trend of decreasing efficiency with increasing firing rate is also evident and they are attributed to low flame temperature. The radiation intensity is directly proportional to the flame temperature

Table 2.3: Variation of radiation efficiency with fuel and air fuel ratio for a surface burner made of honeycomb Al_2O_3 (Arrieta and Amell, 2014).

Operating condition : heat input (kW)	Air to fuel ratio	Fuel	Radiation efficiency (%)
1.0	1.1	CH4	27
1.0	1.1	CH4-syngas	30
1.8	1.1	CH4	10
1.8	1.1	CH4-syngas	13
2.5	1.1	CH4	5
2.5	1.1	CH4-syngas	8
1.0	1.4	CH4	6
1.0	1.4	CH4-syngas	9

Abdelaal *et al.* (2013) showed an effective way to increase the flame temperature and thereby the radiation efficiency by enriching the combustion air with oxygen. Oxygen enrichment noticeably increase rate of reaction enabling an increase in combustion

intensity. In their study they used a mullite ($3Al_2O_3$ $2SiO_2$) burner with 85 % porosity and varied the equivalence ratio from 0.7 to 1.3 and firing rates from 94 to 610 kW/m^2. They observed ~10 % higher efficiency for an equivalence ratio of 1.1 and thermal load of 350 kW/m^2 when the oxygen concentration was raised from 21 % to 25 %. The peak radiation efficiency was stated to occur in the equivalence ratio range of 1-1.1.

Summarizing the literature on flame speed, flame stabilization and radiation efficiency, it can be said that these parameters are largely affected by material properties and operating conditions. Several studies were reported with respect to different materials and methane as a fuel. Few studies were also reported with domestic fuels like LPG, natural gas, and biogas too. However, in comparison to methane, the studies with other fuels are still limited. Liquid fuels are not studied much and the amount of heat required for evaporation, radiation output or efficiency etc. of the burner is still unknown. Examination of the stability limits and radiation, conduction efficiencies of the different burners such as Al_2O_3-SiC, Al_2O_3-ZrO_2, mullite, cordierite etc. with different porosities and with different fuels are needed to be evaluated. Investigations are needed to be performed with non-premixed flame and their effect with respect to stability or radiation is to be elaborated. Surface mode operation is to be largely studied especially with small scale burners as they are designed for domestic application and high efficiency of the burner is of imminent importance. The effect material types used for vaporization of liquid fuels is to be established in detail.

2.8 Thermal and Environmental Performances of PRB

One of the major benefits of the PRB is that it provides better thermal performance compared to the Conventional types and it is because the temperature gradient within the burner is small due to the better recirculation of thermal energy assisted by solid media. Further, the reaction zone is wide and the fuel is preheated due to the internal heat

recirculation and that results in higher heat release rate. Providing of surplus air and enhanced residence time due to the tortuous path of solids makes the pollutant emission characteristics of the burner superior. In the recent years, there have been several reports on design of practical burners and they are assessed in terms of thermal and emission performances.

The thermal performance of the burner is generally evaluated in terms of thermal efficiency and the environmental performance is expressed in terms of combustion efficiency or by providing the emission data like carbon dioxide (CO_2), carbon monoxide (CO), oxides of nitrogen (NO_x), unburnt hydrocarbon (UHC) etc. In the subsequent paragraphs, the thermal and environmental performances of a few recently developed burners are discussed and they are critically evaluated with respect to the fundamental combustion studies discussed in the previous section 2.6. For clarity, thermal and environmental performances are discussed separately.

In the recent time, the main objective of the research in PMC is the design of practical burners and their thermal performance evaluation and most of these studies reveal that PRBs exhibit high thermal efficiencies than their traditional counterparts due to the combined effect of convection and radiation along with conduction. For the same firing rate, high radiation output at the exit of the PRB allows additional heat transfer while operating conditions and burner material decides the total amount of available thermal energy. Firing rate and equivalence ratio are the two major parameters found responsible for thermal performance (Yu *et al.,* 2013; Delalic *et al.,* 2004; Xiong *et al.,* 1995; Jugjai *et al.*, 2001; Jugjai and Sawananon, 2004; Mohamad *et al.,* 1994). Increase in air and fuel flow rates initially results in higher efficiency however beyond a certain point the rate of heat loss becomes significant than the rate of heat release and this makes efficiency to drop (Jugjai and Phothiya, 2007; Shinoda *et al.,* 2002; Jugjai and Rungsimuntuchart, 2002; Tia

et al., 2007). Increasing firing rate shifts the point of maxima to the higher equivalence ratio sides due to higher combustion temperature.

Firing rate and equivalence ratio are the main factors responsible for higher efficiency while burner aspect ratio and size of the load have also significant impact (Shinoda *et al.,* 1998; Tanaka *et al.,* 2001; Arai *et al.,* 1999). Optimum performance can be achieved with the proper aspect ratio of the load (vessel in case of burners for cooking application) as beyond certain point the increase in aspect ratio results in higher heat loss due to increase in surface area. Distance between the burner and load is also an important deciding factor to have high thermal efficiency (Sharma *et al.,* 2011; Yu *et al.,* 2013; Mohamad *et al.,* 1994).

Xiong *et al.* (1995) demonstrated that the porous matrix combustor-heater's thermal efficiency was greatly affected by the horizontal and vertical spacing of the tubes embedded within the burner. Similar observations were reported for the domestic burners designed for cooking applications that large sized vessels were reported to contribute higher efficiency but too large vessel indulge in higher radiant heat transfer from the walls of the vessels (Sharma *et al.,* 2009). Likewise, small sized vessels result in higher convective and radiative heat loss from the sides of the burner. Thus, efficiency peaks and then drops with the increase in vessel size and optimum vessel size with respect to the burner is an important factor to consider.

The inventories of thermal efficiencies on PRB are not very large as most of the burners are designed aiming at lower emissions while evaluation of the thermal efficiency is not generally carried out. A few reports exist where the burners were designed for domestic usage and the efficiencies were evaluated using standard water boiling test (Pantangi *et al.,* 2007; Pantangi *et al.,* 2011; Muthukumar *et al.,* 2011 ; Muthukumar and Shyamkumar, 2013; Kakati *et al.,* 2007; Sharma *et al.,* 2009; Sharma *et al.,* 2011; Mishra *et al.,* 2015).

Besides these, there are few other reports where the thermal efficiencies of the industrial scale burners where water tubes were embedded to extract heat are also available (Trimis and Durst, 1996; Yu *et al.*, 2013; Delalic *et al.*, 2004; Mohamad et al., 1994). In the following section all the work aiming evaluation of efficiencies are discussed.

2.8.1 Thermal Efficiency Studies on High Wattage PRB

Thermal efficiency of a heating device is referred to the amount of heat absorbed by the heating surface to raise the temperature of the working fluid to the chemical energy released due to the combustion of fuel, mathematically:

$$\eta_{th} = \frac{(m_w c_{pw})(T_{w,o} - T_{w,i})}{m_f \left(LCV\right)} \times 100 \qquad \ldots\ldots\ (2)$$

Porous combustor-heaters generally exhibit higher thermal efficiencies than the conventional heaters due to the thermal regeneration mechanism of the combustion heat (Zhang *et al.*, 2013; Park and Kaviany, 2002). The internal heat recirculation process in the PM makes the incoming air preheated and giving rise to higher heat release and transfer to the load (Trimis and Durst, 1996; Yu *et al.*, 2013; Zhang *et al.*, 2013; Park and Kaviany, 2002). The reported thermal efficiencies of the combustor heaters where the heat of combustions used to raise the temperature of the working fluids are found extremely high. For instance, Trimis and Durst (1996) investigated the thermal efficiency (the ratio of the energy absorbed by cooling water to energy released by the fuel) of a combustor heater with inserted cooling tubes. They reported the thermal efficiency at firing rate of 5 kW and informed them to be ~97%. Higher transfer of latent heat of water condensation to the heat exchanger was thought to be cause of this high efficiency. Similar observations were also by Delalic *et al.* (2004). They established a similar system and reported furthermore higher efficiencies. The reason behind this was transfer of heat from the exhaust gases to the water in the heat exchanger. Figure. 2.12 compares the thermal efficiencies of the two systems.

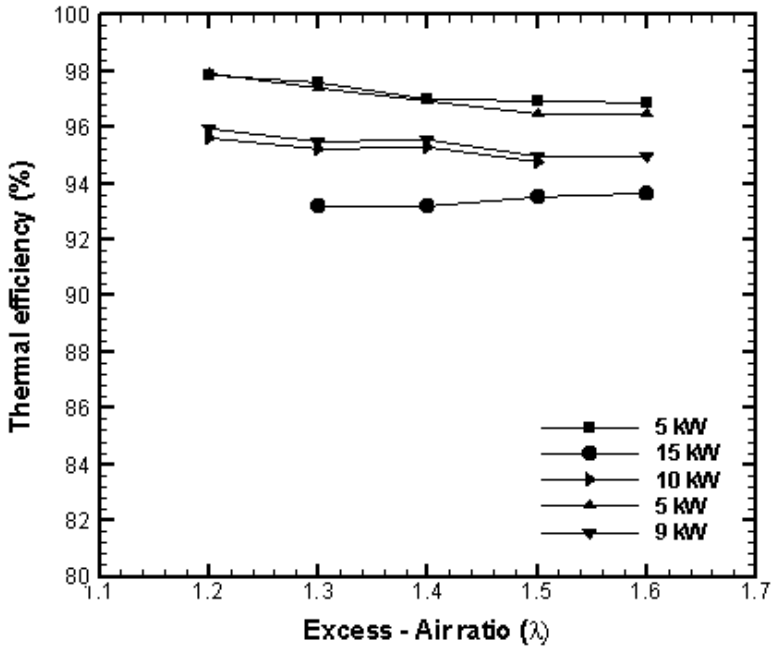

Fig. 2.12: Variations of thermal efficiencies of the combustor heater with excess air ratio and firing rate (Trimis and Durst, 1996; Delalic *et al.*, 2004).

Jugjai and Sawananon (2004) developed a surface combustion heater with a bank of tubes carrying water in it and the burner was made to operate on a novel concept of repeated flow reversal combustion maintained with the help of an alternating valve. The PM was composed of a randomly packed Al_2O_3 balls. Two water-cooled flame traps were installed to assure nearly ambient-temperature boundary conditions and serve as thermal load and flash back arrestor. The thermal efficiencies of the heat exchanger and flame trap were evaluated at the firing rate of 16 kW and equivalence ratio range of 0.38-0.49, and they were found to be in the ~50 % and ~80 % respectively. The flame trap was found to play an important role in maintaining the boundary condition of the packed bed and improving thermal efficiency. There was nearby 35 % enhancement in comparison to their previous studies where PRB was made of magnesia stabilized ZrO_2 and a cooling water in single tube was used as a thermal load (Jugjai *et al.*, 2001). However, in comparison to the design proposed by Trimis and Durst (1996) and Delalic *et al.* (2004), the design employing flow

reversal concepts looks complicated and the window of safe operating equivalence ratio is very narrow.

In a later study, Jugjai and Phothiya (2007) demonstrated that the concept of liquid fuel fired with porous combustor heater removed the atomiser and they found the thermal efficiency to be ~70 % for equivalence ratio of 0.5-0.6 and the firing rate of 10 Kw. Yu *et al.* (2013) used three different types of PM: metal fiber (MF: woven from Fe-Cr alloy), ceramic (CM: cordierite) and stainless steel fin (SF), with a commercial heat exchanger, and tested the thermal efficiencies at various equivalence ratios and firing rates. Fig. 2.13 shows the variations with respect to the firing rate and equivalence ratios.

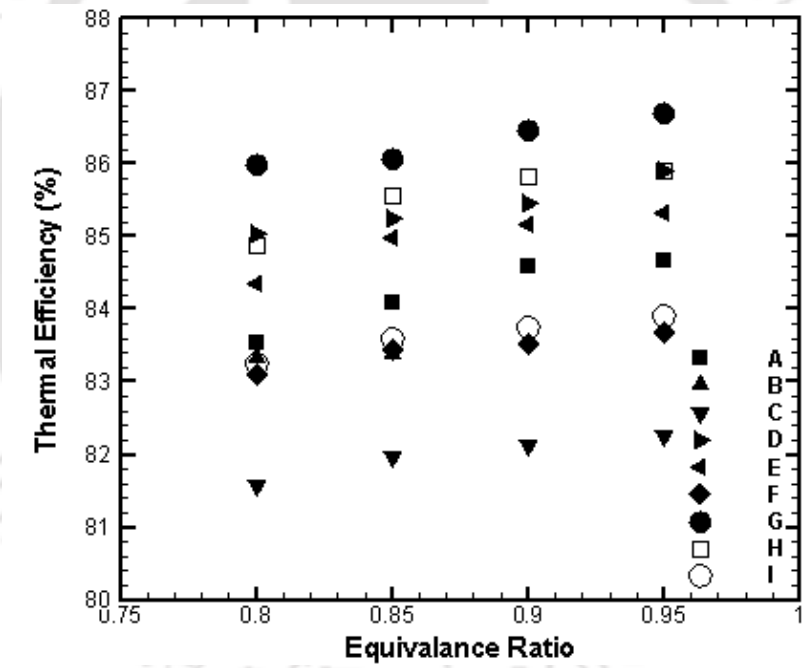

Fig. 2.13: Variations of thermal efficiencies of a PRB made of three different materials with equivalence ratios (Yu *et al.*, 2013).

A: MF, 15 kW; B: CM, 15 kW; C: SF, 15 kW; D: MF, 20 kW; E: CM, 20 kW, F: SF, 20 20 kW; G: MF, 25 kW; H: CM, 25 kW; I: SF, 25 kW

It is observed from Fig. 2.13 that the metal fibre burner exhibits the highest efficiency at all the firing rates tested and it is followed by ceramic and the stainless steel respectively.

The difference in efficiencies was reported to be originated due to the difference in porosities. MF has the highest porosity (89 %), followed by CM (49.5 %) and SF (31.1 %). The low porosity in the SF burner resulted in higher exit velocity and unstable flame causing lift off and lower rate of heat transfer.

With respect to material, Xiong *et al.* (1995) tested SiC and Al_2O_3 and reported that SiC exhibited higher thermal efficiency than the Al_2O_3 burner particularly at higher excess air ratio due to the higher radiative heat transfer to the water tube. Besides having high emissivity of SiC than Al_2O_3, porosity could be another factor but the author did not provide any information on that aspect.

Mohamad *et al.* (1994) modelled a porous matrix combustor-heater with two rows of embedded cooling tubes and studied the effect of excess air on thermal efficiency. The porous matrix was assumed to be made of Al_2O_3 balls (6 mm particle diameter and 43 % porosity) and the percentage of excess air used was 10 %. The results show that the thermal efficiency decreased by ~60 % when the firing rate was increased from 10 kW to 70 kW, while the same had dropped 17 % when the particle diameter was reduced from 6 to 1 mm for a 12.7 mm diameter tube. Further, efficiency drop was observed with the increase in activation energy of the fuel and decrease in cooling tube spacing. It was reported that the predicted results were comparable with the experimental data within an acceptable deviation (± 15 %) for the excess air range of 10-30 %, while the data at the excess air level of 42 % was found significantly deviated from the predicted results. They stated that for more accurate predictions, it was necessary to model the effective thermal conductivity and contact resistance between the embedded tubes and the porous bed in addition to the porosity variation near the walls.

Summarizing, the works reported on thermal efficiencies of the porous combustor-heater

by various researchers, it can be stated that the PM is found effective in improving thermal efficiency of the system to a very high level and firing rate and equivalence are the two key controlling parameters.

2.8.2 Thermal Efficiencies of Low Wattage Burners

Low wattage burners (1-3 kW) are normally served for household applications and mostly for cooking. The thermal efficiencies of those burners are expressed in terms of heat utilized for cooking to the total heat release by the fuel. Conventionally in laboratory, the efficiency is calculated by measuring the amount of heat gained by a cooking vessel placing over the burner and having water in it. The process is known as water boiling test.

Water Boiling Test

Water boiling test is the simplest method utilized for efficiency evaluation. In this, a known quantity of water is taken in a vessel and heated by the thermal power of the burner. The ratio of the energy entering the pot to the energy released through combustion of fuel defines the thermal efficiency. The energy entering the pot produces two measurable effects; (i) raising the temperature of the water to near boiling point and (ii) evaporating water.

Mathematically: $$\eta_{th} = \frac{(m_w c_w + m_p c_p)(T_2 - T_1) + m_{ev} L}{m_f \left(LCV\right)} \times 100 \qquad \ldots\ldots\ (3)$$

Reports on Thermal Efficiencies

Development of PRB for domestic application is a recent trend of PMC research, and many researchers have studied the performance of LPG stoves using PRBs (Mujeebu *et al.*, 2011a; Mujeebu *et al.*, 2011b; Mujeebu *et al.*, 2013; Mujeebu *et al.*, 2007; Pantangi *et al.*, 2011; Muthukumar *et al.*, 2011; Muthukumar and Shyamkumar, 2013; Mishra *et al.*, 2015; Yoksenakul and Jugjai, 2011; Wongwatcharaphon and Theinnoi, 2013). Some recent

reports also indicated the use of PRB in kerosene stoves too (Sharma *et al.,* 2016a; Sharma *et al.,* 2016b). The concept of using PMC for domestic application was first provided by a group of researchers from IIT Guwahati (Pantangi *et al.,* 2007; Kakati *et al.,* 2007; Sharma *et al.,* 2009; Sharma *et al.,* 2011) and thereafter, many reports in this direction have come in the last few years (Mujeebu *et al.,* 2011a; Mujeebu *et al.,* 2011b; Mujeebu *et al.,* 2013; Yoksenakul and Jugjai, 2011; Wongwatcharaphon and Theinnoi, 2013; Jugjai and Rungsimuntuchart, 2002). The pioneering work of IIT Guwahati have established the fact that the PM can successfully be employed in the cooking stoves and it brings significant improvement in efficiency when compared with their traditional counterparts (Pantangi *et al.,* 2007; Muthukumar *et al.,* 2011; Muthukumar and Shyamkumar, 2013; Mishra *et al.,* 2015; Sharma *et al.,* 2016a; Sharma *et al.,* 2016b). The following paragraphs describe the works of various researchers and their findings are critically analysed.

Works Reported from IIT Guwahati

The background of using PRB in LPG stove was linked with the fuel conservation strategy. LPG is served by a bigger (70%) population while fossil fuel reserves are depleting at a faster rate. Keeping efficiency improvement as the main focus, research was conducted with PRB to prove its usability. Among the various works, Pantangi *et al.* (2011) used the SiC and Al_2O_3 as a porous material and made a double-layered PRB. They studied the thermal efficiencies for the input power of 0.8-1.8 kW and equivalence ratio of 0.3-0.7 and they concluded that the equivalence ratio and burner diameter were the key parameter which affect the thermal efficiency significantly. The highest thermal efficiency of 68% observed at the burner diameter was 80 mm. The improvement in thermal efficiency was 3% as compared to CB. Afterwards, Muthukumar *et al.* (2011) had used a ceramic block in its place of Al_2O_3 balls in the preheating zone and they reported that the efficiency of the stove could be improved to 71%. The equivalence ratio range used by Muthukumar *et al.*

(2011) for the stable operation was different from the Pantangi *et al.* (2011) and at an equivalence ratio of 0.68, they observed the maximum efficiency.

In the similar burner (Pantangi *et al.*, 2011), Muthukumar and Shyamkumar (2013) examined the consequence of combustion zone porosity and demonstrated that at 90 % porosity, PRB could yield 75% thermal efficiency at an equivalence ratio of 0.54 and firing rate 1.3 kW. In an another study, Panigrahy *et al.* (2016) studied the effect of combustion zone material thickness. They changed the material thickness from 15 to 40 mm. They concluded that at an equivalence ratio 0.5 and firing rate of 3-5 kW, the burner associates with 15 mm thickness yield higher thermal efficiencies as compared to burner with 30 mm thickness. Panigrahy *et al.* (2016) reported that high thickness burner material becomes responsible for low exit surface temperature due which thermal efficiency becomes lower. Mishra *et al.* (2015) developed a medium wattage (5-10 kW) LPG cooking stove with PRB. The range of equivalence ratio at which the PRB could produce flameless combustion was 0.54-0.72. The observed improvement in thermal efficiency was 9 % as compared to CB.

Study of porous media technology applied to conventional pressurized kerosene stove was also carried out at IIT Guwahati. The very first investigation was carried out by Kakati *et al.* (2007), where they examined the thermal efficiency, kerosene consumption rate and emission of domestic burner with porous inserts of pottery clay, sodium silicate and saw dust and compared the results with the conventional one. Later, Sharma *et al.* (2009) investigated the performance of the same stove by replacing the inserts with four different porous materials, viz. silicon carbide (SiC), zirconia (ZrO_2), wire mesh roll filled with metal balls and alumina (Al_2O_3). They found an optimum value for mass flow rate (130-140 g/hr) and vessel size (260 mm diameter) which resulted in increased thermal efficiency for all the inserts with maximum 7% increase exhibited in SiC inert. Sharma *et al.* (2011) further modified the stove by incorporating ceramic heat shield of low conducting and radiating

alumina (Al_2O_3) which resulted in 15% increase in thermal efficiency. Recently, Sharma *et al.* (2016) extended their research by changing the burner geometry and also incorporated exergy analysis. Experimental stove consisting of two-layer porous matrix of alumina (Al_2O_3) balls and honeycomb structured silicon carbide (SiC) was experimented with three different shapes of burner casing, viz. straight cylindrical, taper and conical. Performance with conical burner casing was found to be the best of all with 10% increase in thermal efficiency at air and fuel flow rate of 120-130 lpm and 220 g/hr respectively. In the same burner, the effect of burner diameter on thermal efficiency, emission and temperature distribution at different air and fuel flow rates was studied by Sharma *et al.* (2016). The burner with 70 mm diameter proved to be the best among the three studied burner diameters of 60 mm, 70 mm and 80 mm. In another study on kerosene stove, Sharma *et al.* (2009) found the optimal thickness of the combustion zone of the PM and it was 20 mm. At this thickness better emissions and higher efficiencies were reported.

Aforesaid PRBs [expect the ones developed by N K Mishra (2015, 2016)] require the supply of external air for its operation, which constrained its potential for commercialization in domestic cooking application. Henceforth, the researchers put in their efforts to make a PRB which would work on naturally induced draft as in the conventional one. This was achieved by bringing changes in the supply pressure of LPG/kerosene, design of orifice, the burner port, the mixing chamber, the preheating zone and the casing. After the experiment, stable combustion was found and thermal efficiency was higher than CB present in market and also reduction of emissions were found in the same burner.

2.8.3 Worldwide PRB Development and Efficiency Studies

Apart from the research conducted at IIT Guwahati, significant amount of work on PRB developments for various applications have been reported by two other groups: (Makmool

et al., 2006; Yoksenakul and Jugjai, 2011a; Yoksenakul and Jugjai, 2011b; Jugjai and Sawananon, 2004; Jugjai and Rungsimuntuchart, 2002) and recently by Mujeebu *et al.* (2011a, 2011b, 2013). Jugjai and Rungsimuntuchart (2002) studied LPG stoves available (5-30 kW) in Thailand and employed the concept of PMC and reported that at 11 kW, the PRB with swirling flame resulted in ~60 % efficiency against ~30 % of the conventional stove. Makmool *et al.* (2006) examined four types of domestic LPG burners: radial flow, swirling flow, vertical flow, and PRB, available in Thailand, and found that the swirling flow burners yielded the highest thermal efficiency.

Yoksenakul and Jugjai (2011) also investigated the thermal efficiency of a self-aspirating PRB made of a packed bed of 15 mm diameter Al_2O_3 balls and reported ~8% higher efficiency than the conventional burner. Wu *et al.* (2014) studied about PRB and they found that PRB lead to higher efficiency than the conventional burner burning with free-flame or bunsen flame. They also reported the efficiency of the CB much affects by the height between the burner exit and load. Herrera *et al.* (2015) too delivered a parallel interpretation in their investigation with PRB of Al_2O_3 and SiC. According to them, the efficiency of the burner is enhanced when the vessel is kept in touch with the burner. They found conduction as an effective mode than convection-radiation that dominates when the load is placed a certain distance apart. However, the maximum thermal efficiency observed with the conduction mode was much lower than the previous reports (Pantangi *et al.*, 2011; Muthukumar *et al.*, 2011; Muthukumar and Shyamkumar, 2013; Mishra *et al.*, 2015). Further, the idea of keeping the vessel just above the burners controverts the conclusions of a few authors like Yoksenakul and Jugjai (2011), Wu *et al.* (2014) etc., where they have presented that the emission of pollutants were relies on the distance and near keeping of vessel attribute to more CO. Mujeebu *et al.* (2011, 2013) made a comparison between the surface combustion and submerged combustion mode of burner operation in context with

the thermal efficiencies. They reported that surface combustion attributed in higher efficiency. Nevertheless, the PM used by them for assembly of surface burner was of much bigger pore that really supports submerged combustion as saw in other reports (Mital *et al.*, 1997; Barra and Ellzey, 2004;

Mathis and Ellzey, 2003; Mital *et al.*, 1998; Viskanta and Gore, 2000). They used Al_2O_3 foam as a preheat zone whose ppi was 66 and for combustion zone they used 20 ppi foam of Al_2O_3. In their surface burner, thickness of the combustion zone was smaller than the preheat zone while basic study (Leonardi *et al.*, 2002) recommends the combustion zone (flame support layer) should be broader to for higher radiation efficiency. Table 2.4 shows the thermal efficiencies of reported by various researcher.

Summarizing, it can be stated that the thermal efficiency of PRB is dependent on many factors such as PM and their geometry, mode of operation, distance between the burner and vessel etc. Self-aspiration mode is found to improve the efficiency of the conventional burner by ~10%. Performance of LPG with PRB is largely reported and better performance is obtained in self-aspiration mode.

2.9 Emission Performance Studies

Emission analysis is an integral component of burner performance studies. PRBs offer lower emissions when compared with their traditional counterparts. Because of the preheating effect, concentration of CO or UHC reduce. The reason behind this increased heat release per unit area in PRB. NO_x emission is depend on the design as it can be built through the thermal (or Zeldovich) mechanism or the prompt (or Fenimore) mechanism and both the mechanism are temperature dependent. The thermal mechanism is "slow" mechanism but contributes the most of the NO_x, and the residence time in the hot region of the combustor is important.

Table 2.4: Thermal efficiencies of different domestic burners (Mital *et al.*, 1997; Bouma and De Goey, 1999; Muthukumar *et al.*, 2011; Leonardi *et al.*, 2002; Williams *et al.*, 1992; Qiu and Hayden, 2006; Wongwatcharaphon and Theinnoi, 2013; Sharma *et al.*, 2016).

Description of PM (material, pore size (ppc/ppi), porosity (%), thickness) and fuel	Firing rate (kW)	Equivalence ratio	Burner type/ Thermal efficiency (%)	
Matrix stabilised PRB Upstream: porcelain foam (18 ppc, 15 mm) Downstream: Al_2O_3 balls (diameter: 30 mm) *Surface stabilized PRB* Upstream: Al_2O_3 foam (26 ppc, 86%, thickness: 12.7 mm) Downstream: Al_2O_3 foam (8 ppc, 84%, thickness: 12.7 mm) Fuel: LPG	0.62	3.14	CB Matrix stabilized Surface stabilized	47 59 71
Upstream: Al_2O_3 balls (diameter: 60-100 mm, thickness: 15- 20 mm) Downstream: Al_2O_3 balls (30 mm diameter) Fuel: LPG	1.3 0.85 1.28-1.72 1.1-1.57	0.45 0.37 0.3-0.4 0.3-0.4	60 mm diameter 70 mm diameter 80 mm diameter 90 mm diameter	63 66 67 66
Upstream: ceramic matrix (thickness:10 mm) Downstream: SiC; Fuel: LPG	1.24	0.68	80 mm diameter	71
Upstream: ceramic matrix (thickness:10 mm); Downstream: SiC (80-90%) Fuel: LPG	1.3	0.55	80 mm diameter	75
Upstream: Al_2O_3 honeycomb (diameter: 120 mm, thickness: 25 mm, 90%) Downstream: SiC (diameter: 120 mm, thickness: 10 mm) Fuel: LPG	 5 10	0.56 0.56	CB (5-10 kW) PRB PRB	32-45 55 58
Fuel: LPG	5	-	Radial flow CB Vertical flow CB Swirl flow CB Porous radiant	43 50 55 47
Stainless steel wire mesh (40 mesh per inch) Fuel: LPG-air	11	-	CB PRB(radial flow) PRB(swirl flow)	30 44 60
Upstream: Al_2O_3 balls (Diameter: 7 mm, 35-40%) Downstream: SiC (80-85%, thickness 20 mm): Fuel: Kerosene	1	-	Pressure stove (compressed air)	58

Temperature and residence time are the strongly relies on burner configurations (Trimis and Durst, 1996). The freedom of using higher excess air without affecting the stabilization process of the burner results the NO_x level lower. However, beyond a certain level the decrease in equivalence ratio is accompanied by lower residence time and this again increases the emissions of CO and NO_x. NO_x is the pollutant responsible for smog and acid rain and imparts severe health effects. PRBs exhibit lower NO_x while they are function of several other parameters as stated before and they are generally evaluated under different operating conditions. Table 2.5 shows the comparison of emission performances which has been reported by several researcher.

From Table 2.5, it was found that the results are too assorted to catch a normal rhythm and it was happened by reason of the different working conditions and also material. CO or NO_x varies with equivalence ratio it depends on operating condition. The PRB, developed by IIT group for the same fuel (LPG), it was found that most of the results (Pantangi *et al.*, 2011; Muthukumar *et al.*, 2011; Mishra *et al.*, 2015) show that increasing CO increases with equivalence ratios. The dissimilarity may be possible due to the application of different material which affects stabilization zone and also due to bigger burner size (90 mm diameter). Minimization of emission calls for optimum burner diameter. In PRB emissions may be affects if burner size smaller or bigger than the optimum size. It happens because sifting the stable zone.

Xu *et al*. (2011) developed a mini-scale PRB (20 mm diameter) with firing rate 0.2-3.8 kW and studied the emission characteristic, and reported that the lower emission of CO was recorded for an equivalence ratio range of 0.46-0.52. Beyond this limit CO level was as high as 548 ppm and it was due to the incomplete combustion owing smaller diameter and difficulty in maintaining self-sustained combustion. Minimum NO_x recorded was 63 ppm and found to increase it with increase in equivalence ratio.

Table 2.5: Comparisons of emission performances of different burners (single and double layered) developed in the last two decades with the stated operating conditions (Yoksenakul and Jugjai, 2011; Wu *et al.*, 2014; Fuse *et al.*, 2003; Arrieta and Amell, 2014; Takami *et al.*, 1998; Yu *et al.*, 2013; Herrera *et al.*, 2015; Ellzey and Goel, 1995; Mishra *et al.*, 2015; Muthukumar and Shyamkumar, 2013; Muthukumar *et al.*, 2011; Pantangi *et al.*, 2011; Jugjai and Phothiya, 2007; Fuse *et al.*, 2005; Jugjai and Polmart, 2003; Jugjai *et al.*, 2002; Tseng and Howell, 1996; Keramiotis *et al.*, 2012; Khanna *et al.*, 1994; Mital *et al.*, 1997).

Single layered			
Material Porosity (%) Pore density (ppi)	Fuel	Emission performance Minimum, maximum	Corresponding equivalence ratio; thermal load (kW) /firing rate (kW/m^2)
Mullite	Kerosene	CO: 0.09% NO_x:20-100 ppm	(at 0.5-0.7); 2205-3879 kW/m^2
Al_2O_3 foam	Kerosene	NO_x:102-360 ppm	(at 0.4-0.6); 4-50 kW
Fe-Cr Cordierite SS	Natural gas	CO: ~200-800 ppm; NO_x: 40-120 ppm CO:~600-1600 ppm; NO_x: 40-90 ppm CO:~600-1600 ppm; NO_x: 30-80 ppm	(at 0.8-0.95); 25 kW
Al_2O_3 balls	LPG	CO: ~200 ppm NO_x: 98 ppm NO_x: 40 ppm	(at 2.08-2.5); 15-55 kW (at 2.08-2.5); (at 54 kW) (at 2.08-2.5); (at 20 kW)
Al_2O_3 balls	LPG	CO: ~1000 -2500 ppm NO_x: 10-59 ppm	21-44 kW
Al_2O_3 honeycomb	CH_4 CH_4+ syngas	CO: ~20 ppm (CH_4) CO: ~30 ppm (syngas) NO_x: 3000 ppm(CH_4) NO_x: 1500 ppm(syngas)	2.5 kW 2.5 kW 2.5 kW 2.5 kW
Bronze pellet	LPG	CO: 6-22 g/kg CO: 4g/kg NO_x: 6 g/kg NO_x: 7 g/kg	(at 1.2 & at 0.6); 1 kW (at 1.0) ; 1 kW (at 0.6) ; 1 kW (at 1.2) ; 1 kW

Double layered			
Material Porosity (%) Pore density (ppi)	Fuel	Emission performance Minimum, maximum	Corresponding equivalence ratio; thermal load /firing rate
Upstream: PSZ (80%,45 ppi) Downstream: SiSiC, Al_2O_3 (10 ppi, 20 ppi)	Natural gas	CO: ~1-3 g/kg NO_x: 0.16-0.32 g/kg UHC:0.1-1.2 g/kg	(at 0.6-1.0) (at 0.6-0.87) (at 0.6-0.87)

Upstream: SiC foam (90%) Downstream: Al_2O_3 balls	LPG	CO:110 mg/m^3 CO:350 mg/m^3 NO_x: 162-216 mg/m^3	(at 0.35); 1.2 kW (at 0.45); 1.7 kW	
Upstream: SiC foam (90%) Downstream: Al_2O_3 honeycomb (40%)	LPG	CO: 10 ppm CO: 16 ppm NO_x:0-2ppm	(at 0.60); 1.4 kW (at 0.68); 1.4 kW 1.2-1.4 kW	
Upstream: SiC foam (80%, 85%, and 90%) Downstream: ceramic matrix (40%)	LPG	CO: 20 mg/m^3 CO: 140 mg/m^3 NO_x:0.1 mg/m^3 NO_x:0.9mg/m^3	(at 0.70); 1.3 kW (at 0.57); 1.7 kW (at 0.54); 1.3 kW (at 0.70); 1.5 kW	
Upstream: SiC foam Downstream: Al_2O_3 honeycomb	LPG	CO: 40 ppm CO: 250 ppm NO_x:3 ppm NO_x:16 ppm	(at 0.50); 5 kW (at 0.70); 10 kW (at 0.50); 5 kW (at 0.70); 10 kW	
Stainless steel wire mesh	Kerosene	CO: ~0.08 % NO_x: ~20-40 ppm	(at 0.50) (at 0.50)	2.06-3.49 kW
Upstream: Stainless steel wire mesh Downstream: Al_2O_3 balls	Kerosene	CO: 700 ppm CO: 100 ppm NO_x: ~100-160 ppm	(at 0.35); 9.15 kW (at 0.45); 9.15 kW (at 0.35-0.85)	
Upstream: Al_2O_3 foam (80%) Downstream: Al_2O_3 foam (68%)	Ethanol	CO: ~100 ppm NO_x: ~59-97ppm	(at 0.60-0.80) (at 0.60-0.80)	1.2 kW
Upstream: Stainless steel wire mesh Downstream: Al_2O_3 balls	Kerosene	CO: ~600 ppm CO: ~2900ppm NO_x: ~130 ppm NO_x: ~110 ppm)	(at 0.50); 15 kW (at 0.65); 15 kW (at 0.70); 15 kW (at 0.30); 10 kW	
Upstream: Stainless steel wire mesh Downstream: Al_2O_3 balls LPG	Kerosene	CO: ~50 ppm (LPG) CO: 200 ppm (SKO) NO_x:130ppm (LPG) NO_x:180ppm (LPG)	(at 0.50-0.95) (at 0.50-0.95) (at 0.50-0.95) (at 0.50-0.95)	5 kW
Upstream: SiSiC foam(5ppi) Downstream: Al_2O_3 foam (10 ppi)	CH_4	CO: ~25-270 ppm NO_x: ~3-30 ppm	200-1000 kW/m^2 200-1000 kW/m^2	
Upstream: PSZ (87%; 10 ppi) Downstream: PSZ (84%; 65 ppi)	Heptane	CO: ~10-120 ppm CO: ~5-30 ppm	(at 0.6-0.87) (at 0.6-0.87)	

Upstream: PSZ (87%; 20 ppi) Downstream: PSZ (85%; 30 ppi)	Heptane	CO: ~5-8 ppm NO_x: ~10-40 ppm	(at 0.30-0.8) (at 0.30-0.8)	
Upstream: PSZ (84 %; 65 ppi) Downstream: PSZ (87%; 10 ppi)	CH_4	CO: 8 ppm CO: 10 ppm NO_x:18 ppm NO_x:20 ppm	(at 0.77) (at 0.94) (at 0.77) (at 0.94)	3.9-7.1 kW
Upstream: SiSiC foam (20 ppi) Downstream: Al_2O_3 flakes	LPG	CO: 25 ppm CO: 150 ppm	(at 0.50); 100 kW/m^2 (at 0.70); 230 kW/m^2	

For low NO_x operation of the burner at lower equivalence ratio is important. However, beyond a certain point, dilution creates hot spot and local extinction becomes evident (Scribano *et al.*, 2006). The opposite effects: higher flame temperature and lower residence time at higher firing rate has sometimes leaves NO_x concentration unchanged while CO emission significantly increases with decrease in equivalence ratio due to low flame temperature and residence time (Bakry, 2008).

Mathis *et al.* (2003) reported the UHC concentration to be ~15 ppm at a thermal load of 1000 kW/m^2 and equivalence ratio of 0.75. It was found to decrease with increase in thermal load and decrease in equivalence ratios. CO emissions were about 10 ppm up to a firing rate of 2000 kW/m^2. Emissions of NO_x were below 10 ppm for the entire range considered (500-3500 kW/m^2). Emissions also affects by type of fuel. Gao *et al.* (2013) studied the emission characteristics of methane-air flame with three different diluents: Ar/ N_2/CO_2 and reported that CH_4/Ar mixture exhibited the highest NO_x emissions when compared with the mixture with diluents. But with higher concentrations of CO_2 (40%), the same was lower than CH_4-air mixture. The CO and HC emissions were found insensitive to the inert gas species. In another study Gao *et al.* (2011) measured NO_x, CO and UHC for methane and biogas (mixture of CO_2 and methane)-air combustion. They reported that NO_x reduces with increase in CO_2 fractions of the biogas due to the low flame temperature. While CO and

UHC were found higher at lower flow velocity (< 40 cm/s) in comparison to methane and the same were found in the nearly same range as that of methane at higher flame speed. Similar observation was reported by Keramiotis and Founti (2013). They found ~50 % higher CO with the biogas combustion against pure CH_4-air combustion for the same excess air ratio. NO_x was observed to reduce by ~50-60% due to low flame temperature.

Arrieta and Amell (2014) used the Al_2O_3 honeycomb burner with CH_4 alone and an equimolar mixture of CH_4 and syngas. They reported that the addition of syngas to methane increases the CO emissions while NO_x decreases. Reduction of NO_x owing to low flame temperature. Lower flame temperature happens due to ample heat loss from the flame to the burner. The reason behind this was the addition of syngas was thought be attributed to higher CO emissions. Jugjai and Rungsimuntuchart (2002) too reported about high CO emissions (~5000 ppm) in a LPG burner with swirled central flame due to the low flame temperature (~800°C) inside PRB.

Gao *et al.* (2012) used double layered PRB with different size downstream materials (Al_2O_3 balls: 3, 6, 8, 10, 13 mm diameter) and 3 mm diameter Al_2O_3 balls for upstream materials and evaluated the emission appearances. They used fuel as CH_4 and concluded that CO emissions were nearly free from the balls diameter. It was happened at higher flow velocity (> 35 cm/s) although smaller diameter ball presented the highest emission at low flame speed. The UHC emissions very sensitive to balls diameter. With increasing balls diameter UHC decreases. It was for the whole range of flow velocity (10-50 cm/s). Minimum NO_x emission was found at 8 mm diameter.

The same research team: Gao *et al.* (2014) also examined the consequence of porous material on emission. They concluded that CO emissions were not reactive to the materials when they chose 4 materials: ZrO_2, Al_2O_3, SiC and FeCrAl. Further, they worked on the

pore density of SiC (10, 20, 25, 30 ppi) and described that the CO emission of 25, 20, and 10 ppi was remarkably higher than 30 ppi SiC foam. They stated the reason for low CO emission. They reported reduction was related with more flame temperature in the 30 ppi material. Moreover, they observed UHC emissions nearly fixed for ZrO_2, Al_2O_3, and FeCrAl foams although for SiC foams. It was observed that with UHC reduce with the rise in flame speed. Order of SiC pore density (20, 25, 30, and 10 ppi), emission of UHC increases. Because of the low flame temperature (for all materials), emission of NO_x remains relatively low (below 3 ppm). The form of material had also shown no significant effect on NO_x emissions (below 4 ppm for foam, honeycomb and bead structures) (Gao *et al.*, 2014). Gao *et al.* (2014) further found that CO emissions reduce in order of foams, beads, and honeycombs. The reported trend of emission with foam is however found different from that expressed in their earlier study (Gao *et al.*, 2014). For their (Gao *et al.*, 2014) earlier study, they reported that, for the identical pore size and material (10 ppi Al_2O_3 for downstream part and for upstream part: Al_2O_3 with 3 mm diameter bead) concentration of CO emissions reduce when flow velocity varies from 20 cm/s to 60 cm/s and variation in same was from ~270 ppm to ~10 ppm. When the flow velocity was nearby 25 cm/s then CO emissions raised and dropped which has been shown by (Gao *et al.*, 2014) in their latter study and this phenomenon shown in Figs 2.14 and 2.15. Muthukumar and Shyamkumar (2013) reported that CO is a strong function of porosity. They observed ~50% reduction in with the increase in porosity of the burner from 80% to 90%. While Xiong *et al.* (1995) reported the type of material and gap between the combustor and cooling tube is important. Wu *et al.* (2014) has however contradicts this finding.

Yoksenakul and Jugjai (2011b) developed a self-aspirating PRB to work on LPG and investigated the emission levels with varying heights between the burner top and the bottom of the vessel.

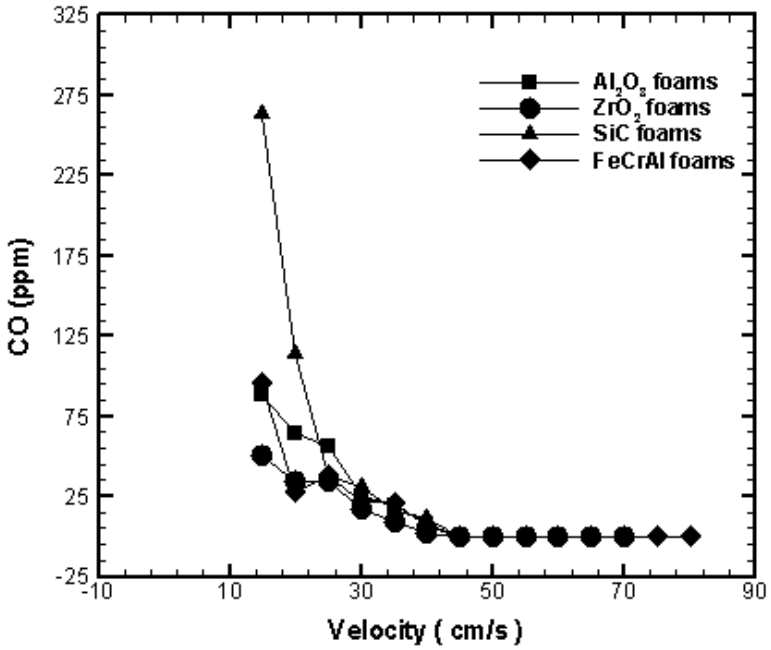

Fig. 2.14: CO emissions as function of flow velocity for different foam materials 10 ppi (Gao *et al.*, 2014).

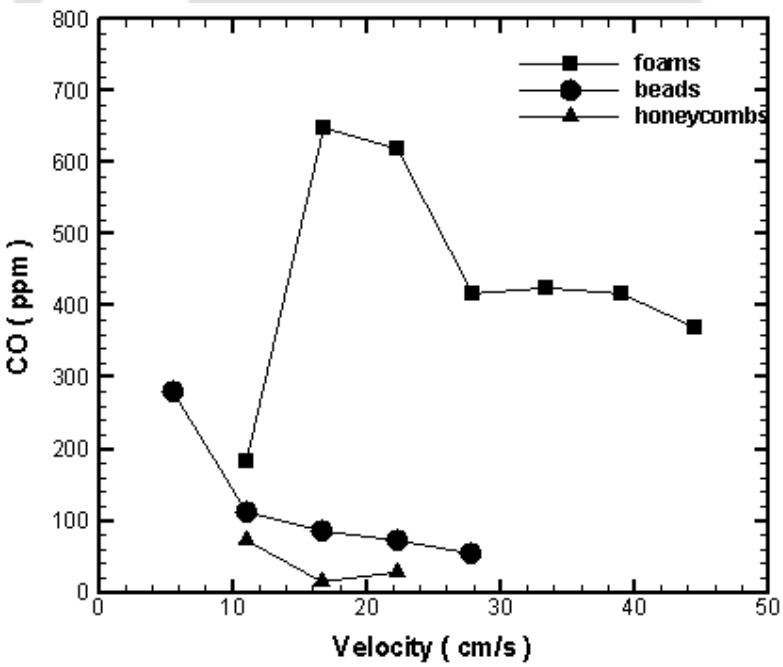

Fig. 2.15: CO emissions of different porous structures as a function of flow velocity (Gao *et al.*, 2014).

They observed about 65% reduction in CO with the change in height from 50 to 120 mm for a firing rate of 44 kW and it was attributed to higher secondary air entrainment at larger

gap. NO_x has shown increasing trend with the increase in distance, though not very significant. Further, CO emission was shown to decrease with decrease in firing rate.

In liquid fuel, Vijykant and Agrawal (2007) studied the effect of injector locations on the emission characteristics of kerosene fired PRB and reported that depending on the injector locations the operating regimes of the combustor varies. The emissions were found lowest when the injector was located far upstream of the PM due to the production of a homogeneous reactant mixture. At the intermediate location, the reactant mixture was found non-homogeneous and at a closer location the combustion was seen to proceed in diffusion mode due to insufficient residence time.

Sharma *et al.* (2016) investigated the emission characteristics of kerosene-air combustion in a domestic stove and reported that the better emission characteristics could be obtained only at the cost of lower efficiency. Liquid fuel combustion in PRB is little tricky due to the need for complete vaporization of the fuel and then combustion of the vaporized fuel. Use of right vaporization technique and optimum distance between the vaporizer and the burner are the two essential criteria for stable combustion.

2.10 Some Recent Patents Based on PMC

With the knowledge of the above early developments, Durst (1996a) and co-researchers patented a porous radiant burner with heat exchanger that could work at low wattage (1-8 kW) with stable combustions and no flash back. This development was mainly meant for European home heating systems. Their burner has increase in the pore size from the inlet to the outlet of the burner. This also allowed the burner to run at high inlet pressures. Some of the recent patents in this area are as follows:

- A porous burner for gas turbine application which was built by Ellzey and William (2004).

- Volkert and peter (2006) patented a porous radiant burner for gas and air mixture. Burning of a gas/air mixture in porous radiant burner leads to improved heat transfer also, they reported low values of emissions.
- Bellucci *et al*. (2006) built a premixed burner with a swirl generator along with two perforated plates which are kept at a defined distance from one another in the inflow region of the combustion air in such a manner that the burner simultaneously allows damping of acoustic combustion chamber pulsations during operation.
- A pore-type burner with silicon–carbide porous body was built by Hoetger *et al*. (2006). This was designed for burning a fuel–air mixture and to generate a hot flue gas. The invention relates to a pore-type burner for burning a fuel/air mixture for the purpose of generating a hot flue gas. The burner includes a housing in which a pore material consisting of porous, high-temperature-resistant silicon carbide (SiC) was provided for combustion, in order to apply a hot stream of flue gas to a steam super heater.
- Redwood and John (2007) invented high efficiency radiant burner, incorporated with heat exchanger.
- Kaeding and Lawrence (2008) invented a burner with a Porous structure. The burner having a burner chamber filled partially by a porous body, an evaporation zone, an igniter for igniting the combustion mixture of evaporated liquid fuel and air supplied. They reported that the developed burner could burnt the liquid fuel with improved combustion.
- Fabrice and Beatrice (2008) designed compact exchanger reactor using a plurality of PRBs. The discovery relates to a novel exchanger for implementing highly endothermic chemical reactions such as steam reforming reactions of naphtha or natural gas reactor.

- Ellzey and Schoegl (2009) developed a super adiabatic counter flow reactor. They reported that in one particular embodiment, fuel/oxidizer mixtures might react in channels in a counter flow arrangement so, that heat from one channel preheats the gas in the neighbouring channel which leads to improved combustion.
- Assmann *et al*. (2010) developed a PRB for heating, drying and keeping hot especially a tundish of a continuous casting installation.
- Franz and Götz (2010) developed a device for burning a fuel/oxidant mixture. The invention consists of a reactor with a combustion chamber containing two different porous material zones. They developed the burner for higher operating temperature up to 2400 °C.
- Yoshida (2011) invented burner for manufacturing porous glass preform. The invention relates to a burner for manufacturing a porous glass preform, which can improve deposition efficiency and gas mixing efficiency without increasing turbulence of the flame.
- Claerbout *et al.* (2012) developed an improved version of PRB which comprises a premixing chamber and a combustion chamber. The premixing chamber was separated from the combustion chamber through radiant burner plate which had multiple levels of burner surface for getting improved combustion.
- Alexander (2012) invented a PRB. The objective of the invention was to provide a radiant burner with high energy efficiency, high radiant power and high flame stability.
- Hwang (2014) designed a special type porous plate burner. The development made for a combustion device, which has a simple structure and burns wood chips, wood pellets or other fuel to achieve high heat efficiency and strong thermal power and generate less soot or air pollution.

- Mishra (2015) developed double-layer self- aspirated LPG domestic cooking stove with PRB for input power range 1-3 kW whose maximum thermal efficiency was 75 % and while for the same input power, thermal efficiency of convention LPG stove was 68 %
- Mishra (2016) invented another double- layer self-aspirated for medium scale LPG cooking stove with PRB with input power range 5-15 kW. The maximum thermal efficiency obtained by this PRB stove was 55 % which was 24 % higher than conventional stove for the same input power.

2.11 Performance Study of Cerium Based Nanofuel

In the combustion process, metals are widely used owing to their properties of producing oxygen while it's burning. It is the property of the metal to follow oxygen is the primary objective of its usage in catalytic application, and is named as oxygen storage capacity (OSC). This property is very much important while heating the metals in nanosized.

Several harmful gases such as CO, NO_x, CO_2 and unburnt hydrocarbons are reduced to great extent by using the OSC of its three ways catalyst (TWC). Under rich fuel content, the TWC supplies the oxygen to CO and hydrocarbons and also removes oxygen from NO_x from lean fuel mixture. While TWC is now widely used in exhaust manifolds, the application of cerium based oxides in the form of catalyst is found to have remarkable improvement in combustion efficiency as well as reduction in emission level.

2.11.1 High Oxygen Storage Capacity (OSC) Materials

Researchers are being attracted towards cerium based oxides due to its applicability in catalytic usage. It is popular in earth metals as its ability to alter valance position from Ce^{4+} position to Ce^{3+} position and opposite to it. In cerium based oxides, with addition or loss of oxygen, the electronic re-configuration takes place and this happens in the temperature

range of 300° C to 800° C (Ozawa *et al.*, 2000; Crozier *et al.* 2008). When in the metal, oxygen vacancies are available, ion moves in lattice quickly leading to playing major role in catalytic usage and opposite to it. While using ceria as a catalytic form, during reduction of NO_x, it absorbs O_2, and release O_2 for the oxidation of CO. It is because of its ability to transform, Ce^{+4} to Ce^{+3} state that depends on the partial pressure of exhaust gas. Nanosized ceria make it more operative in context of redox property (Sayle *et al.*, 2005).

Hirano *et al.* (1999) applied the ultrafine CeO_2 (cerium (IV) oxide) powder in the range of 10-25 nm during hydrothermal condition. They applied urea with a precursor of cerium (IV) sulfate and cerium (IV) ammonium sulfate. They concluded that the effect of concentration of urea and hydrothermal treatment temperature on the morphology and crystallite size of the synthesized particles and stated that the crystallinity and particle size of ceria was seen to be to less with an rise of urea quantity.

Hirano *et al.* (2000) made the crystalline cerium (IV) oxide nanoparticles during thermal hydrolysis in addition to cerium di-ammonium nitrate in the form of precursor. Further, they were prepared nanoparticles mixed with H_2SO_4 or $(NH_4)_2SO_4$ to find the effect of SO_4^{2-} on the ceria particles. Nanoparticles thus obtained were of 10 nm size. H_2SO_4 in addition to, the nano sized crystals were seen to be agglomerated into bigger 150-180 nm sized spherical particles.

Rao *et al.* (2003) investigated properties related to the structural and redox of ceria and ceria based materials. They concluded that under reduced atmosphere, the fluorite structure of ceria had retained up to 900 K. The lattice constant was seen to be enhanced with reduction temperature which indicates that the lattice expansion of its crystal structure, which was attributed to the reduction of Ce^{4+} ions into Ce^{3+}.

2.11.2 Evaluation of OSC in a Materials

The OSC can be determined by showing the equivalent amount of O_2 absorption/release per unit weight of the catalyst, (O_2) μmol/g of catalyst, Gupta *et al.* (2010). The change in valence of Ce^{4+} to Ce^{3+} or vice versa and the release of O_2 mostly takes place on the surface at while working at relatively less temperature moreover it is also feasible to average value of the temperature. This can be visualized from the temperature reduction program (TPR) profiles. Suitable redox property, i.e, the reduction at low temperature, is the necessary characteristics for oxygen storage materials, which is also narrated by Wang *et al.* (2006). Another author, Xiaodong *et al.* (2006) depicted the CO step pulses in lieu of H_2 and O_2 to evaluate the OSC. The total output quantity of CO_2 per gram of catalyst in the first ten CO pulses was measured and it suitably given the information on full OSC of the catalyst. Jia *et al.* (2008) also determined the CO and H_2 pulse injection to measure OSC in a material of catalytic.

Zhang *et al.* (2009) shown that the phenomenon of ceria has two points of reduction at 500˚C and 830˚C during TPR, that is related with the discharge of surface oxygen and bulk oxygen, respectively. In case of CeO_2-ZrO_2 mixed oxide, only a single peak was visible, which was attributed to the fact to the simultaneous release of oxygen from the surface and bulk owing to its high oxygen mobility. Meng *et al.* (2010) perfumed experiment and obtained the OSC of ceria-zirconia by the applied area of up-take H_2 in place of getting 600 ˚C in TPR. The average H_2 used peak area of two TPR profiles was used to determine the catalyst of OSC. Hongmei *et al.* (2010) calculated the value of OSC by injecting pulses of oxygen into the sample bed up to the point no oxygen drawn. Redox temperature of catalyst has been measured by thermo gravimetric analysis. Reduction temperature had shrunk from 757 to 486 ˚C when zirconia was doped with ceria. Lattice of CeO_2-ZrO_2 could generate oxygen vacancies which lead to rise the channel diameter for oxygen movement in the

lattice when doping of ZrO_2 in the CeO_2 and the reason of modifying the lattice structure in CeO_2-ZrO_2 was due to ZrO_2 (Wang *et al.,* 2006).

Measurement of OSC at constant oxidation and reduction state, which is called dynamic OSC can be used to excite the real operational condition, where exhaust gas fluctuated amongst the oxidizing and reducing atmosphere (Jia *et al.,* 2008)

Chung *et al.* (2009) employed the TGA method to describe the OSC by observing the variations in the weight under repeated heating in air atmosphere. Repeated Heating process consists three following step (i) first heating upto 900 ˚C (ii) make cold upto 150 ˚C and (iii) next heating up to 900 ˚C. the rates of heating and cooling were 5 ˚C/min. In the second cyclic heating there was a loss in weight of sample (Al_2O_3-$Ce_{0.5}Zr_{0.5}O_2$). This loss was used to measure the oxygen discharge characteristics of the catalyst in temperature between 300 to 800 ˚C. They also used H_2/CO pulse injection method for calculating the OSC of the sample.

Morikawa *et al.* (2008) calculate the OSC by using method of TGA with pretreatment at 500 ˚C of the sample (Al_2O_3-CeO_2-ZrO_2). The duration of treatment was 15 min. under the environment of H_2/N_2 and O_2/N_2. The change of environment was cyclic until weight balance of sample under both environments come to be nearly same.

2.11.3 Study of Surfactant and Synthesis Method to Prepare Nanofuel

Priya N S (2016) made cerium based high OSC different type nanoparticles, for example CeO_2, $Ce_xZr_{1-x}O_2$ ($0.4 \leq x \leq 0.8$), $Ce_{0.6}Zr_{0.4-x}Y_{1.3x}O_2$ and $Ce_{0.6}Zr_{0.4-x}Mn_xO_2$ (x =0.0, 0.1, 0.2, 0.3, 0.4; Y = Al, Bi, La, Nd). They also made structural characterization of these nanoparticles by X-rays diffractometric (XRD) technique. They found OSC capacity of these nanoparticles by TGA method. Physical and chemical characteristics was also found

by them. In the following section, some parts of her research has discussed, which is related to objective of this thesis. They are

- Selection of suitable surfactant.
- Selection of suitable nanoparticle in context of dispersion stability.
- Selection of suitable method of synthesis of nanofuel.
- Optimum concentration of nanoparticles.

They used different method and surfactant for preparing the highly stable nanofuel which could be used at least one week. Sodium dodecyl sulfate (SDS, anionic), Cetyl Trimethyl ammonium bromide (CTAB, cationic) and tween 20, tween 80 and oleic acid (which are non- ionic) used by them as a surfactant. In order to prepare nanofuel, they used tip sonication, magnetic stirring and combination of both method for selection of suitable technique for highly stable nanofuel. For the purpose of selection of a suitable surfactant, they used the CeO_2 with concentration 0.06 wt. % with and without adding surfactants and compare the relative stability of nanofuel which is shown in Figure 2.16.

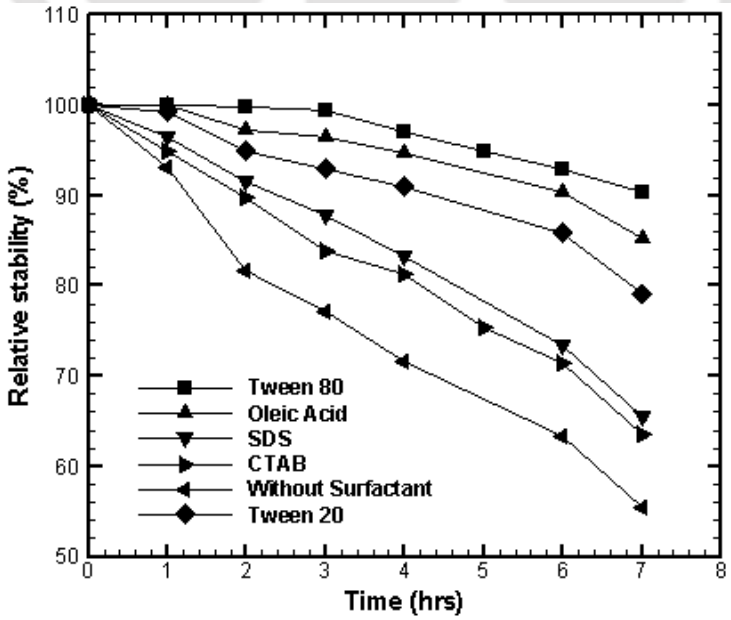

Fig. 2.16: Influence of different surfactants on the relative stability of nanofuel having 0.06 wt. % of CeO_2 (Priya N S, 2016).

Preparation technique was tip sonication method and the period preparation was 1 hr. under the static conditions (samples were examined for 7 hr). The relative stability of nanofuel was noticed 80 and 55 % after 2 and 7 hr respectively when there was no adding of surfactant. While relative stability of nanofuel was 63, 65, 78, 84 and 89 % when they used surfactants as CTAB, SDS, tween 20, oleic acid and tween 80 respectively at the end of 7 hr. It was 100 % stability upto 3 hr, when fuel was prepared by tween 80 while in case of tween 20 and oleic acid as a surfactants, stability was 100 % upto 1hr only. It was seen that after the 2 hr of nanofuel preparation by tween 20, a rapid sedimentations was found as compared to the oleic acid. The relative stability of nanofuel based on CTAB, SDS, tween 20, oleic acid and tween 80 were 14, 17, 42, 53 and 63 % respectively as compared to nanofuel based on without any surfactant at the end of 7 hr. It was observed that surfactant promote the physical stability of the nanofuel. Stability promotion was low in anionic/cationic surfactants while high in non-ionic surfactants as compared to without any surfactants. The reason behind of this was surfactant retained the particles dispersed in base fluid by electrostatic repulsive forces between the particles and hydrophobic surface force due to physical adsorption of surfactant by solid particles. This concept was also supported by Murshed *et al.* (2005).

Due to the size of ceria nanoparticles and high surface energy of solvent, ceria nanoparticles showed the tendency of grouping to each other and construction of the large entangled agglomerates. It was seen that the sedimentation rate of nanoparticles was more when no used of surfactant. Reason behind of this was the strong Van der Waals force of attraction between the nanoparticles because of their size. Enhancement of stability of nanofuel with adding of surfactant was because of ceria particle adsorbed the surfactant molecules by their hydrophobic segments with hydrophilic head directed towards the base fluid, which was also supported by Lisunova *et al.* (2006).

In case of CTAB and SDS surfactants, an electrostatic stabilization had achieved (as shown in Fig. 2.17) because of occurrence of negative and positive hydrophilic head charge in SDS and CTAB, serially which result in leading to higher rate of sedimentation of nanoparticles in solvent. The reason behind this was the formation of micelles and this tendency was come due to the occurrence of single carbon chain in CTAB and SDS (Tah *et al;* 2011). No doubt CTAB and SDS provided homogeneous solution by suitable technique, nevertheless preferably, it was not used in CI engine because of possibility of blocking or chocking in fuel injector and nozzle.

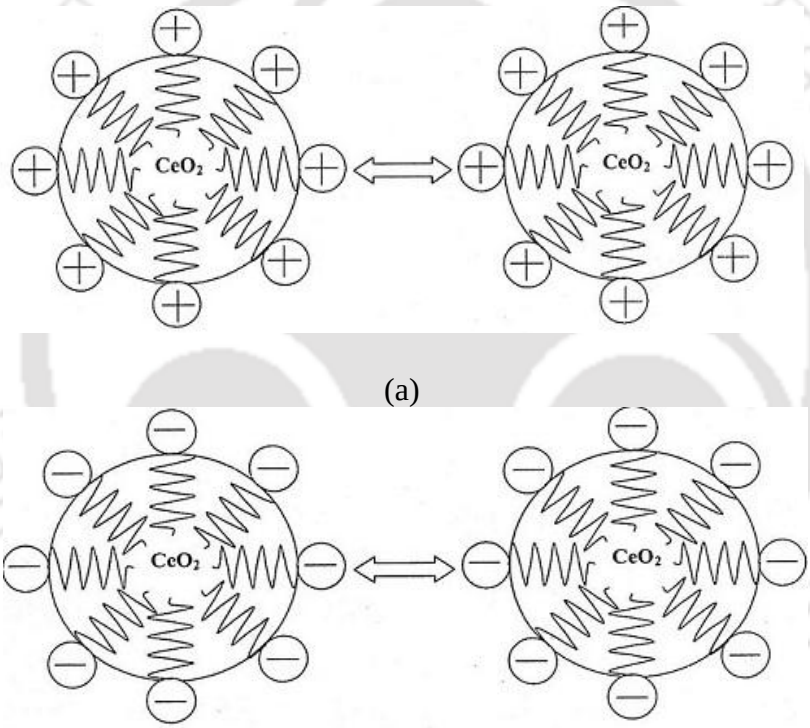

Fig. 2.17: Electrostatic stabilization mechanism of (a) CTAB and (b) SDS surfactant on nanofuel (Priya N S, 2016).

Non-ionic surfactants provided steric stabilization mechanism in nanofuel. Tween 80, tween 20 and oleic acid were associated with long chain molecules that attached with nanoparticles. Nonionic surfactant and nanoparticles were formed a layer between the particles and base fluid and δ was the thickness of adsorbed layer. These layers were

responsible for enhancement of potential between the particles and transmitted repulsive force between them. If h is the separate distance of two particles and $h < 2\delta$, resulting, solid repulsion between the particles due to adsorbed layers can overlap or become compressed. Steric stabilization mechanism of non-ionic surfactant has been shown in Fig. 2.18.

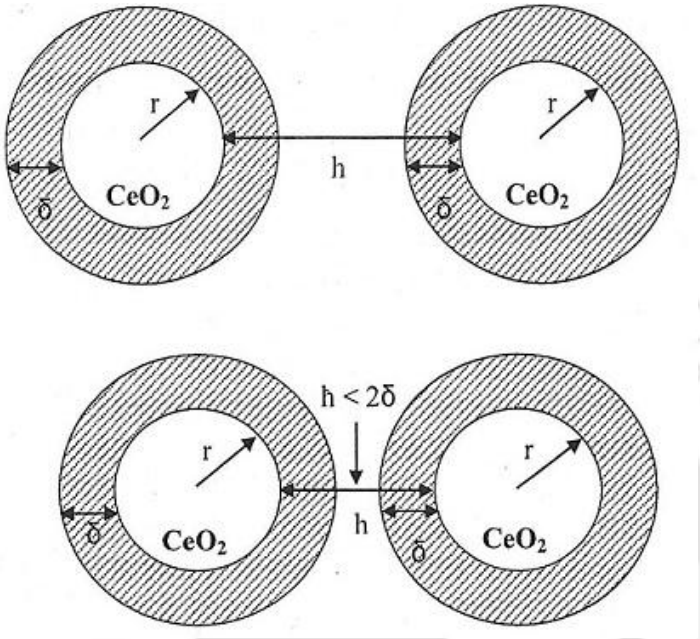

Fig. 2.18: Steric stabilization mechanism of non-ionic surfactant (Priya N S, 2016).

Tween 80 and tween 20 has different hydrophobic compound though they belong to same group. Lauric acid associates with tween 20 while oleic acid with tween 80 (Lorenz *et al.*, 1977). Due to steric stabilization, distance between the particles remain more that overcomes the Van der Waals force of attraction among the particles and that stabilization happens due existence of steric obstacles from non-ionic molecules. Because of ethylene oxide and long hydrocarbon chain as compared to oleic acid and shows the both lipophilic and hydrophilic properties, tween 80 makes more stable nanofuel as compared to tween 20 and oleic acid (Som *et al.*, 2012).

From the above observation and discussion, it was concluded that tween 80 based nanofuel provides enhanced stability. Up to 3 hr, rate of sedimentation was 0% and 10% upto 7hrs.

In case of oleic acid, 100 % stability was for one hour only and at the end of 7 hr, it was seen that increased of sedimentation was 33% as compared to tween 80 based nanofuel. With progress of time, stability of nanofuel decreases reason behind of this weakening of surfactant layer of nanoparticles because of repeated impact between them. It was observed that after the synthesis, nanoparticles remain stable, but after the progress of time, it starts to settle down and rate of sedimentation depends on which type of surfactant has used to prepare the nanofuel. Consequently, for further examination to select a most suitable preparation technique of nanofuel, tween 80 was used as a surfactant with different concentration of nanoparticles.

2.11.4 Effect of Preparation Technique on the Relative Stability of Nanofuel

Priya (2016), in order to find more suitable technique for preparation of nanofuel, firstly magnetic stirrer method was used surfactant as a tween 80. The period of method was 2 hr and the observation period was 72 hr. Nanoparticles had taken as CeO_2 at different concentration. After the preparation of nanofuel, it was observed that fast sedimentation was happening in all cases. During the test sample were retained motionless. For the period of 2 hr after synthesis of nanofuel relative stability was 100 % but after 2 hr of the nanofuel synthesis, it was seen that rapid settle down of nanoparticles with increase of nanoparticle (CeO_2) concentration. Because of small concentration of nanoparticles, particles control the repulsive force and attractive force acting amongst them and this was due to the enough space between them. Due to the lack of repulsive and attractive forces, nanoparticles repeatedly collides against each other and the reason behind this Brownian motion which leading to weakening of adsorbed surfactant layer. Due to progress of time, even at small concentration of nanoparticles, particles began to grouping and then collection and consequently gravitational force also impacted the rate of sedimentation. Effectiveness of van der Waals force of attraction was increased, when concentration of particles was

increased and this was because of low distance among the particle which leading to grouping and collection of particles. Consequently, rapidly fell of stability of nanofuel. In case of magnetic stirring method, due to the viscous effect, temperature was also enhanced resulting weakening of adsorbed layer of the nanoparticles. Thereby, it was seen that agglomeration of nanoparticles which results sedimentation of nanoparticles. For the particle concentration of 0.02, 0.04, 0.06, 0.08 and 0.1 wt. % of CeO_2, the respective relative stability was 72.8, 71.3, 68, 64.6, and 61.5 % and this stability was after 72 hr of nanofuel preparation which has been shown in Fig. 2.19.

The second method for nanofuel preparation was tip sonication method. Surfactant used as tween 80 with different concentration of nanoparticles (CeO_2). Period of nanofuel preparation was 2 hr and observation period was the 72 hr. Nanofuel was prepared in tip sonicator device. Ice bath was used to maintain the constant temperature and that constant temperature was 35 ˚C. after the sample preparation it was observed that relative stability was in the range of 93 % for all concentration of CeO_2 after 72 hr of sample preparation.

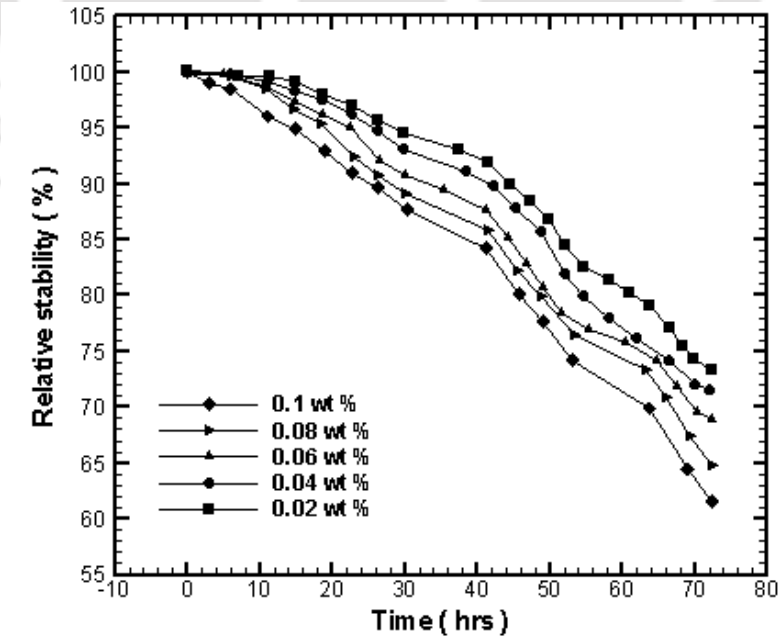

Fig. 2.19: Relative stability of nanofuel prepared by magnetic stirrer for 72 hrs (Priya N S, 2016).

It was also observed that, stability of nanofuel prepared by tip sonication method was more as compared to magnetic stirrer method. At the finishing of 168 hr, the relative stability of nanofuel was 93.5, 91.4, 87.0, 86.0 and 84.6 % at the concentration of 0.02, 0.04, 0.06, 0.08 and .10, respectively and the 100 % stability was seen for the period of 4, 3, 3, 2 and 1 hr for corresponding nanoparticles concentration, which is shown in Figure in 2.20. With progress of time, reduction of stability of nanofuel was due to depletion of adsorbed layer of surfactant covering the nanoparticle. Reason behind this was, collision among the particles which leading to reduction of electrostatic repulsive forces and hydrophobic surface forces. In this situation, Van der Waals forces dominant over electrostatic repulsive forces and hydrophobic surface forces resulting aggregation and agglomeration and due to gravitational force, nanoparticle was started to settle down. Comparison of result from Figs 2.16 and 2.20, it was observed that sedimentation of nanofuel was 1 and 11 % for the sonication period of nanofuel by 2 and 1 hr, respectively at end of 7 hr.

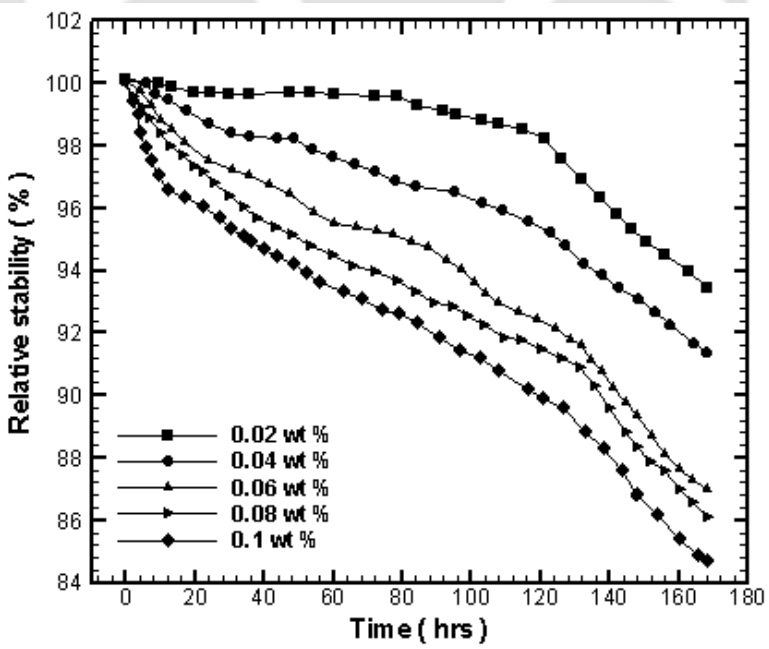

Fig. 2.20: Relative stability of nanofuel prepared by tip sonicator for 168 hrs (Priya N S, 2016).

Spreading stability of nanofuel depends on various forces such as Van der Waals force of attraction, electrostatic force of repulsive and gravitational force. In both methods of nanofuel preparation (magnetic stirrer and tip sonication) as discussed above, it was observed that 0.02 wt. % particle concentration was the optimum value for more stable for longer period of time as compared to other value. Van der Waals force of attraction happen more Influential when nanoparticles occur nearby under the range of equilibrium distance and this happens in the course of Brownian motion of nanoparticles which leading to attraction of two particles resulting increasing the size of accumulation and consequently force of gravitation effect the sedimentation. When concentration of CeO_2 becomes more then above incidence is more considerable. For the nanoparticle concentration of 0.02, 0.04, 0.06, 0.08 and 0.10 wt. %, the respective ratio between volume of liquid and volume of particle was 3.6×10^{10}, 1.8×10^{10}, $1.2x\ 10^{10}$, 0.9×10^{10} and 0.72×10^{10}. From the above data, it was seen that, volumetric ratio was decreased with an increase of nanoparticle concentration. Nanoparticle concentration is proportional to rate of sedimentation and that information confirms the above observation. Rate of sedimentation is assisted by force of gravitation and it is more effected in nanofuel even in lower concentration of particles but with time.

For the best suitability of synthesis technique of nanofuel based on relative stability comparison of synthesis technique namely tip sonication, magnetic stirrer and combined of both was carried out (shown on Fig. 2.21). In case of magnetic stirring method, because of rapid sedimentation, 72 hr were taken for observation of relative stability of nanofuel while in case of tip sonication technique 168 hr were taken for observation of relative stability of nanofuel. For case of combined technique, it was the same as tip sonication. In three method of nanofuel synthesis, poor quality of stability was shown by magnetic stirrer method under

the range of 72 hr while excellent result was shown by combined method of nanofuel synthesis as compared to other individual method till 168 hr of sample preparation.

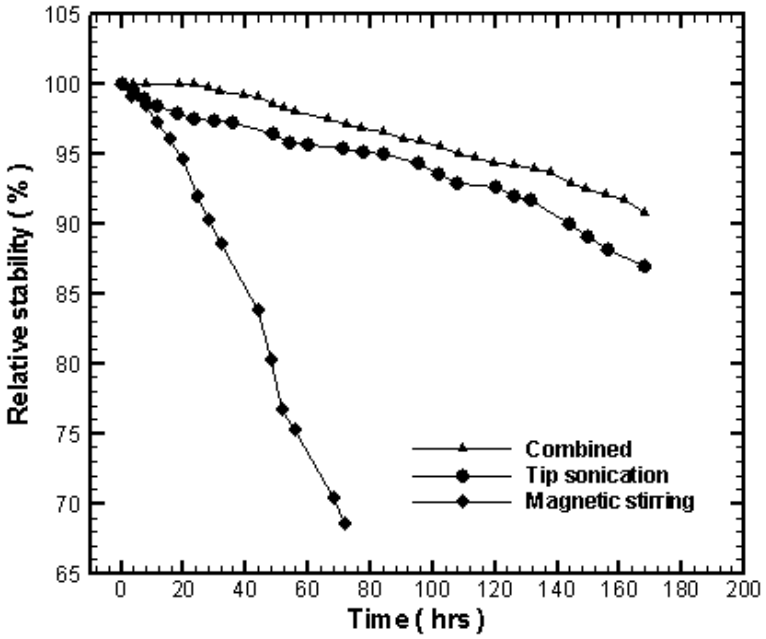

Fig. 2.21: Comparison of relative stability of 0.06 wt. % of nanofuel (Priya N S, 2016).

Table 2.6: Relative stability of nanofuel based on synthesis technique (Priya N S, 2016).

	Magnetic Stirring	Tip Sonication	Combined Technique
After 72 hr	68.4 % relative stability	95.3 % Relative stability	97 % Relative stability
After 168 hr	Not applicable	87 % Relative stability	91.6 % Relative stability
100 % relative stability till	1 hr	3 hr	24 hr

Table 2.6 shows that the combined method of nanofuel synthesis prepares highly stable nanofuel as compare to other method. Table 2.6 also discussed about the relative stability of nanofuel after 72 hr and 168 hr. It included the time for 100 % relative stability. In combined method, sample sonicates for 30 min and then 30 min for magnetic stirring alternatively for the duration of 2 hr. Because of this, nanoparticles get sufficient time for

coating of surfactant. From the above discussion and investigation, it was concluded that combined method of nanofuel synthesis provides homogeneous distribution of nanoparticle in base fluid and this method also provides greater stability.

2.12 Literature Closure

PMC is a primitive combustion technology which provides several advantages. PMC in now days is a new dimension in the field of combustion which belong to IC engine, heat exchanger, turbine and many more and in the current times, more attention has been paid towards the development of burners which works on PMC for domestic and industrial applications. Basic studies and research have been carried out with different PM and the contribution of it in giving healthier stabilization or great efficiency and small emissions were discussed largely. The following important points have been highlighted of the above studies.

- Variety of PMC materials whose range belong from metal to ceramic were investigated. The application of two dissimilar materials (one with high emissivity, conductivity and the other with smaller) or it has been also conceptualized with the two layers of the similar material with different thermo-physical and radiative properties.
- The study on single layer burners have been explored to a greater extend. After the vast discussion, it was found that the porosity of material largely affects the flame stabilization process. The reason behind this was change of radiative properties and this radiative property greatly rely on porosity.
- Optimum selection of porous material is important because the properties of material largely affect the flame speed, radiation output and heat recirculation. From

the studies, it was concluded that working conditions are also largely accountable for the flame to stabilize at a specific location.

- Large number of studies were explored with different materials and methane as a fuel. Regarding the domestic cooking applications, fuel such as LPG, natural gas, biogas and kerosene were used. Nevertheless as compared to CH_4 the reports on the other domestic fuel still inadequate.
- The current invention in LPG cooking stove with porous radiant burner without external air supply called self-aspirated has added a new promising scope for this technology in domestic sector. In recent past, this self-aspirated PRB with LPG have been developed for the input power range of (1-3 kW) and medium scale (5-15 kW) in IIT Guwahati. For low wattage applications, self-aspirated PRBs are economically and also environment friendly. Studies on such burners with liquid and gaseous fuels are yet to be carried out.
- Currently, amongst the gaseous fuels, LPG has gained large attention. The reports on Liquid fuels combustion associate with PM are not much and the details about complete evaporation of the liquid fuel such as kerosene is not available. Further, no studies high thermal efficiency employing liquid fuels is reported.
- Therefore, it is necessary to focus on liquid fuel especially on complete vaporization. It was observed that PRB has been tested in pressure kerosene cooking stove but with external air supply which is not suitable for domestic purpose. Therefore, so it is essential to investigate or develop a self-aspirated pressurized kerosene with porous radiant burner, which can produce high thermal efficiency and low emissions.
- In the combustion process, metals are widely used owing to their properties of producing oxygen while it's burning. It is the property of the metal to follow oxygen

is the primary objective of its usage in catalytic application, and is named as oxygen storage capacity (OSC). This property is very much important while heating the metals in nanosized.

- Several harmful gases such as CO, NO_x, CO_2 and unburnt hydrocarbons are reduced to great extent by using the OSC of its three ways catalyst (TWC). Under rich fuel content, the TWC supplies the oxygen to CO and hydrocarbons and also removes oxygen from NO_x from lean fuel mixture. The OSC can be determined by showing the equivalent amount of O_2 absorption/release per unit weight of the catalyst, (O_2) µmol/g of catalyst.
- Researchers are being attracted towards cerium based oxides due to its applicability in catalytic usage. It is popular in earth metals as its ability to alter valance position from Ce^{4+} position to Ce^{3+} position and opposite to it. In it the electronic placing in the orbit is attributed to loss or addition of oxygen, which is performed at high temperature. While using ceria as a catalytic form, during reduction of NO_x, it absorbs O_2, and release O_2 for the oxidation of CO. It is because of its ability to transform, Ce^{+4} to Ce^{+3} state that depends on the partial pressure of exhaust gas. Nanosized of ceria make it more operative in context of redox property. There are various type of cerium based high OSC nanoparticles, for example CeO_2, $Ce_xZr_{1-x}O_2$ ($0.4 \leq x \leq 0.8$), $Ce_{0.6}Zr_{0.4-x}Y_{1.3x}O_2$ and $Ce_{0.6}Zr_{0.4-x}Mn_xO_2$ (x =0.0, 0.1, 0.2, 0.3, 0.4; Y = Al, Bi, La, Nd). From this cerium based nanoparticles, $Ce_{0.6}Zr_{0.1}Al_{0.26}O_2$ was the best nanoparticle in context of OSC and specific surface area. Combined method was the best suitable technique for nanofuel preparation. Tween 80 was the superior surfactant as comparison to tween 20, CTAB and oleic acid. This nanofuel already used in diesel engine without changing any design of engine.

- Results shows that, performance was superior with this nanofuel in diesel engine compared to conventional diesel. But yet, it has not used in modified kerosene cooking stove like pressure kerosene cooking stove with porous radiant burner. So it is also necessary to investigate the performance of modified kerosene stove with this nanofuel.

2.13 Objectives of the Present Work

In view of the above literature summary made on the available literatures, the following objectives are considered in the present work.

- To develop a self-aspirated porous radiant burner for pressure kerosene cooking stove for domestic cooking application (1.5-3 kW) and also to investigate the effects of the power input on the thermal efficiency and emissions of porous radiant burner and compare the same with conventional pressure kerosene cooking stove of same capacity.
- To test the effect of environmental temperature, vessel diameter and nozzle diameter on thermal efficiency and emissions of the self-aspirated pressurized kerosene cooking stove with porous radiant burner of capacity 1.5-3 kW.
- To measure the temperature distribution in axial and radial directions of the self-aspirated pressurized kerosene cooking stove with porous radiant burner of capacity 1.5-3 kW.
- To prepare a cerium based nanofuel with kerosene and test it with the newly developed self-aspirated pressurised kerosene cooking stove with porous radiant burner and in conventional pressure kerosene cooking stove (1.5-3 kW).
- To find the thermal efficiency and emissions at different nanoparticle concentration prepared in different methods of nanofuel preparation with self-aspirated

pressurised kerosene cooking stove with porous radiant burner and conventional pressure kerosene cooking stove of capacity 1.5-3 kW.

- To find the optimum concentration of nanoparticle prepared in different methods of nanofuel preparation with self-aspirated pressurised kerosene cooking stove with porous radiant burner and conventional pressure kerosene cooking stove of capacity 1.5-3 kW.

Chapter 3

Experimental Setup and Procedure

In this chapter, the complete description of the experimental is presented. Methodology and technique for finding the thermal performances of the newly developed PRB based stove as well as the conventional stove are discussed. Different experimental tools and instruments with specification related to the experiment are also discussed in this chapter. Finally, the formulations used for the calculation of the thermal efficiency of the burners are presented.

3.1 Introduction

It is a well-known fact that the porous media combustion technology is an established technology. However, in the case of liquid fuel, the technology is not matured enough. In certain industrial applications, some study has been done to perceive the combustion characteristics of liquid fuels such as kerosene, heptane, ethanol, etc. However, for domestic applications, no study has been reported. In a developing country like India, kerosene is mostly used for cooking application in the rural areas and some of the urban areas. Generally, pressure kerosene cooking stoves are used for this purpose. Free flame mode of combustion exists in pressure kerosene cooking stove. To utilize the benefits and also to examine the suitability of porous medium combustion in improving the thermal performance of a conventional burner, a pressure kerosene stove with PRB has been developed.

3.2 Design Criteria of Cooking Stove

Output power requirement is the basic design criteria of the cooking stove. For domestic cooking stove, the required output power varies in the range of 0.6 – 2 kW (Mukunda *et al*., 1988). Others parameters considered for the design criteria of the cooking stove are low ignition time and high combustion efficiency. High combustion efficiency means low CO and NO_x emissions and better flame stability. In general, the commercially available kerosene cooking stoves are operated at 2 kW input power. In the present case, a BIS (Bureau of Indian Standards) specified pressure kerosene stove has been employed, which was manufactured by M/s. Mira Udyog, Rajkot, Gujrat. In the following sections, construction details and performance of conventional pressure kerosene stove with different types of burners available in the market have been described.

3.3 Construction Details of Conventional Pressure Kerosene Stove

A BIS pressure kerosene stove consists of fuel tank, hand operated plunger, a spirit cup, a vapour burner, a fuel regulator, a flame holder, a heat shield and a potholder. These are the principal components of the BIS pressure kerosene stove, which is shown in Figure 3.1 (a). Others parts of the pressure kerosene stove are fuel supply line, pressure gauge and pin. Pin is used for removing the foreign particles that create a blockage in the nozzle. Vapour burner comprises of one rising tube, two ascending and two descending tubes. It also contains a flat circular chamber called vaporizer (or) flame holder as shown in Figure 3.1 (b). A spray nozzle is attached in between the two descending tubes. The working principles of the major components of the pressure kerosene stove have been listed below.

- Fuel tank – It stores the kerosene. It is connected to the spray nozzle through the supply line.
- Hand operated plunger – It is used to pressurize the kerosene with the help of hand.

- Spirit cup – It collects the small amount of kerosene for initial burning.
- Vapour burner / Flame holder – It helps to vaporize the kerosene and to guide the flame.
- Fuel regulator – It is intended to control the fuel flow rate.
- Heat shield – Its work is to prevent the heat loss to the surrounding.
- Pot holder – Its work is to provide support to the cooking vessel.

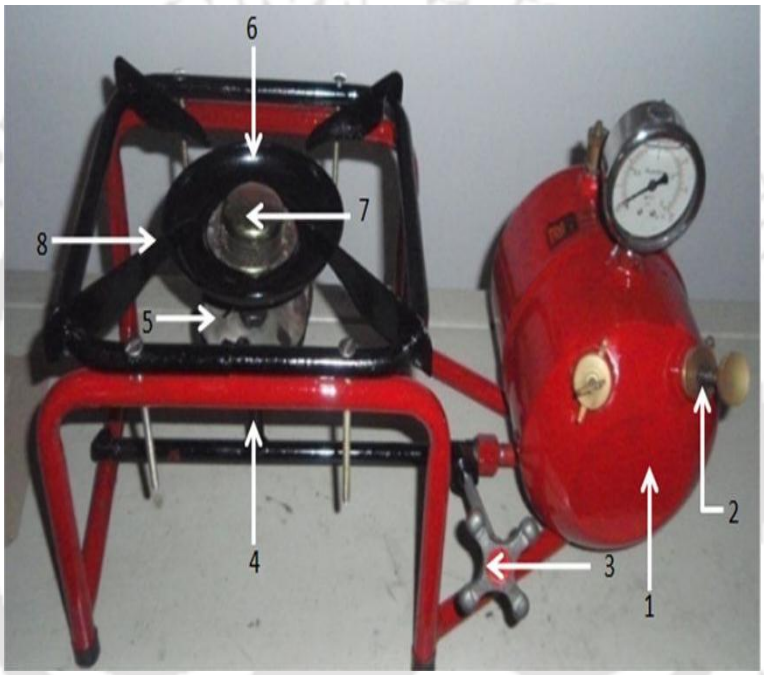

Fig. 3.1: (a) Different part of kerosene stove 1: Fuel tank, 2: Hand operated plunger pump, 3: Fuel regulator, 4: Rising tube, 5: Spirit cup, 6: Heat shield, 7: Vapour burner with flame holder, 8: Pot holder.

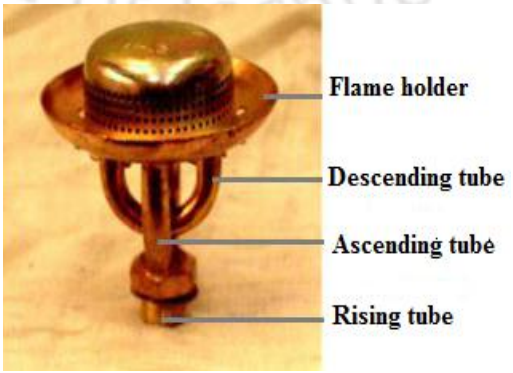

Fig. 3.1: (b) Vapour burner.

When the fuel tank is pressurized by means of hand plunger, kerosene flows to the vapour burner through the rising tube. Kerosene is vaporized here and the vapour is sprayed through nozzle. This kerosene vapour mixes with air and burn after mixing, which gives a rising yellowish orange flame that indicate incomplete combustion. The yellowish orange flame can be seen from Figure 1.2 which is already illustrated in Chapter 1. This type of combustion takes place in gaseous environment and is called as free flame combustion. In this type of combustion, the convection heat transfer remains dominant.

3.4 Performance Study on Conventional Kerosene Stoves

The performance study on cooking stoves comprises the evaluation of thermal efficiency and emissions. A survey has been done on the different types of burners present in the market, which are used in conventional pressure cooking stoves. Generally, three types of burners are used in the Indian houses and commercial places namely venus burner, silent burner and roarer type burner (shown in Fig. 3.2). Thermal efficiency of the CB and PRB of the BIS pressure kerosene stove were estimated by conducting water boiling test (WBT) following the guidelines prescribed in the Bureau of Indian Standards (IS 10109:2002). The emission analysis has been done by the hood method. Construction details and operating principle of PRB with BIS kerosene pressure stove are discussed in the following section.

(a) (b) (c)

Fig. 3.2: Conventional burners available in the market: (a) venus burner (b) silencer type burner (c) roarer type burner.

3.5 Description of Experimental Setup Based on PRB

PMC is the flameless combustion, which is different from the free flame combustion. In PMC, the flame is entrapped in the porous media due to which, the radiation becomes the dominant mode of heat transfer. Experimental set up was developed using a BIS pressure kerosene cooking stove (as shown in Fig. 3.3) in which, the burner uses the concept of PMC. Burner operates in the radiant mode and there is no flame seen over the burner surface and hence, this is called flameless combustion. Same as the conventional stove, experimental setup comprises of fuel tank, hand operated plunger, pressure gauge and pressure valve. Other parts of experimental setup are stainless steel metal casing also called burner casing, which holds the PRB and mild steel perforated sheet (vaporizer plate), conical ring, vaporizing cup, a rising tube attached to the vaporizer pipe, burner port, combustion zone and conical ring. The mild steel perforated sheet acts as a preheater. In the following section, the working principle of the components of the experimental setup are discussed. These final dimensions of the burner have been finalized based on the stablizaiton criteria, which has been discussed in chapter 4 (refer to section 4.2)

- Vaporizer pipe (galvanized steel, ID = 6 mm, OD = 8 mm, height = 105 mm) – The role of vaporizer pipe is to assist the vaporization process that happens during the combustion.
- Burner port – It is an air entrainment system. When vaporized kerosene is coming through nozzle, due to the high velocity of vapour, static pressure of air around the nozzle is decreased. As a result, the primary air is sucked in the burner port through the slots provided near the nozzle. This can also be seen in Figure 3.3.
- Vaporizing cup (bottom diameter = 80 mm, top diameter = 120 mm, height = 20 mm) – Its work is to collect small amount of kerosene for initial burning.

- Vaporizer plate – Its work is to preheat the incoming air fuel mixture.
- Combustion zone – Combustion zone is made of silicon carbide porous matrix with diameter 70 mm and thickness 20 mm. In the combustion zone, due to high porosity, combustion takes place and flame propagates.
- Burner casing (stainless steel, ID = 72 mm, OD = 76 mm) – It holds the PRB and vaporizer plate. Base plate of the burner casing has a central hole of diameter 30 mm and two 32 mm × 9 mm slots to allow the two top ends of the vaporizer pipe to bring in contact with the vaporizer plate (refer Fig. 4.12)
- Conical ring – It is also called radiation shield. It is provided across the top surface of the casing to restrict the heat transfer to the sides and direct the same to the load.
- Stand – It holds the cooking vessel.

The operating principle of the stove is as follows. Same as conventional pressure kerosene stove, initially through a burning wick, a small amount of kerosene is burnt in the vaporizing cup. During the burning of kerosene, vaporizer plate receives heat from the flame. Kerosene converts into vapour form, when the vaporizer plate receives a sufficient amount of heat. The kerosene vapour mixes with air and moves to the PRB and burns within the porous matrix. Initially, air fuel mixture obtain heat through convection and then porous matrix starts appearing in the radiant mode. Vaporizer plate continues to receive heat from the porous media and transfers this heat to kerosene and the cycle continues. At this position, the burning wick is extinguished and on attainment of steady state, various measurements were taken.

Figure 3.3 shows the schematic view of the experimental setup. This image gives a better - comparison with the conventional stove shown in Figure 3.1 (a). There are two important parts of PRB stoves, which are not present in the conventional stove: burner casing (holds porous burner) and burner port. Additionally, in the developed stove, there is no flame

holder because porous media itself act as a flame holder. Flame is trapped in the porous media and stabilize due to its porous nature. Several experiments were conducted at different stand heights and nozzle diameters.

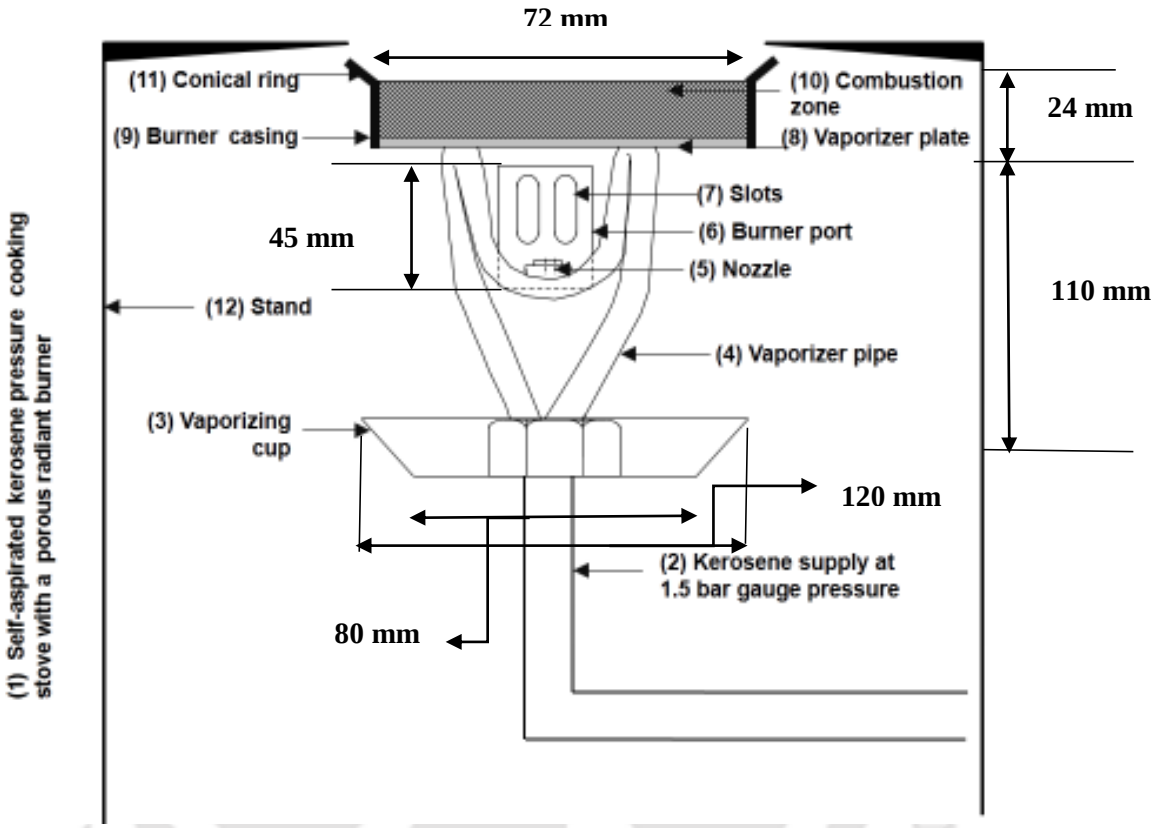

Fig. 3.3: Schematic of the self – aspirated kerosene stove with PRB.

3.6 Measurement Tools and Techniques

For the measurement of weight of stove, water, aluminium vessel and fuel consumption, a strain gauge weighing machine (least count: 1 g, range: 30 kg) is used, which is shown in Figure 3.4. Thermal efficiency is defined as the ratio of heat absorbed by the load to the heat given by fuel. Thermal efficiency of both the CB and PRB are measured by WBT following the guidelines in Bureau of Indian Standard (IS 10109:2002). The procedure followed in WBT is briefly described in the following section.

Fig.3.4: Strain gauge based weighing balance machine.

Ignition of the stove is done by burning wick. Optimal size of aluminum vessel along with lid and stirrer for the experiment are selected and filled with a known amount of water at room temperature (~30 °C). In the WBT, initially the stove is allowed to operate for 5 min (according to BIS for the attainment of steady state) and then it is kept over the platform (dimension: 400 mm x 300 mm) of the weighing machine, for measuring the initial weight of the stove. Weight of the vessel (with lid and stirrer) along water is measured separately with the help of a weighing balance machine. Initial temperature (T_1) of water is measured using glass-in-mercury thermometer (accuracy ± 0.5 °C). After measuring the initial weight of stove, it is unloaded from platform and then vessel is kept above the burner. Water is heated up to 90 °C and for maintaining the uniform temperature in the vessel, stirring is done parallel and continued until the end of the test, when the temperature of water is reached (T_2) 90 ± 0.5°C. At this phase, the burner is quenched. The time required to heat the water from room temperature to 90 °C is noted and the mass of the fuel consumed during this period is recorded by the difference in weights of the stove before and after heating. In every case, the experiments were repeated at least three times and the average

of the three was taken for the analysis. The percentage of thermal efficiency η_{th} of the stove is calculated based on IS 10109:2002 prescribed formula given by Eq. (4).

$$\eta_{th} = \frac{Heat\ Output}{Heat\ Input} = \frac{\left(m_w \cdot C_w + m_p \cdot C_p\right)\left(T_2 - T_1\right)}{m_f \cdot \mathrm{CV}} \qquad \text{.....(4)}$$

Where m_w is the mass of water, C_w is the specific heat of water, m_p is mass of vessel along with the lid and stirrer, C_p is the specific heat of the vessel material (aluminium), m_f is the mass of the kerosene consumed and CV is the lower calorific value of kerosene (43890 kJ/kg). The calorific value is taken from the BIS standard (IS 10109:2002). Properties of the kerosene is presented in Appendix – I. The uncertainty in the thermal efficiency was found to be ± 1.40 %. The detailed uncertainty analysis is presented in Appendix – II.

To compare the thermal efficiency and emissions of the CB with PRB, a market survey was carried out to get the various types of burners used in the conventional pressure kerosene cooking stoves (discussed in section 3.4). Three types of burners were selected from the Indian market (shown in Fig. 3.2). The measured thermal efficiency of the CB (venus burner) was in the range of 48.5 – 58 %. For different powers, the measured efficiencies of the conventional pressure kerosene cooking burners are shown in Figure 3.5.

Height of the flame increases with the increase in the power input and this causes an enhanced heat loss by convection. Hence, the observed trend is the reduction of the thermal efficiency with the increase in input power. For emission analysis, the flue gas sampling was done according to the IS 10109: 2002. For flue gas sampling, a standard specified hood shown in Figure 3.6 was used. It is made according to the BIS standard as per the dimensions mentioned. The hood is placed above the burner.

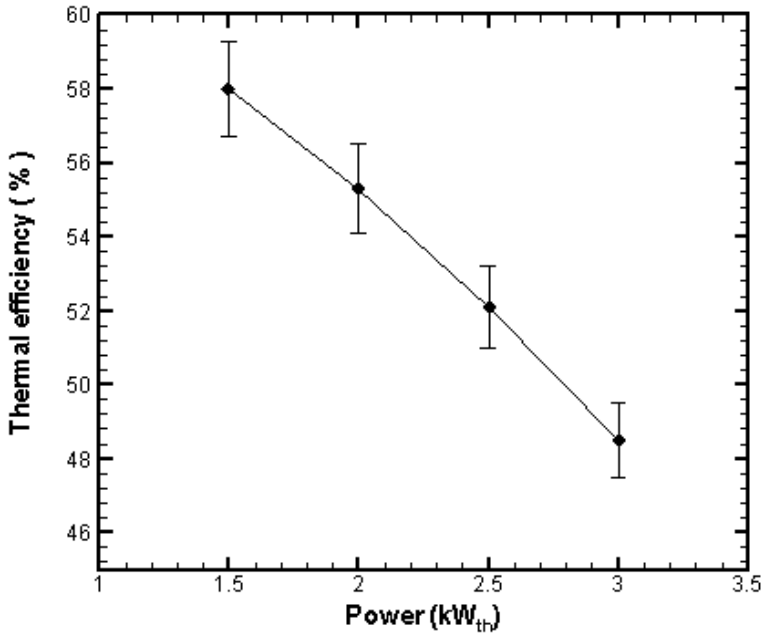

Fig. 3.5: Effect of power intensity on the thermal efficiency of the conventional pressure kerosene cooking stove.

A portable flue gas analyser probe is placed in the first sampling hole of the hood. The main aim of the hood is to separate the flue gases from the atmospheric air. The portable flue gas analyser (Greenline 8000) is used for recording the CO and NO_x emissions.

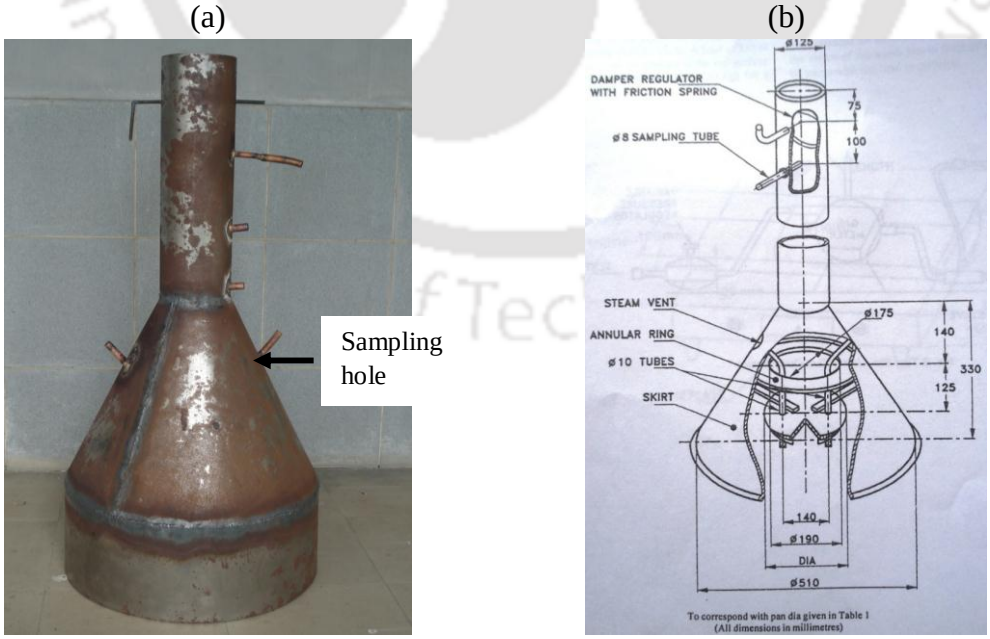

Fig. 3.6: Flue gas sampling (a) Pictorial view of the hood (b) Schematic of the hood (imported from IS: 4246).

The detailed specifications of the instrumentation/ equipment used in the experiments are given in Appendix - III.

The typical measured emission levels of the pressure kerosene cooking stove with the CB is shown in Figure 3.7. From Fig. 3.7, it was found that with the increase in the input power, both the CO and NO_x emissions increases. In CB, the combustion remains incomplete resulting in high CO emission. Reason behind this is the lower residence time combined with insufficient air. With increase in power input, the requirement of air increases. However, in the case of CB, the design is done in such a way that the burner does not permit more air entrainment. As a result, the air-fuel mixture is more fuel rich and hence results in the increased amount of CO emission. A similar rhythm of NO_x emission has been also observed with the increase of input power. Because the fuel rich combustion is responsible for the attainment of high temperature in the reaction zone, which leads to high NO_x emission. Both the rise in CO and NO_x emissions and the maximum values of emissions observed were much higher than the recommended values of World Health Organisation (Kandpal *et al.*, 1995). It is required to measure the temperature distribution of the PRB as well as CB because temperature distribution shows the physical symptoms of burner. Temperature distribution gives certain insights on the amount of CO and NO_x emissions. The temperature of the PRB at several locations are measured using specially made metal-sheathed K-type thermocouples shown in Fig. 3.8 in axial as well as radial directions. Axial and radial temperature distributions have been discussed in the next chapter. The readings from the thermocouples were interpreted with a data acquisition system, Agilent 34972A), which converts the electrical output into the corresponding temperature.

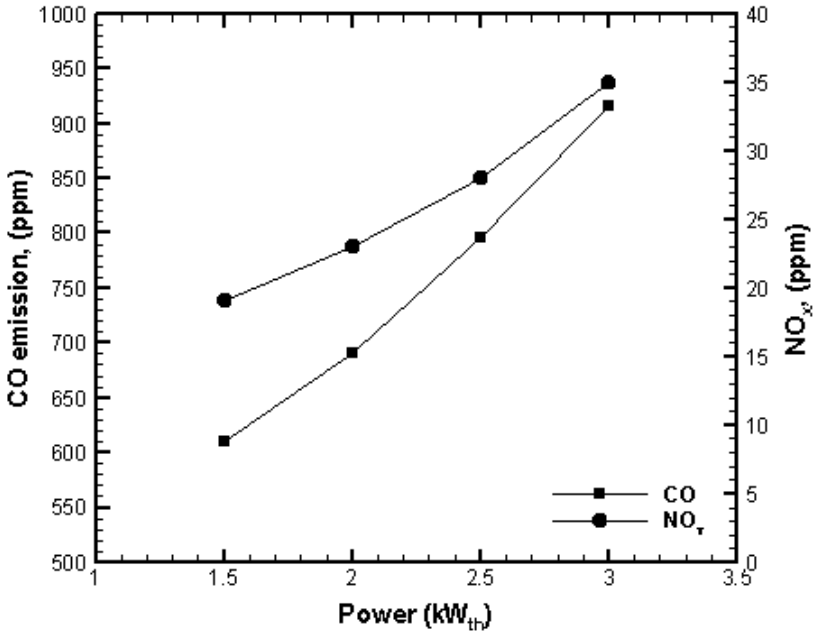

Fig. 3.7: Emission characteristics of a pressure kerosene cooking stove with CB.

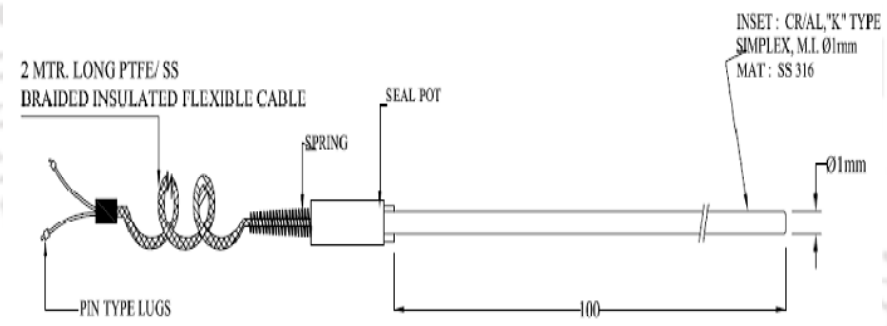

Fig. 3.8: Specifications of the metal-sheathed K- type thermocouple (all dimensions are in mm).

3.7 Preliminary Studies on PMC with Conventional Kerosene Burners

Basic criterion for the selection of a cooking stove is based on the output power requirement. For domestic cooking, the required output power range is 0.6 – 2 kW (Mukunda *et al*., 1988). Low ignition time, high combustion efficiency, low pollutant emission and better flame stability are the other parameters to be considered for the design

of a stove. In the present study, a BIS specified pressure stove was used. From the literature survey, it is observed that many researchers claim that the PMC with kerosene has a complete vaporization problem. This lead to the usage of LPG or electricity as a secondary heat source for vaporization of kerosene by many researchers. Reason behind this is the low contact area between the vaporiser tube and porous media. The present section discusses about four different types of burners (shown in Figure 3.9) whose surface area was increased to avoid the problem of vaporization. The burner pipe is of 8 mm diameter and made of copper. As the proper accuracy of nozzle and difference between the height of nozzle surface and burner surface could not be maintained properly, the burner was not used for further experiments.

Fig. 3.9: (a) Different type of helical copper wire burner.

Fig. 3.9: (b) Different type of non-helical copper wire burner.

3.8 Design Criteria and Selection of Porous Radiant Burner

The most important design criterion for PRB construction is the selection of the material. The material should possess good thermo-physical properties such as high emissivity, high thermal conductivity, low thermal expansion and high temperature resistance, as it helps in improving the heat transport from the burned gases to the unburned reactants. Besides this,

the other factors to be considered are the length of the porous bed, length of the preheating and combustion zones, shape and orientation of the combustion chamber etc. (Mujeebu *et al*., 2009a). The flame stabilization process is very complex as it involves an intimate coupling of combustion, heat transfer and fluid dynamics. Therefore, a proper selection of porous medium helps in the stabilization of flame within the PRB. The materials used in the experiments for the construction of porous burners are SiC, Al_2O_3 balls and perforated sheets, which are shown in Figure 3.10. Table 3.1 gives the dimension of the porous material.

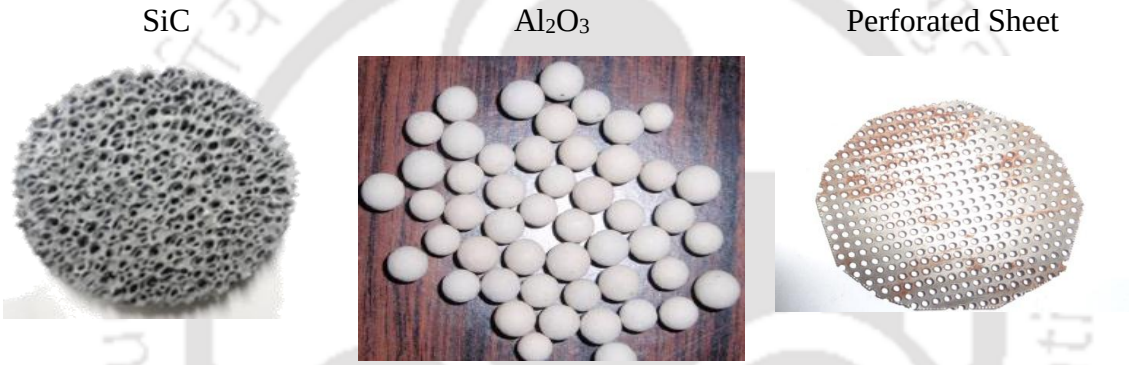

Fig. 3.10: Pictures of different types of materials used for PRB construction.

Table 3.1: List of materials used for PRB construction (all data in mm).

Materials	**Pore size (ppi)**	**Diameter**	**Thickness**	**Porosity (%)**	**Hole diameter**
SiC	10	70	20	90	-
Al_2O_3	-	5	-	30, 40	-
Perforated sheet	-	70	2	12, 17, 25	1.25, 1.5, 1.8

3.9 Modification of Burner Design (Vaporizer Tube)

As discussed earlier, in PMC for liquid fuel such as kerosene, complete vaporization is very difficult to achieve. Reason behind this is the less contact area available between the porous media and burner (vaporizer tube). Many researchers had used LPG, electric heater etc. for achieving complete vaporization in the pressure kerosene stove with PRB. During the

experiment, it was found that combustion inside the porous media was not uniform. It was due to a blockage of vaporizing plate between the nozzle and porous media. Therefore, a new set of burners are developed with modified dimensions without the vaporizing plate as shown in Figs. 3.11 and 3.12. The burners were fabricated in collaboration with Servals Automation Pvt. Ltd., Chennai. The main objective of the design is to allow the fuel mixture completely combusted inside the porous media without any blockage between the nozzle and porous media.

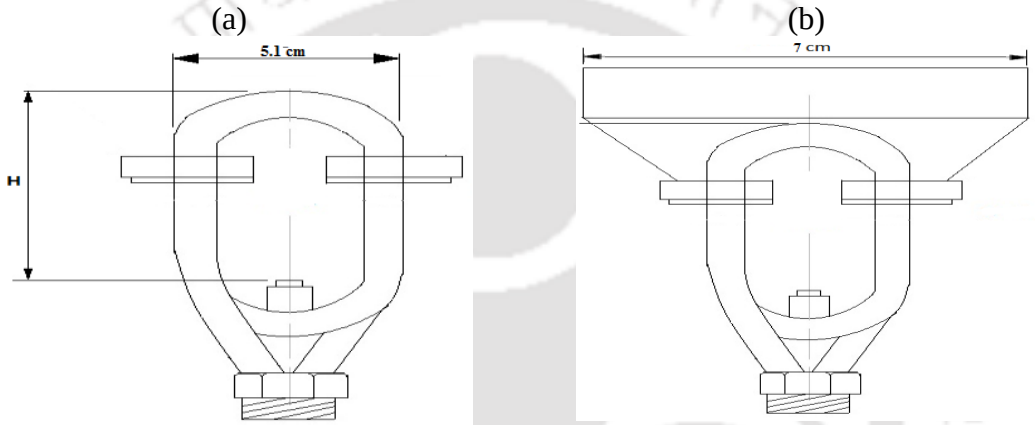

Fig. 3.11: Schematic of the newly designed burner: (a) without burner casing (H= 4.5 cm) (b) with burner casing.

Fig. 3.12: Picture of the newly designed burners.

3.10 Study on Venturi Effect (Burner Port)

The conventional pressure stove is generally designed in such a way that it cannot permit more air entrainment resulting in rich combustion or more CO emission. Even after getting

the red-hot condition in the porous media, it was found that flame color was yellowish orange, which indicates the deficiency of oxygen or signifies that the combustion was incomplete. For providing sufficient oxygen supply, different types of venturies were made. When the vaporized kerosene flows through the nozzle, due to the high velocity of vapour, static pressure of air decreases. As a result, the primary air is sucked in at the opening provided near the nozzle, which is called venturi slot. Venturi is available in two forms depending on the contour: conical venturi and cylindrical venturi.

3.10.1 Conical Venturi

Figure. 3.13 shows the conical venturi. After using this venturi, blue flame was coming out from the burner, which indicates complete combustion. Still the vaporization problem exists in a minimal level due to the large surface area of the conical Venturi.

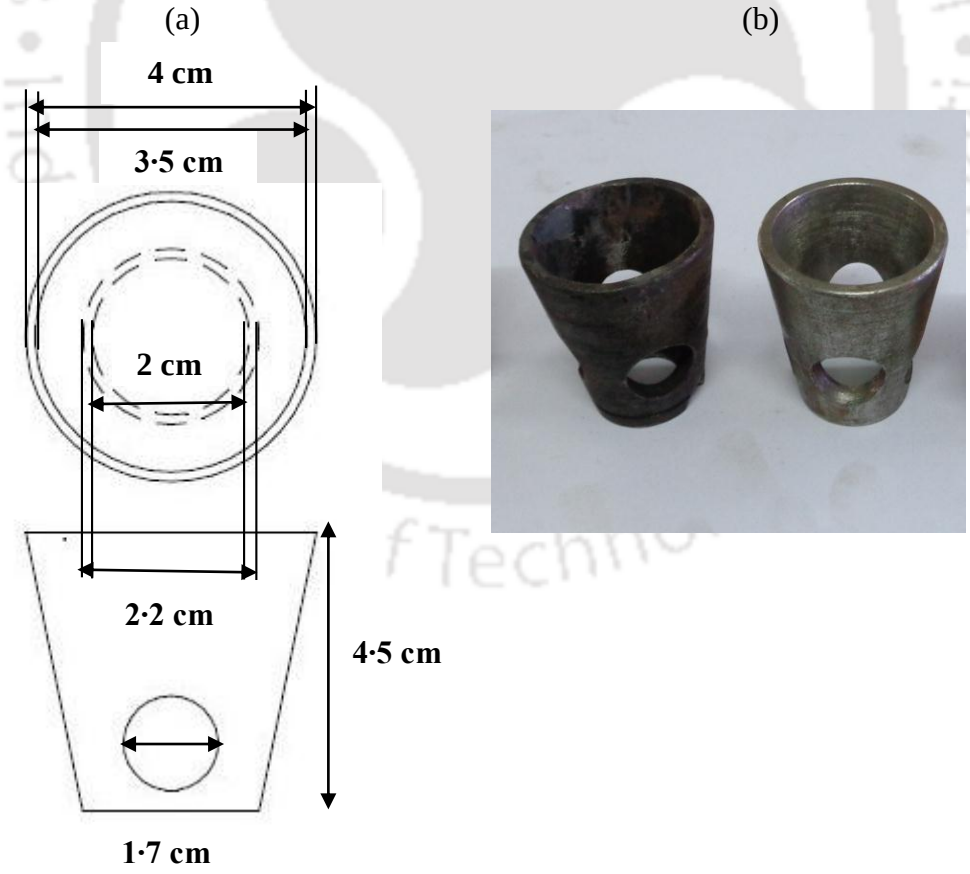

Fig. 3.13: (a) Schematic of conical venturi (b) image of conical venturi.

3.10.2 Cylindrical Venturi

In this venturi which is shown in Figs. 3.14, the contact surface area with the burner was less, so there was no problem of vaporization. After complete combustion, blue flame was coming out from the burner. This indicates the complete combustion. So cylindrical venturi was found to be the optimum venture, which has been selected for the further investigations.

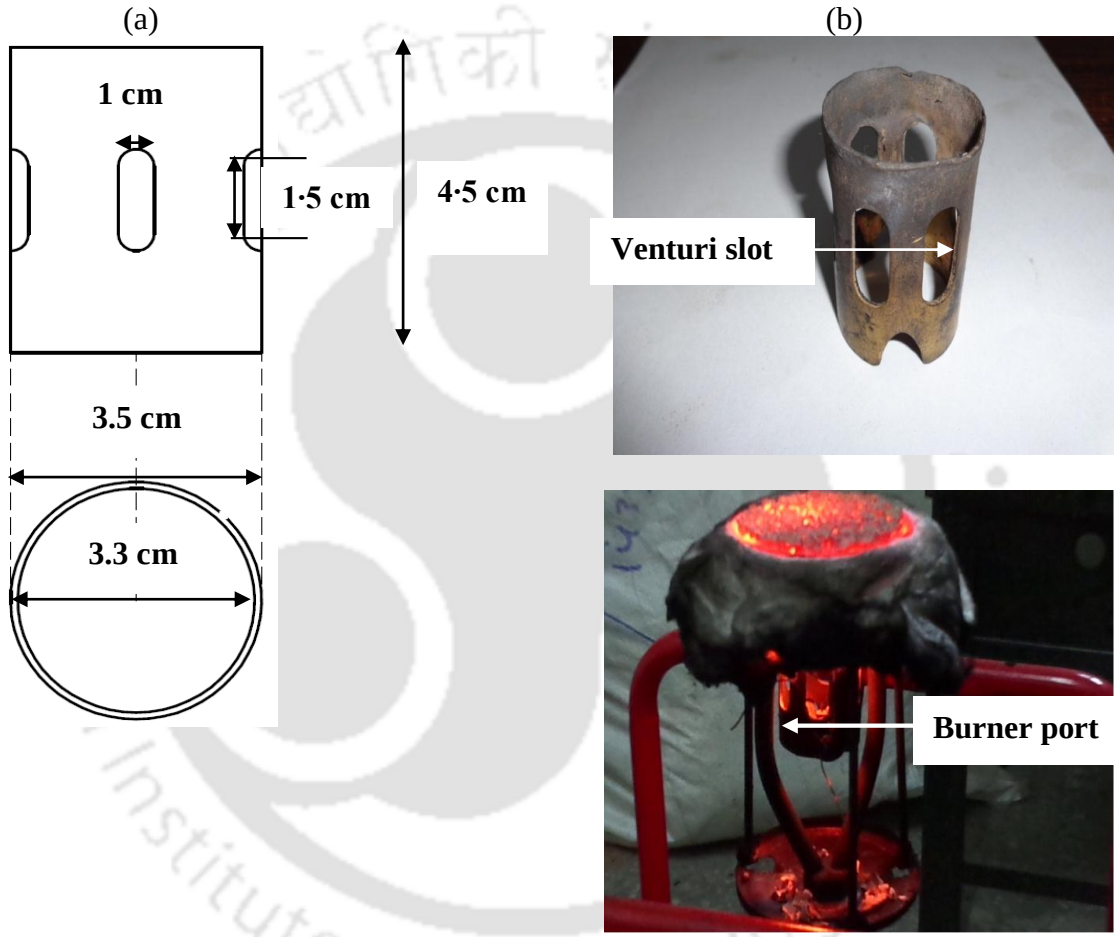

Fig. 3.14: (a) Schematic of cylindrical venturi (b) picture of cylinder venturi.

3.11 Study on Insulation

PRBs of LPG stove and kerosene pressure stove have a major problem regarding the heat loss to the surroundings. There are two types of heat loss in porous media, convective heat loss and radiative heat loss. Convective heat loss takes place at periphery of cylinder, while the radiative heat loss occurs between the vessel and surface of the burner. For reducing

these losses, certain arrangements have been done, which are discussed in the following section.

3.11.1 Insulation for Convective Heat Loss

Castable cement was initially used as an insulation material to avoid the convective heat loss. The sustaining temperature of castable cement is about 1700 ˚C. But after the combustion process during the initial experiments, a crack was found in the insulation. Hence for proper insulation, ceramic wool was used, which has a sustaining temperature of about 3000 ˚C. Figure.3.15 shows the pictorial representation of the ceramic wool insulation. For the proper decoration, aluminium sheet was used.

3.11.2 Insulation for Radiative Heat Loss

Radiation heat loss is proportional to the fourth power of temperature. Hence, maximum heat loss occurs in the kerosene pressure stove with PRB is due to radiative heat loss. To avoid the radiation heat loss, a radiation heat shield made of stainless steel was used, which is shown in Fig. 3.16. The radiation shield was tilted to 45˚ angle from the base. This radiation heat shield reduces the radiation heat loss to the surrounding.

Fig.3.15: (a) Heat insulation by ceramic wool (b) ceramic wool covered by aluminum sheet.

Fig. 3.16: Radiation shield.

3.12 Summary

Porous media combustion is an age-old technology in several applications. But for liquid fuel, it is quite a new technology, especially for kerosene. In a developing country like India, kerosene is mostly used for cooking purpose and generally pressure kerosene stoves are used for cooking applications. In the present study, a BIS specified pressure kerosene stove, manufactured by M/s. Mira Udyog, Rajkot, Gujarat, was used. Certain parts of the BIS stove such as metal casing, porous material, burner port (venturi) and stainless steel perforated sheet are modified to achieve higher efficiency. Complete vaporization of the fuel is the vital problem in the liquid fuel combustion in porous media. To avoid this problem, many arrangements were performed such as the usage of copper burner, vaporizer, metal casing, etc. Thermal efficiency of the conventional burner was investigated and the efficiency (48.5 – 58 %) was found to with input power (3 – 1.5 kW). It is found that with the increase in input power, the efficiency decreases. Reason behind this is the higher heat loss associated with the increased power. CO and NO_x emissions were also measured for conventional burner and the CO and NO_x emissions were found to be in the ranges of 610 – 915 ppm and 19 – 35 ppm for the input power range of 1.5 – 3 kW. It is

observed that with increase in input power, emission also increases. Due to the rich combustion that takes place at higher input powers, CO emissions were more at high input power. High local temperature formed at higher input power is responsible for more NO_x emissions. To avoid the convection heat loss, ceramic wool was used as the insulation material. Similarly, to avoid the radiation heat loss, stainless steel radiation shield was used. Different types of PRB configurations, major results obtained from the experimental investigations on PRBs, effect of nozzle diameter on efficiency and emissions and effect of environmental temperature on thermal efficiency of PRB have been discussed in the next chapter.

Chapter 4

Self-aspirated Domestic Pressurized Kerosene Cooking Stove with Porous Radiant Burner

In this chapter, tests on different configurations of PRB integrated with pressurized kerosene stove are presented. Performance investigations of a domestic conventional pressure kerosene cooking stove are discussed. Details about the experimental set up and procedure are outlined. Thermal efficiency and emission characteristics of different conventional burners at different input powers are also presented.

4.1 Performance Analysis of Domestic Pressure Kerosene Cooking Stove

In rural areas, the main source of energy for cooking are firewood and cow dung cake, which are used in generally in mud stove (shown in Figure 4.1). But this type of cooking device produces more emissions resulting in a poor efficiency. Moreover, large consumption of firewood leads to deforestation and highly necessitates the urge in the modification of the existing less efficient combustion systems. Due to the poor supply of electricity in rural areas, the usage of electric stove is restricted. Because of the technical and management issues, usage of solar and biogas stoves is also limited. It is of course no doubt that LPG is a cleaner fuel when compared to other fuels for cooking purpose. But in rural areas, because of inadequate distribution and high cost, people could not afford LPG. It is known that kerosene is of lower cost and easy to handle and transport (as compared to LPG). In addition, the government also gives subsidies for kerosene purchase. Hence, kerosene is affordable for low-income group people in rural, suburban and urban areas. Also by the usage of kerosene for cooking purpose, it may reduce the dependency on

biomass especially in rural areas. Two types of kerosene stoves are generally used for cooking purpose, viz., wick type and pressure type. Wick type stove works on the capillary action of the kerosene, in which the wick draws kerosene from the fuel tank. At the end of wick, ablaze is done for flame production and that flame is used for cooking purpose. In pressure type stoves, the preheated kerosene in the form of vapour is pressurized and passed through the nozzle. It is then mix with air and ignites for producing the flame (shown in Figure 4.2.).

Fig. 4.1: Mud stove.

This flame is used for cooking purpose, and so it is called as free flame combustion. As discussed in chapter 1, the thermal efficiency of pressure kerosene cooking stoves is higher than the wick type kerosene stoves. Average thermal efficiency of pressure kerosene cooking stoves are 45 %, while in the case of BIS stoves, it varies from 55 – 58 %. As discussed in Chapter 3, there are three types of burners available in the market, namely venus burner, silent burner and roarer type burner (shown in Figure 3.2). The measured maximum and minimum efficiency of the burners are presented in Table 4.1.

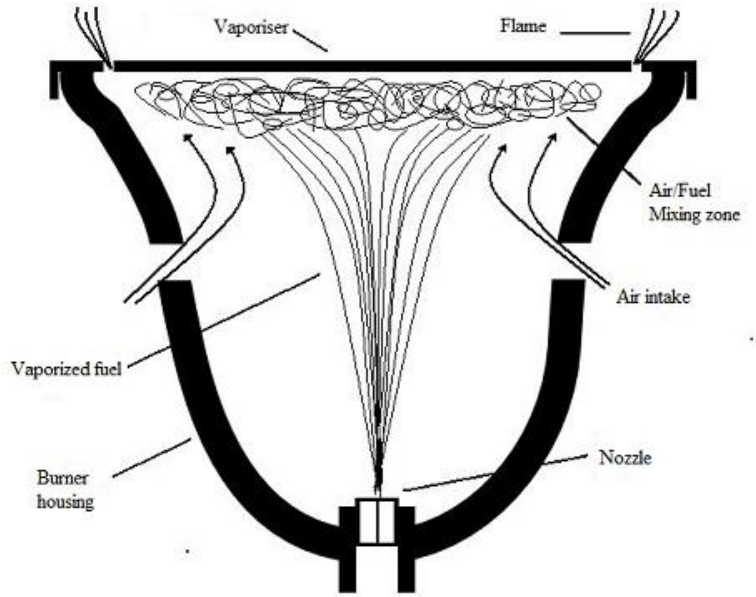

Fig. 4.2: Mechanism of pressure kerosene stove.

Table 4.1: Efficiency of different types of burners.

Types of burners	Thermal Efficiency (%)	
	Maximum	Minimum
Venus burner	58	48.5
Roarer burner	55	45.0
Silencer burner	54	44.1

Further, effect of each burner with input power in context of thermal efficiency is also presented in Figure 4.3. The overall maximum and minimum thermal efficiencies are achieved in Venus and silencer burners. So for further studies, Venus burner has been selected as the conventional burner. Construction details of general conventional burner have been discussed in the Chapters 1 and 3. A brief discussion about the general conventional burner is presented here.

As shown in Figure 4.4, the general conventional burner consists of two ascending and two descending tubes. These tubes touch the vaporizer (which is a flat circular chamber) and

the ascending tubes remain connected with the riser. Middle section of the descending tubes contains the spray nozzle, through which kerosene vapour is sprayed in air. For ignition of the kerosene stove, little amount of kerosene is put in spirit cup initially (Figure 2.3) and is burned with ablaze wick.

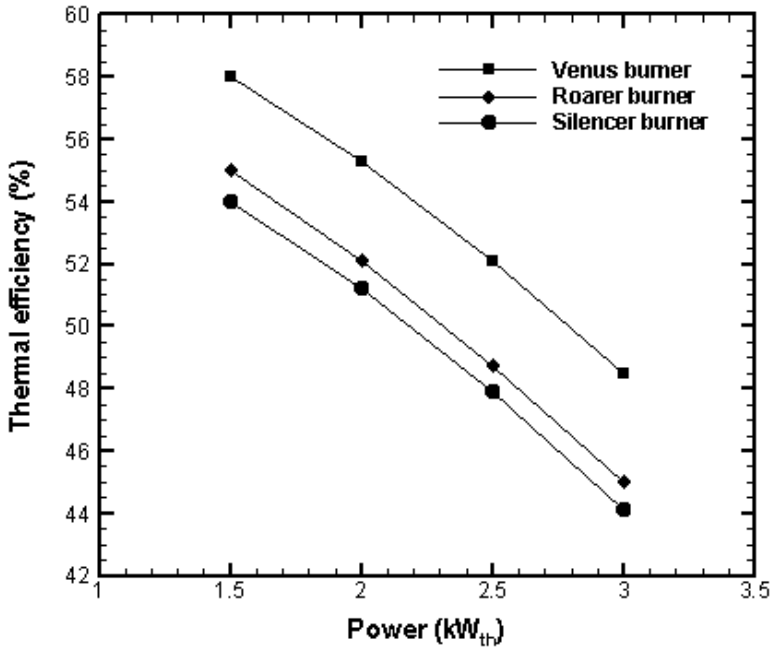

Fig. 4.3: Thermal efficiency of different conventional burner.

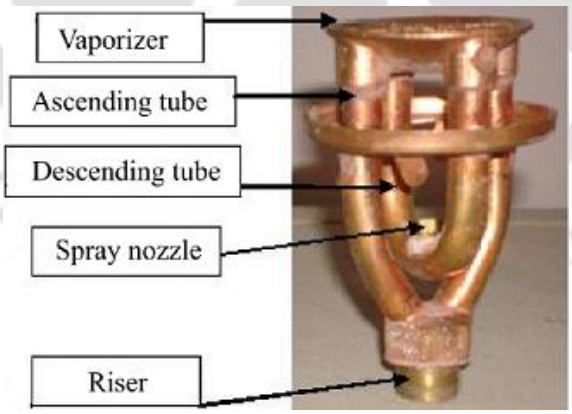

Fig. 4.4: Construction of general conventional burner.

During the burning of kerosene, pressure pushes the liquid kerosene to vaporizer through the riser and ascending tube. Vaporizer gains heat from the burning kerosene through convection and becomes hot. Liquid kerosene becomes vapour when they pass through the

hot vaporizer. Under the force of pressure, vapour kerosene passes through the descending tubes and finally emits from the spray nozzle and then mixes with air and burns with yellowish orange flame (as shown in Figure 1.2) in the place between the vaporizer and flame holder. The initial flame in the spirit cup is quenched and vaporizer takes heat continuously from the kerosene-air flame.

Combustion in conventional pressure stove is free flame, which is treated as gas whose emissivity and thermal conductivity are very low. Because of this reason, convection mode of heat transfer is predominant in the conventional pressure kerosene cooking stove. Due to insignificant conduction and radiation modes of heat transfer, performance of the pressure kerosene cooking stoves is very low like low thermal efficiency and high emissions (CO: 610 – 915 ppm, NO_x: 19 – 35 ppm). The emissions are higher than the prescribed limit of the World health organization (WHO) for indoor air pollution (Kandpal *et al.*, 1995; Zhang *et al.*, 1999). Reason for the low efficiency and high emission is the incomplete combustion. As discussed in chapter 3, through the usage of novel concept of PRB, thermal efficiency can be improved and emissions can be minimized, which results in the saving of kerosene. But the important aspect to be considered in the design of any novel concept is the requirement of external air. It is difficult to provide compressed air for domestic purpose, especially in rural areas. So it is required to design a cooking stove with PRB without the requirement of any external air (natural draft). This chapter discusses the various efforts to make a cooking stove with PRB without external air. Different configurations of PRB with their outcomes have been discussed in the next section.

4.2 Different Configuration of PRB with Conventional Stove

For exploring different configurations of PRB, BIS specified pressure kerosene cooking stove have been used. Alumina ball (Al_2O_3), silicon carbide (SiC) and stainless steel were

used for fabricating the PRB. Castable cement, stainless steel and mild steel were used for the fabrication of casing, which holds the porous burner.

Configuration 1

In configuration 1, casing was made by stainless steel wire mesh and vaporizer tube was surrounded by same casing material for air entering and it was bound by metal clip as shown in Figure 4.5. Two layers (total thickness, 10 mm) of alumina balls (diameter, 5 mm) were used as the porous media. The bed diameter was about 70 mm. Combustion process was done same as in conventional stove.

Observation

During the experiment, it was found that the air-fuel mixture did not move up and combustion was occurred below the bottom of the composed bed. During the experiment, it was found that, only a small area of porous bed was found to be red hot while the remaining major part was black. It was also observed the formation of soot. It was due to non- uniform distribution of the air-fuel supply.

Technical Reason

Small passage between the alumina balls resulting in a large pressure drop. Due to the large pressure drop, high resistance to the flow was created below the bottom of the porous bed. Because of this, the air-fuel mixture could not move up and red hot did not take place to whole area of porous bed. Reason behind of soot formation was high resistance offered by porous bed. Based on this observation, it was concluded that by the increasing the number of alumina ball layer, the pressure drop increases and hence the number of alumina ball layer should be kept less than 2. In the next configuration, number of ball layers has been reduced to one.

(a) (b)

Fig. 4.5: Double layer alumina bed (a) before combustion (b) after combustion.

Configuration 2

Same experimental setup was used in configuration 2 as in configuration 1, except that a single layer (thickness, 5 mm) of alumina ball was used for the porous burner. Bed diameter (70 mm) and ball diameter (5 mm) were the same as in configuration 1. Stainless steel wire mesh was used for casing and burner cover.

Observation

During the combustion, it was observed that a blue flame appeared above the porous bed and the bed was heated to incandescence to some area of porous bed as shown in Figure. 4.6 (a) - (b). After the combustion, it was found that there was soot on the porous bed.

Technical Reason

The reason behind the blue flame over the bed was the insufficient bed thickness which was unable to trap flame inside the porous bed. Soot was present due to the initial burning of porous bed. From the above two configurations, it was concluded that the alumina balls were not suitable for the porous burner.

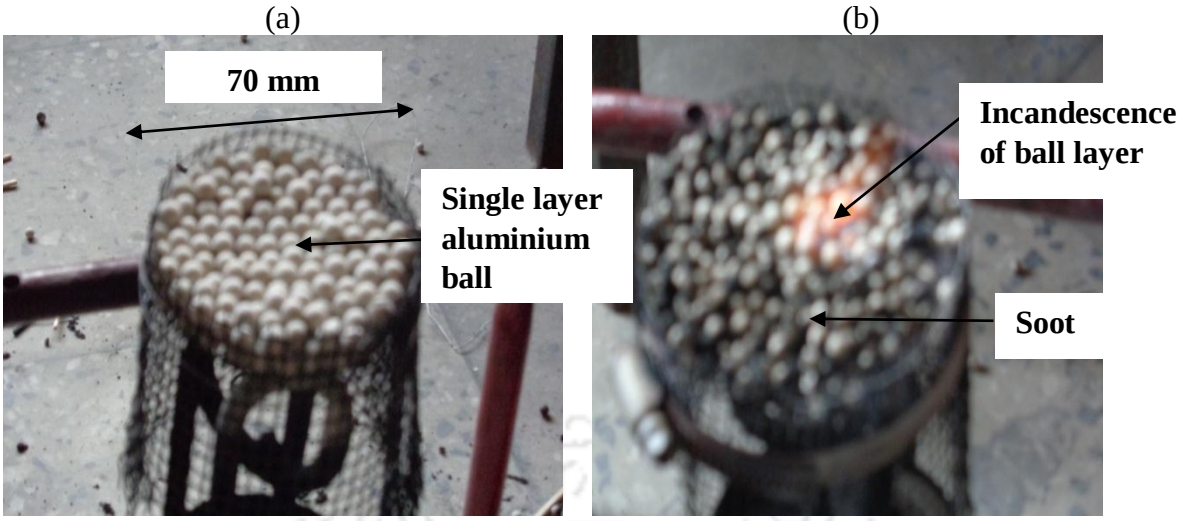

Fig. 4.6: Single layer alumina bed (a) before combustion (b) after combustion.

Conclusions from configurations 1 and 2

It was also seen in both configurations 1 and 2 that more heat loss occurred from the peripheral side of the casing. For reducing the heat loss, a special type of cement called castable cement was fabricated. The sustaining temperature of the castable cement is about 1700 ˚C, which is more than the maximum temperature produced during PMC (1100 – 1200 ˚C). The selected castable cement is the combination of Al_2O_3 (85.8 %), CaO (6.2 %) and Fe_2O_3 (1.6 %). The fabrication procedure of casing with castable cement is as follow. A wood mould (as shown in Figure 4.7) was made initially according to the desired contour of the casing. The castable cement was mixed with small amount of water (8 – 10 %) and the wet mixture was poured into the wood mould. It was then left curing for 2 days. Prepared cemented casing is shown in Figure 4.8. The inner diameter, outer diameter, thickness and height of the casing are 72 mm, 112 mm, 20 mm and 50 mm, respectively. The casing has a central hole of diameter 30 mm and two 32 mm × 9 mm slots to allow the two top ends of the vaporizer pipe to bring in contact with the porous burner. The purpose of central hole is to allow the vaporised air-fuel mixture into the casing so that combustion

could take place inside the casing. These dimensions were fixed to facilitate the selected porous matrix.

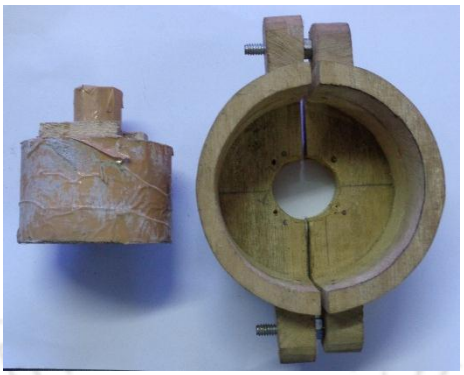

Fig. 4.7: Wood mould.

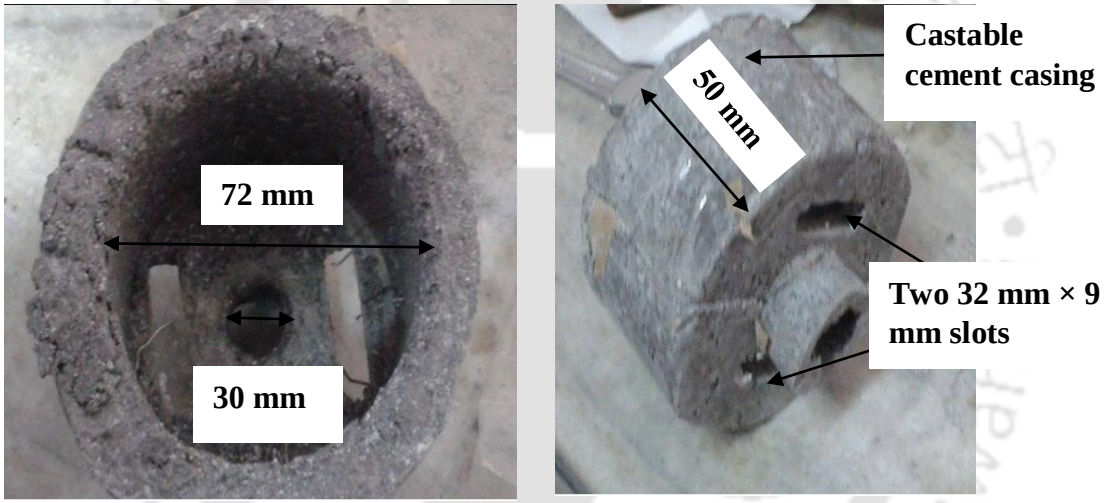

Fig. 4.8: Castable cement casing.

Configuration 3

Configuration 3 is totally different from the previous two configurations, though the same BIS stove was used for the experiment. In this configuration, for PRB, circular SiC (silicon carbide) insert was used as shown in Figure 3.10. Thickness and diameter of the RRB were 20 mm and 70 mm, respectively. Porosity and pore size were 90 % and 10 ppi (pore per inch), respectively. Pictorial view of the burner with configuration 3 is shown in Figure 4.9, in which the cemented casing was attached to vaporiser tube through slot made in casing and the porous burner was kept inside the cemented casing.

Observation

During the experiment, it was found that only partial red hot occurred in the porous burner. There was no soot formation observed, which was the major advantage of this configuration. It was also observed that during the initial period of combustion, there was a problem of vaporisation of fuel.

Technical Reason

Due to the low pressure of the stove, flame did not extend much towards downstream of burner and partially red hot occurred in porous burner. Reason behind the problem of vaporisation of fuel was improper heat transfer from porous burner (SiC) to vaporiser tube.

Configuration 4

Configuration 4 was same as that of configuration 3, except the supply pressure of fuel. In this configuration, the supply pressure of fuel was increased to 1.5 bar.

Observation

During combustion, it was seen that burner was 80 % red hot (area wise) as shown in Figure 4.10. Percentage of red hot was determined by the ratio of area of red hot to total area of SiC. Although, no soot formation was found, problem of vaporisation of fuel was still existed.

Technical Reason

Due to increased pressure, flame was able to move downstream to combustion zone (burning SiC) and flame propagated to radial direction. Reason behind the problem of vaporisation of fuel was improper heat transfer from porous burner (SiC) to vaporiser tube.

Fig. 4.9: Combustion of single layer of SiC.

Fig.4.10: Combustion of single layer of SiC at higher pressure.

Configuration 5

From configurations 3 and 4, it was observed that the problem of complete vaporisation of fuel hinders the performance of the stove. So to overcome from the problem of vaporisation, three types of perforated sheet of mild steel with holes of different diameters (1.25 mm, 1.5 mm and 1.8 mm) were used (shown in Figure 3.10). This perforated sheet acts as a preheater and was placed beneath of SiC. The diameter of the sheets is 70 mm.

Observation

During the experiment, it was found that 100 % red hot of porous burner was occurred (shown in Figure 4.11). This was the best configuration when compared with the previous four configurations, but problem of vaporisation was still existed. Soot formation was not found.

Technical Reason

Due to the increasing the pressure and the use of perforated sheet as a preheater, flame was trapped in reaction zone as well as in combustion zone resulting in 100 % red hot condition. But the issue remained was the incomplete vaporisation of fuel. The reason behind this is

the insufficient heat gain by the vaporiser tube. Because of preheater, some part of the heat is gained by the vaporiser, but due to cemented casing, no heat is gained by the vaporiser tube from the casing. Hence, to solve the problem of vaporisation, other casing materials, viz., mild steel and stainless steel have been tried (shown in Figure 4.12).

Fig. 4.11: Double layer of PM after combustion in cement casing.

In the case of mild steel casing, there was a crack and corrosion observed after performing several experiments. But, in the case of stainless steel casing, there was no crack and corrosion observed even after several experiments. Therefore, it was decided to use stainless steel casing in the further experiments.

Configuration 6

As discussed above, stainless steel material was used as a casing in configuration 6. It holds the perforated sheet of diameter 70 mm (hole diameter, 1.25 mm) and porous burner (SiC). Pictorial view of the base plate of the burner casing having a central hole of diameter 30 mm, and two 32 mm × 9 mm slots to allow the two top ends of the vaporizer pipe to bring in contact with the vaporizer plate (perforated sheet or preheater) is shown in Figure 4.12.

Observation

During the experiment, it was found that complete vaporisation of the fuel occurred. There was no soot formation and 100 % red hot condition of porous burner was happened. It was also observed that during the experiment, flame was coming out from the surface of burner (shown in Figure 4.13) and however, the flame height was short.

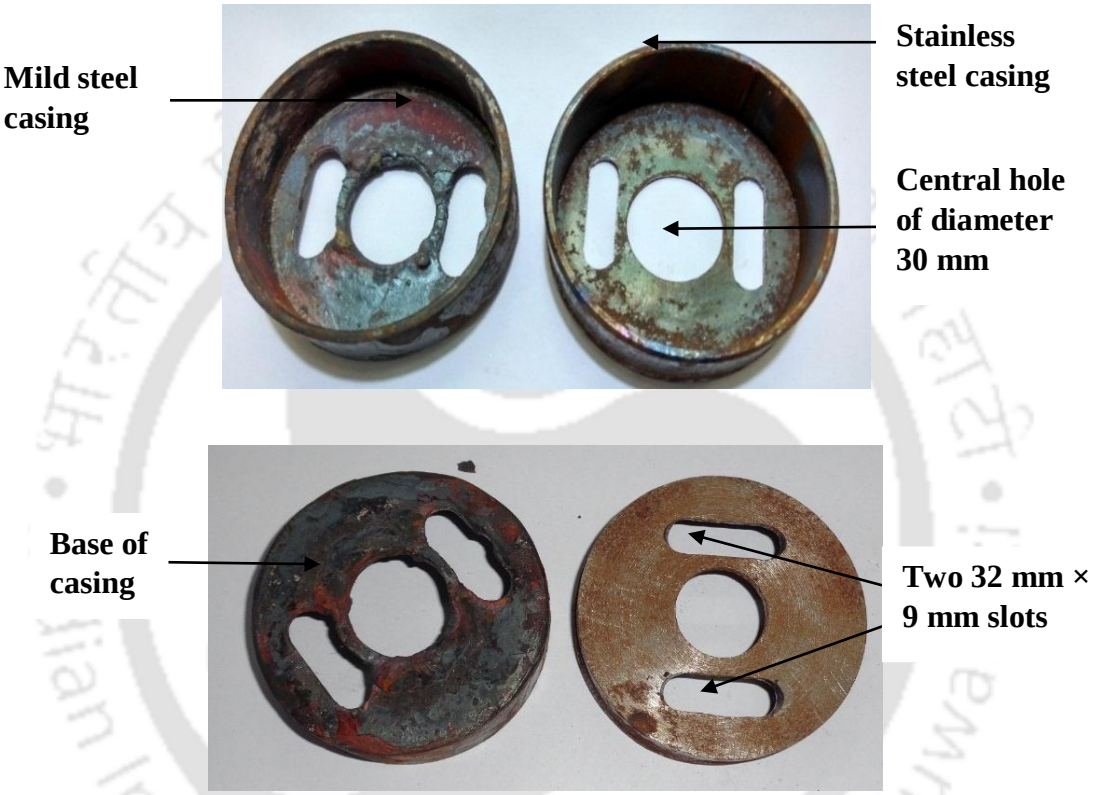

Fig.4.12: Casing of mild steel and stainless steel.

Technical Reason

Due to the lower porosity (12 %) of the preheater flame trapped inside the burner but to some extent and flame was coming out from the burner. Because of metal casing, good heat transfer taken place between vaporiser tube and burner casing resulting in no vaporisation problem in PRB stove.

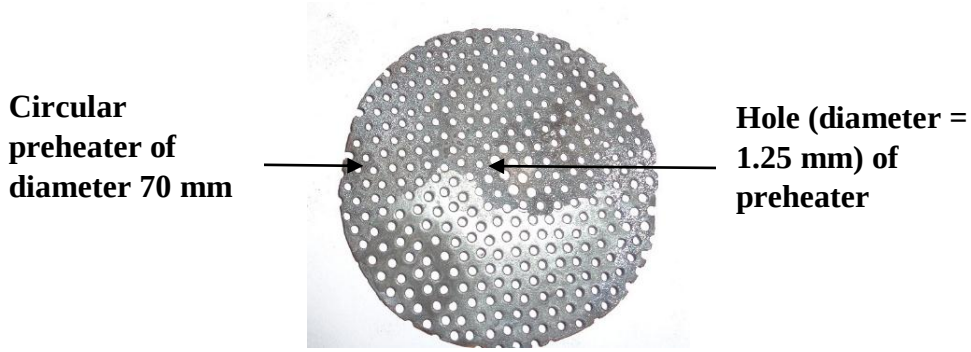

(a)

Fig. 4.13: (a) Perforated sheet of hole diameter 1.25 mm.

(b)

Fig. 4.13: (b) Combustion after using 1.25 mm hole diameter preheater.

Configuration 7

In configuration 7, diameter of the preheater was taken as 70 mm (which was optimized by the earlier researchers at IIT Guwahati (Sharma *et al.*, 2009) and diameter of the holes was chosen as 1.8 mm. The diameter, porosity and ppi the porous burner (SiC) were 70 mm, 90 % and 10, respectively. As in configuration 6, same stainless steel casing (same dimension) was used in configuration 7.

Observation

During the experiment, it was observed that soot formation did not occur and 100 % red hot condition of porous burner was occurred. In this configuration, it was also seen that a long flame was observed on the surface of burner (shown in Figure 4.14). Length of this flame was greater than length of flame as found in configuration 6.

Technical Reason

Due to the high porosity (25 %) of perforated sheet (preheater), flame was not trapped inside the porous burner and long flame was observed on the surface of the porous burner.

Configuration 8

Configuration 8 is the same as configuration 7, except the preheater. In this configuration, the hole diameter of preheater was reduced to 1.5 mm. The diameter, porosity and ppi of the porous burner (SiC) were 70 mm, 90 % and 10, respectively.

Observation

During the experiment, it was seen that porous burner became a highly bright with 100 % red hot condition. After the experiment, soot formation did not occur on the surface of the burner. An improved performance was observed in this configuration, because during the experiment, no flame was seen over the surface of the burner which is shown in Figure 4.15. So the configuration 8 is considered to be the optimum because combustion was flameless which not only enhances the efficiency but also lowers the emission.

Technical Reason

Medium porosity of preheater was the important character for flameless combustion in which porous burner and preheater are able to trap the flame in the porous matrix. Hence, the preheater of hole diameter 1.5 mm is found to be the optimum.

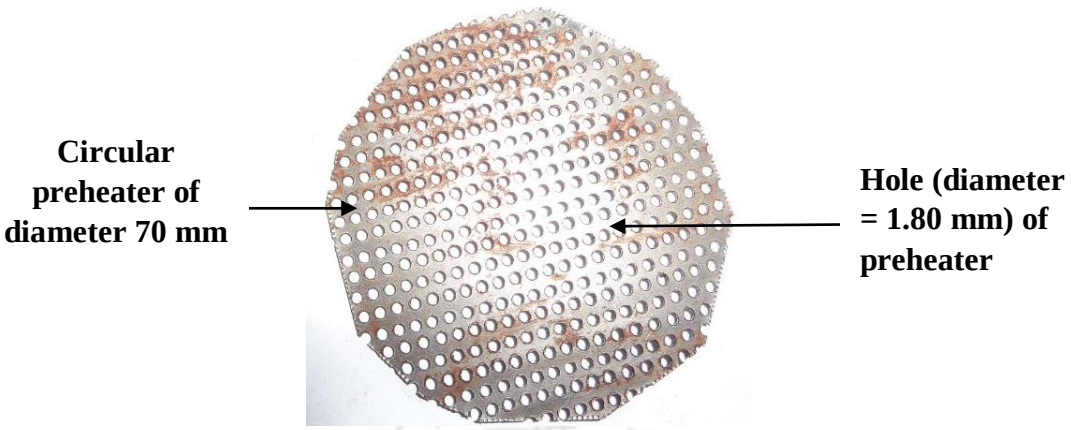

(a)

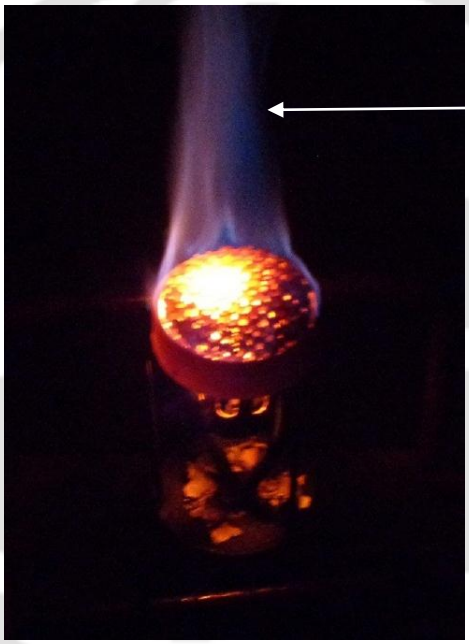

(b)

Fig. 4.14: (a) Perforated sheet of hole diameter 1.80 mm (b) Combustion after using this preheater.

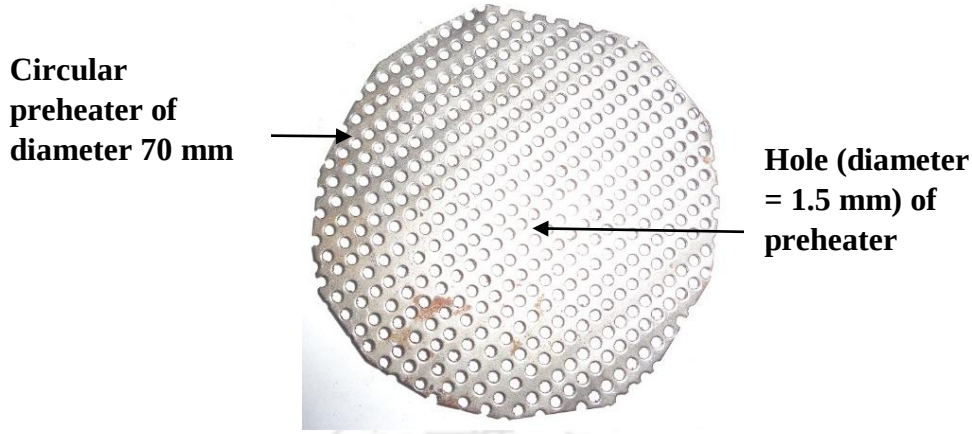

(a)

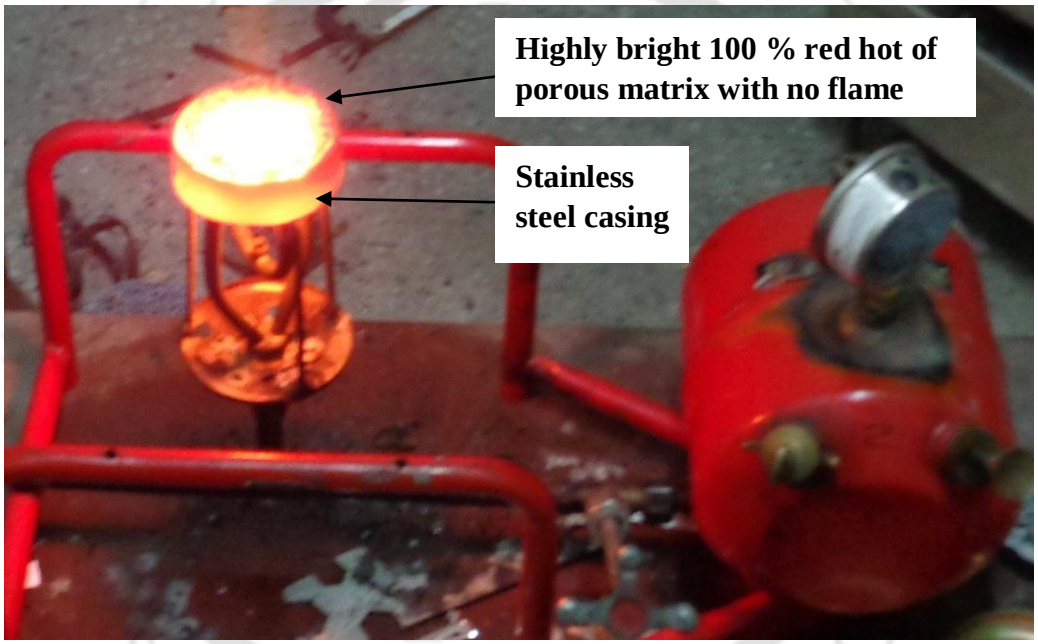

(b)

Fig. 4.15: (a) Perforated sheet of hole diameter 1.50 mm (b) combustion after using 1.50 mm hole diameter preheater.

So for further experiments, configuration 8 was selected as the PRB in which the thermal efficiency and emissions (CO and NO_x) were measured and the same was compared with conventional burner (CB) which has been discussed in the next section. A rough schematic diagram of whole set up of PRB is presented in Figure 4.16.

In flameless combustion, as the combustion occurs in highly emissive and conductive solid matrix (SiC), conduction and radiant modes of heat transfer become significantly active and due to large internal surface area of porous media and also the convective mode of heat transfer got improved. Hence, in flameless combustion all the three modes of heat transfer become active. Free-flame combustion that occurs in conventional burner happens in the gaseous environment, in which only convective heat transfer becomes dominant. Because free flame is treated as a gas whose emissivity and thermal conductivity are very low and hence the radiation and conduction modes of heat transfer becomes insignificant. Because of this, the thermal efficiency of conventional stove is low with more emissions. A comparison is made among all the configurations studied which is shown in Table 4.2.

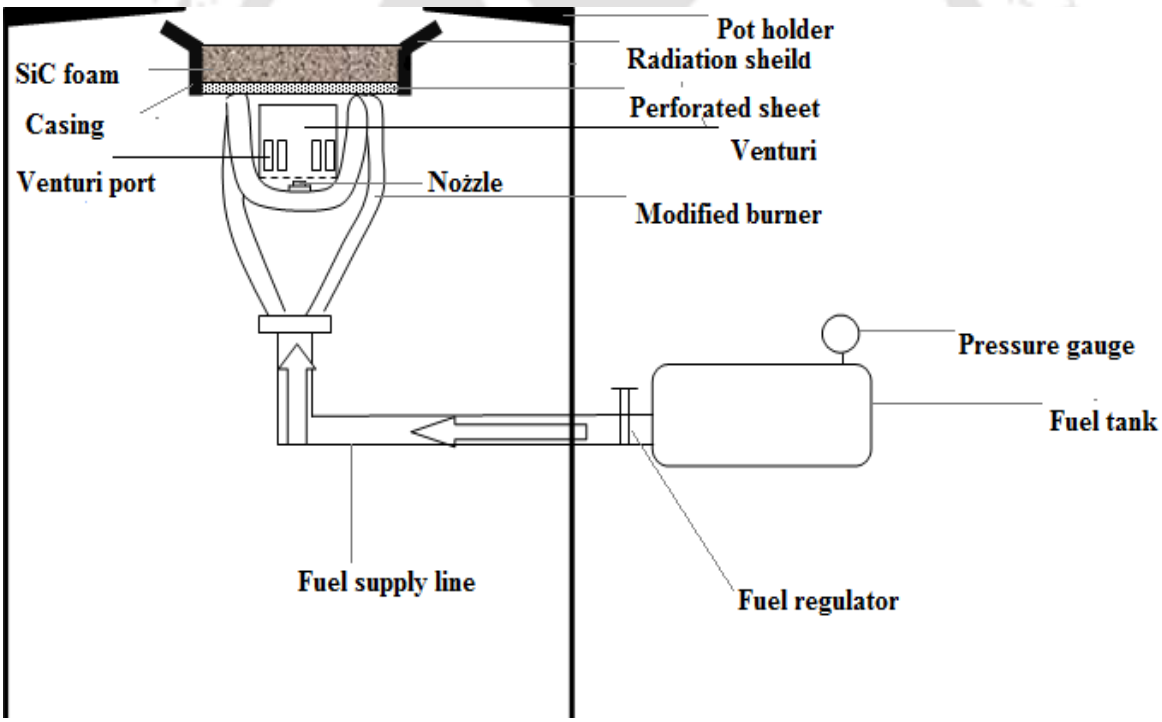

Fig. 4.16: Schematic of the experimental setup used in self-aspirated PRB.

Table 4.2: Comparison performances of all configurations of PRB

Conf. No.	Design details	Major Observation	Technical Reason
1	Two layer of alumina balls.	Burning took place below the layer.	Small passage between the alumina balls resulting in a large pressure drop.
2	Single layer of alumina balls.	Blue flame seen over the surface of burner.	Insufficient bed thickness which was unable to trap flame inside the porous bed.
3	Cemented casing, SiC as porous media.	Partially red hot condition took place.	Low pressure of the stove, flame did not extend much towards downstream of burner.
4	Cemented casing, SiC as porous media, increased pressure up to 1.5 bar.	80 % red hot condition took place, but vaporization problem exist.	Increased pressure, flame was able to move downstream to combustion zone, improper heat transfer from porous burner (SiC) to vaporiser tube.
5	Used preheater of hole diameter 1.5 mm.	100 % red hot condition took place, but vaporization problem exist.	Increasing pressure, use of perforated sheet as a preheater, flame trapped in reaction zone as well as in combustion zone, no heat is gained by the vaporiser tube from the casing.
6	Used metal casing, preheater with hole diameter 1.25 mm.	Vaporization problem eliminated, but short flame was observed.	Use of metal casing, lower porosity of the preheater, flame trapped inside the burner but to some extent,
7	Used preheater of hole diameter 1.8 mm.	Long flame was observed.	High porosity of perforated sheet (preheater), flame was not trapped inside the porous burner.
8	Used preheater of hole diameter 1.5 mm.	No flame, flameless combustion.	Medium porosity, porous burner and preheater are able to trap the flame in the porous matrix.

4.3 Development of Self-aspirated Porous Radiant Burner

As discussed in chapter 3, due to the low air entrainment in conventional stove, a rich combustion takes place due to which high CO emissions are produced. In the case of PRB after converting to the red hot condition, a short yellowish orange flame comes from surface of the burner which indicates the deficiency of oxygen. Due to this, the combustion process

that occurred is said to be incomplete. For domestic purpose, it is not suitable to use air compressor for air entrainment. For more air entrainment, a venturi (Burner port) was used. When vaporized kerosene flows through the nozzle, due to the high velocity of vapour, static pressure of air decreases. As a result, primary air is sucked through the venturi at the opening provided in the venturi (venturi slot) and this process is called venturi effect. As more air entrainment is achieved without any external agent, the method is called self-aspirated air entrainment. There are two types of venturi namely conical and cylindrical venturi are used in the PRB stove as shown in the Figs. 3.13 and 3.14. As discussed in chapter 3, conical venturi has the problem of incomplete vaporisation and higher emissions. As the cylindrical venturi does not possess these adverse issues, cylindrical venturi was considered to be the optimum.

4.4 Design and Fabrication of Porous radiant Burner

Design and fabrication of the porous radiant burner have been done in three steps: (i) selection of dimensions of the porous radiant burner, (ii) selection of vaporizer tube and (iii) selection of burner casing.

Selection of Size of Porous Burner

Proper selection of porous matrix is the key factor for achieving better thermal efficiency and reduced emissions. SiC porous burner is available in the commercial market in the range of 60 mm - 120 mm diameter with thickness 20 mm. In order to study the effect of porous matrix diameter on the thermal efficiency of the burner, series of experiments have been performed (Sharma *et al.*, 2009; Pantangi *et al.*, 2007; Sharma *et al.*, 2011; Sharma *et al.*, 2016a; Sharma *et al.*, 2016b). It was found that the burner with 70 mm diameter yielded the maximum thermal efficiency. Therefore, SiC matrix of 70 mm has been chosen for the present investigations.

Selection of Vaporizer Tube

This work was extension of the earlier PhD work on the development of pressurize kerosene burner for kerosene stove (Sharma, 2010). Figure 4.17 shows the schematic of the earlier development. Retrofitting the PRB in the commercial pressure kerosene stove, significant improvement in thermal efficiency and reduction in emissions have been achieved (Sharma *et al.*, 2011). However, this burner required compressed air for its operation. Therefore, in this present work, vaporizer tube has been modified with focus on the development self-aspirating PRB.

During the experiment (with old design), it was found that combustion inside the porous media was not uniform. It was due to obstruction between the nozzle and porous media. So it was necessary to develop a vaporizer tube with no burner head. For the same purpose, a conventional venus burner, which is available in the commercial market without burner head has been chosen (which is shown in Figure 4.18) for the initial investigations.

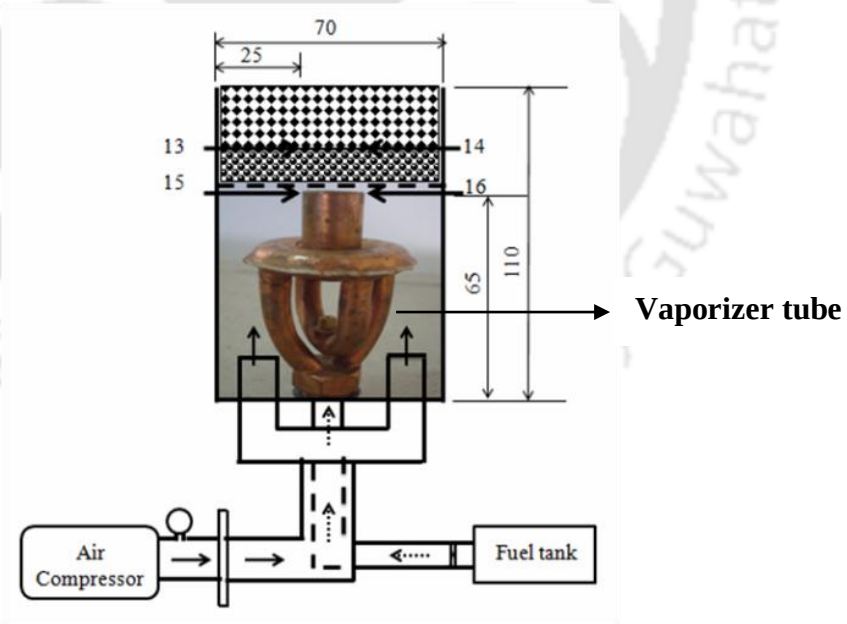

Fig. 4.17: Vaporizer tube associated with compressed air (all dimension in mm).

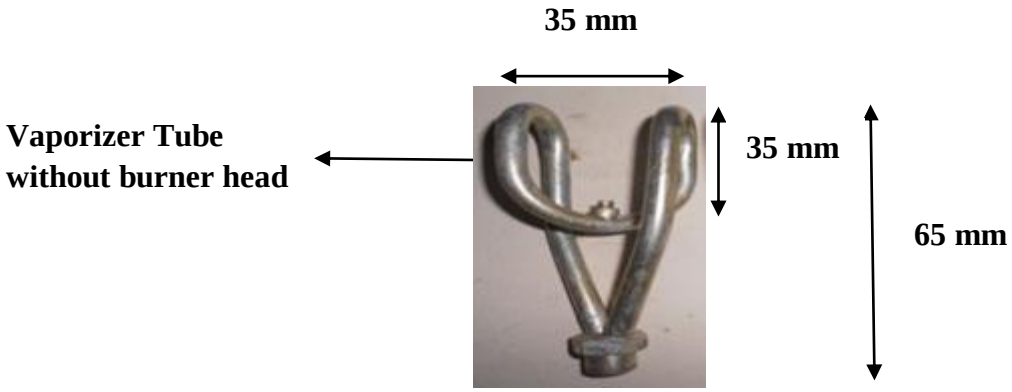

Fig. 4.18: Venus burner without burner head.

During experiment, porous radiant burner with SiC as combustion zone has been inserted at the top of venus burner. It was observed that only partial red hot was noticed in SiC. It was due the small distance between nozzle and burner surface which diverts the air fuel mixture during the high strike of air fuel jet on bottom of porous matrix surface. To avoid this issue, the distance between the nozzle and burner surface has been increased to 45 mm. It was also observed that beyond the distance of 45 mm, air fuel mixture partially wetted the porous matrix, resulting in non-uniform distribution of red hot. The modified vaporizer tube is shown in Figure 4.19.

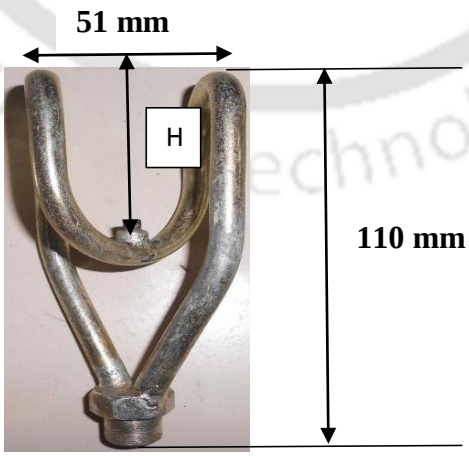

Fig. 4.19: Modified vaporizer tube with dimension (H = 45 mm).

After increasing the height to 45 mm, air-fuel mixture gets enough space for entering into the porous matrix and it wetted the whole area of porous material.

Selection of Casing

Selection of burner casing depends on porous burner size. Normally, burner casing can be made from three different materials viz., stainless steel, mild steel and castable cement. While testing with low cost castable cement casing, it was observed that during the initial period of combustion, there was a problem of vaporisation of fuel. This was due to the poor heat transfer from porous matrix (SiC) to the cemented casing and vaporiser tube. Hence, to achieve better (complete) vaporisation, stainless steel and mild steel made burner casing were tried. After repeated experiments, corrosion has been observed in mild steel based burner casing. Therefore, stainless steel based burner casing, which provided the satisfactory results has been selected for the further investigations. Dimension of stainless steel casing are given in Figure 4.12.

With stainless steel (or mild steel) based casing, there was no issue of vaporization in PRB based kerosene pressure stove reported. This is mainly due to the better heat transfer between porous matrix and casing. With these modifications, the final configuration of the burner has been arrived.

Usually, kerosene cook stoves are meant for domestic cooking application in the rural and remote areas and it is not recommended for large scale cooking application due to large emissions of CO. As evident from the test report of LPG stove with PRB (Mishra *et al.*, 2015; Pantangi *et al.*, 2007), the expected thermal efficiency of the kerosene stove with PRB at higher wattage will be very low and it's not economical to operate the kerosene burner at higher thermal inputs.

4.5 Summary

For the conventional burners, higher thermal efficiency was observed in venus burner (58-48.5 %) as compared to roarer burner (55- 45 %) and silent burner (54- 44.1 %). Flameless and stable combustion was observed in configuration 8. SiC as porous matrix (porosity 90 %, and diameter 70 mm) and preheater (mild steel perforated sheet of hole diameter 1.5 mm) were used in configuration 8. Distance between the nozzle and bottom surface has been found as an important parameter for stable combustion and 45 mm distance was found as the optimum distance.

Chapter 5

Preparation and Characterization of Alumunium Based Ceria Nanoparticles with Kerosene

In this chapter, the preparation of aluminium based ceria nanoparticle blended with kerosene is discussed. Different method of nanofuel synthesis is also presented. Performances of the burners at different concentrations of nano particles blended with kerosene and its comparison with pure kerosene are discussed. Specific surface area and oxygen storage capacity of different nanoparticle is also discussed. Further, optimization of nanoparticle concentration is also highlighted in this chapter.

5.1 Introduction

As discussed in chapter 2, nowadays cerium based oxide gained more attention among the researchers due to its catalyst property in several chemical reactions. Because of its properties towards altering the valence from Ce^{+4} to Ce^{+3} and vice versa, it is widely popular among the earth metals. This property attributes towards the loss or addition of oxygen, which happens in the high temperature range (300 ˚C to 800 ˚C). When a vacancy of oxygen ion or molecule is available in metal, oxygen ion moves in the lattice quickly leading to the catalytic usage and opposite to it. During the combustion, when ceria is used as the catalyst, it absorbs the O_2, which is formed due to the reduction of NO_x. The same O_2 is released then for the oxidation of CO. This happened due to the ability of the ceria to transform from Ce^{+4} to Ce^{+3} (redox properties) that depends on the partial pressure of the exhaust gas. Ceria occurs more effective when they are available in nano-sized state in the context of redox properties. Property of the metal to follow oxygen is the primary objective of its usage in

catalytic application, and is called as oxygen storage capacity (OSC). This property is very much effective while heating the metals in nano-sized form. Harmful emissions such as NO_x, CO and unburned hydrocarbons can be reduced to a greater extent using OSC of the nanoparticle by its three-way catalyst (TWC). Under rich combustion, TWC supplies O_2 to CO and hydrocarbon and extract O_2 from NO_x from the lean mixture. Using cerium based oxide as catalyst in fuel showed potential improvement in combustion efficiency as well as reduction in the emission (Ozawa *et al.,* 2000; Crozier *et al.,* 2008)

5.2 Nanofuel Preparation Method

As discussed in chapter 2, there are three methods of nanofuel preparation namely magnetic stirrer method, tip sonication method and combination of both the methods. In these methods, combination of both the methods is found to be the optimum method (refer to Table 2.6). Surfactants are required for making a more stable solution. Tween 80, Tween 20, SDS, CTAB and Oleic acid are the different types of surfactants, which are primarily used in nanofuel preparation. Among the available surfactants, Tween 80 provides a more stable homogeneous solution (as discussed in section 2.11.3).

Cerium based solid solution is made by two different methods namely co–precipitation (COP) and Sol-gel (SOL) method. Both the methods provide a homogeneous solid solution. Crystallite size of the solid solution $Ce_xZr_{1-x}O_2$ ($0.4 \leq x \leq 8.8$) made by the Sol-gel technique is less as compared to that made by the COP method. It is also observed that the OSC of the solid solution made by the Sol-gel method is higher than that made by the COP technique. For example, the OSC of $Ce_{0.6}Zr_{0.4}O_2$ prepared by COP and SOL method is found to be 0.140 and 0.147 mol of O_2/CeO_2, respectively. The reason behind this is the higher lattice expansion and higher substantial of OSC band in SOL samples as compared to COP sample. Table 5.1 shows the comparison of the characteristics of solid solutions of

$Ce_xZr_{1-x}O_2$ ($0.4 \leq x \leq 8.8$) prepared by SOL and COP methods. The materials, $Ce_{0.4}Zr_{0.6}O_2$, $Ce_{0.5}Zr_{0.5}O_2$, $Ce_{0.6}Zr_{0.4}O_2$, $Ce_{0.7}Zr_{0.3}O_2$ and $Ce_{0.8}Zr_{0.2}O_2$ have been denoted as CZ1, CZ2, CZ3, CZ4 and CZ5, respectively. In all the materials considered, the sample made by Sol-gel method is having higher OSC than that made by COP method. $Ce_{0.6}Zr_{0.4}O_2$ (CZ3) possessed the highest OSC among the samples. From the details provided in Table 5.1, it is concluded that the Sol-gel (SOL) method of solid solution preparation is the best method as compared to the COP method. It is due to the significant OSC band in the Sol- gel synthesized sample as compared to the COP synthesized sample and it is seen in XRD pattern of sample

Table 5.1: Characteristics comparison of solid solution preparation of $Ce_xZr_{1-x}O_2$ by SOL and COP method (Priya N S, 2016).

	$Ce_{0.4}Zr_{0.6}O_2$ (CZ1)		$Ce_{0.5}Zr_{0.5}O_2$ (CZ2)		$Ce_{0.6}Zr_{0.4}O_2$ (CZ3)		$Ce_{0.7}Zr_{0.3}O_2$ (CZ4)		$Ce_{0.8}Zr_{0.2}O_2$ (CZ5)	
	COP	SOL	COP	SOL	COP	SOL	COP	SOL	COP	SOL
Crystallite size (nm)	6.0	5.6	6.0	5.7	9.8	7.5	9.0	6.0	10.0	7.5
OSC-(δ) (mol of O_2/mole of CeO_2)	.024	.043	.067	.121	.140	.147	.102	.131	.079	.102

Generally, three types of techniques are used for nanofuel preparation namely magnetic stirrer method, tip sonication method and combination of both the methods. Nanofuel is generally prepared by distributing the certain amount of nanoparticle in kerosene. Due to the van der Waals force of attraction, the nanoparticles starts to accumulate. Kerosene with the accumulated nanoparticles cannot be readily used as a full-fledged nanofuel and hence this type of fuel formed is considered as unstable. For getting a stable nanofuel, prevention of accumulation of nanoparticles is required and for this purpose, certain materials called as surfactants are mixed with the solution. The ratio of nanoparticles (solid solution) to

surfactant, generally used is 1:2 (Sharif *et al.*, 2009). As discussed above, Tween 80 is the optimum surfactant and it is selected as surfactant in the present work. In case of tip sonication technique, Tip sonicator (M/s. Sonics USA, model: VCX 750) is used for the synthesis of nanofuel. During the synthesis of nanofuel, the temperature of sample (kerosene + nanoparticles + surfactant) was maintained at 35 ˚C. Figure 5.1 shows the pictorial view of the setup used for the synthesis of nanofuel. An ice bath arrangement was made in the tip sonicator for maintaining the sample container (capacity 1litre) at the required temperature during the sonication period. Along with the suitable surfactant (Tween 80) different concentrations of nanoparticle (solid solution) was distributed in kerosene. Due to high frequency (20 kHz) of sonorod tip, a high field of conical energy was built up in kerosene.

Fig. 5.1: Tip sonicator used to prepare nanofuel.

Fig. 5.2: Sample of pure kerosene and nanofuel prepared using tip sonicator.

Because of this high conical energy, nucleate boiling takes place in kerosene which produces limitless number of macro bubbles. When theses bubbles fall down, an enormous amount of energy produces, which disperse the nanoparticles thereby avoiding the accumulation of nanoparticles (Krause *et al.*, 2010). Sonication period for the current study was about 1 hr. Figure 5.2 shows the sample prepared by tip sonication technique.

Another method of nanofuel synthesis is the magnetic stirrer technique. Figure 5.3 shows magnetic stirrer (IKAC – Mag, Model: HS7) device. In the magnetic stirrer method of nanofuel preparation, a suitable concentration of nanoparticles was added in kerosene with the required amount of surfactant (Tween 80) at a proportion of 1:2. The duration of stirring is about 2 hrs and sample was maintained at room temperature for the same period. The polarity of the developed magnetic field on the magnetic stirrer plate was altered by the AC supply. The magnetic bead (shown in Figure 5.4) was kept inside the sample container to respond the altered magnetic field due to which rotation of magnetic bead took place inside the sample. This leads to the dispersion of nanoparticles in kerosene. Prepared sample is shown in Figure 5.5.

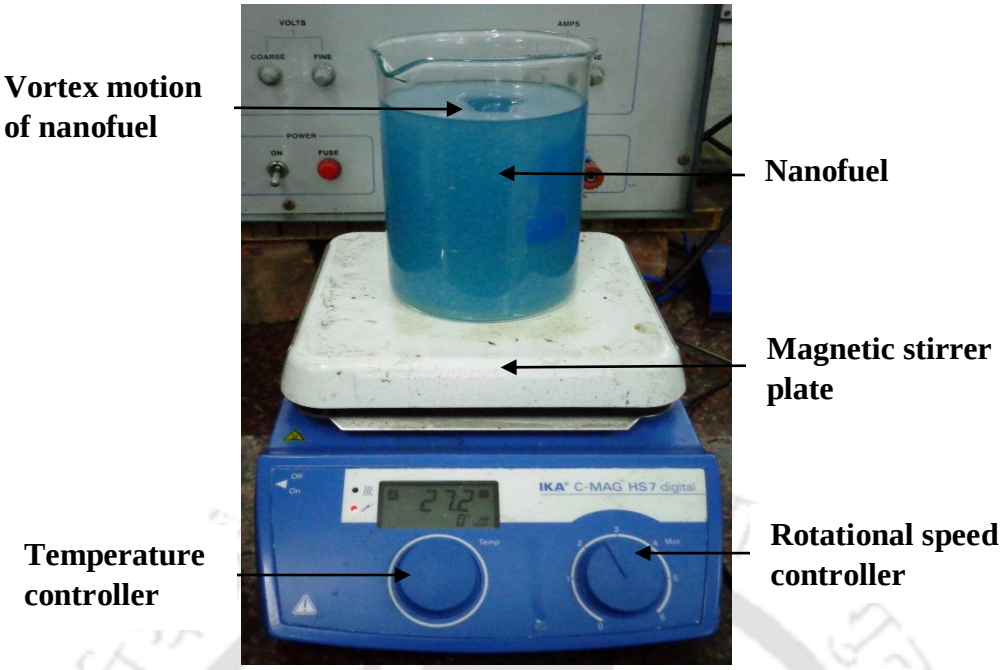

Fig. 5.3: Preparation of nanofuel using magnetic stirrer.

Fig. 5.4: Magnetic bead.

Fig. 5.5: Sample prepared using magnetic stirrer.

Third method of synthesis of nanofuel is the combined method in which both the tip sonication and magnetic stirrer were used. The duration of this method is about 2 hrs in

which 30 minute is used by both the methods alternatively. In tip sonication method as discussed above, the probe sonicates inside the limited conic volume so magnetic stirrer method is used after tip sonication in order to make the uniform dispersion of nanoparticles in kerosene. As discussed earlier, among the three methods, tip sonication and combined method for nanofuel preparation are the best methods as compared to the magnetic stirrer method. So for the preparation of optimum concentration of nanoparticle, tip sonication and combined method were used.

5.3 Selection of Suitable Nanoparticles (Solid Solution)

As discussed earlier, there are various types of cerium based high OSC nanoparticles, such as CeO_2, $Ce_xZr_{1-x}O_2$ (CZ) ($0.4 \leq x \leq 0.8$), $Ce_{0.6}Zr_{0.4-x}Y_{1.3x}O_2$ (CZA, CZB, CZL, CZN) and $Ce_{0.6}Zr_{0.4-x}Mn_xO_2$ (CZM) (x =0.0, 0.1, 0.2, 0.3, 0.4; Y = Al, Bi, La, Nd). All these nanoparticles have different OSC, specific surface area and crystallite size. Also they have their own limitation in terms of thermal performance and thermal stability. In CZ, CZA, CZM, CZB, CZL and CZN group, $Ce_{0.6}Zr_{0.4}O_2$ (CZ3), $Ce_{0.6}Zr_{0.2}Al_{0.26}O_2$ (CZA2), $Ce_{0.6}Zr_{0.2}Mn_{0.2}O_2$ (CZM2), $Ce_{0.6}Zr_{0.1}Bi_{0.39}O_2$ (CZB3), $Ce_{0.6}Zr_{0.2}La_{0.26}O_2$ (CZL2) and $Ce_{0.6}Zr_{0.1}Nd_{0.13}O_2$ (CZN1) have high OSC and specific surface area respectively, which is shown in Table 5.2.

Table 5.2: Nanoparticles with different OSC and specific surface area (Priya N S, 2016).

S. No.	Ceria based high OSC nanoparticles	Nomenclature	OSC (mol. of O_2/mol of CeO_2)	Specific surface area (m^2/g)
1	CeO_2	CeO_2	-	3.676
2	$Ce_{0.6}Zr_{0.4}O_2$	CZ3	0.1470	50.743
3	$Ce_{0.6}Zr_{0.2}Al_{0.26}O_2$	CZA2	0.2293	121.496
4	$Ce_{0.6}Zr_{0.1}Al_{0.39}O_2$	CZA3	0.2131	60.125
5	$Ce_{0.6}Zr_{0.2}Mn_{0.2}O_2$	CZM2	0.1799	51.199
6	$Ce_{0.6}Zr_{0.1}Bi_{0.39}O_2$	CZB3	0.0327	23.903
7	$Ce_{0.6}Zr_{0.2}La_{0.26}O_2$	CZL2	0.0817	27.106
8	$Ce_{0.6}Zr_{0.1}Nd_{0.13}O_2$	CZN1	0.1256	31.458

Among these nanoparticles, CZA2 possess higher OSC and specific surface area. OSC of CZA2 is 0.2293 mole of O_2/ mole of CeO_2 while specific surface area is 121.496 m^2/g. The crystallite size of CZA2 is found to be 4.7 nm. Although the crystallite size of CZA2 is greater than CZM2 (2.7 nm) and CZA3 (2.6 nm), but its OSC and specific surface area are greater than that of CZM2 and CZA3. Hence, CZA2 is selected for further study.

5.4 Optimization of Nanoparticle Concentration

Tip sonication and combined method of nanofuel preparation are found to be the best method for nanofuel preparation. For the preparation of highly stable nanofuel, the best surfactant is Tween 80 which has been discussed in chapter 2. Amount of nanoparticles (concentration of nanoparticles) play an important role in the context of relative stability of nanofuel and thermal performance of kerosene stove. For the present work, focus has been made on effect of concentration of nanoparticles on thermal performance of kerosene stove. For this purpose, the concentration of CZA2 was varied from 0.02, 0.03, 0.04 0.05 0.06 and 0.07 wt. %. Prepared nanofuel samples by varying the concentration of CZA2 with surfactant Tween 80 were tested with CB and PRB. Performances of the burners were tested in terms of thermal efficiency at 1.5 kW input power. Figure 5.6 shows the effect of nanoparticles concentration on thermal efficiency of PRB and CB. From the investigation, it was found that with the increase in the CZA2 concentration in kerosene, thermal efficiency of PRB and CB were increasing till 0.05 wt. % of CZA2 and after that they were found to decrease. Maximum thermal efficiency was obtained at 0.05 wt. % of CZA2 and the reason behind this is the maximum activation energy works for of this particular concentration of CZA2 as compared to the other concentrations of CZA2. Minimum thermal efficiency was obtained at 0.02 wt. % of CZA2, which has been shown in Figure 5.6.

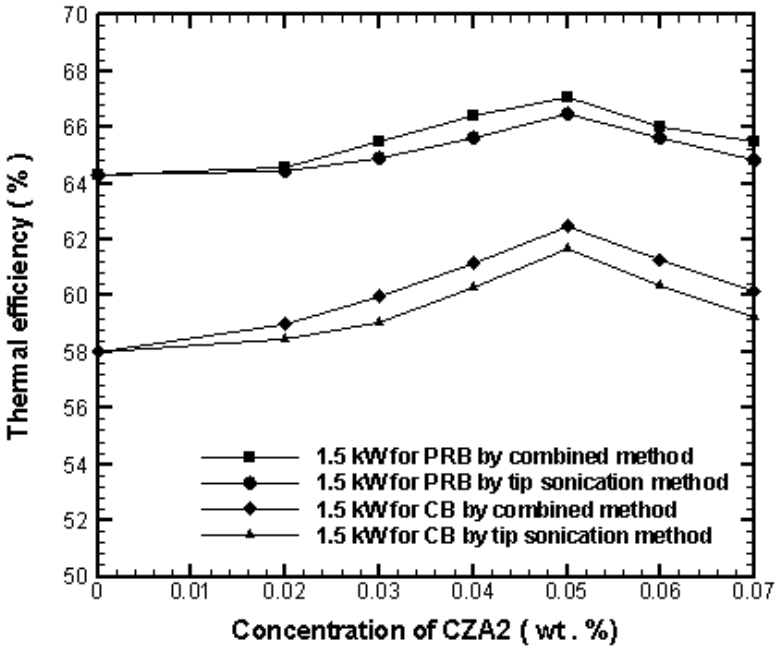

Fig. 5.6: Effect of nanoparticle concentration on thermal efficiency of CB and PRB.

Table 5.3 shows the thermal efficiency and improvement in thermal efficiency of CB at different concentrations of CZA2 for both the methods of nanofuel preparation. From the Table 5.3, it is found that the maximum improvement in the thermal efficiency is obtained at 0.05 wt. % of CZA2 and they were 7.70 % and 6.32 % by combined and tip sonication method, respectively. Table 5.4 shows the comparison between CB without nanofuel and PRB with nanofuel at different CZA2 concentrations with the combined method and tip sonication methods. From Table 5.4, it is observed that maximum improvement in thermal efficiency occurred at 0.05 % of CZA2 and they are 15.68 % and 14.65 %, respectively for nanofuel prepared employing combined method and tip sonication method, respectively.

In the case of PRB, maximum thermal efficiency obtained were 67.10 % and 66.50 % for combined method and tip sonication method, respectively at 0.05 wt. % of CZA2 while in case of CB, the maximum thermal efficiency were 62.47 % and 61.67 % for combined method and tip sonication method respectively at 0.05 wt. % of CZA2. Figure 5.7 shows the effects of concentration of CZA2 (wt. %) on power output for the input power of 1.5

Table 5.3: Comparison of thermal efficiency of CB at different concentration of CZA2.

CZA2 concentration (wt. %)	Combined Method		Tip Sonication Method	
	Thermal efficiency (%)	Increase in Thermal efficiency (%)	Thermal efficiency (%)	Increase in Thermal efficiency (%)
0.00	58	0.00	58	0.00
0.02	58.9	1.67	58.4	0.81
0.03	59.9	3.39	59.0	1.84
0.04	61.1	5.46	60.2	3.91
0.05	62.4	7.70	61.6	6.32
0.06	61.2	5.63	60.3	4.08
0.07	60.1	3.74	59.2	2.18

Table 5.4: Comparison of thermal efficiency of PRB at different concentration of CZA2

CZA2 concentration (wt. %)	Combined Method		Tip Sonication Method	
	Thermal efficiency (%)	Increase in Thermal efficiency (%) w.r.t CB	Thermal efficiency (%)	Increase in Thermal efficiency (%) w.r.t CB
0.00	64.3	10.86	64.3	10.86
0.02	64.6	11.37	64.4	11.12
0.03	65.5	12.93	64.9	11.89
0.04	66.4	14.48	65.6	13.10
0.05	67.1	15.68	66.5	14.65
0.06	66.0	13.84	65.6	13.10
0.07	65.0	12.93	64.8	11.72

kW. Trend of output power with concentration of CZA2 is the same as in thermal efficiency. Maximum and minimum output power was obtained at 0.05 and 0.02 wt. % of CZA2. Table 5.5 shows the output power of PRB with both the methods of nanofuel preparation.

From Table 5.5, it is found that, same kind of trend is observed for output power as in Table 5.3 and Table 5.4. For the concentration of 0.05 wt. % of CZA2, the maximum output

power is 1.063 kW and 1.053 kW in the combined method and tip sonication method, respectively. Whereas for the same concentration, the enhancement of power output achieved was 15.64 % and 14.55 % in the combined method and tip sonication method, respectively.

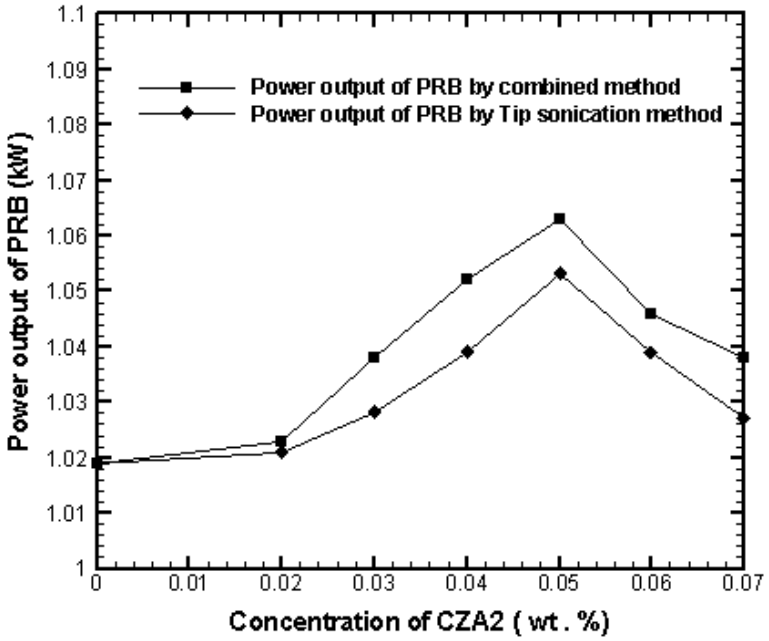

Fig. 5.7: Effect of CZA2 concentration (wt. %) on power output.

Table 5.5: Comparison of output power of PRB w.r.t CB at different concentration of CZA2.

CZA2 concentration (wt. %)	Combined Method		Tip Sonication Method	
	Power output (kW)	Increase in power output (%) w.r.t CB	Power output (kW)	Increase in power output (%) w.r.t CB
0.00	1.019	10.85	1.019	10.85
0.02	1.023	11.29	1.021	11.07
0.03	1.038	12.92	1.028	11.83
0.04	1.052	14.44	1.039	13.03
0.05	1.063	15.64	1.053	14.55
0.06	1.046	13.79	1.039	13.03
0.07	1.038	12.92	1.027	11.72

Hence, from the above information, it is concluded that the optimum concentration of CZA2 is 0.05 wt. % and the best method of nanofuel preparation is the combined method. The optimum surfactant is tween 80 in the context of relative stability. So for further experiments, nanofuel is prepared by the combined method with surfactant Tween 80 and the concentration of CZA2 is chosen as 0.05 wt. %.

5.5 Nanofuel Characterization

It is necessary that nanofuel properties should be in range of base fuel so that performances of the system should not get affected. Viscosity, flash point and fire point were measured at the concentration of 0.05 % wt. of CZA2. For the flash point and fire point of nanofuel variation were only 1°C and 1°C respectively as compared to pure kerosene. Dynamic viscosity of nanofuel was observed to be high (14.26 %) compared to pure kerosene. The addition of nanoparticles in the fuel increased the resistance between the fluid layers and hence increased the viscosity. Table 5.6 shows the properties of CZA2 based nanofuel and kerosene.

Table 5.6: Properties of CZA2 based nanofuel and kerosene.

Particulars	Fuel Types	
	Kerosene	Nanofuel (at 0.05 wt. % concentration)
Flash point (˚C)	55	56
Fire point (˚C)	61	62
Dynamic viscosity (Ns/m^2)	1.30×10^{-3}	1.49×10^{-3}

5.6 Summary

Cerium based oxide gained more attention among the researchers because of its property to switch over from Ce^{+4} to Ce^{+3} and vice versa. During combustion, cerium based oxide

absorbs the oxygen through the reduction of NO_x and same oxygen is supplied to CO and other unburned hydrocarbon for oxidation. This process not only reduces the emissions but also makes the combustion more efficient. $Ce_{0.6}Zr_{0.2}Al_{0.26}O_2$ (CZA2) nanoparticle has the high oxygen storage capacity (OSC) as compared to other nanoparticles. Sol-gel method was the best method for the preparation of nanoparticles, which lead to more OSC. For nanofuel preparation, combined method (comprises tip sonication and magnetic stirrer method) was the best method. 0.05 wt. % concentration of CZA2 was found to be the optimum concentration which provides high thermal efficiency.

भारतीय प्रौद्योगिकी संस्थान गुवाहाटी
Indian Institute of Technology Guwahati

Chapter 6

Result and Discussion - Self-aspirated Porous Radiant Burner

In this chapter, performance evaluation of the self-aspirated PRB stove are discussed in terms of various performance parameters such as thermal efficiency and emissions (CO and NO_x). The influence of various parameters such as nozzle diameter, distance between burner and vessel, vessel diameter and ambient temperature on the performance of the PRB stove have been also presented. Temperature distribution measured along the axial and radial directions and the effect of power intensity on the temperature distribution have been also discussed.

6.1 Thermal Efficiency

As discussed in chapter 3, the thermal efficiency was measured by conducting water boiling test (WBT) following the guidelines of bureau of Indian standard (IS 10109:2002). Figure 6.1 shows two different nozzles (orifice) used in PRB having diameters, 0.454 mm and 0.376 mm, respectively. Due to reduction in the nozzle diameter, velocity of the upcoming vaporized kerosene increases resulting in the creation of a higher pressure difference between the nozzle section and the surrounding air. Because of this, more air is sucked in the mixing chamber (venture region), which increases the air entrainment. This increased air entrainment not only improves the combustion; but also increases the thermal efficiency. Figure 6.2 shows the measured thermal efficiency for different input power for PRB with the two different nozzle diameters, 0.454 mm and 0.376 mm. The thermal efficiency of the PRB varies from 52.5 – 61.3 % for 0.454 mm nozzle and 55.5 – 64.3 % for 0.376 mm

nozzle in the input power range of 1.5-3 kW. In the case of PRB with venture effect, the increased air entrainment plays an important role on both efficiency and emissions.

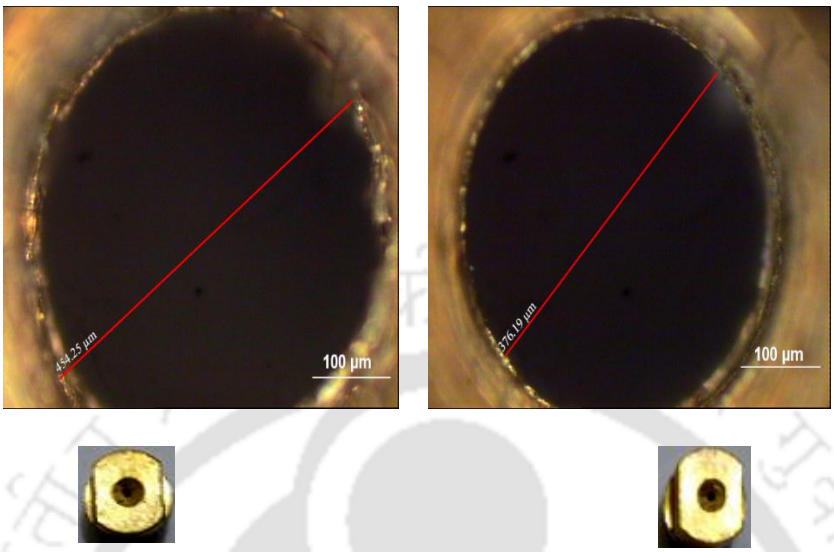

Nozzle of diameter 0.454 mm Nozzle of diameter 0.376 mm

Fig. 6.1: Different type of nozzles.

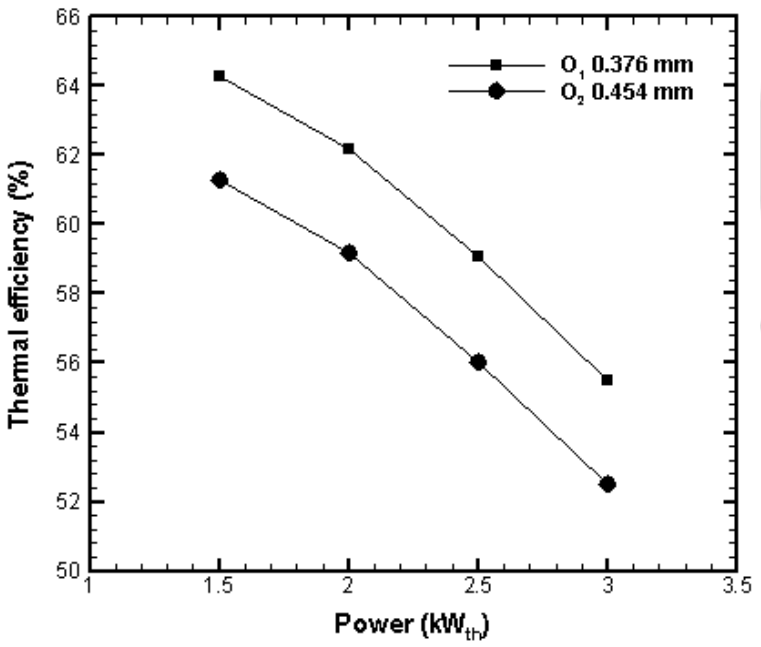

Fig. 6.2: Thermal efficiency at different nozzle (orifice) diameter at different power input for PRB.

The percentage of increase of efficiency for the PRB with 0.376 mm diameter nozzle was about 4.9 % when compared with the 0.454 mm diameter nozzle. So the nozzle having a

diameter of 0.376 mm was considered as optimum and it was selected for further experiments.

Figure 6.3 shows the comparison of thermal efficiency between the CB and PRB. The thermal efficiency varies from 48.5 – 58 % for CB and 55.5 – 64.3 % for PRB in the input power range of 1.5 – 3 kW. The percentage increase in thermal efficiency for the PRB at an input power of 1.5 kW was about 10.86 % when compared with the CB. The maximum improvement in thermal efficiency observed was about 14.43 % at 3 kW input power. As discussed earlier, with the usage of PRB, conduction, radiation and convection heat transfer modes become active which leads to better combustion of the fuel. This results in the higher thermal efficiency.

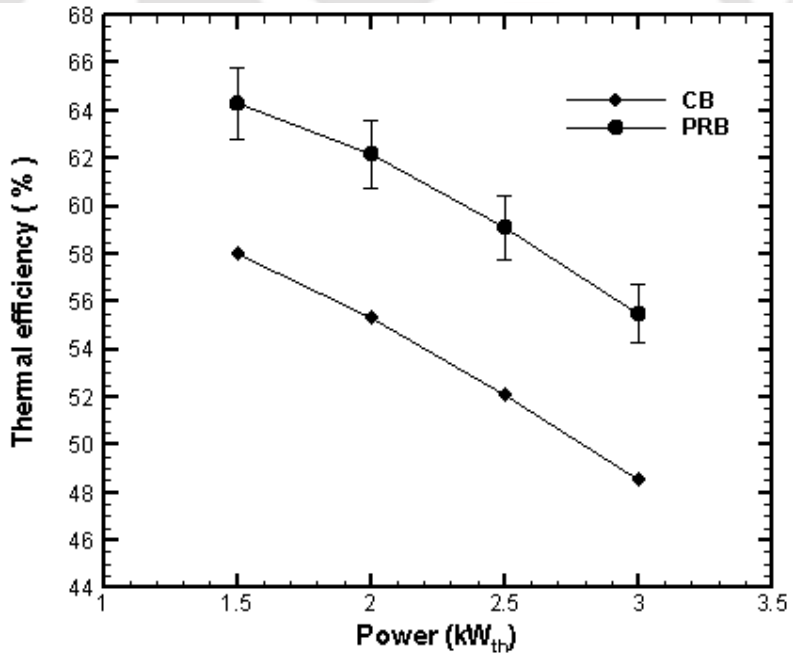

Fig. 6.3: Thermal efficiency of different burners.

It is further observed from Figure 6.3 that with the increase in the input power, thermal efficiency was found to decreases in both CB and PRB. The reason behind this is the higher heat loss to the surrounding at higher power input, due to which the net power output decreases as compared to the input power. Further, in PRB with smaller nozzle diameter

(0.376 mm), the downward shifting of the reaction zone takes place, and this augments the volumetric heat release. It can be seen that the maximum thermal efficiency of the PRB is 64.3 % for the case with nozzle diameter 0.376 mm at thermal input power 1.5 kW.

Thermal efficiency depends on various factors such as vessel diameter, distance between the burner surface and vessel, and ambient temperature. Figure 6.4 shows the effects of vessel diameter on the thermal efficiency. For this purpose, 4 vessels were selected with different diameters, viz., 255 mm, 270 mm, 285 mm and 300 mm, respectively. The capacity of these vessels accordingly was 5 kg, 7 kg, 9 kg and 12 kg, respectively. For any given condition with the increase in vessel diameter, the thermal efficiency increases, reaches a peak value and then decreases to a minimum value (Lucky and Hossain, 2001). It is observed from the experiments that, with increase in vessel diameter from 255 mm to 270 mm, an improvement in the thermal efficiency (4.8 %) was noted. But on the contrary, with the increase of vessel diameter beyond 270 mm, the thermal efficiency was found to reduce, 1.6 % (for 285 mm) and 5.2 % (for 300 mm), when compared with the vessel with diameter 270 mm. The decrease in thermal efficiency is attributed to the higher convective and radiative heat losses from the burner, resulting in a low amount of heat, received by the vessel. The decrease in thermal efficiency beyond a certain vessel diameter is due to the large surface area of the vessels by which more amount of heat is lost to the surroundings for the same input load. So for achieving the best efficiency, vessel diameter should be of optimum size. In present case, 270 mm diameter is the optimum vessel diameter which gave the highest thermal efficiency (64.3 %) under the same operating condition.

Figure 6.5 shows the variation of thermal efficiency due to the impact of the distance between the bottom of vessel surface and top of burner surface. For this purpose, thermal efficiency was measured at three different distances, 10 mm, 30 mm and 50 mm respectively. Thermal efficiency was found to high (64.3 %) when the vessel was placed

close to the porous burner (10 mm). Drop in thermal efficiency as compared to the highest efficiency was about 3.5 % and 6 % when the vessel was placed at a distance of 30 mm and 50 mm, respectively. When the vessel is closer to the burner, minimum heat loss occurred to the surrounding, while in the case of larger distance between the vessel and burner, maximum amount of heat loss occurred to the surrounding. Ambient temperature also influences the thermal efficiency of the burner. Figure 6.6 shows the variation of thermal efficiency with respect to the ambient temperature.

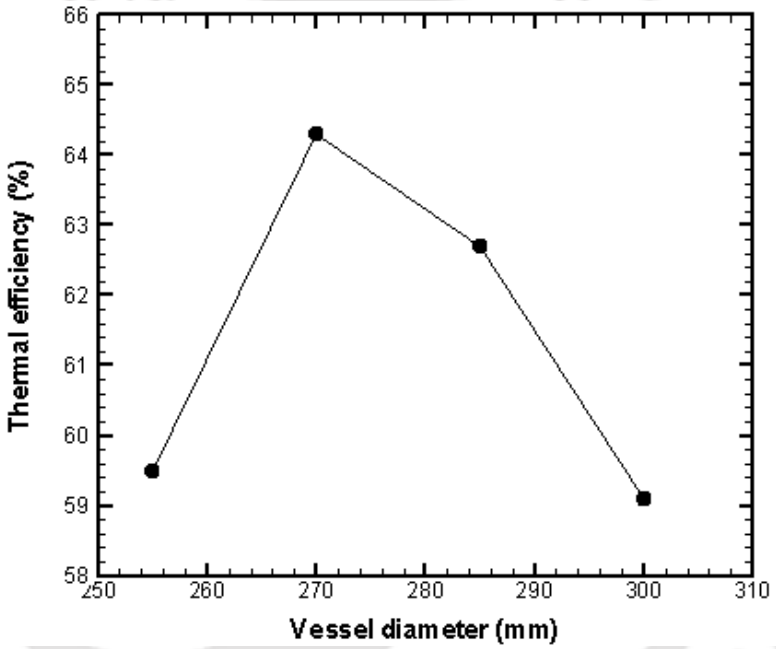

Fig. 6.4: Variation of thermal efficiency with vessel diameter with PRB.

In PRB, two types of heat losses occur: convective and radiative heat loss. But in the case of CB, only convective heat loss takes place. Hence the rate of heat loss is lower in CB as compared to PRB. Also in cold weather conditions, more heat loss occurred as compared to the hot weather conditions. So in order to investigate the thermal efficiency with ambient temperature, the thermal efficiencies of both CB and PRB were measured at different ambient temperatures (10 ˚C, 15 ˚C, 20 ˚C, 25 ˚C, and 30 ˚C). The maximum thermal efficiency for both CB and PRB was obtained at 30 ˚C.

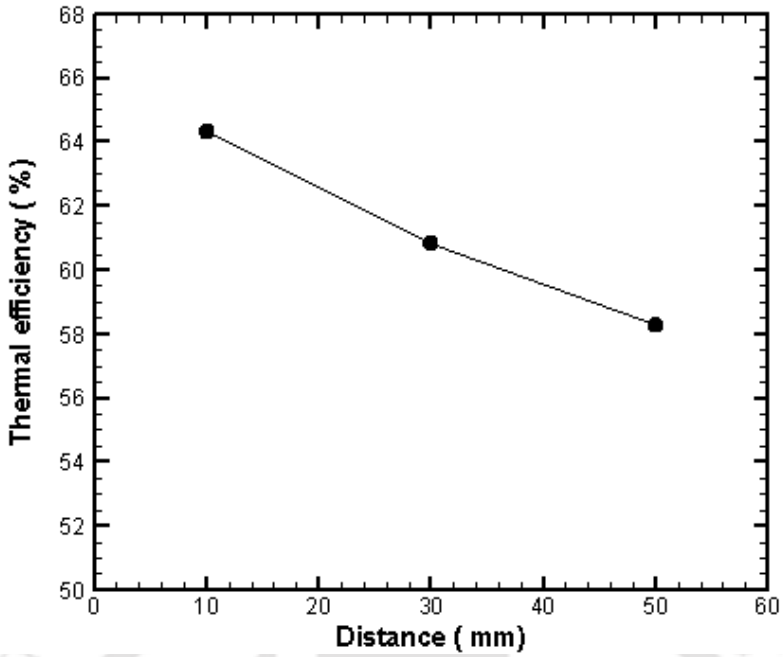

Fig. 6.5: Variation of thermal efficiency with distance between vessel and burner.

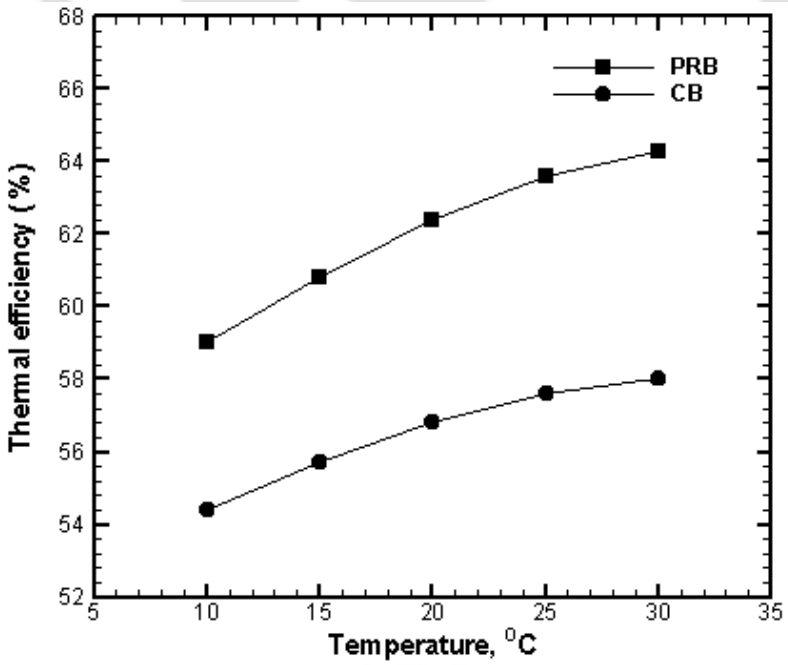

Fig. 6.6: Variation of thermal efficiency with ambient temperature.

6.2 Thermal Output Power

Figure 6.7 shows the thermal output of PRB and CB at different input powers. Power output can be obtained from the thermal efficiency of the stoves of different burners (Output power = thermal efficiency × input power). Table 6.1 shows the comparison of output power and

improvement in output power achieved in PRB as compared to CB. From the Figure 6.7, it was observed that at particular input power, output power of PRB was more than that for CB. It was due to higher thermal efficiency of PRB when compared with the CB. It is also observed that with the increase in input power, improvement in output power of PRB with respect to CB also increases. Reason behind this is the time factor of the WBT. In the case of higher input power, WBT time is much lesser for the PRB, which leads to higher improvement in the output power as compared to the lower input power. Nevertheless, high input power is more responsible for CO, NO_x and other harmful gases which has been discussed in the next section.

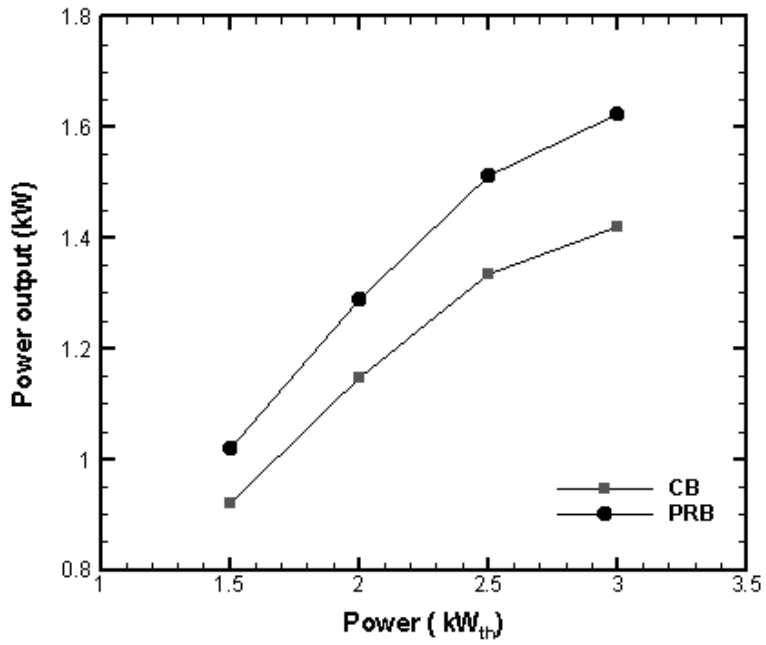

Fig. 6.7: Power output of CB and PRB with different input power.

Table 6.1: Comparison of output power of CB and PRB.

Power input (kW)	Power output (kW)		Increase in power output (%)
	CB	PRB	
1.5	0.9192	1.0190	10.85
2.0	1.1460	1.2890	12.47
2.5	1.3338	1.5130	13.43
3.0	1.4191	1.6239	14.43

6.3 Emission Analysis

As discussed in chapter 3, NO_x and CO were measured by using Greenline 8000 portable flue gas analyzer. For emission analysis, the flue gas sampling was done according to the IS 10109: 2002. For gas sampling, a standard specified hood as shown in Figure. 3.6 is used. It is made according to the BIS standard in which all the dimensions are mentioned. As discussed earlier, modification in the nozzle diameter also changes the NO_x and CO emissions. Figure 6.8 (a) - (b) shows the emissions of PRB with different nozzle (orifice) diameters.

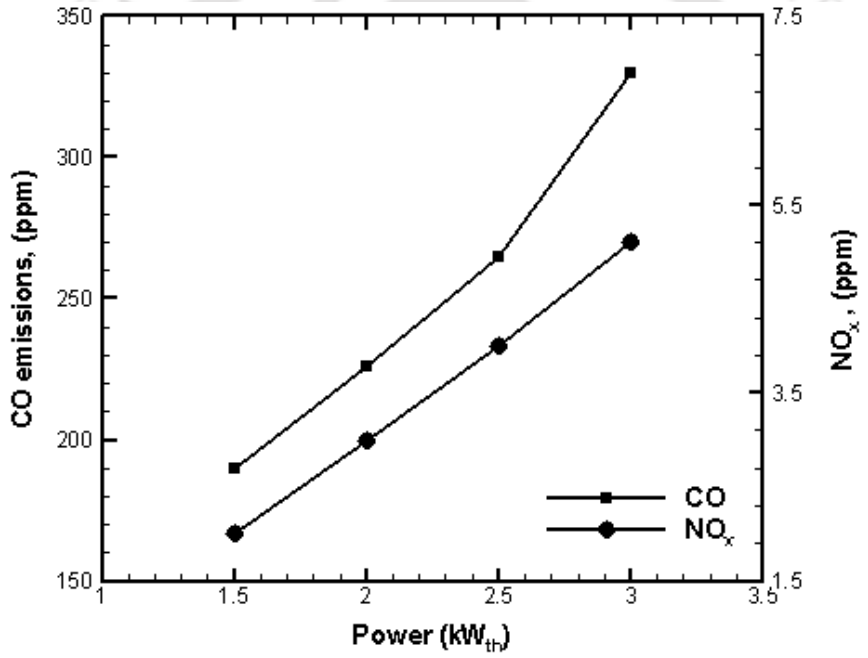

Fig. 6.8: (a) Emissions of PRB at 0.454 mm diameter nozzle.

In PRB with lower diameter nozzle, more air entrainment happen resulting in better combustion which leads to lower CO emissions. Figure 6.9 (a) - (b) shows the comparison of the amount of CO and NO_x emissions between the CB and PRB. It is to be noted that in the CB, with lean combustion, the undesirable feature of flame lift-off occurs. To avoid this, conventional pressure kerosene cooking stove is designed for a fuel rich combustion and hence the emissions are high. Measured emissions of PRB are lower than that of CB

because of better combustion and more residence time, which leads to lower CO emissions. In the PRB, due to the lower global temperature (surface temperature of the burner) when compared with the CB, the NO_x emission was also found to be much lower than that of the CB.

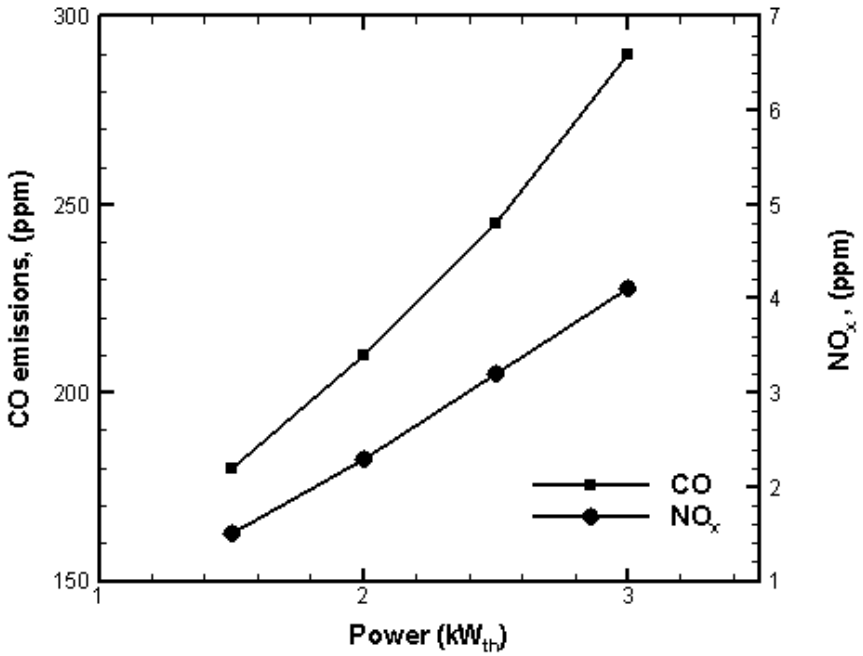

Fig. 6.8: (b) Emission of PRB at 0.376 mm diameter nozzle.

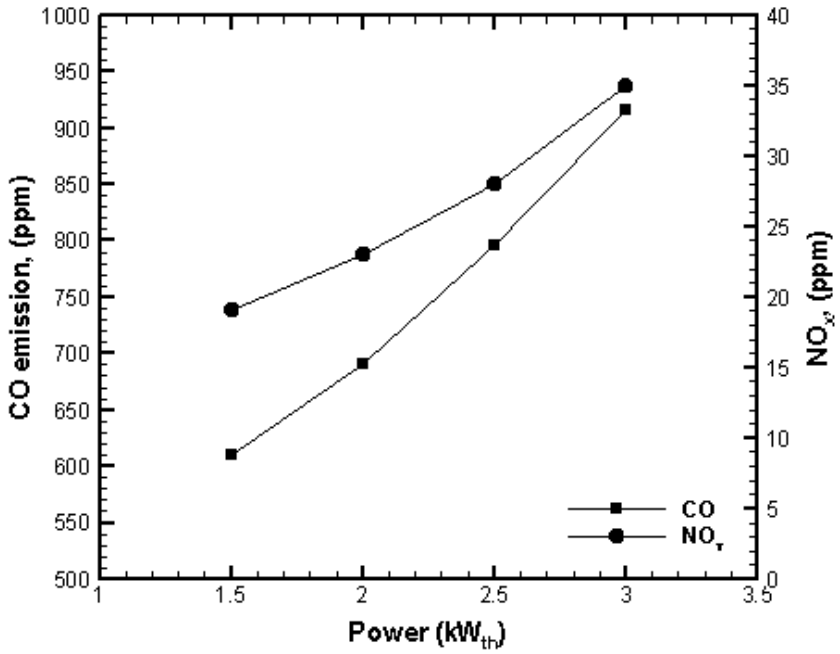

Fig.6.9: (a) CO and NO_x emissions for different thermal loads for CB.

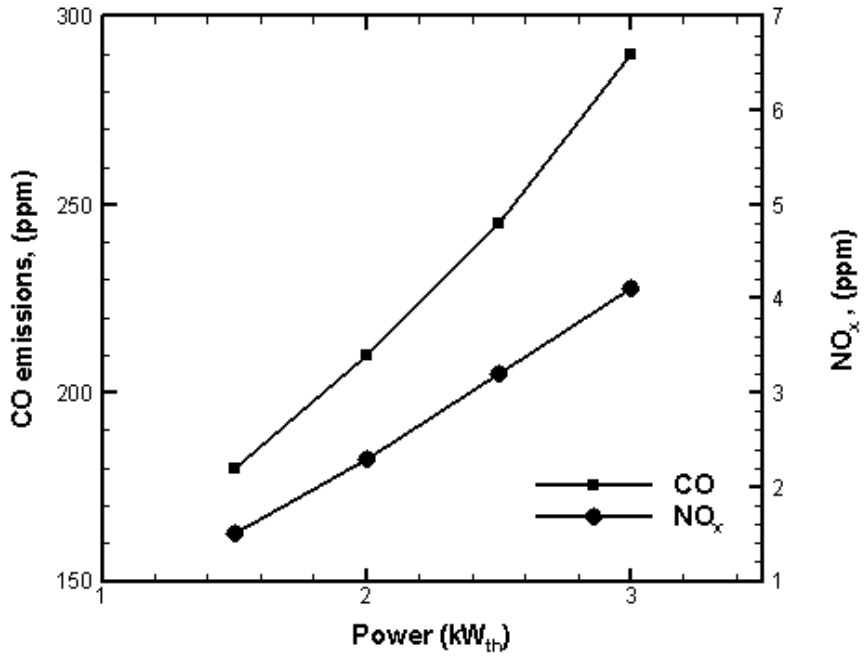

Fig.6.9: (b) CO and NO_x emissions for different thermal loads for PRB.

6.4 Temperature Distribution

Temperature distribution in the axial and radial directions of the PRB plays a vital role in thermal performance. It gives the reason for the variation of thermal efficiency and emissions at different input powers. Radial and axial temperatures were measured in the surface and thickness of the burner, respectively. K-type thermocouples were employed for the measurement of temperature and the respective thermocouple positions are shown in Figs. 6.10 (a). The outputs of thermocouples were acquired through a data acquisition system, consisting of a data logger and multiplexer. Figure 6.10 (b) shows the temperature profile in radial direction for the power input range of 1.5 – 3 kW. Surface temperature of the PRB indicates the amount of heat transferring from the burner to the load. Measurement of surface temperature is important as it directly measures the transferrable heat flux, which decides the thermal efficiency of the system. Radiant heat transfer occurred in the PRB is proportional to the fourth power of temperature and hence PRB with high temperature is preferable. Besides this, due to the high temperature difference that exists between the PRB

and surrounding, convective heat transfer increases. Knowledge of temperature distribution is needed for observing the uniformity of the temperature. Non-uniform temperature distribution leads to local *hot spot*, which increases the NO_x emission. It is observed from Figure 6.10 (b) that the maximum temperature occurs at the center of the PRB and the temperature decreases radially and reaches a minimum at the periphery. It is also inferred from Figure 6.10 (b) that the surface temperature distribution is uniform, which is a desirable feature of the PRB, as non-uniformity results in the release of thermal NO_x.

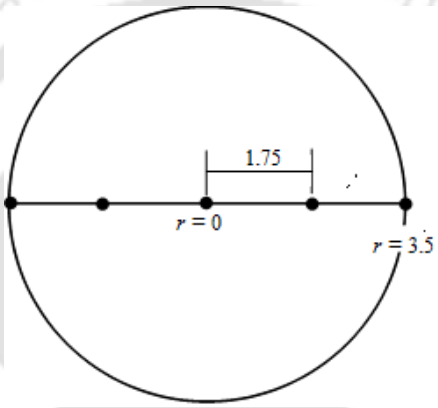

Fig. 6.10: (a) Radial positions of thermocouples on top surface of the PRB (in cm).

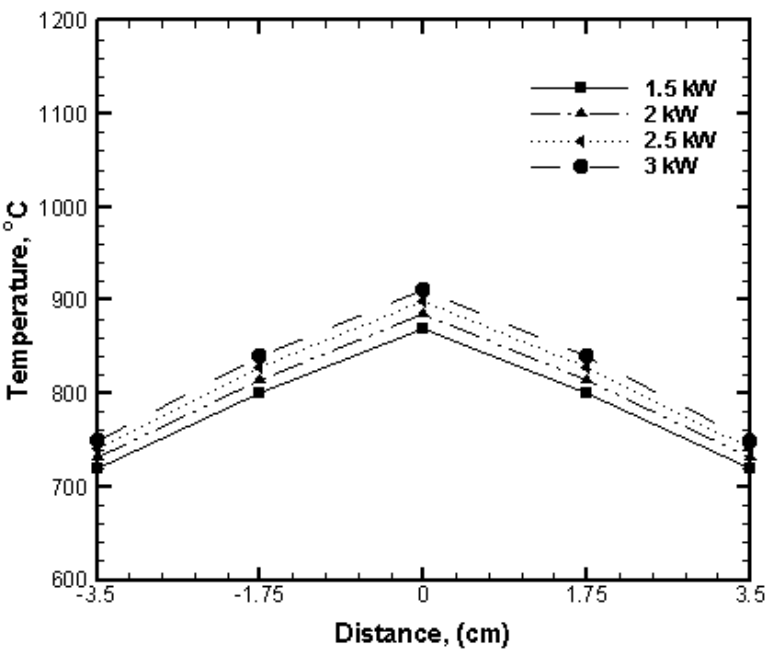

Fig. 6.10: (b) Radial temperature distribution of PRB with input power.

Similar to the radial temperature distribution, the axial temperature distribution of the PRB is also studied. The position of thermocouples in the axial direction is shown in Figure 6.11 (a). T0, T1, T3 and T4 represent the thermocouple positions located below the preheating zone, reaction zone, combustion zone 1 (center of combustion zone) and the combustion zone 2 (5 mm above the center of combustion zone), respectively. Temperature measurements were done 1 cm from the periphery of the burner in the locations, 0.0, 0.3, 2.3 and 2.8 cm, respectively from the base point of the perforated sheet.

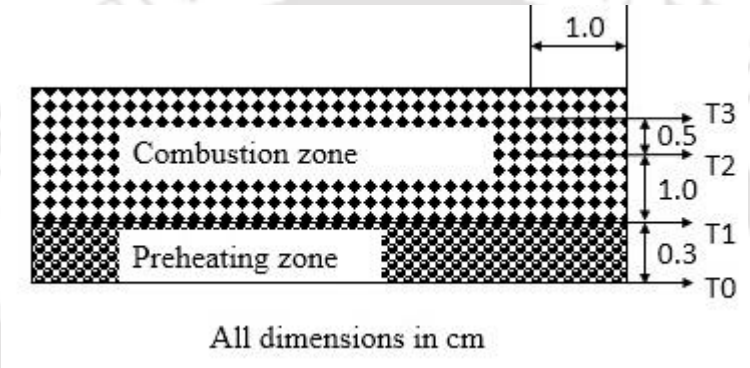

Fig. 6.11: (a) Axial positions of thermocouple in the PRB.

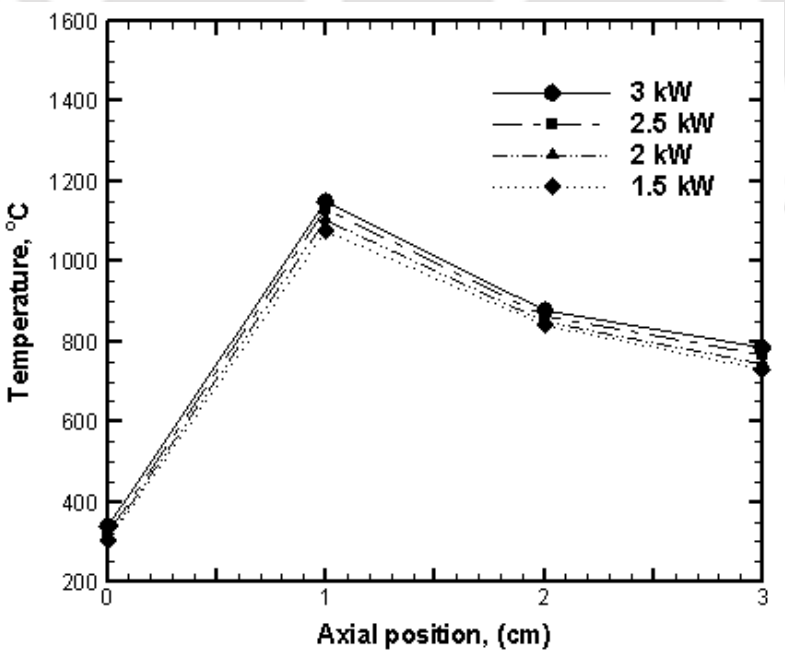

Fig. 6.11: (b) Axial temperature distributions in PRB.

At position T0 (below the preheating zone), temperature of the PRB is in the range of 300 – 340 ˚C, which is higher than the auto ignition temperature of kerosene (220 ˚C). This indicates that the combustion reaction is started below the preheat zone and the perforated sheet acts as a flame supporting layer. Liu and Hsieh (2004) observed similar condition in their set up, in which they studied the combustion characteristics of LPG in a porous burner. In their setup also, the burning took place in the entire PM, indicated by high preheat temperature. However, they reported that the high preheat temperature has a good implication on the CO emissions, as a significant portion of the energy generated through combustion was transferred to the upstream to preheat the reactants. Reduction of CO emission is very much desirable as there is a greater concern exists for the environmental protection. At location T1 (reaction zone), temperature varies in the range of 1076 – 1150 ˚C. This is the highest temperature zone when compared with other zones as shown in Figure 6.11 (b). This temperature range provides better emission (Trimis and Durst, 1996). At positions T2 (combustion zone 1) and T3 (combustion zone 2), the temperature varies from 840 to 876 ˚C and 730 to 786 ˚C. At any location, with the increase in the input power, temperature also increases. Radiation and conduction heat transfer in the PRB preheats the incoming air-fuel mixture and also helps in achieving faster transfer of heat from the reaction zone in the downward direction. As a result, the temperature rise is lower in the PRB.

6.5 Cost Analysis

From the previous study, it was observed that thermal efficiency of kerosene stove with PRB was enhanced. This enhancement can be used to find fuel saving and cost reduction and the formoula which is used for calculation of energy cost are following (Mukunda *et al.*, 1988).

Energy cost = heat release by the fuel × cost of 1MJ of fuel

Heat released by the fuel = fuel consumed × C.V

The cost of one kilogram of kerosene ≈ 43 Rs.

The energy content in one kilogram of kerosene = 43.890 MJ

So, cost of 1MJ = 43/43.890 = 0.97 Rs. /MJ

Energy cost = fuel consumed ×C.V × .97 Rs.

For CB Energy cost = 64g ×C.V × .97 Rs. = 2.7 Rs.

For PRB = 58g × C.V × .97 = 2.4 Rs.

Fuel saved = 9.375 %

Money saved = 11.11 %

This cost analysis was done based on the maximum thermal efficiency.

Figures 6.12, 6.13. 6.14, 6.15 and 6.16 show the pictorial views of pressure kerosene stove with PRB taken during different stages of the investigations.

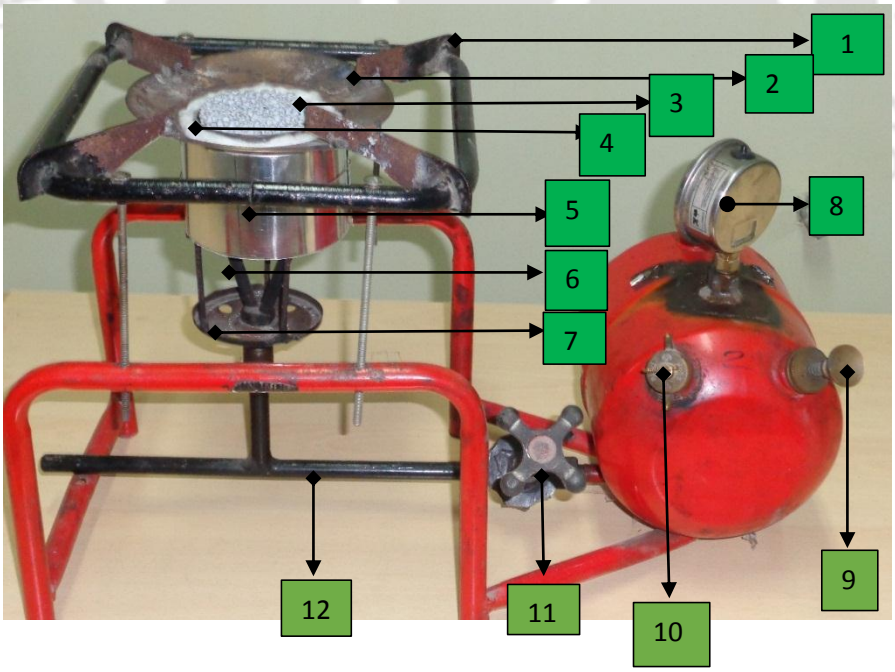

Fig. 6.12: Pressure kerosene stove with PRB (1: Pot-holder; 2: Radiation shield; 3: Porous burner; 4: Ceramic wool; 5: Aluminium sheet; 6: Vaporiser tube; 7: Vaporiser cup; 8: Pressure gauge; 9: Hand plunger; 10: Stove key; 11: Fuel regulator; 12: Fuel supply line)

Fig. 6.13: Photographic view of experimental setup for measuring thermal efficiency.

Fig. 6.14: Photographic view of experimental setup for measuring emissions.

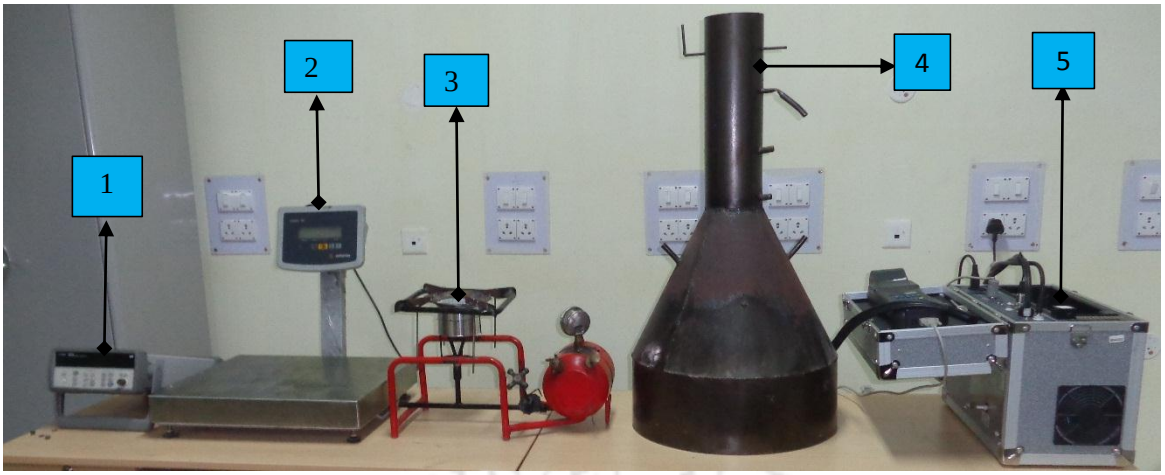

Fig. 6.15: Experimental tool (1: data acquisition system; 2: weighing balance machine; 3: PRB kerosene stove; 4: Emissions hood; 5: Flue gas analyzer).

Fig. 6.16: Burning of PRB stoves

6.6 Summary

Performance analyses of the self-aspirated pressurized kerosene cooking stove with PRB (1.5 – 3 kW) have been carried out in terms of thermal efficiency, CO and NO_x emission characteristics. The maximum thermal efficiency of PRB obtained was about 64.3 % with nozzle diameter of 0.376 mm at 1.5 kW, while for the same input power, thermal efficiency

of the CB was found to be about 58 %. Therefore, an ample amount of kerosene fuel can be saved by using the self-aspirated pressurized kerosene cooking stove with PRB. Measured CO and NO_x emissions in the self-aspirated pressurized kerosene cooking stove with PRB were found in the range of 180 – 290 ppm and 1.5 – 4.1 ppm, respectively for the input power range of 1.5 – 3 kW. While in case of CB, measured CO and NO_x emissions were in the range of 610 – 915 ppm and 19 – 35 ppm for the same input power. As the developed stove is self-aspirated, it works on natural draft and hence it is perfectly suitable for domestic cooking purpose.

भारतीय प्रौद्योगिकी संस्थान गुवाहाटी
Indian Institute of Technology Guwahati

Chapter 7

Result and Discussion - Self aspirated Porous Radiant Burner with CZA2 Based Nanofuel

In this chapter, thermal efficiency and thermal output power of CB and PRB with and without nanofuel are presented for the input power of 1.5 – 3 kW. Improvement in thermal efficiency and output power are also presented. Emission analysis of different burners with and without nanofuel are also discussed.

7.1 Thermal Efficiency

Thermal efficiency is estimated by conducting WBT (as discussed in chapter 3). Thermal efficiency of both conventional burner and porous radiant burner are estimated at different input power. Figure 7.1 shows the comparison of thermal efficiency of CB and PRB with and without nanofuel. In all the cases, trend is the same i.e. with increased in input power, thermal efficiency decreases. The reason behind this is the higher heat loss to the surrounding at higher input powers. Maximum and minimum thermal efficiency are found at 1.5 kW and 3.0 kW, respectively. In the case of CB, the maximum and the minimum thermal efficiency are 58 % and 48.5 % respectively. While in the case of CB with nanofuel, the maximum and the minimum thermal efficiency are 62.47 % and 52.5 % respectively. For PRB without nanofuel, the maximum and the minimum thermal efficiency are 64.3 % and 55.5 % respectively. While in the case of PRB with nanofuel, the maximum and the minimum thermal efficiency are 67.10 % and 58.5 % respectively.

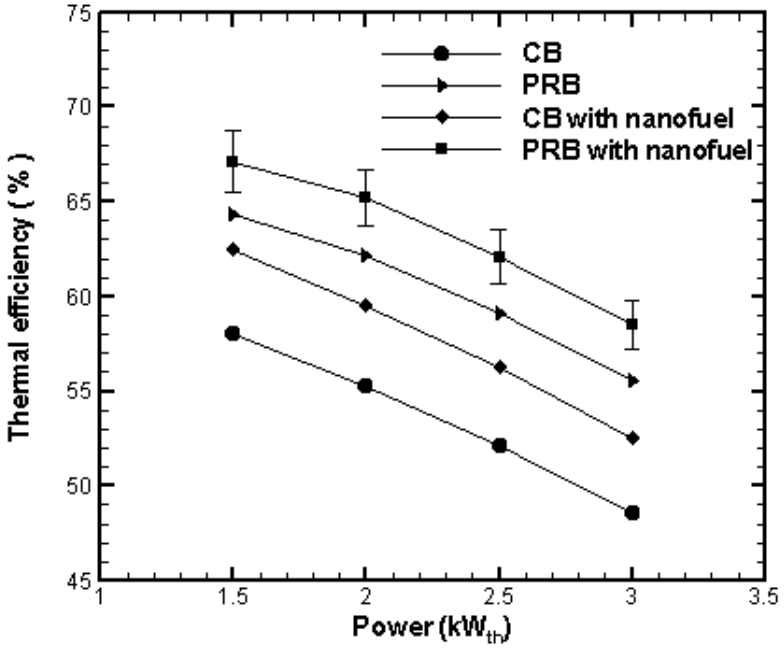

Fig. 7.1: Comparison of thermal efficiency of CB and PRB at different input power.

Table 7.1 shows the improvement in thermal efficiency of CB and PRB with nanofuel w.r.t CB without nanofuel. With increasing the input power, improvement in thermal efficiency also increases as shown in Figure 7.2. The reason behind this is at high input power the time taken to reach the water temperature up to 90 ˚C is less. In the case of CB with nanofuel, the thermal efficiency improvement varies from 7.70 – 8.24 %, while in the case of PRB with nanofuel, it varies from 15.68 – 20.61 %.

Table 7.1: Comparison of thermal efficiency of CB and PRB with nanofuel w.r.t CB

Power input (kW)	Thermal efficiency (%)		Increase in thermal efficiency (%)	Thermal efficiency (%)		Increase in thermal efficiency (%)
	CB	CB with nanofuel		CB	PRB with nanofuel	
1.5	58.0	62.4	7.70	58.0	67.1	15.68
2.0	55.3	59.5	7.59	55.3	65.2	17.93
2.5	52.1	56.2	7.86	52.1	62.1	19.19
3.0	48.5	52.5	8.24	48.5	58.5	20.61

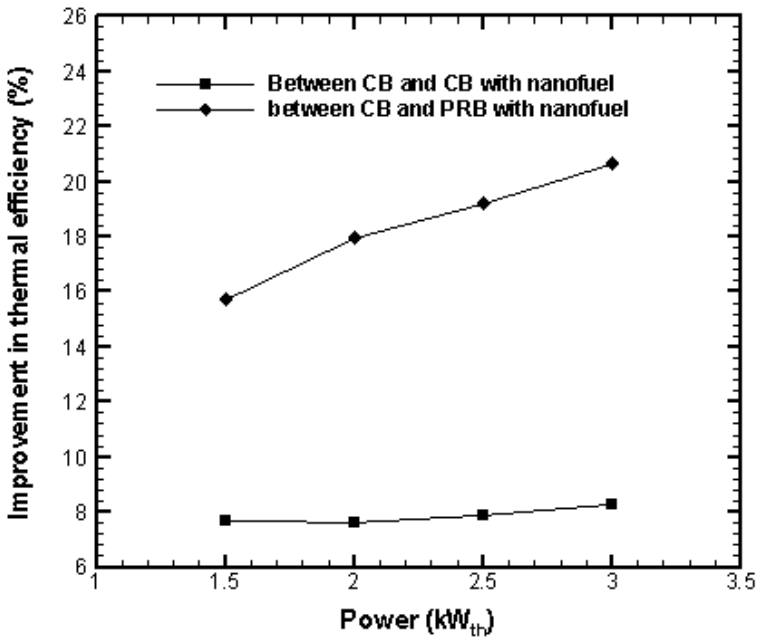

Fig. 7.2: Improvement in thermal efficiency of CB and PRB with nanofuel w.r.t CB.

The improvement in thermal efficiency of CB with nanofuel w.r.t CB is low as compared to PRB with nanofuel. During combustion, CZA2 based nanofuel extracts O_2 through the reduction of NOx and provides the same O_2 to CO for oxidation due to which it makes the combustion lean, which leads to efficient combustion. While in the case of PRB with nanofuel, both principle works first is CZA2 effects and second is highly conductive and emissive porous burner effects. Nanofuel provides O_2 to CO for oxidation which reduces the emission and reduces the fuel consumption while PRB actives three mode of heat transfer, homogenizes and preheats the incoming air-fuel mixture which lead to efficient combustion and this reduces the emission level and fuel consumption, resulting in higher thermal efficiency.

Environment temperature plays an important role in the efficiency. In PRB kerosene stove, two types of heat losses exist; convective and radiative heat loss. While in the case of conventional kerosene stove, there is only convective heat loss. In cold weather conditions, more heat loss occurs as compared to hot weather conditions. So in order to investigate the

efficiency at different ambient temperatures, efficiency was estimated at different ambient temperature, which is shown in Figure. 7.3. At an ambient temperature of 30 ˚C, maximum efficiency is obtained. In the case of PRB with nanofuel, the drop in thermal efficiency is 8.37 % while in case of CB with nanofuel, the drop in thermal efficiency is 5.60 % for temperature range (30 – 10 ˚C).

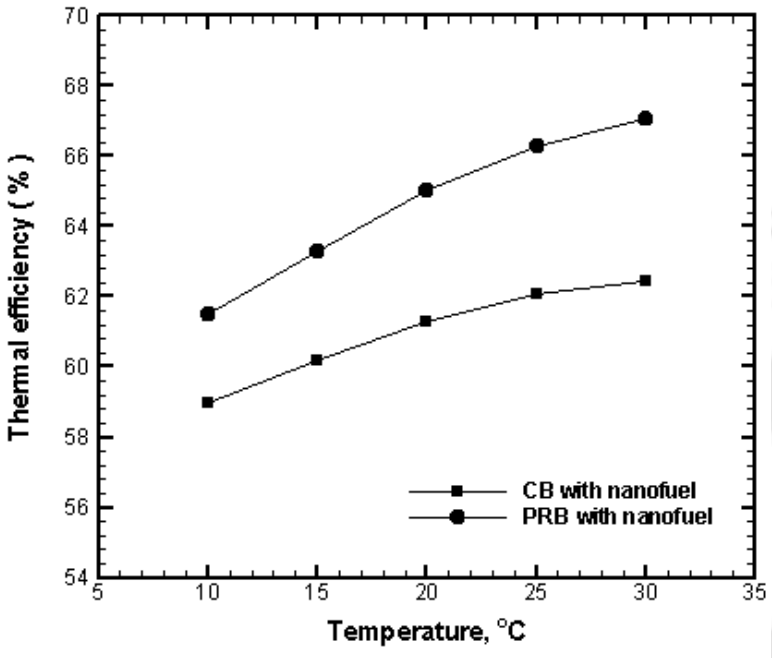

Fig. 7.3: Variation of thermal efficiency with ambient temperature.

7.2 Thermal Output Power

Figure 7.4 shows the output power of CB and PRB with and without nanofuel at different input power. Power output can be obtained from the thermal efficiency of the stoves of different burners. From Figure 7.4, it is observed that, at a particular input power, the output power of PRB with nanofuel is the maximum while the output power of CB is the minimum. It is due to the higher thermal efficiency of PRB with nanofuel and lower thermal efficiency of CB. It is also observed that with the increase in input power, output power also increases. Table 7.2 shows the comparison of output power of CB and PRB with nanofuel w.r.t CB.

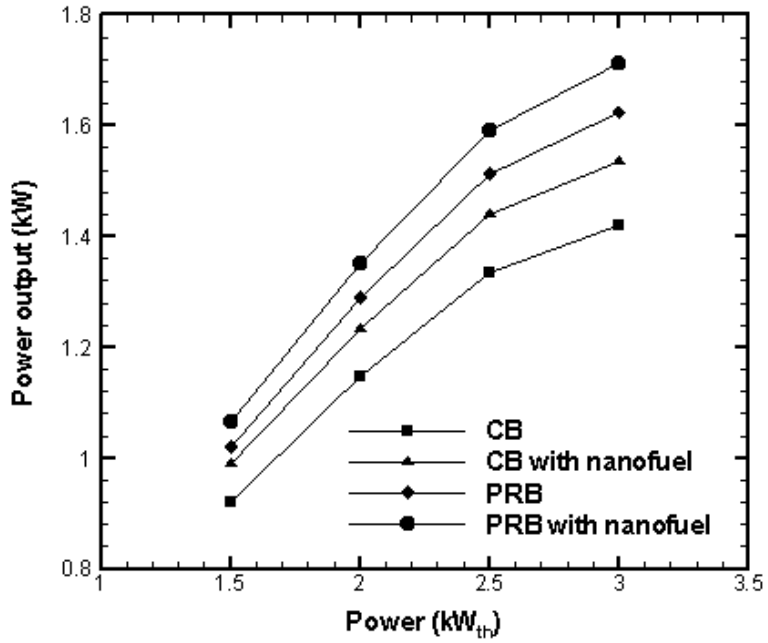

Fig.7.4: Power output of different burners at different input power.

In the case of CB with nanofuel, maximum and minimum output power are 1.5361 kW and 0.9900 kW respectively while the maximum and minimum enhancement are 8.24 % and 7.70 % respectively. In the case of PRB with nanofuel, maximum and minimum output are 1.0634 kW and 1.7117 kW respectively while the maximum and minimum enhancement are 20.61 % and 15.68 % respectively.

Table 7.2: Comparison of output power of CB and PRB with nanofuel w.r.t CB.

Power output (kW)		Increase in power output (%)	Power output (kW)		Increase in power output (%)
CB	CB with nanofuel		CB	PRB with nanofuel	
0.9192	0.9900	7.70	0.9192	1.0634	15.68
1.1460	1.2331	7.60	1.1460	1.3516	17.94
1.3338	1.4388	7.87	1.3338	1.5898	19.19
1.4191	1.5361	8.24	1.4191	1.7117	20.61

Figure 7.5 shows the improvement in output power of PRB and CB with nanofuel w.r.t CB. The trend of improvement in output power is same as improvement in the thermal efficiency as shown in Figure 7.2. It is due to the fact the output power is directly

proportional to the thermal efficiency, the variation of output power is same as thermal efficiency. From Fig 7.5, it is observed that with increasing input power, output power increases. Reason behind this is the time factor of the WBT. In the case of higher input power, WBT time is much lesser for the PRB, which leads to higher improvement in the output power as compared to the lower input power. Nevertheless, high input power is more responsible for CO, NO_x and other harmful gases which has been discussed in the next section.

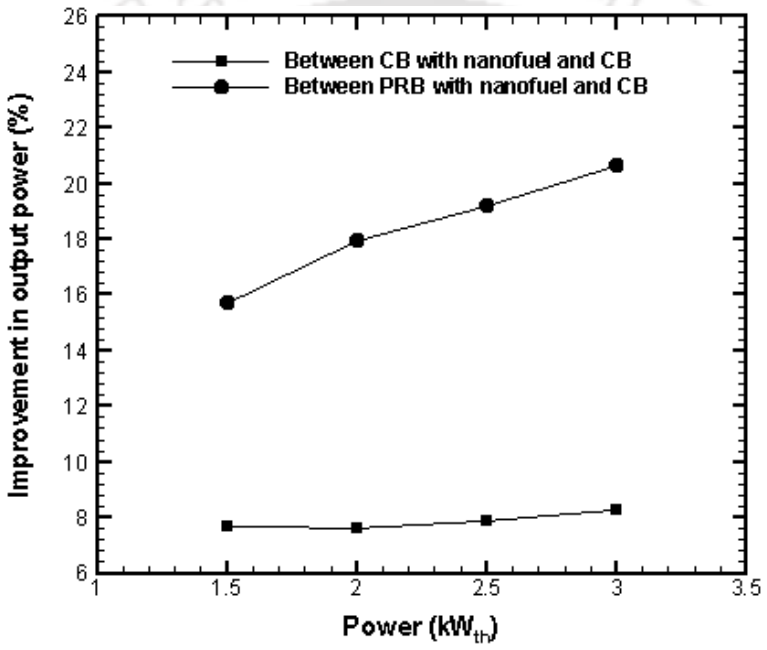

Fig. 7.5: Improvement in output power of PRB and CB with nanofuel w.r.t CB.

7.3 Emission Analysis

Greenline 8000 portable flue gas analyzer was used to measure the CO and NO_x emissions. For emission analysis, the flue gas sampling was done according to the IS 10109:2002. A standard specific hood was used for gas sampling which is shown in Figure 3.6. This standard specific hood was made according to BIS standard. Figures 7.6 and 7.7 show CO and NO_x emissions of CB and PRB with nanofuel respectively. From Figures 7.6 and 7.7, it is observed that, with the increase in input power, CO and NO_x emissions increases.

Increasing input power makes rich combustion which leads to incomplete combustion resulting low residence time. Residence time is defined as the time taken for conversion of CO to CO_2. Due to low residence time, conversion of CO to CO_2 does not take place properly, which results in the increased CO formation. Due to the increase in input power, global temperature (surface temperature of burner increases) increases and high global temperature is responsible for NO_x emission.

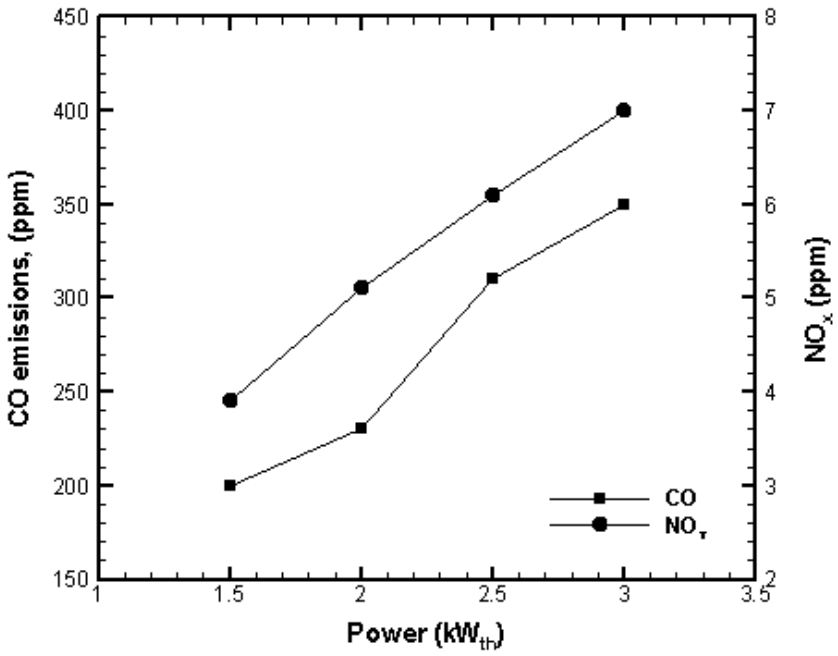

Fig.7.6: CO and NO_x emissions for different thermal loads for CB with nanofuel.

Table 7.3 compares the emissions of CB and PRB with and without nanofuel. For CB, CO varies in the range of 610-915 ppm, while NO_x varies in the range of 19-35ppm for input power 1.5 – 3 kW. For CB with nanofuel, CO varies in the range of 200-350 ppm, while NO_x varies in the range of 3.9-7 ppm for input power 1.5 – 3 kW. From Table 7.3, it is observed that, the maximum reduction of CO and NO_x is 67.21 % and 80 % respectively. During the combustion, nanoparticles of CZA2 are used as a catalyst. It absorbs O_2 through the reduction of NO_x and supplies the same O_2 to CO for oxidation. After the oxidation, CO converts to CO_2, which not only decreases the concentration of CO but also reduces

the soot formation on the burner. Decrease in NO_x emissions occurs through the reduction of NO or NO_2 by C and CO formed by the combustion.

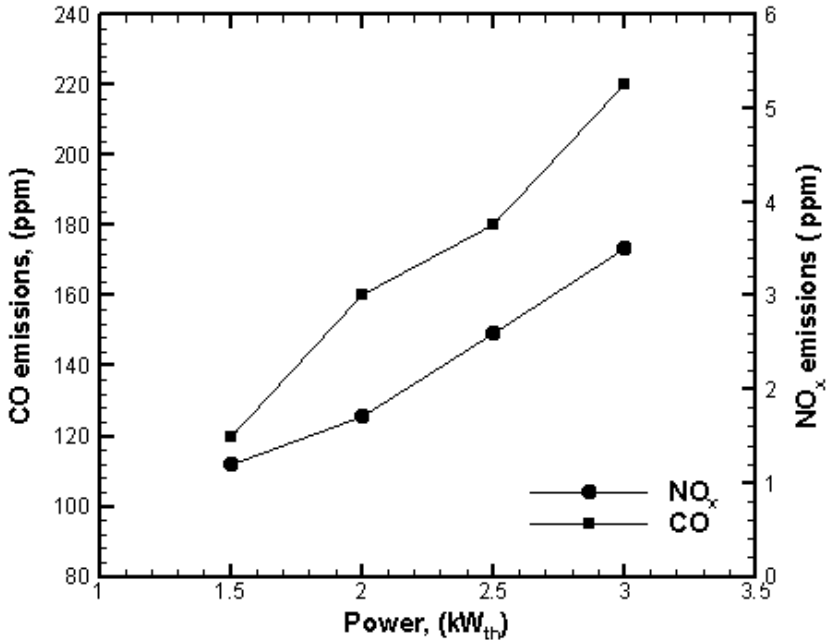

Fig.7.7: CO and NO_x emissions for different thermal loads for PRB with nanofuel.

Maximum reduction in CO and NO_x in PRB with nanofuel is approximately 81 % and 94 % respectively. It is mainly due to the combined effects of nanoparticle and porous radiant burner. Porous radiant burner preheats the incoming air-fuel mixture which not only boost the combustion reaction but also reduce the CO emission (Liu and Hsieh, 2004). At the same time, CZA2 provides O_2, which makes the combustion lean and hence the level of CO decreases. Porous radiant burner homogenises the air fuel mixture, which lead to uniform temperature distribution. Uniform temperature distribution is responsible for low NO_x emissions. In addition, due to the CZA2 nanoparticles, NO_x level decreases because of the reduction of NO or NO_2 through C and CO formed by combustion.

Figure 7.8 shows the reduction in CO and NO_x of CB and PRB with nanofuel w.r.t CB without nanofuel. From Fig 7.8, it is observed that with increase in the input power, reduction of emissions decreases. It is due to fact that, with the increase in input power, the

combustion becomes rich and also it increases the surface temperature of burner, which led to increase in CO and NO_x respectively.

During the experimental investigation, no sticking of nano particles on the porous medium has been observed. Since, flame velocity inside the PBR is high, even if the nano particles try to stick on the surface, which may be blown out easily during combustion itself.

Table 7.3: Comparison of emissions of CB and PRB with nanofuel w.r.t CB.

Power input (kW)	Emissions (CB) in ppm		Emissions (CB with nanofuel) in ppm		Reduction in emissions (%)		Emissions (PRB with nanofuel) in ppm		Reduction in emissions (%)	
	CO	NO_x	CO	NO_x	CO	NO_x	CO	NO_x	CO	NO_x
1.5	610	19	200	3.9	67.21	79.47	120	1.2	80.32	93.68
2.0	691	23	230	5.1	66.71	77.82	160	1.7	76.84	92.60
2.5	795	28	310	6.1	61.00	78.21	180	2.6	77.35	90.71
3.0	915	35	350	7.0	61.74	80.00	220	3.5	75.95	90.00

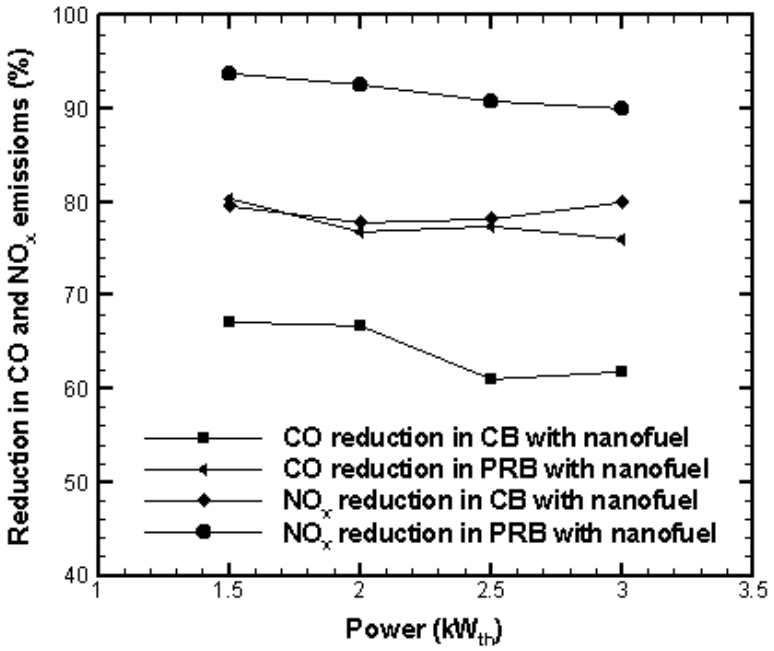

Fig. 7.8: Reduction of CO and NO_x of PRB and CB with nanofuel w.r.t CB.

7.4 Quantity Analysis of Nanofuel

From the previous study, it was observed that thermal efficiency of stove incorporated with PRB with nanofuel was enhanced. This enhancement can be used to find fuel saving. Preparation of nano-particles is not the objective of present work and hence, the cost analysis has not been considered for present study. However, the quantity of CZA2 used is very less (0.05 % wt.), so it will not influence the fuel cost much.

$$WF(\%) = \frac{Wn}{Wt} \qquad \ldots\ldots\ldots (5)$$

WF = weight fraction, *Wn* = weight of nanoparticle (gm), *Ws* = weight of kerosene (gm)

Wt = W*s* + W*n*.

For optimum concentration of nanoparticles

Ws = 1000 ml ×810 kg/m^3

Wn = 0.4052 gm and weight of surfactant = 2×W*n*

Mass of nanofuel consumed in PRB based kerosene pressure stove = 55 gm

Mass of kerosene consumed in CB = 64 gm

Fuel saved (%) = 14.06 %

This calculation is based on maximum thermal efficiency of CB with kerosene and PRB with nanofuel.

7.5 Summary

Maximum thermal efficiency obtained by CB with nanofuel was 62.47 % while CO emission varies in the range of 200-350 ppm and NO_x emission varies in the range of 3.9-7 ppm for input power 1.5 – 3 kW. The maximum thermal efficiency obtained through self-aspirated pressure kerosene cooking stove with PRB with nanofuel (kerosene +CZA2) was about 67.10 %. For the same self-aspirated pressure kerosene stove with PRB with

nanofuel, the CO emission varies in the range of 120-220 ppm while NO_x emission varies in the range of 1.2-3.5 ppm for the input power 1.5 – 3 kW. The maximum improvement in thermal efficiency in PRB with nanofuel was 15.68 % while for same NO_x reduction was 93.68 % and CO reduction was 80.32 % w.r.t CB without nanofuel.

भारतीय प्रौद्योगिकी संस्थान गुवाहाटी
Indian Institute of Technology Guwahati

Chapter 8

Conclusions and Future Work

This chapter deliberates the conclusions of all the outcomes that came from the proposed objectives which includes the development of self-aspirated pressurised kerosene cooking stove with porous radiant burner and testing of PRB with and without nanofuel. It also includes the synthesis of cerium oxide based nanofuel, which comprises of $Ce_{0.6}Zr_{0.2}Al_{0.26}O_2$ (CZA2) and kerosene. The prepared nanofuel is tested for combustion performance in CB and in newly developed self-aspirated pressurised kerosene cooking stove with PRB. The core objective of the thesis is to achieve improvement in the performance of conventional pressure kerosene cooking stove in terms of thermal efficiency and emissions adapting the novel concept of porous media combustion. For the self-aspirated kerosene cooking stove with PRB, various parameters such as nozzle diameter, vessel diameter, and air-entrainment arrangement have been optimised for maximum thermal efficiency and minimum emissions. Major conclusions obtained from the various stages of PhD work is summarized below.

8.1 Selection of Burner for Conventional Pressure Kerosene Stove

Generally, three types of CB are available in the market namely silencer burner, roarer burner and Venus burner. Thermal efficiency was measured for the different conventional burners at laboratory conditions at IIT Guwahati. Maximum thermal efficiency of about 58 % was obtained for the Venus burner. For the same condition, maximum thermal efficiency of 55 % and 54 % were obtained for the roarer and silencer burners, respectively. Hence,

Venus burner was found to be the best CB with the available options and hence, they were selected for further experimental study.

8.2 Design and Development of Self-aspirated Pressurized Kerosene Cooking Stove with Porous Radiant Burner.

About eight different configurations of self-aspirated Pressurized Kerosene Cooking Stove with Porous Radiant Burner were developed and tested discussed. Among these, configuration no. 8 was found to be the best suited for domestic cooking applications. In configuration no. 8, the porous burner achieved 100 % red hot condition with no flame, no vaporisation problem and no flash back and lift off. So with the potential advantages, the configuration no. 8 embraces itself to be the best configuration.

8.2.1 Selection of Preheater

Preheater was used to preheat the incoming air-fuel mixture thereby solving the problem associated with complete vaporisation for achieving the stable porous media combustion (flame less combustion). For this purpose, three types of mild steel perforated sheet with different hole diameter (1.25 mm, 1.5 mm and 1.8 mm) have been fabricated. Of the three types, the preheater with 1.5 mm hole diameter was found to be more suitable in the context of stable combustion.

8.2.2 Selection of Nozzle

Nozzles with different diameters (generally used in cooking stoves) viz., 0.454 mm and 0.376 mm were tested in the PRB for performance comparison. From the experimental studies it was observed that the nozzle with 0.376 mm diameter yielded the thermal efficiency of 64.3 %, while for the nozzle with 0.454 mm diameter, the maximum thermal efficiency was 61.3 %. Hence an improvement in thermal efficiency of about 4.9 % is

achieved through the nozzle with lesser diameter as compared to that of the nozzle with larger diameter. Due to reduction of the nozzle diameter, velocity of the upcoming vaporized kerosene increases, this creates a pressure difference between the nozzle section and surrounding air. So the optimum size of the nozzle diameter was found to be 0.376 mm.

8.2.3 Selection of Venturi

Conventional pressure stove has been designed to operate in rich combustion mode to avoid flame stabilization issue. For achieving sufficient oxygen supply, different types of venturies were fabricated. When vaporized kerosene is passed through the nozzle, due to the high velocity of vapour, the static pressure of air is decreased. Due to this, the primary air is sucked in through the opening provided near the nozzle (venturi slot). Two different venturi configurations were tested for better performance: conical venturi and cylindrical venturi. While using conical venturi, a blue flame was observed and this indicates complete combustion. But, due to the larger surface area and thickness of conical venturi, it creates a problem of vaporization. In cylindrical venturi, the surface area and thickness of the venturi, which contacts the vaporizer tube was less and no problem of vaporization was observed. After combustion, a blue flame was also observed and this indicates a complete combustion. Hence, cylindrical venturi was considered to be the optimum venturi.

8.2.4 Selection of Vessel Diameter

Vessel diameter also plays a moderate role in the variation of thermal efficiency. Four vessels with different diameters (255 mm, 270 mm, 285 mm and 300 mm) were chosen. Maximum and minimum thermal efficiencies were achieved with vessel diameters, 270 mm (64.3 %) and 300 mm (59.1 %). The decrease in thermal efficiency in the smaller vessel is attributed to the higher convective and radiative heat losses, resulting in transfer of low amount of heat to the vessel. The decrease in thermal efficiency beyond a certain vessel

diameter is due to the large surface area of the vessel by which more amount of heat is lost to the surroundings for the same input load. The optimum vessel diameter for the present study was found to be 270 mm.

8.2.5 Selection of Optimum Distance between Surface of Burner and Bottom of Vessel

Distance between the burner and bottom of the vessel was varied from 10 mm to 50 mm Maximum and minimum thermal efficiencies were obtained at 10 mm and 50 mm. Due to the closer burner surface, minimum heat loss occurred to surrounding while in the case of far from the burner surface, maximum heat loss occurred to the surrounding. So, 10 mm distance was found to be more suitable for the present design.

8.2.6 Effect of Ambient Temperature on Thermal Efficiency

In PRB, two types of heat losses occur: convective and radiative heat loss. While in the case of CB, only convective heat loss takes place. So the rate of heat loss is low in CB as compared to PRB. Also in cold weather conditions, more heat loss occurs as compared to hot weather conditions. So in order to investigate the effect of ambient temperate on thermal efficiency, the thermal efficiency was estimated at 10 ˚C, 15 ˚C, 20 ˚C, 25 ˚C, and 30 ˚C by conducting the experiments from November to April. The maximum thermal efficiency was obtained at 30 ˚C.

8.3 Selection of Synthesis Method of Nanofuel preparation

Three methods were used to synthesize the nanofuel namely magnetic method, tip sonication method and combined method (which includes magnetic stirring and tip sonication method). Relative stability of nanofuel prepared by combined method was more as compared to tip sonication and magnetic method. In the case of magnetic stirrer method, tip sonication method and combined method, 100 % relative stability remained for 1 hour,

3 hours and 24 hours. The maximum thermal efficiency obtained by the combined method was more than the tip sonication method. Hence, combined method was considered to be the best suited method for the synthesis of nanofuel.

8.3.1. Selection of Optimum Concentration of Nanoparticle CZA2

Tip sonication and combined methods were used for synthesizing the nanofuel with different concentrations of CZA2 (0.00, 0.02, 0.03, 0.04, 0.05, 0.06 and 0.07 wt. %) and Tween 80 in the ratio of 1:2. The nanofuel with different concentrations was tested in CB and PRB. After the experiment, it was observed that the maximum thermal efficiency was obtained at 0.05 wt. % in both CB and PRB. So, 0.05 wt. % was chosen as the optimum concentration for efficient combustion in the present study.

8.3.2 Thermal Efficiency and Emissions Tests with Nano-fuel blended Kerosene

The maximum thermal efficiency obtained from the self- aspirated pressured kerosene stove with PRB was 64.3 % which is 10.86 % higher than their conventional counterpart. Similarly, for PRB with nanofuel, the maximum thermal efficiency found was 67.10 %, which is 15.68 % greater than the conventional burner. The minimum CO and NO_x emissions measured from the PRB were 180 and 1.5 ppm, respectively, which are 70.49 % and 92.10 % lesser than their conventional counterpart. In the case of PRB with nanofuel, the reduction in percentage of CO and NO_x emissions were 80.32 % and 93.68 %, respectively as compared to CB.

8.4 Scope of Future Work

The present work opens different gateways for further improvement in the performances of the self-aspirated pressurised kerosene cooking stove with porous radiant burner. The scope of future work is outlined as follows.

- The newly developed stove can be tested with waste vegetable oil.
- Different nanofuels can be explored with different nanoparticles and tested with the developed stove.
- A numeral tool can be developed for investigating the combustion behaviour of kerosene stove with PRB.

References

Abdelaal M, El-Riedy M, El-Nahas A (2013) Effect of oxygen enriched air on porous radiant burner performance and NO emissions, *Experimental Thermal and Fluid Science*, vol.45, pp. 163-168.

Alexander M (2012), Radiant Burner, *Patent No. US20120164590 A1*.

Annual Report (2016-17) *Ministry of Petroleum and Natural Gas***.**

Arai N, Shinoda M, Churchill S W (1999) The characteristics of a heat-recirculating ceramic burner, *Transactions of the Canadian Society for Mechanical Engineering*, vol. 23, pp. 147-158.

Arrieta C E, Amell A A (2014) Combustion analysis of an equimolar mixture of methane and syngas in a surface-stabilized combustion burner for household appliances, *Fuel*, vol.137, pp. 11-20.

Assmann M, Falkenreck U, Hecken H J, Schlüter J, Weischedel W (2010), Burner arrangement, *Patent No. US 20100104989A1*

Avdic F (2004) Application of the porous medium gas combustion technique to household heating systems with additional energy sources, *PhD Thesis, University of Erlangen-Nuremberg*.

Avdic F, Adzic M, Durst F (2010) Small scale porous medium combustion system for heat production in households. *Applied Energy*, vol. 87, pp. 2148-2155.

Babkin V, Korzhavin A A, Bunev V A (1991) Propagation of premixed gaseous explosion flames in porous media, *Combustion and Flame*, vol. 87, pp. 182-190.

Bakry A (2008) Stabilized premixed combustion within atmospheric gas porous inert medium (PIM) burner, Proceedings of the Institution of Mechanical Engineers, Part A, *Journal of Power and Energy*, vol. 222, pp. 781-789.

Bakry A, Al-Salaymeh A, Ala'a H, Abu-Jrai A, Trimis D (2011) Adiabatic premixed combustion in a gaseous fuel porous inert media under high pressure and temperature: Novel flame stabilization technique, *Fuel*, vol. 90, pp. 647-658.

Barra A J, Diepvens G, Ellzey J L, Henneke M R (2003) Numerical study of the effects of material properties on flame stabilization in a porous burner, *Combustion and Flame*, vol. 134, pp. 369-379.

Barra A J, Ellzey J L (2004) Heat recirculation and heat transfer in porous burners. *Combustion and Flame*, vol. 137, pp. 230-241.

Basu P, Cen K, and Louis J (2012) Boilers and burners: design and theory, Springer Science & Business Media.

Bellucci V, Meili F, Paschereit O C and Schuermans B (2006), Premix burner, *Patent No. US 20060101825.*

Bouma P, De Goey L P H (1999) Premixed combustion on ceramic foam burners, *Combustion and Flame*, vol. 119, pp. 133-143.

Bubnovich V, Zhdanok S, Dobrego K (2006) Analytical study of the combustion waves propagation under filtration of methane-air mixture in a packed bed, *International Journal of Heat and Mass Transfer*, vol. 49, pp. 2578-2586.

Colorado A, Avila D, McDonell V (2015) An experimental study of the stability limits and emissions of a surface-stabilized combustion burner using biogas and natural gas, *9th U. S. National Combustion Meeting, Central States Section of the Combustion Institute, Cincinnati, Ohio*.

Cookson E J, Floyd I, Donald E (2007) Application of reticulated metal foam to gas fired infrared burners, *High Temperature Materials and Processes*, vol. 26, pp. 269-274.

Cho K W, Han K, Lee Y K, Noh D S, Yoon H M, Riu K J (2001) Premixed combustion of coke oven gas in a metallic fibre mat, *Fuel*, vol. 80, pp. 1033-1036.

Chen Y, Matthews R, Howell J (1987) The effect of radiation on the structure of premixed flame within a highly porous inert medium, *ASME HTD*, vol. 81, pp. 35-42.

Chung C C, Hsianga H I, Hwang J S, Wang T S (2009) Synthesis and characterization of Al_2O_3-$Ce_{0.5}Zr_{0.5}O_2$ powders prepared by chemical to Co-precipitation method, *Journal of Alloys and Compounds*, vol. 470, pp. 387-392.

Claerbout K, Dumortier G and Olalde V (2012), Improved radiant burner, *Patent No. US 20110111356 A1*.

Crozier P, Wang R, Sharma R (2008) In situ environment TEM studies of dynamic changes in cerium-based oxides nanoparticles during redox processes, *Ultramicroscopy*, vol. 108, pp. 1432-1440.

Dhamrat R S, Ellzey J L (2006) Numerical and experimental study of the conversion of methane to hydrogen in a porous media reactor, *Combustion and Flame*, vol. 144, pp. 698-709.

Di Mare L, Mihalik T A, Continillo G, Lee J (2000) Experimental and numerical study of flammability limits of gaseous mixtures in porous media, *Experimental Thermal and Fluid Science*, vol. 21, pp. 117-123.

Dillon J (1999) Combustion in porous media, Los Alamos National Lab, Final report, *California Institute of Technology*.

Delalic N, Mulahasanovic D, Ganic E N (2004) Porous media compact heat exchanger unit-experimental analysis, *Experimental Thermal and Fluid Science*, vol. 28, pp. 185-192.

Delalic N, Mulahasanovic D, Ganic E (2004) Porous media compact heat exchanger unit-experiment and analysis, *Experimental Thermal and Fluid Science*, vol. 28, pp. 185-192.

Dendukuri G, Mittal J P (1993) Some field experiences with improved chulhas in introduced in rural households of Andhra Pradesh , India, Energy Conversion and Management, vol. 34, pp. 457-464.

Deshaies B, Joulin G (1980) Asymptotic study of an excess-enthalpy flame, *Combustion Science and Technology*, vol. 22, pp. 281-285.

Dixit C S B, Paul P J, Mukunda H S (2006) Experimental studies on a pulverized fuel stove, *Biomass Bioenergy*, vol. 30, pp. 673-683.

Djordjevic N, Habisreuther P, Zarzalis N (2012) Experimental study on the basic phenomena of flame stabilization mechanism in a porous burner for premixed combustion application, *Energy & Fuels*, vol. 26, pp. 6705-6719.

Du L, Xie M (2006) The influences of thermo physical properties of porous media on superadiabatic combustion with reciprocating flow, *Heat Transfer-Asian Research*, vol. 35, pp. 336-350.

Durst F, Trimis D, and Dimaczek G (1996a), Burner having material of varying porosity, *United States Patent, No: 5522723.*

Durst F, Keppler M, Weclas M (1997) Air-assisted nozzle applied to very compact, ultra-low emission porous medium oil-burner, *Proceedings of the 3rd Workshop on Spray*.

Echigo R (1991) Radiation enhanced/controlled phenomena of heat and mass transfer in porous media, *Proceedings: ASME-JSME Thermal Engineering Joint Conference, vol. 4, pp. 21-32.*

Echigo R (1982) Effective energy conversion method between gas enthalpy and thermal radiation and application to industrial furnaces, *Proceedings of The International Heat Transfer Conference.*

Echigo R, Kurusu M, Ichimiya K, Yoshizawa Y (1983) Combustion augmentation of extremely low calorific gases (application of the effective energy conversion method from gas enthalpy to thermal radiation), *Proceedings: ASME-JSME Thermal Engineering Joint Conference, Honolulu*, vol. 4, pp. 99-104.

Echigo R, Yoshizawa Y, Hanamura K, Tomimura T (1986) Analytical and experimental studies on radiative propagation in porous media with internal heat generation, *Heat Transfer, Proceedings of the International Heat Transfer Conference.*

Echigo R (1984) Method and Device for Combustion, *Application No. 57-160456. Int. CI. F23C11/00*

Ellzey J L and Schoegl I M (2009), System and method for super adiabatic counter flow reactor, *Patent No. WO2007121004A2*

Ellzey J L, Goel R (1995) Emissions of CO and NO from a two stage porous media burner, *Combustion Science and Technology*, vol. 107, pp. 81-91.

Ellzey J L and William J M (2004), Porous burner for gas turbine applications, Patent No. US2003024655.

Fabrice G and Beatrice F (2008), Compact exchanger reactor using a plurality of porous burners, *Patent No. WO2008132313 A2*

Fleming D K (1987) Non-catalytic porous-phase combustor, *US4643667A.*

Franz M and Götz S (2010), Device for burning a fuel/oxidant mixture, *Patent No. WO2010031869A3*

Francisco R W, Rua F, Costa M, Catapan R, Oliveira A (2009) On the combustion of hydrogen-rich gaseous fuels with low calorific value in a porous burner, *Energy & Fuels*, vol. 24, pp. 880-887.

Fuse T, Araki Y, Kobayashi N, Hasatani M (2003) Combustion characteristics in oil-vaporizing sustained by radiant heat reflux enhanced with higher porous ceramics, *Fuel*, vol. 82, pp. 1411-1417.

Fuse T, Kobayashi N, Hasatani M (2005) Combustion characteristics of ethanol in a porous ceramic burner and ignition improved by enhancement of liquid-fuel intrusion in the pore with ultrasonic irradiation, *Experimental Thermal and Fluid Science*, vol. 29, pp. 467-476.

Fu X, Viskanta R, Gore J P(1998) Prediction of effective thermal conductivity of cellular ceramics, *International Communications in Heat and Mass Transfer*, vol. 25, pp. 151-60.

Fu X, Viskanta R, Gore J P (1998) Measurement and correlation of volumetric heat transfer coefficients of cellular ceramics, *Experimental Thermal and Fluid Science*, vol. 17, pp. 285-293.

Ganesh D, Gowrishankar G (2011) Effect of nano-fuel additive on emission reduction in a biodiesel fuelled CI engine, *IEEE*, pp. 3453-3459.

Gao H, Qu Z, Tao W, He Y, Zhou J (2011) Experimental study of biogas combustion in a two-layer packed bed burner, *Energy & Fuels*, vol. 25, pp.2887-2895.

Gao H B, Qu Z G, He Y, Tao W Q (2012) Experimental study of combustion in a double-layer burner packed with alumina pellets of different diameters, *Applied Energy*, vol. 100, pp. 295-302.

Gao H B, Qu Z G, Tao W Q, He Y L(2013) Experimental investigation of methane/(Ar, N_2, CO_2)–air mixture combustion in a two-layer packed bed burner, *Experimental Thermal and Fluid Science*, vol. 44, pp. 599-606.

Gao H, Qu Z, Feng X, Tao W(2014) Methane/air premixed combustion in a two-layer porous burner with different foam materials, *Fuel*, vol. 115, pp. 154-161.

Gao H, Qu Z, Feng X, Tao W (2014) Combustion of methane/air mixtures in a two-layer porous burner: A comparison of alumina foams, beads, and honeycombs, *Experimental Thermal and Fluid Science*, vol. 52, pp. 215-220.

Gupta A, Waghmare U V, Hegde M S (2010) Correlation of oxygen storage capacity and structural distortion in transition-metal, noble- metal, and rare-earth-ion-substituted CeO_2 from first principles calculation, *Chemistry of Materials*, vol. 22, pp. 5184-5198.

Hale M J, Bohn M S (1993) Measurement of the radiative transport properties of reticulated alumina foams, *ASME/ASES Joint Solar Energy Conference, New York*, pp. 1-9.

Hanamura K, Echigo R, Zhdanok S A (1993) Superadiabatic combustion in a porous medium, *International Journal of Heat and Mass Transfer*, vol. 36, pp. 3201-3209.

Hansen J, **Sato M** (2016) Regional climate change and national responsibilities, *Environmental Research Letters*, vol. 11, pp.1-9.

Hardesty D, Weinberg F (1973) Burners producing large excess enthalpies, *Combustion Science and Technology*, vol.8, pp. 201-214.

Hendricks T, Howell J (1996) Absorption/scattering coefficients and scattering phase functions in reticulated porous ceramics, *Journal of Heat Transfer*, vol. 118, pp. 79-87.

Herrera B, Cacua K, Villalba L O (2015) Combustion stability and thermal efficiency in a porous media burner for LPG cooking in the food industry using Al_2O_3 particles coming from grinding wastes, *Applied Thermal Engineering*, vol. 91, pp. 1127-1133.

Hirano M, Kato E (1999) Hydrothermal synthesis of nanocrystalline cerium (IV) oxide powders, *Journal of American Ceramic Society*, vol. 82, pp 786-788.

Hirano M, Fukuda Y, Iwata H, Hotta Y, Inagaki M (2000) Preparation and spherical agglomeration of crystalline cerium (IV) oxide nanoparticles by thermal hydrolysis, *Journal of American Ceramic Society*, vol. 83, pp. 1287-1289.

Hoetger M and Thiele W (2006), Pore-type burner with silicon-carbide porous body, *United States Patent No. 20060035190*.

Hoffmann J G, Echigo R, Tada S, Yoshida H (1996) Analytical study on flame stabilization in reciprocating combustion in porous media with high thermal conductivity, *Symposium (International) on Combustion*, vol. 26, pp. 2709-2716.

Homraruen A, Jugjai S (2014) An experimental study on combustion performance of a flexible porous medium burner (FPMB), *The 5th TSME International Conference on Mechanical Engineering, The Empress, Chiang Mai.*

Hongmei L, Qingchao Z, Yile L, Maochu G, Yongdong C, Jianli W, Yaoqiang C (2010) Effects of ceria/zirconia ratio on properties of mixed CeO_2-ZrO_2-Al_2O_3 compound, *Journal of Rare Earths*, vol. 28, pp. 79-83

Howell J, Hall M, Ellzey J (1996) Combustion of hydrocarbon fuels within porous inert media, *Progress in Energy and Combustion Science*, vol. 22, pp. 121-45.

Hsu P, Howell J R (1992) Measurements of thermal conductivity and optical properties of porous partially stabilized zirconia, *Experimental Heat Transfer An International Journal*, vol. 5, pp. 293-313.

Hsu P F, Evans W D, Howell J R (1993) Experimental and numerical study of premixed combustion within nonhomogeneous porous ceramics, *Combustion Science and Technology*, vol. 90, pp.149-172.

Hwang S J (2014), Combustion device, Patent No. EP2738459 A1.

Indian Standard, Burners for oil pressure stoves and oil pressure heaters, specification, (Second Revision): IS 10109, 2002, *Bureau of Indian Standard.*

Jia L, Shen M, Hao J, Rao T, Wang J (2008) Dynamic oxygen storage and release over $Mn_{0.1}Ce_{0.6}O_x$ complex compounds and structural characterization, *Journal of Alloys and compounds*, vol. 454, pp. 321-326.

Jugjai S, Phothiya C (2007) Liquid fuels-fired porous combustor-heater. *Fuel*, vol. 86, pp. 1062-1068.

Jugjai S, Polmart N (2003) Enhancement of evaporation and combustion of liquid fuels through porous media, *Experimental Thermal and Fluid Science*, vol. 27, pp. 901-909.

Jugjai S, Pongsai C (2007) Liquid fuels-fired porous burner, *Combustion Science and Technology*, vol. 179, pp. 1823-1840.

Jugjai S, Rungsimuntuchart N (2002) High efficiency heat-recirculating domestic gas burners, *Experimental Thermal and Fluid Science*, vol, 26, pp. 581-592.

Jugjai S, Sawananon A (2004) The surface combustor-heater with cyclic flow reversal combustion embedded with water tube bank, *Fuel*, vol. 83, pp. 2369-2379.

Jugjai S, Wongpanit N, Laoketkan T, Nokkaew S (2002) The combustion of liquid fuels using a porous medium, *Experimental Thermal and Fluid Science*, vol. 26, pp. 15-23.

Jugjai S, Wongveera S, Teawchaiitiporn T, Limbwornsin K (2001) The surface combustor–heater with cyclic flow reversal combustion. *Experimental Thermal and Fluid Science*, vol. 25, pp. 183-192.

Jung H, Kittlelson D B, Zachariah R (2005) The influence of a cerium additive on ultrafine diesel particle emissions and kinetics of oxidation, *Combustion and Flame*, vol. 142, pp. 276-288.

Jungbluth N, Kollar M Koβ V (1997) Life cycle inventory for cooking-some results for the use of liquefied petroleum gas and kerosene as cooking fuels in India, Energy Policy, vol. 25, pp. 471-480.

Kaeding S and Lawrence J (2008), Burner device with a porous body, *Patent No. US20080020336 A1*.

Kakati S, Mahanta P, Kakoty S (2007) Performance analysis of pressurized kerosene stove with porous medium inserts, Journal of Scientific & Industrial Research, vol. 66, pp. 565-569.

Kayal T K, Chakravarty M (2006) Modeling of trickle flow liquid fuel combustion in inert porous medium, *International Journal of Heat and Mass Transfer*, vol. 49, pp. 975-983.

Kandpal J B, Maheshwari R C, Kandpal T C (1995) Indoor air pollution from domestic cookstoves using coal, kerosene and LPG**,** *Energy Conversion and Management*, vol. 36, pp. 1067-1072.

Kaplan M, Hall M J (1995) The combustion of liquid fuels within a porous media radiant burner, *Experimental Thermal and Fluid Science*, vol. 11, pp. 13-20.

Kaspar J, Fornasiero P, Hickey N (2003) Automotive catalytic converters: current status and some perspectives, *Catalytic Today*, vol. 77, pp. 419-449.

Keramiotis C, Founti M A (2013) An experimental investigation of stability and operation of a biogas fueled porous burner, *Fuel*, vol. 103, pp. 278-284.

Keramiotis C, Katoufa M, Vourliotakis G, Hatziapostolou A, Founti M (2015) Experimental investigation of a radiant porous burner performance with simulated natural gas, biogas and synthesis gas fuel blends, *Fuel*, vol. 158, pp. 835-842.

Keramiotis C, Stelzner B, Trimis D, Founti M (2012) Porous burners for low emission combustion: An experimental investigation, *Energy*, vol. 45, pp. 213-219.

Khanna V K (1992) Experimental analysis of radiation for methane combustion within a porous medium burner, *M. S. Thesis, Department of Mechanical Engineering, The University of Texas at Austin*.

Khanna V, Goel R, Ellzey J L (1994) Measurements of emissions and radiation for methane combustion within a porous medium burner, *Combustion Science and Technology*, vol. 99, pp. 133-142.

Kotani Y, Behbahani H, Takeno T (1985) An excess enthalpy flame combustor for extended flow ranges, *Twentieth Symposium (International) on Combustion/The Combustion Institute*, vol. 20, pp. 2025-2033.

Krause B, Mende M, Potschke P, Petzold G (2010) Dispersability and particle size distribution of CNTs in an aqueous surfactant dispersion as a function of ultrasonic treatment time, *Carbon*, vol. 48, pp. 2746-2754.

Krittacom B, Kamiuto K (2009) Radiation emission characteristics of an open-cellular porous burner, *Journal of Thermal Science and Technology*, vol. 4, pp.13-24.

Kulkarni M, Peck R (1996) Analysis of a bilayered porous radiant burner, *An International Journal of Computation and Methodology*, vol. 30, pp. 219-232.

Lammers F, De Goey L P H (2003) A numerical study of flash back of laminar premixed flames in ceramic-foam surface burners, *Combustion and Flame*, vol. 133, pp. 47-61.

Leonardi S, Viskanta R, Gore J P (2003) Analytical and experimental study of combustion and heat transfer in submerged flame metal fiber burners/heaters. *Journal of Heat Transfer*, vol. 125, pp. 118-125.

Leonardi S, Viskanta R, Gore J P (2002) Radiation and thermal performance measurements of a metal fiber burner, *Journal of Quantitative Spectroscopy and Radiative Transfer*, vol. 73, pp. 491-501.

Li Y, Suzuki M, Ogawa H, (2009a) Effect of ethyl tert-butyl ether addition to diesel fuel on characteristics of combustion and exhaust emission of diesel engines, *Fuel*, vol. 88, pp. 2017-2024.

Lisunova M O, Lebovka N I, Melezhyk O V, Boiko Y P (2006) Stability of the aqueous suspensions of nanotubes in the presence of non-ionic surfactant, *Journal of Colloid and Interface Science*, vol. 299, pp. 740-746.

Liu J F and Hsieh W H (2004) Experimental investigation of combustion in porous heating burners. *Combustion and Flame*, vol. 138, pp. 295-303.

Lorenz W, Reimann H J, Schmal A, Dormann P, Schwarz B, Neugebauer E (1977) Histamine release in dogs by cremophor EI and its derivatives: oxethylated oleic acid is the most effective constituent, *Agent Action*, vol. 7, pp. 63-67.

Lucky A R and Hossain I (2001) Efficiency study of Bangladeshi cookstoves with an emphasis on gas cookstoves, *Energy*, vol. 26, pp. 221-237.

Makmool U, Tia S, Valikul P, Fungtammasan B, Jugjai S (2006) Performance and Diagnostic by PIV of LPG Cooking Burners in Thailand, *The 20th Conference of Mechanical Engineering Network of Thailand, Nakhon Ratchasima, Thailand*.

Malico I, Mujeebu M A (2015) Potential of porous media combustion technology for household applications, *International Research Establishment for Energy and Environment (IREEE)*, vol. 1, pp. 50-69.

Malico I, Pereira J C F (2001) Numerical study on the influence of radiative properties in porous media combustion, *Journal of Heat Transfer*, vol. 123, pp. 951-957.

Marbach T L, **Agrawal A K** (2003) Experimental study of surface and interior combustion using composite porous inert media, *Journal of Engineering for Gas Turbines and Power*, vol. 127, pp. 307-13.

Marbach T L, Sadasivuni V, Agrawal A K (2007) Investigation of a miniature combustor using porous media surface stabilized flame. *Combustion science and technology*, vol. 179, pp. 1901-1922.

Masui T, Minami K, Koyabu K, Imanaka N (2006) Synthesis and characterisation of new promoters based on CeO_2-ZrO_2-Bi_2O_3 for automotive exhaust catalysis, *Catalysis Today*, vol. 117, pp. 187-192.

Mathis W M, Ellzey J L (2003) Flame stabilization, operating range, and emissions for a methane/air porous burner, *Combustion Science and Technology*, vol. 175, pp. 825-839.

Meng L, Liu L, Zi X, Dai H, Zhao Z, Wang X, , He W (2010) Preparation ceria-zirconia solid solution with enhanced oxygen storage capacity and redox performance, *Front Environmental Science Engineering China*, vol. 24, pp. 164-171.

Min D K, Shin H D (1991) Laminar premixed flame stabilized inside a honeycomb ceramic, *International Journal of Heat and Mass Transfer*, vol. 34, pp. 341-356.

Mishra S, Steven M, Nemoda S, Talukdar P, Trimis D, Durst F (2006) Heat transfer analysis of a two-dimensional rectangular porous radiant burner, International Communications in Heat and Mass Transfer, vol. 33, pp. 467-474.

Mishra N K, Mishra S C, Muthukumar P (2015) Performance characterization of a medium-scale liquefied petroleum gas cooking stove with a two-layer porous radiant burner. *Applied Thermal Engineering*, vol. 89, pp. 44-50.

Mishra S C, Muthukumar P, Mishra N K (2015) Self-aspirated LPG domestic cooking stove with a two-layer porous radiant burner, *Patent No: 543/KOL/2015*.

Mishra S C, Muthukumar P, Mishra N K, Panigrahi S (2016) Medium-Scale Self-Aspirated Improved Air Entrainment LPG Cooking Stove with a Two-Layer Porous Radiant Burner, *Patent No: 201631015526.*

Mital R, **Gore J P**, **Viskanta R** (1997) A study of the structure of submerged reaction zone in porous ceramic radiant burners. *Combustion and Flame*, vol. 111, pp. 175-184.

Mital R, Gore J P, Viskanta R, Mcintosh A C (1998) An experimental evaluation of asymptotic analysis of radiant burners, *Symposium (international) on combustion, Elsevier*, vol. 27, pp. 3163-3171.

Mital R, Gore J P, Viskanta R (1998) A radiation efficiency measurement procedure for gas-fired radiant burners, *Experimental Heat Transfer An International Journal*, vol. 11, pp. 3-21.

Mjaanes H P, Chan L, Mastorakos E (2005) Hydrogen production from rich combustion in porous media, *International Journal of Hydrogen Energy*, vol. 30, pp. 579-592.

Mohamad A A, Ramadhyani S, Viskanta R (1994) Modelling of combustion and heat transfer in a packed bed with embedded coolant tubes, *International Journal of Heat and Mass Transfer*, vol, 37, pp. 1181-1191.

Morikawa A, Suzuki T, Kanazawa T, Kikuta K, Suda A, Shinjo H (2008) A new concept in high performance ceria-zirconia oxygen storage capacity material with Al_2O_3 as a diffusion barrier, *Applied Catalysis B: Environmental*, vol. 78, pp. 210-221.

Mößbauer S, Pickenäcker O, Pickenäcker K, Trimis D(2002) Application of the porous burner technology in energy- and heat-engineering, *Clean Air*, vol. 3, pp. 185-198.

Mujeebu M A, Abdullah M Z, Bakar M A, Mohamad A, Muhad R, Abdullah M (2009a) Combustion in porous media and its applications-A comprehensive survey, *Journal of environmental management*, vol. 90, pp. 2287-2312.

Mujeebu M A (2016) Hydrogen and syngas production by superadiabatic combustion-A review, *Applied Energy*, vol. 173, pp. 210-224.

Mujeebu M A, Abdullah M, A. Bakar M, Mohamad A (2011a) A mesoscale premixed LPG burner with surface combustion in porous ceramic foam. *Energy Sources, Part A: Recovery, Utilization, and Environmental Effects*, vol. 34, pp. 9-18.

Mujeebu M A, Abdullah M, Mohamad A (2011b) Development of energy efficient porous medium burners on surface and submerged combustion modes, *Energy*, vol. 36, pp. 5132-5139.

Mujeebu M A, Abdullah M, Bakar M A, Mohamad A, Abdullah M (2009b) Applications of porous media combustion technology-A review, *Applied Energy*, vol. 86, pp. 1365-1375.

Mujeebu M A, Abdullah M Z, Zuber M (2013) Experiment and simulation to develop clean porous medium surface combustor using LPG, *Journal of Thermal Science and Technology*, vol. 33, pp. 55-61.

Mujeebu M A, Abdullah M Z, Mohamad A, Bakar M A (2010) Trends in modeling of porous media combustion, *Progress in Energy and Combustion science*, vol. 36, pp. 627-650.

Mukunda H S, Shrinivasa U, Dasappa S (1988) Portable single pan wood stove for high efficiency, *Sadhana*, vol. 13, pp. 237-270.

Murshed S M S, Leong K C, Yang C (2005) Enhanced thermal conductivity of TiO_2-water based nanofluids, *Internatinal Journal of Thermal Sciences*, vol. 44, pp. 367-373.

Muthukumar P, Anand P, Sachdeva P (2011) Performance analysis of porous radiant burners used in LPG cooking stove, *International Journal of Energy and Environment*, vol. 2, pp. 367-374.

Muthukumar P, Shyamkumar P (2013) Development of novel porous radiant burners for LPG cooking applications. *Fuel*, vol. 112, pp. 562-566.

Nakamura Y, Itaya Y, Miyoshi K, Hasatani M (1993) Mechanism of methane-air combustion on the surface of a porous ceramic plate, *Journal of Chemical Engineering of Japan*, vol. 26, pp. 205-211.

Natarajan R, Karthikeyan N S, Agarwal A, Sathiyanarayanan K (2008) use of vegetable oil as fuel to improve efficiency of cooking stove, *Renewable Energy*, vol. 33, pp. 2423-2427.

NSSR (2010) Implementation energy sources of Indian households for cooking and lighting, *Ministry of Statistics and Programme*.

Orenstein R M, Green D J (1992) Thermal shock behaviour of open-cell ceramic Foams, *Journal of the American Ceramic Society*, vol. 75, pp. 1899-1905.

Ozawa M, Matuda K, Suzuki S (2000) Microstructure and oxygen release properties of catalytic alumina-supported CeO_2-ZrO_2 powders, *Journal of Alloys and Compounds*, vol. 303, pp. 56-59.

Panigrahy S, Mishra N K, Mishra S C, Muthukumar P (2016) Numerical and experimental analyses of LPG (liquefied petroleum gas) combustion in a domestic cooking stove with a porous radiant burner, *Energy*, vol. 95, pp. 404-414.

Pantangi V, Kumar A K, Mishra S C, Sahoo N (2007) Performance analysis of domestic LPG cooking stoves with porous media. *International Energy Journal*, vol. 8, pp. 139-144.

Pantangi V K (2010) Development and performance analysis of porous radiant burners for cooking applications, *PhD Thesis, Indian Institute of Technology Guwahati, Guwahati.*

Pantangi V, Mishra S C, Muthukumar P, Reddy R (2011) Studies on porous radiant burners for LPG (liquefied petroleum gas) cooking applications. *Energy*, vol. 36, pp. 6074-6080.

Park C W, Kaviany M (2002) Evaporation-combustion affected by in-cylinder, reciprocating porous regenerator. *Journal of Heat Transfer*, vol. 124, pp. 184-194.

Periasamy C, Sankara-Chinthamony S K, Gollahalli S (2007) Experimental evaluation of evaporation enhancement with porous media in liquid-fueled burners, *Journal of Porous Media*, vol. 10, pp. 137-150.

Periasamy C, Gollahalli S (2010) Numerical modeling of evaporation enhancement of aviation-grade kerosene spray in porous media combustors, *Journal of Porous Media*, vol. 13, pp. 707-723.

Periasamy C, Gollahalli S R (2011) Experimental investigation of kerosene spray flames in inert porous media near lean extinction, *Energy & Fuels*, vol. 25, pp. 3428-3436.

Pickenäcker O, Pickenäcker K, Wawrzinek K, Trimis D, Pritzkow W E C, Müller C, Goedtke P, Papenburg U, Adler J, Standke G, Heymer H, Tauscher W, Jansen F (1999) Innovative ceramic materials for porous-medium Burners II, *Interceram*, vol. 48, pp. 424-433.

Pohekar S D, Kumar D, Ramachandran M (2005) Dissemination of cooking energy alternatives in India- a review. *Renewable Sustainable Energy Review*, vol. 9, pp. 379-393.

Pontree K, Jugjai S (2014) Self-aspirating, liquid fuel, annular porous burner (SLAPB), *The 5th TSME International Conference on Mechanical Engineering, The Empress, Chiang Mai.*

Primus stove, Wikipedia 2010, viewed 10th December 2010, https://en.wikipedia.org/wiki/Primus_stove

Priya N S (2016) Synthesis and characterization of high oxygen storage capacity nanoparticles dispersed diesel for the emission reduction and performance enhancement of a direct injection engine, *PhD Thesis, IIT Guwahati, Guwahati*.

Qiu K, Hayden A C S (2006) Premixed gas combustion stabilized in fiber felt and its application to a novel radiant burner, *Fuel*, vol. 85, pp. 1094-1100.

Qiu K, Hayden A C S (2009) Increasing the efficiency of radiant burners by using polymer membranes, *Applied Energy*, vol. 86, pp. 349-354.

Rao R, Mishra B G (2003) Structural redox and catalytic chemistry of ceria based materials, *Bulletin of the Catalysis Society of India*, vol. 3, pp. 122-134.

Redwood D S and John P (2007), High efficiency Radiant Burner, *Patent No. WO2007027379A1*

Scribano G, Solero G, Coghe A (2006) Pollutant emissions reduction and performance optimization of an industrial radiant tube burner, *Experimental Thermal and Fluid Science*, vol. 30, pp. 605-612.

Sathe S B, Kulkarni M R, Peck R E, Tong T W (1989a) An experimental study of combustion and heat transfer in porous radiant burners, *Western Sates Section, Combustion Institute, Livermore, CA.*

Sajith V, Sobhan C B, Peterson G P (2010) Experimental investigation on the effects of cerium oxide nanoparticle fuel additives on biodiesel, *Advance in Mechanical Engineering*, Article ID 581407, pp. 1-6

Sathe S B, Peck R E, Tong T W (1989b) A numerical analysis of combustion and heat transfer in porous radiant burners, *ASME/ HTD*, vol. 106, pp. 93-109.

Sathe S B, Peck R E, Tong T W (1990) A numerical analysis of heat transfer and combustion in porous radiant burners, *International Journal of Heat and Mass Transfer*, vol. 33, pp. 1331-1338.

Sathe S B, Kulkarni M R, Peck R E, Tong T W (1991) An experimental and theoretical study of porous radiant burner performance, *23rd Symposium (International) on Combustion*, vol. 23, pp. 1011-1018.

Sayle T X T, Parker S C, Sayle D C (2005) Oxidising CO to CO_2 using ceria nanoparticles, *Physical Chemistry Chemical Physics*, vol. 7, pp. 2936-2941.

Sharif S M, Fard F G, Khatibi E, Sarpoolaky H (2009) Dispersion and stability of carbon black nanoparticles, studied by ultra-violet spectroscopy, *Journal of Taiwan Institute of Chemical Engineers*, vol. 40, pp. 524-527.

Sharma M, Mahanta P, Mishra S C (2016a) Usability of porous burner in kerosene pressure stove: An experimental investigation aided by energy and exergy analyses, *Energy*, vol. 103, pp. 251-260.

Sharma M, Mishra S C, Acharjee P (2009) Thermal efficiency study of conventional kerosene pressure stoves equipped with porous radiant inserts, *International Energy Journal*, vol. 10, pp. 247-254.

Sharma M, Mishra S C, Mahanta P (2011) An experimental investigation on efficiency improvement of a conventional kerosene pressure stove, *International Journal of Energy for a Clean Environment*, vol. 12, pp. 79-93.

Sharma M, Mishra S C, Mahanta P (2016b) Effect of burner configuration and operating parameters on the performance of kerosene pressure stove with submerged porous medium combustion, *Applied Thermal Engineering*, vol. 107, pp. 516-523.

Sharma M, Mukunda H, Sridhar G (2009) Solid fuel block as an alternate fuel for cooking and barbecuing: Preliminary results, *Energy Conversion and Management*, vol. 50, pp. 955-961.

Shinoda M, Maihara R, Kobayashi N, Arai N, Churchill S W (1998) The characteristics of a heat-recirculating ceramic burner, *Chemical Engineering Journal*, vol. 71, pp. 207-212.

Shinoda M, Tanaka R, Arai N (2002) Optimization of heat transfer performances of a heat-recirculating ceramic burner during methane/air and low-calorific-fuel/air combustion, *Energy Conversion and Management*, vol. 43, pp. 1479-1491.

Singh R, Kasana H S (2004) Computational aspects of effective thermal conductivity of highly porous metal foams, *Applied Thermal Engineering*, vol. 24, pp. 1841-1849.

Smith K, Uma R K V V N (2000) Greenhouse gases from small-scale combustion devices in developing countries, Phase IIa, *Household Stoves in India*, USEPA, EPA-600-00-052.

Smucker M T, Ellzey J L (2004) Computational and experimental study of a two-section porous burner, *Combustion Science and Technology*, vol. 176, pp. 1171-1189.

Som I, Bhatia K Y, Asir M (2012) Status of surfactants as a penetration enhancers in transdermal drug delivery, *Journal of Pharmacy and Bioallied Sciences*, vol. 4, pp. 2-9.

Surange J R, Patil N K, Rajput A V (2014) Performance analysis of burners used in LPG cooking stove-A review, *International Journal of Innovative Research in Science, Engineering and Technology*, vol. 3, pp. 87-97.

Tah B, Pal P, Mahato M, Talapatra G B (2011) Aggregation behavior SDS/CTAB catanionic surfactant mixture in aqueous solution and at the air/water interface, *The Journal of Physical Chemistry B*, vol. 115, pp. 8493-8499.

Takami H, Suzuki T, Itaya Y, Hasatani M (1998) Performance of flammability of kerosene and NOx emission in the porous burner, Fuel, vol. 77, pp. 165-171.

Takeno T, Murayama M (1986) One-dimensional flame with extended reaction zone, *Dynamics of Reactive Systems*, 105 (part I), 246.

Takeno T, Hase K (1983) Effects of solid length and heat loss on an excess enthalpy flame, *Combustion Science and Technology*, vol. 31, pp. 207-215.

Takeno T, Sato K (1979) An excess enthalpy flame theory, *Combustion Science and Technology*, vol. 20, pp. 73-84.

Takeno T, Sato K, Hase K (1981) A theoretical study on an excess enthalpy flame, *Eighteenth Symposium (International) on Combustion/The Combustion Institute*, vol. 18, pp. 465-472.

Talukdar P, Mishra S C, Trimis D, Durst F (2004) Heat transfer characteristics of a porous radiant burner under the influence of a 2-D radiation field. *Journal of Quantitative Spectroscopy and Radiative Transfer*, vol. 84, pp. 527-537.

Tanaka R, Shinoda M, Arai N (2001) Combustion characteristics of a heat-recirculating ceramic burner using a low-calorific fuel, *Energy Conversion and Management*, vol. 42, pp. 1897-1907.

Thukral K, Bhandari P M (1994) The rationale for reducing the subsidy on LPG in India, *Energy Policy*, vol. 22, pp. 81-87.

Tia S, Jugjai S, Tia W, Tanatvanit S (2007) Effect of burner type on thermal efficiency and emission of LPG cookstoves, *Research and Development Journal*, vol. 18, pp. 50-57.

Tiwari A, Alenezi M R, Jun S C (2016) Advanced Composite Materials, *John Wiley & Sons*.

Tong T W, Li W (1995) Enhancement of thermal emission from porous radiant burners, *Journal of Quantitative Spectroscopy and Radiative Transfer*, vol. 53, pp. 235-248.

Trimis D, Durst F (1996) Combustion in a porous medium-advances and applications, *Combustion science and technology*, vol. 121, pp. 153-168.

Trimis D, Wawrzinek K, Hatzfeld O, Lucka K, Rutsche A, Haase F, Kruger K, Kuchen C (2001) A novel porous burner for liquid fuels based on porous media combustion and cool flame vaporization. *Combustion and Enviroment: XXIV Event of the Italian Section of the Combustion Institute, S Margherite Ligure, Italy*.

Tseng C J, Howell J R (1996) Combustion of liquid fuels in a porous radiant burner, *Combustion Science and Technology*, vol. 112, pp. 141-161.

Turns S R (1996) An introduction to combustion: concepts and application, *McGraw-Hill*, 2nd edition.

Vijaykant S, Agrawal A K (2006) Effect of porous media configuration on combustion of kerosene. *44th AIAA Aerospace Sciences Meeting Exhibit Reno, Nevada*, pp. 11577

Vijaykant S, Agrawal A K (2007) Liquid fuel combustion within silicon-carbide coated carbon foam, *Experimental Thermal and Fluid Science*, vol. 32, pp. 117-125.

Viskanta R (1995) Interaction of combustion and heat transfer in porous inert media, *8th International Symposium on Transport Phenomena in Combustion, San Francisco*.

Viskanta R, Gore J (2000) Overview of cellular ceramics based porous radiant burners for supporting combustion, *International Journal on Environmental Combustion Technology*, vol. 1, pp. 167-203.

Volkert J and Goebel P (2006), Burner for a gas and air mixture, *United States Patent No. 6997701*.

Wang X, Rodriguez J A, Jonathan, Hanson J C, Gamarra D, Arias A M, Garcia M F (2006) In situ studies of the active sites for the water gas shift reaction over Cu-CeO_2 catalysts: complex interaction between metallic copper and oxygen vacancies of ceria, *Journal of Physical Chemistry B*, vol. 110, pp. 428-434.

Weclas M (2005) Porous media in internal combustion engines, *Cellular Ceramics: Structure, Manufacturing, Properties and Applications*, pp. 580-595.

Weclas M (2010) Potential of porous-media combustion technology as applied to internal combustion engines, *Journal of Thermodynamics*, vol. 2010, pp. 1-39.

Wei M, Wang Y, Reh L (2002) Experimental investigation of the prevaporized premixed (vpl) combustion process for liquid fuel lean combustion. *Chemical Engineering and Processing: Process Intensification*, vol. 41, pp. 157-164.

Weinberg F J (1971) Combustion temperatures: the future, *Nature*, vol. 233, pp. 239–241.

Williams A, Woolley R, Lawes M (1992) The formation of NO_x in surface burners, *Combustion and Flame*, vol. 89, pp. 157-166.

Wongwatcharaphon K, Tongtem P, Jugjai S (2012) Modulating dual fuel porous burner, *The 3rd TSME International Conference on Mechanical Engineering*, Chiang Rai .

Wongwatcharaphon K, Theinnoi K (2013) Effect of physical properties of porous combustor on radiant output and fuel-preheated efficiency of a non-sprayed porous burner, *Applied Mechanics and Materials*, vol. 421, pp. 819-825.

Wongwatcharaphon K, Tongtem P, Jugjai S (2013) Numerical and experimental study of a nonsprayed porous burner for liquid kerosene, *Journal of Porous Media*, vol. 16, pp. 227-239.

Wood S, Harris A T (2008) Porous burners for lean-burn applications, *Progress in Energy and Combustion Science*, vol. 34, pp. 667-684.

Wu C Y, Chen K H, Yang S Y (2014) Experimental study of porous metal burners for domestic stove applications, *Energy Conversion and Management*, vol. 77, pp. 380-388.

Xiong T Y, Khinkis M J, Fish F F (1995) Experimental study of a high-efficiency, low emission porous matrix combustor-heater, *Fuel*, vol. 74, pp. 1641-1647.

Xiaodong W, Qing L, Xiaodi W, Duan W (2007)Role of surface adsorption in fast oxygen storage and release of CeO_2-ZrO_2 mixed oxides, *Journal of Rare Earth*, vol. 25, pp. 416-421.

Xu K, Liu M, Zhao P (2011) Stability of lean combustion in mini-scale porous media combustor with heat recuperation, *Chemical Engineering and Processing: Process Intensification*, vol. 50, pp. 608-613.

Yetter R A, Risha G A, Son S F (2009) Metal particle combustion and nanotechnology, *Proceedings of the Combustion Institute*, vol. 32, pp. 1819-1838.

Yoksenakul W, Jugjai S (2011a) Design and development of a SPMB (self-aspirating, porous medium burner) with a submerged flame, *Energy*, vol. 36, pp. 3092-3100.

Yoksenakul W, Jugjai S (2011b)Thermal efficiency of self-aspirating porous medium burner for Small and Medium Scale Enterprises (SMEs*), Proceedings of The 2nd TSME International Conference on Mechanical Engineering*, pp. 1-8.

Yoshio Y, Kiyoshi S, Ryozo E (1988) Analytical study of the structure of radiation controlled flame. *International Journal of Heat and Mass Transfer*, vol. 31, pp. 311-319.

Younis L, Viskanta R (1993) Experimental determination of the volumetric heat transfer coefficient between stream of air and ceramic foam. *International Journal of Heat and Mass Transfer*, vol. 36, pp. 1425-1434.

Yoshida M (2011), Burner For Manufacturing Porous Glass Preform, *Patent No. US20110259056 A1*.

Yu B, Kum S M, Lee C E, Lee S (2013) Combustion characteristics and thermal efficiency for premixed porous-media types of burners, *Energy*, vol. 53, pp. 343-350.

Zhang J C, Cheng L M, Zheng C H, Luo Z Y, Ni M J (2013) Development of non-premixed porous inserted regenerative thermal oxidizer, *Journal of Zhejiang University SCIENCE A*, vol. 14, pp. 671-678.

Zhang J, Smith K R, Uma R (1999) Carbon monoxide from cookstoves in developing countries: 1. Emission factors, *Chemosphere-Global Change Science*, vol. 1, pp. 367-375.

Zhang X, Long E, Li Y, Guo J, Zhang L, Gong M, Wang M, Chen Y (2009) CeO_2-ZrO_2-La_2O_3-Al_2O_3 composite oxide and its supported palladium catalystfor the treatment of exhaust of natural gas engined vehicles, *Journal of Natural and Gas Chemistry*, vol. 18, pp. 139-144.

Zhdanok S A, Martynenko V V, Shabunya S I (1993) Obtaining superadiabatic temperatures in combustion of gaseous fuel in a system of two porous plates with a periodic change of the direction of pumping, *Journal of Engineering Physics and Thermophysics*, vol. 64, pp. 463-469.

Zumbrunnen D A, Viskanta R, Incropera F P (1986) Heat transfer through porous solids with complex internal geometries, *International Journal of Heat and Mass Transfer*, vol. 29, pp. 275-284.

भारतीय प्रौद्योगिकी संस्थान गुवाहाटी
Indian Institute of Technology Guwahati

APPENDIX-I

1. Properties of kerosene and nanofuel

Particulars		Fuel Types	
		Kerosene	Nanofuel (at 0.05 wt. % concentration)
Chemical Formula	:	($C_{10}H_{22}$)	-
Higher calorific value in kJ/kg.	:	46200	46149.40
Lower calorific value kJ/kg.	:	43890	43837.33
Flash point (˚C)	:	55	56
Fire point (˚C)	:	61	62
Dynamic viscosity (Ns/m^2)	:	1.30×10^{-3}	1.49×10^{-3}

2. Input Power/ Thermal load of a burner:

To find the power/thermal load of the burner, kW = Mass flow rate of the fuel × calorific value of the fuel

For example:

If the flow meter shows a reading of 150 g/h,

then the power at which the burner is running = 150 g/h × 43890 kJ/kg

= 1.82 kW

APPENDIX-II

Klein and McClintock (1953) proposed a procedure for estimating the uncertainty of any measured quantity in experimental studies. If an estimated quantity, R depends on the independent variables like x_1, x_2, x_3,…….x_n then,

$$R = R (x_1, x_2, x_3,…….x_n)$$

Then the maximum value of uncertainty is given by:

$$W_R = \left[\left(\frac{\partial x_1}{x_1} \right)^2 + \left(\frac{\partial x_2}{x_3} \right)^2 + \left(\frac{\partial x_3}{x_3} \right)^2 ..... \left(\frac{\partial x_n}{x_n} \right)^2 \right]^{1/2}$$

In the present case, the formula for efficiency is as given below:

$$\eta = \frac{\left[m_w C_w \Delta T_w \right] + \left[m_p C_p \Delta T_p \right]}{m_f \times CV}$$

Since $\Delta T_w = \Delta T_p = \Delta T$

$$\eta = \frac{\left[(m_w C_v) + (m_p C_p) \right] \left[\Delta T \right]}{m_f \times CV_f}$$

m_f is the fuel consumed to raise the water temperature from T_1 to T_2

The uncertainty in the thermal efficiency mainly comes due to the measured quantities of mass and temperature.

Assumptions:

1. Temperature rise of water and vessel are equal.
2. No error in values of specific heat of pan (C_p) and water (C_w), and Calorific value (CV) of fuel. Hence the Calculation formula:

$$\frac{\partial \eta}{\eta} = \left[\left(\frac{\partial \eta}{\partial m_v} \Delta m_v \right)^2 + \left(\frac{\partial \eta}{\partial m_w} \Delta m_w \right)^2 + \left(\frac{\partial \eta}{\partial (\Delta T)} \Delta(\Delta T) \right)^2 + \left(\frac{\partial \eta}{\partial m_f} \Delta m_f \right)^2 \right]^{1/2}$$

Where $\Delta m_v = \pm 1$ gm, $\Delta m_w = \pm 1$ gm

$\Delta(\Delta T) = \pm 1°C$, $\Delta m_f = \pm 1$ gm

At a condition of $m_v = 1.195$ kg, $m_w = 6$ kg

$\Delta T = (90\text{-}25) = 65°C$, $m_f = 0.061$ kg

We get $\frac{\partial \eta}{\eta} = 0.0139$

Therefore the maximum uncertainty in efficiency is $1.39 \approx 1.40$

APPENDIX-III

1. Pressure gauge

Make	: Waree instruments
Dial size	: 100 mm
Range	: 0-2 bar
Readability	: 0.05 bar
Housing Materials	: 300 Series SS
Accuracy	: ±0.05% full scale
Temperature Limits	: 0 °C to 120 °C

2. Weighing balance

Make	: SARTORIUS
Model	: CLWP1 – 30ED-I
Capacity	: 30 kg
Platform size	: 400 mm × 300 mm
Least count	: 1 g

3. Thermocouple

Type	: K
Range	: 20 ^{o}C to 1350 ^{o}C
Accuracy	: ±1.5 ^{o}C

4. Data acquisition unit (DAQ)

Make	: Agilent Technologies
Model	: 34970A
Scan rate	: 60 to 250 channels/second
Scan intervals	: 0 to 99 hours; 1 ms time step
Accuracy	: 6 digits of resolution with 0.004%

5. Portable gas analyser

Make	: Green Line
Model	: 8000
O_2	: 0 – 25 Vol%
Resolution	: 0.1 Vol%
Accuracy	: <0.1 Vol%
CO	: 0 – 20000 ppm
Accuracy	: <5 ppm (0 – 300 ppm)
Resolution	: 1 ppm
NO	: 0 – 4000 ppm
Accuracy	: <1 ppm (0 – 100 ppm)
Resolution	: 0.1 ppm
NO_2	: 0 – 500 ppm
Accuracy	: <1 ppm (0 – 99 ppm)

भारतीय प्रौद्योगिकी संस्थान गुवाहाटी
Indian Institute of Technology Guwahati

List of Patents and Publications

1. Patents

1. Subhash C. Mishra, P. Muthukumar, Gyan Sagar Sinha, Monikankana Sharma, Niraj Kumar Mishra, P. Mahanta. Self-Aspirated Pressurized Kerosene Cooking Stove with a Porous Radiant Burner, patent application no. 201631037245.

2. P. Muthukumar, Gyan Sagar Sinha, Lav Kumar Kaushik, Monikankana Sharma, N. Shanmuga Priya, S. Kanagaraj. Self-Aspirated Pressurized Kerosene Cooking Stove with a Porous Radiant Burner with Nanoparticles blended (Send to patent attorney, review is going on).

2. Journal

1. Muthukumar Palanisamy, Monikankana Sharma, Lav Kumar Kaushik, Gyan Sagar Sinha, Sangjukta Devi, Niraj Kumar Mishra, Subhash C Mishra, Recent Progress in Porous Media Combustion Technology: Burners Development and Performance Estimation. Renewable and Sustainable Energy Reviews (under review).

2. Gyan Sagar Sinha**,** P. Muthukumar, Monikankana Sharma, Niraj Kumar Mishra : Use of ceramic porous media as a burner for the improvement of thermal and emission performance of a kerosene pressure stove, Energy (under review).

3. Conferences

1. Snehasish Panigrahy**,** Gyan Sagar Sinha and Subhash C. Mishra and P. Muthukumar, Analysis of combustion of premixed kerosene –air mixture in a porous radiant burner, Proceedings of the 23rd National Heat and Mass Transfer Conference and 1st International ISHMT-ASTFE Heat and Mass Transfer Conference IHMTC, ISRO Thiruvananthapuram, India, Dec. 17-20, 2015.